Multivariate Geostatistical Analysis of Evapotranspiration and Elevation for Various Climatic Regimes in Oregon

by

Antonio Martínez-Cob

A THESIS

submitted to

Oregon State University

in partial fulfillment of

the requirements for the degree of

DOCTOR OF PHILOSOPHY

Completed May 4, 1990

Commencement June 1990

AN ABSTRACT OF THE THESIS OF

Antonio Martínez Cob for the degree of Doctor of Philosophy in Soil Science presented on May 4, 1990

Title: Multivariate Geostatistical Analysis of Evapotranspiration and Elevation for Various Climatic Regimes in Oregon

Abstract approved:

Richard H. Cuenca

This work investigated the feasibility of applying multivariate geostatistics in evapotranspiration studies. The major goals of this study were: 1) to analyze and model the spatial correlation between evapotranspiration and elevation above sea level; and 2) to investigate whether the use of cokriging improves the accuracy of the evapotranspiration estimates over a regular grid by including the effects of topography.

A total of 11 study cases for each of four different climatic regions within the state of Oregon were analyzed. The climatic regions were labeled as Willamette Valley, North Central, South Central and East. Long-term monthly averages of daily reference evapotranspiration (ET_r) were available at 199 locations within those regions for the months of February to November as well as values of total annual (cumulative) ET_r. Values of elevation above sea level were available at those locations and at additional 8570 locations on a grid of approximately 5 *km* per side.

Application of the geostatistical concept of the direct-semivariogram was required to describe the spatial variability of a single variable. The description of the spatial correlation between ET_r and elevation required the application of the cross-semivariogram concept. Experimental direct-semivariograms for ET_r were fit with isotropic, spherical models with small nugget effects. Experimental direct-semivariograms for elevation were fit with isotropic models with nugget effects and two

nested structures (spherical and gaussian) for the Willamette Valley region, one nested structure (spherical) for the North Central region, and two nested structures (spherical and linear) for the South Central and East regions. The experimental cross-semivariograms were fit with spherical models.

The direct- and cross-semivariogram models were applied to interpolate monthly and cumulative ET_r using the geostatistical tools of kriging and cokriging at 8570 locations on a 5 *km* grid. Kriging and cokriging estimation error standard deviations were computed for each study case. ET_r estimates and estimation error standard deviations were plotted as contour maps. Maximum, minimum and average kriging and cokriging estimates of ET_r were in general agreement, although minimum and average values tended to be lower for cokriging. However, contour lines of cokriged ET_r reflected more closely the elevation features of the climatic regions. Maximum and average estimation error standard deviations were lower for cokriging, while the minimum values being very similar for both kriging and cokriging. Average cokriging standard deviations decreased by about 20 to 30 % in the Willamette Valley and North Central regions and by 5 to 13 % in the South Central and East regions. The difference between regions was caused by the lower correlation coefficient between ET_r and elevation observed in the latter two regions. Contour maps of standard deviations showed cokriging had a more uniform distribution of estimation errors than kriging, for which errors tended to decrease in the vicinity of the sample ET_r points at the weather stations. Errors along regional borders increased for both kriging and cokriging, although maximum estimation error values were lower for cokriging.

APPROVED:

Assoc. Prof. of Agricultural Engineering in charge of Major

Head of Soil Science Department

Dean of Graduate School

Date Thesis is presented: May 4, 1990

Thesis presented by Antonio Martínez Cob

ACKNOWLEDGEMENT

The purpose of these lines is to show my recognition and gratitude to the many people that contributed to the completion of this project. I would like to thank Dr. Richard H. Cuenca for his constant and generous support, guidance and, more important, friendship during these school years. I would like to thank the rest of my committee members for their time and excellent suggestions: Dr. Richard Morris, Dr. Jonathan Istok, Dr. Harry Mack, Dr. David Thomas and Dr. Don Grabe.

I would like to express my respect and gratitude to the graduate students that I worked with under the direction of Dr. Cuenca: Osmar Carrijo, William Nichols, Jeffery Nuss, Gabriel Katul and Samuel Ortega. The support, assistance, conversation and coffee we have shared together has been one of the most enjoyable aspects of graduate school. Thanks should also go to the rest of the faculty, staff and fellow graduate students of the Agricultural Engineering and Soil Science Departments at Oregon State University.

Several other persons deserve my gratitude. The assistance of Joe Hevesi (U.S. Geological Survey, Mercury, Nevada), Kelly Redmond (State Climatologist, Climatic Research Institute, Corvallis), Clint Jensen (National Weather Service, Portland) and Phil Brown (Computer Center, Oregon State University) in the data collection and processing was invaluable. Special thanks should go to Dr. José Faci González and Dr. Ramón Aragüés Lafarga (Servicio de Investigación Agraria, Zaragoza, Spain) for their constant and sincere support. I wish to express my gratitude to the Autonomous Government of Aragón (Spain) and the U.S. - Spain Joint Committee for Scientific and Technological Cooperation for their financial support.

Finally, the most sincere thanks and special recognition goes to my parents, brothers and sisters. Their support, encouragement and love was a true blessing, which gave me strength during the more difficult moments of my years far away from home.

A mis padres y hermanos

TABLE OF CONTENTS

LIST OF TABLES

LIST OF FIGURES

Multivariate Geostatistical Analysis of Evapotranspiration and Elevation for Various Climatic Regimes in Oregon

1 INTRODUCTION

1.1 Statement of the problem

The rate of evapotranspiration from land surfaces is an important component of the hydrological balance. Due to this phenomenon, a major fraction of the total amount of water falling as precipitation on land surfaces is returned to the atmosphere. On average, evapotranspiration represents about two-thirds of the annual precipitation falling over the land (Shukla and Mintz, 1982; Sharma, 1985). Substantial variations in hydrological regimes have been reported in various parts of the world. These changes have been attributed to alterations in evapotranspiration rates caused by significant modifications of the surface vegetative cover (Rose and Sharma, 1984; Eagleson, 1986).

Quantitative evaluation of evapotranspiration rates is required within the context of many problems. Among others, these topics include crop production, management of water resources for agricultural, industrial and urban uses, and environmental assessments. In irrigated areas of the world, an increasing competition for water use between agriculture, industry, and human populations has stressed the need of more accurate crop water use estimates. These estimates are critical for improving the efficiency of irrigation systems and irrigation scheduling.

Unfortunately, evapotranspiration is still among the less understood aspects of the hydrological cycle. It is still difficult to estimate this quantity on a regional basis (Brutsaert, 1982; Jackson, 1985).

Evapotranspiration rates in a given region for a period of time may be determined as the residual of the water balance equation (Brutsaert, 1982) when the other terms are known

$$P - ET + Q_i - Q_o = \frac{dS}{dt} \qquad [1]$$

where: P = precipitation rate
ET = evapotranspiration rate
Q_i = water inflow rate
Q_o = water outflow rate
dS/dt = rate of change in soil water storage

However, this method is not always practical. Large absolute errors in the evapotranspiration rate may result from relatively small but inevitable errors in the determination of the various terms of equation [1] (Brutsaert, 1982). Likewise, this method cannot be applied to predict evapotranspiration in the design of planned water storage. Neither can it be used when irrigation systems are designed to supply water required for growing crops in a given region. In such situations, evapotranspiration is usually determined independently from the water balance equation. Generally for irrigation, evapotranspiration is estimated on the basis of meteorological parameters recorded at a weather station located at a site considered as representative of the project area.

The fields to be irrigated may be several times larger than the supposedly representative weather station site. As a consequence, these local evapotranspiration estimates must be extrapolated. The extrapolation region may be several kilometers away from the weather station site

and hundreds of square kilometers in area. Errors incorporated in such an approximation may lead to over irrigation or under irrigation of crops and may cause to water storage reservoirs to be over-designed or under-designed.

Increased concern in regional scale evapotranspiration studies has also resulted from two other relatively recent developments. First is the availability of remotely sensed data of surface conditions. The frequency and the relatively dense grid at which these data are being recorded make them particularly suitable for water resources planning and management (Cuenca and Amegee, 1987). The second development is the worldwide increasing concern in the prediction of both short-term and long-term climatic changes at a global scale. This concern has focused the attention on global circulation models (Eagleson, 1986). Regional evapotranspiration estimates are one of the input parameters of these models which normally operate on a minimum grid size ranging from 100 to 500 *km* (Cuenca and Amegee, 1987).

The considerations mentioned above justify efforts to improve the accuracy of regional evapotranspiration estimates and to quantify the error associated with the application of a local estimate to a region a certain distance away. As proposed by Amegee (1985), such efforts must rely on the modeling of the spatial variability of evapotranspiration, i.e. the change in evapotranspiration with respect to the distance between weather stations at which meteorological data are collected. It is customary to represent such spatial variability with weekly, monthly or annual isolines of evapotranspiration based on long-term meteorological parameters (Cuenca *et al.*, 1981).

In the hydrological sciences, the drawing of contour lines is generally expedited by the estimation of the values of the hydrological variable under study at each node of a regular grid. This estimation is done by interpolation of data available at other sites (Delhomme, 1978). This interpolation should be based on the variation of the hydrological variable as a function of the distance between measurement points. The

topographic characteristics of the region where the estimations are to be made should also be taken into consideration. It is known that changes in elevation above sea level within a region may significantly affect the structure of the spatial variability of the hydrological variable of interest (Cuenca *et al.*, 1981; Nuss, 1989).

1.2 Alternative methods of approach

Several approaches have been suggested in the literature to study and quantify evapotranspiration at regional scales. Recent progress in remote sensing techniques has greatly encouraged this type of study (André *et al.*, 1986, 1988). In this approach, remotely sensed data (e.g. the soil-plant canopy temperature and the surface incoming and reflected radiation) can be used in combination with ground based parameters measured at traditional weather stations. Subsequently, evapotranspiration is computed as a residual of the energy balance equation. Although the resulting formulas offer promising results, their validity has not yet been fully verified over large regions. They also need to be evaluated under conditions of partly cloudy skies and the methodology is still subject to several constraints (Jackson, 1985; Hatfield, 1988a). One of these constraints is the extension of the punctual ground based parameters to a region.

Different empirical and physically based formulas have been developed to estimate evapotranspiration at locations where meteorological parameters are recorded. Section 2.2 is devoted to a review of these formulas. In all cases, the quantification of regional evapotranspiration requires the extension of these local estimates to locations where meteorological parameters are not available. If the objective is the contour-

ing of evapotranspiration, values of this variable must be estimated at each node of a regular grid covering the study region. Various computerized techniques have been used for distributing data to a grid. Such techniques include distance weighting of the data, polynomial interpolation, least squares, and others. However, all of these methods give arbitrary weights to the data, regardless of the physical aspects of the problem. Another important disadvantage is that most of them cannot provide any indication as to the precision of the results (Delhomme, 1978).

The need for a preliminary recognition of the spatial variability of a variable for the optimization of a data weighting system and the quantification of the estimation error was emphasized as early as the 1940's by the Soviet school of hydrometeorology (Delhomme, 1978). At the beginning of the 1960's, Matheron (1963) built his Theory of Regionalized Variables. Geostatistics, as this theory is usually known, uses the correlation between neighboring measurements to construct a model which characterizes the structure of the spatial variability of the parameter under study, such as evapotranspiration (Journel and Huijbregts, 1978). The model spatial variability can be applied to estimate the required parameter by spatial interpolation at locations where no measurements are available. The method also provides a tool to quantify the error of the estimation. These errors can be related to station density so that a sampling design network can be optimized (Delhomme, 1978; Warrick *et al.*, 1986).

Geostatistics has been applied to a large variety of fields, including mining (Journel and Huijbregts, 1978), agrometeorology (Vieira *et al.*, 1983), water resources (Delhomme, 1978), and soil science (Warrick *et al.*, 1986). Recently, the feasibility of applying geostatistics to evapotranspiration has been analyzed for the state of Oregon (Cuenca and Amegee, 1987; Nuss, 1989). As a result of their analyses, contour maps of evapotranspiration on a monthly basis have been developed. Cuenca and Amegee (1987) analyzed the spatial variability of evapotranspiration for

the whole state of Oregon. Their research indicated the presence of a bias in those estimates. This bias was due to the fact that the topographic characteristics of Oregon were not included in the model of spatial variability. They suggested dividing the state into uniform climatic regions and applying geostatistics within each region. This task was performed by Nuss (1989) with an improvement over the original work, but topographic characteristics were again excluded. His results also supported the need of including topographic information to analyze the spatial variability of evapotranspiration within each climatic region.

Elevation values are available at many more locations than evapotranspiration. In such situations, it has been pointed out that the estimates of the under-sampled variable can be improved if the additional information provided by the more frequently sampled variable is included in the model spatial variability (McBratney and Webster, 1983; Aboufirassi and Mariño, 1984). The magnitude of the improvement depends, among other factors, on the degree of correlation between the two variables (Ahmed and De Marsily, 1987; Hoeksema *et al.*, 1989; Hevesi *et al.*, 1990). Because of the known influence of elevation on the spatial variability of several meteorological parameters, such as air temperature, a strong correlation between evapotranspiration and elevation is to be expected.

1.3 Objectives and scope

The use of geostatistics to analyze and model the spatial variability of evapotranspiration has proven to be feasible. However, the influence of changes in topography on that spatial variability has not yet been considered. In this thesis, the general objective was to analyze and

model the spatial correlation between local estimates of evapotranspiration and values of elevation above sea level. The main goal of this work was to investigate the improvement in accuracy in the estimates of evapotranspiration over a regular grid by including the effects of elevation using a geostatistical interpolation technique termed cokriging. The final product was the contour of these estimates of evapotranspiration for those climatic regimes in Oregon in which the analysis technique was feasible. The specific objectives of this work were:

1. To analyze and model the spatial variability of evapotranspiration within each climatic region when long-term meteorological parameters were used to estimate evapotranspiration at weather station sites.
2. To analyze and model the spatial correlation and variability of evapotranspiration and elevation within each climatic region.
3. To estimate evapotranspiration within each region at grid points where weather data were not available. The model spatial variability developed in the first two objectives, in conjunction with kriging and cokriging interpolation techniques, was used.
4. To quantify and compare of the errors associated with the estimation of evapotranspiration with both kriging and cokriging interpolation techniques.
5. To produce contour maps of evapotranspiration for each climatic region.

The scope of this project was limited to the state of Oregon. Within the state six climatic regions were identified. Four of these regions were used in this work. A small number of weather stations and a lack of significant correlation between evapotranspiration and elevation at the

other two regions precluded further analysis. Estimates of long-term monthly averages of daily reference evapotranspiration (see section 2.1) were available at 199 locations within these four climatic areas for the months of February to November. In each of these locations, estimates of total annual (cumulative) reference evapotranspiration were also available. This study was not performed for January and December because the majority of the estimates of reference evapotranspiration at the weather stations were zero. Elevation data were available at the 199 weather station sites and at additional locations distributed on a grid interval of approximately 5 *km* (section 3.3).

2 LITERATURE REVIEW

This chapter is divided into three sections. The first section presents some basic definitions related to evapotranspiration. The second section discusses several approaches used to estimate evapotranspiration at both local and regional scales. The third section introduces principles of the theory of regionalized variables or geostatistics.

2.1 Basic definitions of evapotranspiration

Consistent definitions are extremely important in maintaining communication within the research community. For this reason, some basic definitions related to evapotranspiration are given.

Evapotranspiration

Evapotranspiration is the loss of water from the ground surface to the atmosphere through vaporization of liquid water (Sharma, 1985). This process includes water evaporated directly from the soil surface (evaporation) or from live and dead vegetation foliage, and water lost through plant surfaces, particularly leaves (transpiration). Evapotranspiration is expressed as the latent heat transfer per unit area or its equivalent depth of water per unit area per unit time (Burman *et al.*, 1983).

Potential evapotranspiration

Potential evapotranspiration is the maximum rate at which water, if fully available, would be removed from the ground surface and transpired by the plant. This definition is not restricted to a standard surface. It is vague and offers various interpretations of its meaning (Burman *et al.*, 1983). Due to this ambiguity, the research community is moving towards the use of the term reference evapotranspiration.

Reference evapotranspiration

Two definitions of reference evapotranspiration (ET_r) are commonly used. The first definition uses alfalfa (*Medicago sativa* L.) as the reference crop and is given as (Burman *et al.*, 1983)

> "... the upper limit or maximum evapotranspiration that occurs under given climatic conditions with a field having a well watered agricultural crop with an aerodynamically rough surface, such as alfalfa, with 30 to 50 *cm* of top growth".

The second definition, the one employed in this thesis, expresses ET_r as (Burman *et al.*, 1983)

> "... the rate of evapotranspiration from an extensive surface of 8 to 15 *cm*, green grass cover of uniform height, actively growing, completely shading the ground, and not short of water".

Local and regional evapotranspiration

Local evapotranspiration represents the evapotranspiration rate of surfaces of about 1 km^2. It is the evapotranspiration rate computed using meteorological parameters recorded at a single weather station. The evapotranspiration rate representative of an area between 1 to 100 km^2 is generally considered as regional evapotranspiration (Sharma,

1985). However, in the context of general circulation models (GCM), regional evapotranspiration refers to grid sizes of about 100 to 500 *km* per side (Cuenca and Amegee, 1987).

2.2 Evapotranspiration estimating methods

The complexity of the evapotranspiration process has long been recognized. In general terms, evapotranspiration research has two main goals: 1) the quantification of water losses from a given area; and, 2) an improved understanding of the various mechanisms involved in that process (Sharma, 1985). In the context of the first purpose, time and spatial scales are relatively large, and empirical and semi-empirical approaches, with appropriate calibration, may be adequate. However, an improved understanding of evapotranspiration requires smaller time and spatial scales. Consequently physically based models which include soil and plant parameters would be preferable (Sharma, 1985). A discussion of all methods developed for evapotranspiration studies is beyond the scope of this work. The reader is referred to several excellent reviews of the subject (Jensen, 1974; Brutsaert, 1982; Sharma, 1985).

This section describes several methods in which the main input parameters are meteorological data. The first subsection presents approaches to estimate local ET_r and focuses on the temperature-based methods. The second subsection briefly reviews some approaches to estimate regional evapotranspiration. The methods discussed in that section are, in general, within the scope of the first objective mentioned in the previous paragraph.

2.2.1 Local evapotranspiration estimating methods

Several methods are available to estimate local ET_r from meteorological parameters (Jensen, 1974; Sharma, 1985). Their degree of complexity and accuracy and their time scales are diverse (Hatfield, 1985; Sharma, 1985). One of the first attempts to develop a function relating local ET_r and several meteorological parameters was done by Penman (1948). His approach combines two factors affecting evapotranspiration: the energy available for the evaporation process and the action of the wind to remove water vapor from the evaporating surfaces. Penman's equation is the following

$$ET_r = \frac{\Delta}{\Delta+\gamma} R_n + \frac{\gamma}{\Delta+\gamma} E_a \qquad [2a]$$

$$E_a = f(u)\ (e_s - e_a) \qquad [2b]$$

where: ET_r = reference evapotranspiration, $mm\ d^{-1}$

Δ = slope of the saturation vapor pressure-temperature curve, $mb\ ^{\circ}C^{-1}$

γ = psychrometric constant, $mb\ ^{\circ}C^{-1}$

R_n = net long-wave and short-wave radiation, $mm\ d^{-1}$

$f(u)$ = empirically derived aerodynamic wind function

$e_s - e_a$ = vapor pressure deficit, mb

The variable E_a represents the drying power of the air or advection ($mm\ d^{-1}$). Although Penman's approach is based on theory, some empiricism exists to account for simplification needed for practical use. The Penman equation has been calibrated in different climates and several versions of this equation exist (Doorenbos and Pruitt, 1977; Wright, 1982). This equation offers the advantage of being based on theory and its accuracy allows estimates of daily values of ET_r to be made (Dooren-

bos and Pruitt, 1977). However, it requires the input of a number of meteorological parameters, including incoming solar radiation and wind speed. Unfortunately, these variables are only recorded at a limited number of weather stations.

Several other empirical or semi-empirical equations to estimate local ET_r have been formulated. These methods can be grouped according to their main meteorological parameter input (Jensen, 1974; Sharma, 1985). It is possible to distinguish between radiation methods, pan evaporation methods, humidity methods and air temperature methods. The accuracy of these methods is highly variable and most of them only perform relatively well in climatic conditions very similar to the ones in which they were developed (Burman *et al.*, 1983). The temperature-based methods have the most widespread use because air temperature is the variable most frequently recorded at weather stations. Some methods use other parameters (secondary weather data) for additional calibration. These secondary weather parameters allow for adjustment (local calibration) based on the general climatic conditions of the station site. Improved ET_r estimates have been made by applying local calibration or, at least, an adjustment that considers the general climatic conditions (Doorenbos and Pruitt, 1977; Burman *et al.*, 1983).

Erpenbeck (1981) evaluated and compared seventeen empirical local ET_r estimating methods at fourteen meteorological sites in the state of Washington. Seven of these methods used air temperature as the primary weather parameter. The other ten methods used most of the data available at a relatively complete weather station, including solar radiation, wind speed, and saturation deficit of the air. The Blaney-Criddle method, as modified by the Food and Agriculture Organization (FAO) of the United Nations (Doorenbos and Pruitt, 1977), was selected as the best state-wide local ET_r estimating method for Washington. The selection was based on the weather data available throughout the state and on statistical ranking using the coefficient of determination for each estimating method compared to lysimeter measurements.

Allen and Brockway (1982) compared eight local ET_r estimating methods using daily weather data from the U.S. Department of Agriculture (USDA) Research Center at Kimberly, Idaho. Again, the FAO-modified Blaney-Criddle method was selected as the best state-wide local ET_r estimating method for Idaho based on accuracy and the primary data requirement of air temperature only.

For the state of Oregon, Basketfield (1986) analyzed and contrasted two temperature based local ET_r estimating methods: the Soil Conservation Service (SCS) modified Blaney-Criddle and the FAO-modified Blaney-Criddle methods. Results indicated that the SCS-modified Blaney-Criddle method seriously under predicted ET_r at relatively high altitude and semiarid locations. The FAO-modified Blaney-Criddle method with additional adjustments recommended by the USDA (Doorenbos and Pruitt, 1977; Allen and Brockway, 1982) was chosen for this research because of results previously indicated for Washington, Idaho and Oregon, and because the air temperature is the most frequent meteorological parameter recorded at weather stations throughout Oregon (Redmond, 1985).

FAO-modified Blaney-Criddle method

The method presented in this subsection is the result of work done under the direction of the FAO (Doorenbos and Pruitt, 1977). Later adjustments were introduced after research performed at the USDA Research Center at Kimberly, Idaho (Allen and Brockway, 1982). In this method, the following equation was used to estimate the monthly average of local daily ET_r

$$ET_r = \{a + b\ [p\ (0.46\ T_{ad} + 8.13)]\}\ R_f \qquad [3]$$

where: ET_r = monthly average of local ET_r, $mm\ d^{-1}$

p = monthly mean of daily percentage of annual daytime hours

T_{ad} = monthly average of daily mean air temperature, $^{\circ}C$, adjusted to account for the aridity of the surroundings of the station

a, b = climatic calibration coefficients

R_f = reference ratio coefficient

The values of the variable p were estimated as a function of the latitude of the station and month from a look-up table (Doorenbos and Pruitt, 1977). The climatic calibration coefficients partially account for local climatic conditions. They were developed by a step-wise regression analysis on meteorological and lysimeter data (Doorenbos and Pruitt, 1977). The authors presented the following equation for coefficient a

$$a = 0.0043RH_{min} - \frac{n}{N} - 1.41 \qquad [4]$$

where: RH_{min} = long-term monthly average of daily minimum relative humidity, %

n/N = long-term monthly average of daily ratio of actual to maximum possible sunshine hours, dimensionless

Frevert *et al.* (1983) published a regression equation for coefficient b based on the original computerized look-up table produced by Doorenbos and Pruitt (1977). Further simplification of that regression equation resulted in the following expression (Cuenca, 1989)

$$b = 0.82 - 0.0041(RH_{min}) + 1.07\left(\frac{n}{N}\right) + 0.066(U_{day}) - 0.006(RH_{min})\left(\frac{n}{N}\right) - 0.0006(RH_{min})(U_{day}) \qquad [5]$$

where: U_{day} = long-term monthly average of daily daytime wind speed at 2 m height above ground, $m\ s^{-1}$

The original tabulated values of coefficient b are always more accurate than the regression equation which does not have a perfect fit for every coefficient in the table. The tabulated values were used in this study instead of equation [5].

For climatic conditions at Kimberly, Idaho, the ratio of ET_r for an alfalfa reference crop to ET_r for a grass reference crop should be 1.15 (Doorenbos and Pruitt, 1977). However, the results of Allen and Brockway (1982) showed that the FAO-modified Blaney-Criddle method overpredicted grass ET_r. A set of reference ratio coefficients, R_f, was developed to correct this situation (Allen and Pruitt, 1986). Two sets of these coefficients were given dependent upon whether or not equation [3] is corrected to account for the site elevation above sea level. Because of the objectives of this work, this latter correction was not included. Thus, the reference ratio coefficients used (Table 1) were those developed for the case in which equation [3] is not corrected for elevation.

Reference evapotranspiration is supposed to be representative, by definition, of moist, non-arid sites. However, some weather stations were located in completely arid environments. These stations tended to have higher temperatures than adjacent stations exposed to the same meteorological conditions but in irrigated environments. Allen and Brockway (1982) developed an additional calibration to adjust for the aridity of the station surroundings. They proposed the following adjustment for the mean air temperature

$$T_{ad} = T - A_{ad} \qquad [6]$$

where: T = monthly average of daily mean air temperature, $^{\circ}C$, as recorded at the station

A_{ad} = temperature adjustment aridity factor, $^{\circ}C$

The temperature adjustment aridity factor was given by the following expression

$$A_{ad} = A_a \; A_c \qquad [7]$$

where: A_a = average monthly aridity effect, $^{\circ}C$

A_c = cumulative aridity of the station, dimensionless

The monthly aridity effects represent the departure of air temperature over arid areas from air temperature over irrigated areas. These values were given by Allen and Pruitt (1986) for Southern Idaho. They are listed in Table 1. These coefficients were used in this research because of the proximity of Oregon to Idaho.

TABLE 1. Monthly reference ratios, R_f, without elevation correction and monthly aridity effects, A_a (adapted from Allen and Pruitt, 1986).

Month	R_f	A_a, $^{\circ}C$
April	1.36	1.0
May	1.28	1.5
June	1.20	2.0
July	1.13	3.5
August	1.12	4.5
September	1.21	3.0
October	1.37	0.0

Cumulative aridity ratings were a constant for each station. These ratings ranged from 0, for a completely irrigated environment, to 100 percent, for a completely unirrigated environment. They were computed by the following equation (Allen and Pruitt, 1986)

$$A_c = 0.4A_s + 0.5A_a + 0.1A_r \quad [8]$$

where: A_s = site aridity, %

A_a = area aridity, %

A_r = regional aridity, %

Site aridity represents the aridity of the environment within a 50 *m* radius of temperature sensor. Area aridity is the aridity of the environment within a 1.5 *km* radius in the predominant upwind direction of the temperature sensor. Regional aridity represents the aridity of the environment within a 50 *km* radius in the predominant upwind direction of the temperature sensor (Allen and Pruitt, 1986).

2.2.2 Regional evapotranspiration estimating methods

In the previous section, methods to estimate ET_r at a local scale were discussed. Several approaches are available in the literature to extend these local estimates to a regional scale. Most of these approaches employ traditional weather data to estimate evapotranspiration in regions of about 100 km^2, while methods applying remote sensing techniques estimate evapotranspiration at larger scales (Hatfield, 1985). It must be kept in mind that as the spatial scale increases, input data availability rather than model adequacy becomes the principal limitation to estimate regional evapotranspiration (Rose and Sharma, 1984). Very often regional evapotranspiration is called actual evapotranspiration, i.e. the rate of evapotranspiration under non-reference conditions.

Two main criteria should be used to design techniques for estimating regional evapotranspiration (Amegee, 1985): 1) estimates must be representative of the whole area and hence take into consideration the heterogeneity of individual surfaces within the area; 2) techniques must also be simple enough to be used routinely for practical purposes using traditional weather station networks.

It is common practice to obtain estimates of evapotranspiration at different locations and to use these values to draw contours of evapotranspiration over large areas (Hatfield, 1985). This approach has been used recently in California where ET_r values were available for 400 sites (Pruitt *et al.*, 1987). A question which arises using this approach is how to interpolate the available estimates at points where evapotranspiration information is not available. In general, a weighted average is employed but the weights given to the known points are often arbitrary. Thompson *et al.* (1981) used meteorological parameters recorded at one or more weather stations within 40-*km* squared grids in Great Britain to compute a weighted average meteorological data set. This data set was subsequently used to estimate evapotranspiration within the grid area. The geostatistical interpolation methods described in section 2.3 may represent an improvement of these weighted average procedures.

Doorenbos and Pruitt (1977) proposed to estimate ET_r at a location considered representative of the area under study. Actual evapotranspiration for a particular crop (ET_{crop}) is computed by multiplying the corresponding ET_r values by a coefficient (K_c) specific for the crop. The proposed formulation is the following

$$ET_{crop} = ET_r \; K_c \qquad [9]$$

This approach could work if a knowledge of the surface area occupied by different crops is available for the area represented by the weather station. Raymond and Owen-Joyce (1986) used satellite data to

estimate vegetation types and areal extent. This information was used to estimate regional evapotranspiration in the Palo Verde Valley, California.

It has also been proposed to incorporate concepts and relationships of aerodynamic and canopy resistances to water vapor transfer into the Penman method (Thom and Oliver, 1977; Thompson *et al.*, 1981). In this approach, known as the Penman-Monteith method, evapotranspiration is estimated by the following equation

$$ET_r = \frac{\Delta\ (R_n - G)\ +\ \rho c_p\ (e_s - e_a)/r_a}{\Delta\ +\ \gamma(1 + r_c/r_a)} \qquad [10]$$

where: G = soil heat flux, $mm\ d^{-1}$

ρ = air density, $g\ cm^{-3}$

c_p = specific heat of air, 0.24 $cal\ g^{-1}\ ^{\circ}C^{-1}$

r_a = aerodynamic resistance to water vapor transfer, $s\ m^{-1}$

r_c = canopy (bulk stomatal) resistance to water vapor transfer, $s\ m^{-1}$

Allen (1986) compared ten forms of the Penman equation, two of which were Penman-Monteith formulations, with lysimeter measured evapotranspiration at three locations in the U.S. These three locations represented a wide range of climatic conditions. Results showed that the Penman-Monteith equations best predicted daily lysimeter measurements at the three locations based on the reliability and consistency of the estimates. The Penman-Monteith method produces estimates of regional evapotranspiration provided that aerodynamic and canopy resistance values and vegetative areal extents are known for the different crops of an area.

Air which is in contact with a wet surface over a very long fetch tends to become saturated with water vapor. In this situation E_a (equation [2b]) tends to zero. In other words, the first term of the right-

hand side of equation [2a] represents a lower limit to evaporation from moist surfaces. This lower bound is called equilibrium evaporation (Brutsaert, 1982). The second term of the right-hand side of equation [2a] represents a measure of the departure from equilibrium in the atmosphere. In the absence of cloud condensation or radiative divergence, this departure would arise from large-scale or regional advection effects involving horizontal variation of surface or atmospheric conditions.

These arguments lead Bouchet (Brutsaert, 1982) to formulate the following expression which he termed the complementary relationship

$$ET = 2ETW - ETP \qquad [11]$$

In this equation, ET is the regional (actual) evapotranspiration from an area so large that the effects of upwind boundary transition are negligible. ETP is the potential evapotranspiration as estimated from a solution of the vapor transfer and energy-balance equations. It represents the evapotranspiration that would occur from a hypothetical moist surface with radiation absorption and vapor transfer characteristics similar to those of the area. The effects of evapotranspiration from this moist surface on the overpassing air are assumed negligible. ETW is the wet-environment actual evapotranspiration that would occur if the soil-plant surfaces of the area were saturated and there were no limitations on the availability of water.

Equation [11] is applied to estimate actual evapotranspiration rates from large uniform surfaces of regional size (lengths on the order of 1 to 10 *km*). Several alternative formulations, with different time scales, have been proposed to compute ETP and ETW (Brutsaert and Stricker, 1979; Morton, 1983, 1985). The main advantage of methods derived from Bouchet's complementary relationship is that only meteorological parameters are required. In some procedures, calibration is required to determine additional parameters used to compute ETP and ETW (Morton, 1983,

1985). This approach requires input from a meteorological station whose surroundings are representative of the area of interest. Interpolation to areas where weather stations are not available has not yet been solved (Morton, 1983). Bouchet's approach however requires further analysis with different data sets (Brutsaert, 1982; Hatfield, 1985).

Brutsaert and Mawdsley (1976) proposed the extension of the Penman's equation to the planetary boundary layer (PBL). The PBL also is known as the outer region layer and is situated from about 1 *km* to 2 *km* above the ground. According to McNaughton and Spriggs (1986), the PBL is a well-mixed layer of air with specific thickness, potential temperature and relative humidity. Above the PBL is the free atmosphere with specified potential temperature and relative humidity profiles set by larger-scale atmospheric processes. Between the bulk of the PBL and the ground is a 'thin' surface layer where the mixing is not perfect and sizable temperature and humidity gradients may develop. The basic assumption in this approach is that fluxes in the PBL layer are independent of the nature of the surface and will better represent an average of the elementary fluxes. These fluxes may therefore be more representative of the regional evapotranspiration fluxes (Brutsaert and Mawdsley, 1976; McNaughton and Spriggs, 1986) for surfaces larger than 5 to 10 *km*. This approach requires profiles of mean wind speed, temperature and humidity in the lowest 2 *km* or so of the atmosphere. These profiles are measured with devices known as rawinsondes. Difficulties in using this method arise from the inadequacy of rawinsonde networks and inaccuracy of some published rawinsonde data. Moreover, the vertical intervals between the profile measurements are often larger than desirable (Brutsaert, 1982). However, this approach shows potentials for the study of the effect of evapotranspiration on the weather and may serve as a useful interface between the ground and the atmosphere in GCMs (McNaughton and Spriggs, 1986).

Several authors have demonstrated that remotely sensed data together with some ground-based measurements can be used to estimate or measure evapotranspiration at a regional scale (Price, 1982; Gurney and Camillo, 1984; Jackson, 1985; Reginato *et al.*, 1985; André *et al.*, 1988). In all cases, the starting point is the energy balance equation. This equation, with all terms expressed in units of energy per unit time per unit area (Jackson, 1985) can be written as

$$ET = R_n - H - G \qquad [12]$$

where: ET = latent heat flux (evapotranspiration)

R_n = net radiation absorbed at the surface

H = sensible heat flux from the surface to the atmosphere

G = soil heat flux

In a ground-based situation, net radiation, sensible heat flux, and soil heat flux can be directly measured. In the remote sensing case, this is not possible. It is necessary to identify which parameters can be measured, which estimated, and which safely neglected so that the latent heat flux may be determined with acceptable accuracy. In general, the larger number of relevant parameters that can be measured by remote means, the more accurate a regional evaporative flux measurement will be, thereby reducing the need to replicate expensive ground-based instrumentation to obtain the same information.

Net radiation at the surface of the Earth is the sum of the incident and reflected shortwave solar radiation and the incident sky and emitted terrestrial long-wave radiation. By measuring or estimating these four radiation terms, net radiation can be computed. Since remote sensing is the detection of reflected and emitted energy, net radiation could be reliably evaluated by combining ground-based measurements of the incoming radiation terms with remotely measured outgoing terms (Jackson *et al.*, 1985).

Sensible heat flux is function of the temperature gradient between the evaporative surface and the air above it (Price, 1982; Hatfield, 1988b). The surface temperature can be determined using remotely sensed data. The air temperature must be measured by a traditional meteorological station. Still in this approach, the aerodynamic resistance for sensible heat flux transfer must be determined which requires quantification of aerodynamic properties of the surface, stability of the atmosphere and wind speed (Gurney and Camillo, 1984; Hatfield, 1988b).

Soil heat flux must be determined by means of ground-based measurements. The soil heat flux is generally small in magnitude compared to the other terms of equation [12]. Some authors neglect it (Price, 1982), while others employ empirical approaches to estimate soil heat flux as function of crop height and net radiation (Reginato *et al.*, 1985; Choudhury *et al.*, 1987).

The largest drawback of these techniques is the extrapolation of ground-base measurements from single meteorological stations to a regional scale (Hatfield, 1988a). Another main constraint of these techniques is that it is necessary to devise ways to infer values that apply to longer time periods, i.e. daily, from the essentially instantaneous remotely sensed data (Jackson, 1985). The sinusoidal nature of solar radiation under clear skies has been used to approach this problem (Jackson *et al.*, 1983; Seguin and Itier, 1983). However, further evaluation is required under partly cloudy skies or over larger regional scales (Hatfield, 1988a). Effects of the atmosphere on the amount of radiation reaching the sensors, sensor calibration, and the determination of aerodynamic resistance terms to sensible heat flux are the other main constraints for application of remote sensing techniques (Jackson, 1985).

2.3 Fundamental concepts of geostatistics

This section describes elements of the theory of regionalized variables which are relevant to the main geostatistical tools used to characterize spatial variability and to estimate regionalized variables. It is not intended to present a comprehensive treatise of the subject. For an introduction to the subject, the reader is referred to Rendu (1978), Clark (1979) and Journel (1989). For a detailed discussion of the theoretical aspects behind geostatistics, it is recommended to consult David (1977) and Journel and Huijbregts (1978). For an introduction of the application of geostatistics to fields other than mining, the reader is referred to Delhomme (1978), Vieira *et al.* (1983), Warrick *et al.* (1986) and Cuenca and Amegee (1987).

2.3.1 Definition and applications of geostatistics

At the beginning of the 1960's, Matheron (1963) developed his Theory of Regionalized Variables, also termed Geostatistics. Geostatistics is the application of the formalism of random functions to the reconnaissance and estimation of natural phenomena (Journel and Huijbregts, 1978). A natural phenomenon can often be characterized (Delhomme, 1978; Journel and Huijbregts, 1978) by the distribution in space and/or time of one single variable (regionalization) or two or more intercorrelated variables (coregionalization). These variables are known as regionalized variables. Univariate geostatistics refers to the study of regionalization processes and multivariate geostatistics applies to the study of coregionalization processes. It should be noted that geostatis-

tical methods are closely related to time series analysis, many of whose methods can be viewed as one dimensional subsets of geostatistics (Henley, 1981).

The application of geostatistics to the estimation of ore reserves in mining is probably its most well known use. Nevertheless, it has been emphasized frequently that geostatistics can be used wherever the value of a variable is expected to be affected by its position and its relationship with neighboring values of the same variable (Clark, 1979). Therefore, almost all variables encountered in the earth sciences, including the hydrological ones such as ET_r, can be regarded as regionalized variables (Delhomme, 1978).

Geostatistics was developed as a new approach to the problem of estimation of regionalized variables because of the failure of classical statistical methods to solve them (Matheron, 1963). Classical statistical methods are based on the assumption of the random distribution of values. Classical statistics interprets all sample values as independent realizations of the same random variable. Consequently, it is unable to take into account the spatial variability of the regionalized variables. This spatial variability implies a structured aspect, which is precisely its most important feature (Rendu, 1978; Clark, 1979).

Geostatistical methods offer several advantages over other empirical interpolation techniques (Delhomme, 1978; Burguess and Webster, 1980; Hevesi *et al.*, 1990): 1) they provide unbiased estimates; 2) they provide an indication of the precision of the estimates; 3) they minimize the estimation error variance; and, 4) additional, correlated variables can be incorporated in the estimation equations. This latter property offers the potential of significantly decreasing the calculated estimation error variances. The main disadvantage of geostatistics is the complexity of its application when compared to other interpolation techniques (Journel and Huijbregts, 1978). Computational efforts in geostatistics are high and the use of a powerful computer is a must. A more detailed discus-

sion of the advantages and disadvantages of geostatistics and other interpolation techniques can be found in Henley (1981) and Mansur-Marques (1985).

It often happens in resource surveys that some variables are measured more intensively than others due to several reasons. Estimates of sparsely sampled variables using univariate geostatistics are likely to have large errors. If, however, such a variable is spatially correlated with one or more others that have been or can be measured more intensively, its estimates can be improved by using the additional information with multivariate geostatistics (McBratney and Webster, 1983; Aboufirassi and Mariño, 1984). In this thesis, the under sampled variable is ET_r and the more intensively sampled variable is elevation above sea level. The magnitude of the improvement in the estimation variances depends on several factors (Ahmed and De Marsily, 1987; Hoeksema *et al.*, 1989; Hevesi *et al.*, 1990): 1) the number of additional data; 2) the degree of correlation between the two variables; 3) the proximity of the additional data to the point being estimated; and, 4) the arrangement of the additional data around the point to be estimated.

The most common application of geostatistical techniques is the estimation of the value of a regionalized variable at a point in which no data are available. This application is known as point or local estimation and it is the one used in this work. However, geostatistical techniques can be used for other purposes (Journel and Huijbregts, 1978). For instance, they can be used to make estimates of global averages of the regionalized variable for a certain area or volume within the study region. This application is known as global or block estimation and it has been used in numerous cases (Delhomme, 1978).

The potential of geostatistics for sampling network design has also been indicated (Hughes and Lettenmaier, 1981). This design must define the number, location, and sample pattern of sampling sites. Three approaches have been pointed out to perform this task (Loaiciga, 1989): 1) optimization; 2) conditional simulation; and, 3) variance reduction.

In the optimization approach, the minimization of the variance of the estimation error is subject not only to the unbiasedness condition but to resource constraints, e.g. economic restrictions (Loaiciga, 1989). In the conditional simulation approach, other possible realizations of the same regionalized variable are simulated (Delhomme, 1979; Journel, 1989). These other realizations have the same spatial variability as the true natural phenomenon. In the variance reduction approach, additional samples are added until the maximum estimation error variance has been reduced to an acceptable level (Rouhani, 1985; Smyth, 1988).

There are four main steps in a geostatistical point estimation procedure (Journel and Huijbregts, 1978). 1) A model adequately describing the spatial variability of the variables of interest must be proposed. This model must also characterize the dependence between variables. Direct-semivariograms (regionalization) and cross-semivariograms (coregionalization) are the appropriate tools for this task. 2) The unknown parameters of the model must be determined. 3) The suitability of the fit model must be checked by using cross-validation. 4) The variable of interest is estimated at unknown locations. Kriging (univariate geostatistics) and cokriging (multivariate geostatistics) are the interpolation techniques used. These interpolation methods allow computation of the estimation error variance associated with each estimate of the variable of interest. The following sections describe these four steps.

2.3.2 Regionalized variables and random functions

Let consider the value taken by a particular variable, $z(x_1)$, at point x_1 (in one-, two- or three-dimensional space) as a particular realization of a certain random variable (RV), $Z(x_1)$, at that point. The set

of variables $z(x)$ for all sample points x within the domain of interest, i.e. the regionalized variable (ReV) $z(x)$, can be considered as a particular realization of the set of RV's, $Z(x)$, for all points x within that domain (Journel and Huijbregts, 1978). This set of RV's is known as the random function (RF) $Z(x)$. Any regionalized variable has two important characteristics which are expressed by the definition of a RF (Journel and Huijbregts, 1978; Delhomme, 1978):

a) A local, random, erratic aspect. Thus, at a point x_1, $Z(x_1)$ is a RV.

b) A general structured aspect. It is expressed by the (auto) correlation that, in general, exists between the corresponding RV's $Z(x_1)$ and $Z(x_1+h)$ for each pair of points x_1 and x_1+h.

This structured aspect of ReV's is the central point of geostatistics. The autocorrelation depends on both the distance vector h (in modulus and direction) which separates the two points, and on the particular variable considered.

The probabilistic approach to coregionalization is similar to that of the regionalization of a single variable. Therefore, the coregionalization of K ReV's $\{z_1(x),\ldots,z_K(x)\}$ is interpreted as a particular realization of the set of K inter-correlated RF's $\{Z_1(x),\ldots,Z_K(x)\}$.

For a certain RF, $Z(x)$, to have an operative sense, it is necessary to infer all or part of the probability law defining this RF. However, it is not possible to infer this probability law from a single realization, $z(x)$, which is limited to a finite number of sample points, x_i. In order to resolve this situation, certain assumptions, involving various degrees of spatial homogeneity, are necessary. These assumptions are introduced under the general heading of the hypothesis of stationarity (David, 1977; Journel and Huijbregts, 1978; Myers, 1989).

It is also necessary to note that the application of the theory of regionalized variables requires that each RV be normally distributed. Because only a single realization is available for each RV, the distribution of the sample points is used as an indication of this assumption of normality. If the data are not normally distributed, a transformation into a normal distribution is usually applied (Henley, 1981; Myers, 1989).

2.3.3 Hypothesis of stationarity and the semivariogram

Both the role and meaning of stationarity are the source of some confusion. Stationarity refers to the RF and not to the data, although the data are the only information available to test for stationarity or an appropriate weak form. As indicated by Myers (1989), this interchange is the source of some confusion in the literature. The definitions and consequences of different forms of stationarity, both in the univariate and the multivariate cases, follow the discussion presented by David (1977), Journel and Huijbregts (1978) and Myers (1989).

Strong stationarity

A RF, $Z(x)$, is stationary if, for any finite number n of points, $\{x_1,\ldots,x_n\}$, and any vector distance h, the joint distribution of RV's, $\{Z(x_1),\ldots,Z(x_n)\}$, is the same as the joint distribution of RV's, $\{Z(x_1+h),\ldots,Z(x_n+h)\}$. In the multivariate case, this condition must apply for each of the K inter-correlated RF's defining the coregionalization. Unfortunately, in nearly all instances, the data are represented as

a nonrandom sample from one realization of the RF and, therefore, can not be tested for stationarity. For this reason, weaker forms of stationarity are introduced.

Stationarity of order 2

A RF, $Z(x)$, is second-order stationary if the following conditions are met.

a) The mean of the RF exists and does not depend on the support point x .

b) The covariance of the RF exists and depends only on the vector distance h .

The first condition implies that the mean is constant over the domain of interest. The mean, m , of the RF is defined as its mathematical expectation value, symbolized by $E[.]$

$$E[Z(x)] = m \qquad [13]$$

In the multivariate case, the first condition implies that, for each RF, $Z_k(x)$, the mathematical expectation is defined as

$$E[Z_k(x)] = m_k \qquad [14]$$

The covariance, $C(h)$, is defined as the expected value of the product of deviations of two RV's, $Z(x+h)$ and $Z(x)$, separated by the vector distance h , from the mean

$$C(h) = Cov[Z(x+h), Z(x)]$$

$$= E\{[Z(x+h)-m][Z(x)-m]\} \quad [15a]$$

$$= E[Z(x+h)\ Z(x)] - m^2 \quad [15b]$$

In the multivariate case, for each pair of RF's, $Z_k(x), Z_{k'}(x)$, the cross-covariance, $C_{k'k}(h)$, can be defined as

$$C_{k'k}(h) = E\{Z_{k'}(x+h)\ Z_k(x)\} - m_{k'}m_k \quad [16]$$

The stationarity of the covariance has two more implications.

a) The first one is the existence of a finite *a priori* variance. From equation [15a], this variance is equal to the covariance at $h = 0$

$$Var[Z(x)] = E\{[Z(x)-m]^2\} = C(0) \quad [17]$$

b) The direct-semivariogram function, $\gamma(h)$, defined as one-half the variance of the increment $[Z(x+h)-Z(x)]$, is also stationary. From equations [13], [15] and [17], the direct-semivariogram function can be written as

$$\gamma(h) = \frac{1}{2}Var[Z(x+h)-Z(x)]$$

$$= \frac{1}{2}E\{[Z(x+h)-Z(x)]^2\} \quad [18a]$$

$$= C(0) - C(h) \quad [18b]$$

In the multivariate case, for each pair of RF's, $Z_k(x), Z_{k'}(x)$, the cross-semivariogram function, $\gamma_{k'k}(h)$, can be defined as

$$\gamma_{k'k}(h) = \frac{1}{2}E\{[Z_{k'}(x+h)-Z_{k'}(x)][Z_k(x+h)-Z_k(x)]\} \quad [19a]$$

$$= C_{k'k}(0) - \frac{1}{2}[C_{k'k}(h)+C_{kk'}(h)] \quad [19b]$$

When $k' = k$, equations [16] and [19a] yield the definitions of the covariance and direct-semivariogram given in equations [15a] and [18a], respectively. Equations [18b] and [19b] indicate that, under the hypothesis of second-order stationarity, the covariance and the semivariogram function are two equivalent tools for characterizing the spatial variability and correlations between one or more ReV's. The semivariogram function expresses how two RV's, $Z(x)$ and $Z(x+h)$, differ in average according to the distance vector h separating them (David, 1977).

Intrinsic hypothesis

There are many physical phenomena and RF's which have an infinity capacity for dispersion. These RF's have neither an *a priori* variance nor a covariance, but a semivariogram function can be defined. As a consequence, the second-order stationarity hypothesis can be slightly reduced when assuming only the existence and stationarity of the semivariogram function. This condition is known as the intrinsic hypothesis. Under the intrinsic hypothesis, equations [13] and [18a] apply for the univariate case, and equations [14] and [19a] apply for the multivariate case. Under this hypothesis, the expectation of the increment, $[Z(x+h)-Z(x)]$, is zero. The hypothesis of second-order stationarity implies the intrinsic hypothesis but the converse is not true.

Quasi-stationarity

As has been mentioned previously, stationarity is defined by properties of the RF. This would suggest that stationarity is not scale related. However, this is not the case and an example could illustrate it (Myers, 1989). Elevation rapidly changes when proceeding from east to west in the United States and, so, elevation could be assumed non stationary. However, if elevation is considered on a global scale, the mountain ranges represent an insignificant part of the Earth's surface. Hence, in this case, a more reasonable view might be to consider elevation as stationary.

A common practice is to limit the hypothesis of second-order stationarity (or the intrinsic hypothesis if only the semivariogram function is assumed) to only distances smaller than a limit b. This corresponds to an hypothesis of quasi-stationarity (or to a quasi-intrinsic hypothesis). The distance within which the stationarity hypothesis can be assumed is generally difficult to determine as the data are the only information available to test for stationarity. In fact, the hypothesis of quasi-stationarity is a compromise between the scale of homogeneity of the phenomenon and the amount of available data.

When the assumptions are false

The assumptions of second-order stationarity (or intrinsic hypothesis) and normality of the data distribution are not always met. Table 2 outlines different ways in which those assumptions are not satisfied. Table 2 also shows the methods which have been developed to meet progressive breakdown of the stationarity and the normal distribution assumptions (Henley, 1981).

TABLE 2. Kriging (cokriging) methods available when stationarity or distribution assumptions are not satisfied. Adapted from Henley (1981).

	STATIONARITY			
DISTRIBUTION	Stationary	Simple drift	Local trends	Severe anisotropy
Complex	Disjunctive kriging		?	?
Simple known (e.g. lognormal)	Lognormal kriging	?	?	?
Normal	Ordinary kriging (point or block)	Universal kriging	Generalized covariances	?

The most usual of those methods is called universal kriging (David, 1977; Journel and Huijbregts, 1978). In this case, it is said that the RF, $Z(x)$, is weakly stationary with drift. This RF can be written as

$$Z(x) = Y(x) + m(x) \qquad [20]$$

where: $Y(x)$ = a RF which satisfies the intrinsic hypothesis

$m(x) = E[Z(x)]$, the drift

The drift is the mean of the RF, but it is not independent of the support point x. The drift is a linear combination of known linearly independent functions. The essential point when using this form of stationarity is to remove $m(x)$ and then to proceed with $Y(x)$ using the intrinsic hypothesis (David, 1977; Myers, 1989). An adequate modeling of the drift is critical to reduce the estimation error variance and to avoid biased estimators (Boufassa and Armstrong, 1989).

Because of difficulties resulting from simultaneous estimation and modeling of the semivariogram and the drift, a second definition of weak stationarity has been introduced: the generalized covariances approach

(Myers, 1989). It is necessary to define linear combinations that filter out polynomials up to order $k-1$. These generalized differences define second-order stationary RF's.

If the distribution of the data samples is not normal, a logarithm transformation of the original values may lead to a normal distribution. If this is the case, ordinary kriging (Table 2) can be used on the transformed values (Henley, 1981). This method is known as lognormal kriging. However, the estimates will be in terms of logarithms of the original values. If the distribution of the original data is more complex, disjunctive kriging may be employed (Journel and Huijbregts, 1978; Henley, 1981). In this case, a 'best-fit' approximate transformation, consisting of a set of Hermite polynomial functions, is used.

Some authors have proposed the use of a non-parametric approach, whereby the data are used through their rank order (Henley, 1981; Journel, 1983, 1984). In this approach, the minimum of assumptions is required. Usually continuity of the distribution is sufficient. In this approach, the estimators of the unknown points will necessarily be sub-optimal when all the conditions for the ordinary kriging (Table 2) are satisfied (Henley, 1981).

2.3.4 Properties of the semivariograms

In this section, several properties of theoretical direct- and cross-semivariograms are discussed. Most of the material covered in this section can be found in David (1977), Journel and Huijbregts (1978) and Clark (1979).

The definition of the direct-semivariogram entails the following properties

$$\gamma(0) = 0, \qquad \gamma(h) = \gamma(-h) \geq 0 \qquad [21]$$

In general, as the distance vector h increases (Figure 1), the semivariogram increases from its initial value. Very often in practice, the semivariogram stops increasing beyond a certain distance. This distance is known as the range, a. Beyond this distance, the semivariogram becomes more or less stable around a limit value. This value is called sill, C. Semivariograms characterized by a sill value and a range are called transition semivariograms. They correspond to a RF which is not only intrinsic but also second-order stationary.

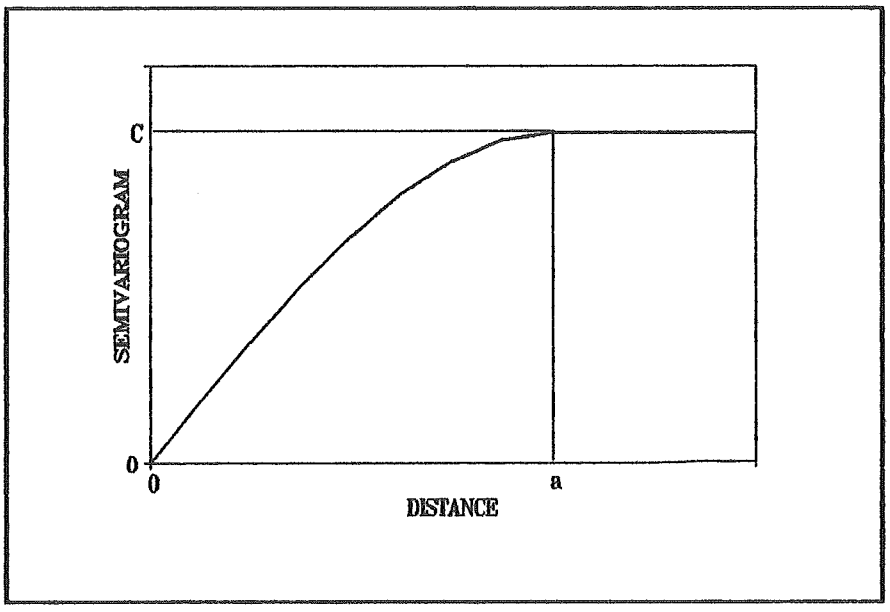

FIGURE 1. Ideal shape for a direct-semivariogram with a range a and a sill C.

The range corresponds to the intuitive idea of a zone of influence of a RV. For any distance h greater than the range, two RV's, $Z(x)$ and $Z(x+h)$, are no longer correlated. The sill is simply the *a priori* variance of the RF, defined in equation [17]. It should be stressed that the existence of a sill is not related to the existence of an experimental variance (variance of the sample values). This experimental variance can always be calculated even when a sill does not exist. There is no reason to expect that a natural phenomenon exhibit the same behavior in every direction. A semivariogram is considered to be anisotropic when its range and sill vary for different directions in space.

The properties of cross-semivariograms are very similar to those of direct-semivariograms. However, some differences do exist. For instance, a cross-semivariogram may take negative values, whereas a direct-semivariogram is always positive. A negative value of the cross-semivariogram indicates that a positive increase in one of the variables, k', corresponds, on average, to a decrease in the other, k. In general, the shape of an ideal semivariogram outlined in Figure 1 is still valid for a cross-semivariogram. Nevertheless, because this cross-semivariogram may take negative values, the cross-semivariogram may decrease from 0 at $h = 0$ to negative values at distances greater than 0. This decrease will flatten out at some distance which is equivalent to the range of the direct-semivariogram. Beyond the range, the cross-semivariogram becomes stable around a limit value, the sill.

Another important remark needs to be pointed out. The cross-semivariogram is symmetric in (k', k) and $(h, -h)$ while this is not necessarily so for the cross-covariance

$$\gamma_{k'k}(h) = \gamma_{kk'}(h) \qquad \text{and} \qquad \gamma_{k'k}(h) = \gamma_{k'k}(-h) \qquad [22a]$$

$$C_{kk'}(h) = C_{k'k}(-h) \qquad \text{and} \qquad C_{k'k}(-h) \neq C_{k'k}(h) \qquad [22b]$$

Finally, the point to point correlation coefficient, $\rho_{k'k}$, between two RF's, $Z_{k'}(x)$ and $Z_k(x)$, located at the same point x, is defined as

$$\rho_{k'k} = \frac{C_{k'k}(0)}{\sqrt{C_{kk}(0)C_{k'k'}(0)}} = \rho_{kk'} \qquad [23]$$

where: $C_{k'k}(0)$ = cross-covariance at distance 0

$C_{kk}(0)$ = variance of the RF $Z_k(x)$

$C_{k'k'}(0)$ = variance of the RF $Z_{k'}(x)$

2.3.5 Structural analysis: fitting models of semivariograms

Structural analysis of a regionalized phenomenon consists in constructing a semivariogram model which characterizes, in an operational way, the main features of the regionalization or the coregionalization of interest (Journel and Huijbregts, 1978). This modeling requires good physical knowledge of the phenomenon under study as well as good "craft" in the practice of fitting geostatistical models. Structural analysis should be adapted to the proposed goal of the study. It is most often a prelude to an intended estimation and, as such, should be limited to the purpose of the estimation. Thus, it is not used to specify structures at smaller scales than the ones at which the estimation is intended (Journel and Huijbregts, 1978).

Before the computation of experimental semivariograms begins, a preliminary statistical analysis must be performed. This statistical analysis must provide the arithmetic mean and the standard deviations of all samples for the variable or variables under study (Journel and Huijbregts, 1978). If more than one variable is analyzed, the correlation coefficient for each pair of variables should also be estimated.

2.3.5.1 Experimental semivariograms

The first step to fit a semivariogram model is to compute an experimental semivariogram using the data available. The experimental semivariogram is based on sample data while the semivariogram model is the underlying theoretical shape of the semivariogram function. The following equation is used to compute an experimental direct-semivariogram value, $\gamma^*(h)$, of the ReV $z(x)$ for a specific distance vector h (David, 1977; Journel and Huijbregts, 1978; Rendu, 1978)

$$\gamma^*(h) = \frac{1}{2N(h)} \sum_{i=1}^{N(h)} [z(x_i+h)-z(x_i)]^2 \qquad [24]$$

where: $N(h)$ = number of pairs of sample points separated by the distance vector h

$z(x_i)$ = measured value at sample point x_i

$z(x_i+h)$ = measured value at sample point x_i+h

For a specific distance vector h , the following expression is used to compute an experimental cross-semivariogram value, $\gamma^*_{kk'}(h)$, for each pair of inter-correlated ReV's (David, 1977; Journel and Huijbregts, 1978)

$$\gamma^*_{kk'}(h) = \frac{1}{2N(h)} \sum_{i=1}^{N(h)} \{[z_k(x_i+h)-z_k(x_i)][z_{k'}(x_i+h)-z_{k'}(x_i)]\} \qquad [25]$$

where: $N(h)$ = number of pairs of sample points separated by the distance vector h

$z_k(x_i)$ = measured value of ReV $z_k(x)$ at sample point x_i

$z_k(x_i+h)$ = measured value of ReV $z_k(x)$ at sample point x_i+h

$z_{k'}(x_i)$ = measured value of ReV $z_{k'}(x)$ at sample point x_i

$z_{k'}(x_i+h)$ = measured value of ReV $z_{k'}(x)$ at sample point x_i+h

In practice, the experimental cross-semivariogram is computed only for pairs of sample points which have data for both ReV's (Smyth, 1988). It must be pointed out that it is necessary to estimate direct-semivariograms for each of the ReV's involved in the coregionalization in addition to cross-semivariograms for each pair of variables (Journel and Huijbregts, 1978).

Ideally, the sample points are spaced in a regular grid at regular intervals. In that case, experimental semivariogram values are computed for several distances (and/or several directions in space), these distances being multiples of the smaller distance between two sample points. It is recommended to limit such computations to approximately half the maximum distance between two sample points (Journel and Huijbregts, 1978; Clark, 1979). It is customary to plot the distance between pairs of samples along the abscissa axis and the values of the experimental semivariogram along the ordinate (Clark, 1979).

In general, sample points are not aligned in a regular manner. In this case, assuming a two dimensional situation, data are grouped into angle (direction) and distance classes (David, 1977; Journel and Huijbregts, 1978). To construct an experimental semivariogram in the direction r, each sample value is associated with every other sample value located within the range defined by $r \pm dr$. Within this angle class, the sample values can be grouped into distance classes. Every data pair separated by a distance $h \pm dh$ is used to estimate the value $\gamma^*(h)$ (Figure 2). The size of the tolerances, dr and dh , depends on the structure of the variable(s) of interest. A good practice is to try several tolerance values (David, 1977). The distance tolerance, dh , should always be small relative to the sample spacing. One rule that should not be forgotten is that the fewer pairs of sample points used to compute a single experimental semivariogram value, the less reliable this value is (Clark, 1979). Journel and Huijbregts (1978) recommend to use distance tolerances such that at least 30 to 50 sample points are used to compute each experimental semivariogram value. In general, the most

reliable points on the semivariogram graph are those for small distances and the reliability drops off slowly and regularly as the distance between sample points increase (Clark, 1979). Again, the experimental semivariogram is computed for distances up to approximately half the maximum distance between two sample points.

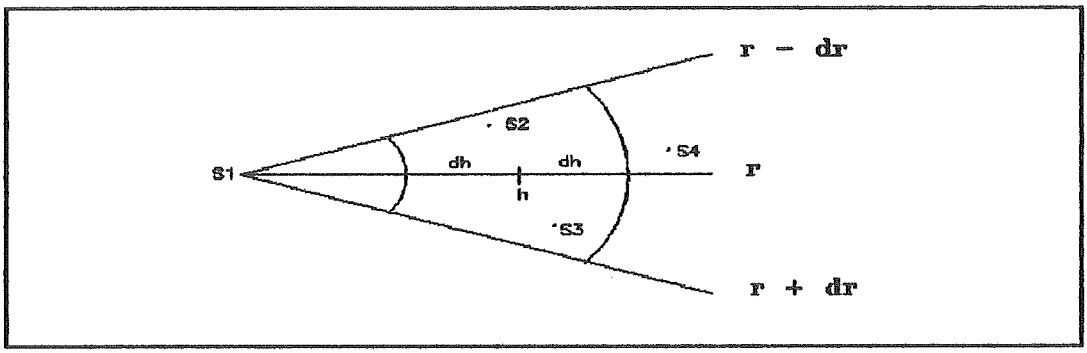

FIGURE 2. Grouping data into distance and angle classes. S1 to S4 are sample values. Adapted from Journel and Huijbregts (1978).

If the experimental semivariogram does not change with the direction in space, a single isotropic semivariogram can be estimated. In this case, the two previous equations can be applied for all pairs of points within the study area, regardless of the direction in space. However, if the experimental semivariogram changes with the direction in space, it is not possible to characterize the spatial variability of the phenomenon under study with a single semivariogram. In this case, anisotropic semivariograms are computed for each direction of the anisotropy.

2.3.5.2 Models of semivariograms

Fitting a theoretical model to the experimental semivariogram is one of the most important aspects of geostatistics. A theoretical model for the semivariogram must satisfy an important condition: it must be a conditionally positive-definite function (Journel and Huijbregts, 1978; Armstrong and Jabin, 1981). This condition is necessary to assure that the variance of any linear combination of RV's is positive (Armstrong and Jabin, 1981). It is time consuming and difficult to test the positive-definiteness of particular models. It is much simpler and safer to adhere to those models for which the conditionally positive-definite condition has been shown (Armstrong and Jabin, 1981). The semivariogram models of most common and widespread use are classified according to whether or not they have a sill value (Journel and Huijbregts, 1978; Rendu, 1978). Table 3 lists the formulas, the slopes at the origin, the ranges and the sills of these different models.

MODELS WITH A SILL. These are known as transition models. They are divided according to their behavior at the origin.

a) Linear behavior at the origin. Two models are included in this category.

   - Spherical model (Figure 3a). This model behaves linearly up to approximately one-third of the range. A line tangent to the points near to the origin will reach the sill at a distance about two-thirds of the range (Vieira *et al.*, 1983).
   - Exponential model (Figure 3b). This model rises more slowly from the origin than the spherical model and never quite reaches the sill (Journel and Huijbregts, 1978; Clark, 1979).

TABLE 3. Models of semivariograms in widest use. Adapted from Delhomme (1978), Journel and Huijbregts (1978) and Rendu (1978).

Type	Formula	Slope at the origin	Range	Sill
Spherical	$\gamma(h) = \begin{cases} C\left(\frac{3h}{2a} - \frac{h^3}{2a^3}\right) & h \le a \\ C & h > a \end{cases}$	$3C/2a$	a	C
Exponential	$\gamma(h) = C(1 - e^{-h/a})$	C/a	$3a$	C
Gaussian	$\gamma(h) = C(1 - e^{-h^2/a^2})$	0	$a\sqrt{3}$	C
Models in h^l	$\gamma(h) = \omega h^l$ $\begin{cases} 0 < l < 1 \\ l = 1 \\ 1 < l < 2 \end{cases}$	∞ ω 0	∞	∞
Nugget effect	$\begin{cases} \gamma(0) = 0 \\ \gamma(h) = C_0 \quad h > 0 \end{cases}$	∞	0	C_0

b) Parabolic behavior at the origin: gaussian model (Figure 3c). This model reaches the sill only asymptotically (Journel and Huijbregts, 1978).

MODELS WITHOUT A SILL. In this case, the RF is only intrinsic. The most common models included in this group are known as models in h^l (Figure 3d) with l being a value strictly greater than 0 and strictly less than 2 (Vieira *et al.*, 1983). If $l = 1$, the semivariogram follows a linear model.

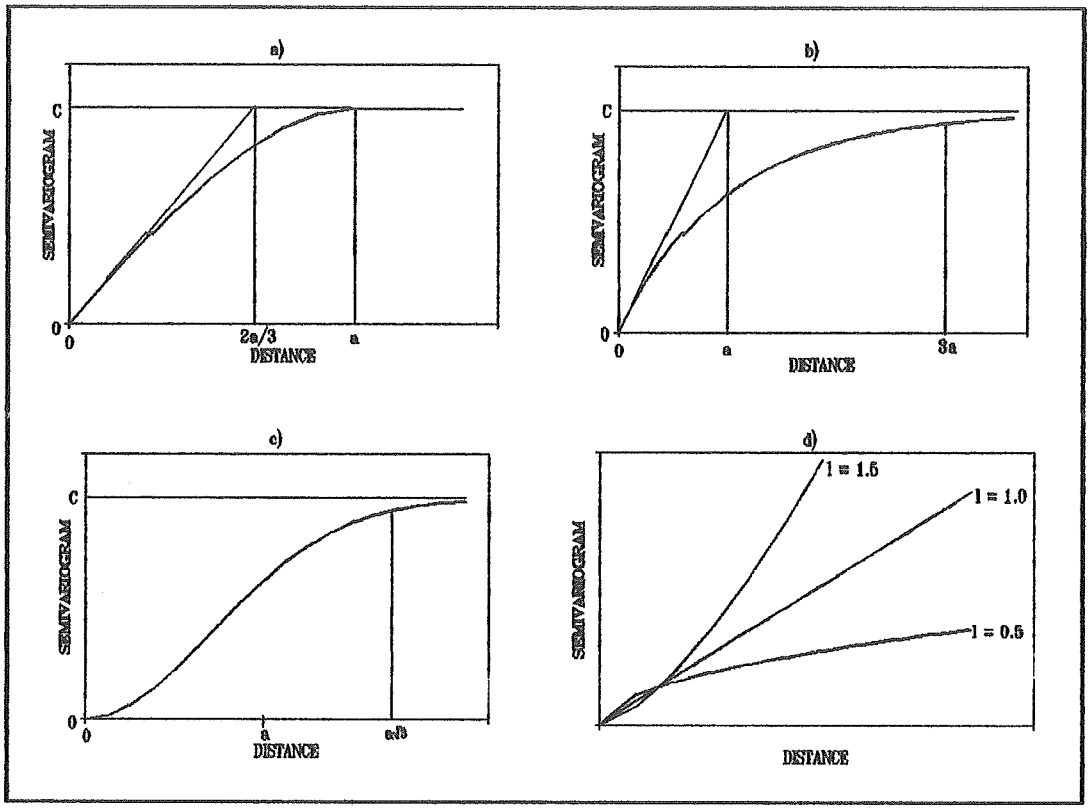

FIGURE 3. Graphs of semivariogram models in widest use: a) spherical model; b) exponential model; c) gaussian model; d) models in h^l. Adapted from Delhomme (1978).

NUGGET EFFECT. This term has been kept to describe an initial discontinuity of the semivariogram: the semivariogram does not tend to zero when the distance tends to zero (Delhomme, 1978; Journel and Huijbregts, 1978). It is a semivariogram with a very small range of influence (Clark, 1979). The nugget effect may be due to a microregionalization on a scale much smaller than the spacing of the data points. It may also be caused by measurement errors (Journel and Huijbregts, 1978; Delhomme, 1978). Table 3 lists the characteristics of a

nugget effect. A pure nugget effect corresponds to the situation where there is a total absence of spatial correlation between two RV's, at least for all available distances (Journel and Huijbregts, 1978).

In several occasions, an experimental semivariogram can be described as a combination of two or more of the previous models. In this case, it is necessary to speak of nested structures. Mathematically, a nested structure can be conveniently represented as the sum of a number of semivariograms, each characterizing the variability of the RF at a particular scale (David, 1977; Journel and Huijbregts, 1978; Clark, 1979)

$$\gamma(h) = \gamma_0(h) + \gamma_1(h) + \gamma_2(h) + \ldots + \gamma_t(h) \qquad [26]$$

There is no reason for the components of a nested structure to have the same directions of anisotropy. For instance, $\gamma_1(h)$ may be isotropic and $\gamma_2(h)$ may be anisotropic (Journel and Huijbregts, 1978). A so-called nested structure commonly found in natural phenomena is composed of a nugget effect plus a structure of larger range and defined by any of the models previously discussed.

Models of coregionalization

LINEAR MODEL OF COREGIONALIZATION. This model is fully discussed in Journel and Huijbregts (1978). The linear model of coregionalization, in terms of semivariograms, is defined as a linear combination of s basic direct-semivariograms $\left\{\gamma_v(h),\ v = 1 \text{ to } s\right\}$

$$\gamma_{kk'}(h) = \sum_{v=1}^{s} b^v_{kk'}\ \gamma_v(h) \qquad \text{with} \quad b^v_{kk'} = b^v_{k'k} \qquad [27]$$

where: $[b^{v}_{kk'}]$ = matrix of parameters of the direct- and cross-semivariogram models

The models for the direct- and cross-semivariogram models must be positive definite, a condition assured if any of the models described previously in this section are chosen. It is also required that the matrix of parameters $[b^{v}_{kk'}]$ be positive definite. For $K = 2$ (the case of two ReV's), verification of the positive definite condition of this matrix amounts to checking that, for all v, the two following inequalities (Schwarz's inequality) hold true

$$b^{v}_{11} > 0 \qquad [28a]$$

$$|b^{v}_{12}| = |b^{v}_{21}| < \sqrt{b^{v}_{11} b^{v}_{22}} \qquad [28b]$$

Schwarz's inequality implies that every basic structure, $\gamma_v(h)$, appearing on the cross-semivariogram, $\gamma_{kk'}(h)$ must also appear on the two direct-semivariograms, $\gamma_{kk}(h)$ and $\gamma_{k'k'}(h)$. Thus, for example, if $\gamma_{kk'}(h)$ reveals two nested ranges, a_1 and a_2, these two ranges must also appear on the two direct-semivariograms. On the other hand, a structure may appear on the direct-semivariograms without being present on the cross-semivariograms. For this, it is sufficient that $b^{v}_{kk'} = 0$ when $b^{v}_{kk} > 0$.

Checking Schwarz's inequality becomes progressively more complicated as the number of nested structures in the semivariogram model increases. Schwarz's inequality can also be written as follows (Myers, 1982)

$$|\gamma_{kk'}(h)| < \sqrt{\gamma_{kk}(h) \quad \gamma_{k'k'}(h)} \qquad [29]$$

Consequently, Hevesi *et al.* (1990) proposed a graphical test of the Schwarz's inequality based in the previous equation. This test is not a strict measure of a positive definite model. However, it has proven to be an invaluable device to select a valid cross-semivariogram model. In this graphical test, a visual comparison of the curve

$$|PDC| = \sqrt{\gamma_{kk}(h) \quad \gamma_{k'k'}(h)} \qquad [30]$$

with the selected cross-semivariogram model is performed. The model is considered to be positive definite if two conditions are met: 1) the absolute value of the model for any distance is smaller than the corresponding absolute PDC value; and 2) the slope of the model does not exceed the slope of the PDC curve.

INTRINSIC COREGIONALIZATION MODEL. This model is also fully discussed in Journel and Huijbregts (1978). This model is a particular example of the linear model. It corresponds to the case in which all the RF's have the same direct-semivariogram, $\gamma_o(h)$. The model of intrinsic coregionalization is then

$$\gamma_{kk'}(h) = b_{kk'} \quad \gamma_o(h) \qquad [31]$$

where $[b_{kk'}]$ is the matrix of parameters and is positive definite.

OTHER MODELS. Myers (1982) and Hoeksema *et al.* (1989) suggest an alternative to the linear model of coregionalization described previously. In their approach, they suggest that rather than computing and plotting sample cross-semivariograms, sample direct-semivariograms for paired sums should be computed and plotted instead. According to these authors, for any pair of RF's, $Z_k(x), Z_{k'}(x)$, their sum, $U_{kk'}(x) = Z_k(x) + Z_{k'}(x)$, is another RF. They define the cross-semivariogram for each pair of RF's as follows

$$\gamma_{kk'}(h) = \frac{1}{2}[\gamma^{*}_{k,k'} - \gamma_{kk}(h) - \gamma_{k'k'}(h)] \qquad [32]$$

where $\gamma^{*}_{k,k'}$ is the direct-semivariogram for the RF $U_{kk'}(x)$, and $\gamma_{kk}(h)$ and $\gamma_{k'k'}(h)$ are the direct-semivariograms for the RF's $Z_k(x)$ and $Z_{k'}(x)$, respectively. Then, spherical, exponential, gaussian and/or linear models can be used to fit these different direct-semivariograms. In general, it will be necessary to verify that the Schwarz's inequality (equation [29]) holds after the separate modelling of those direct-semivariograms.

2.3.5.3 Testing the models: cross-validation

In previous sections, the computation of experimental semivariograms and the different models available to fit them were discussed. The question remains of how to choose the appropriate model to fit to the experimental values and how to determine the parameters of that model. This question is critical and the validity of the geostatistical estimation techniques discussed in section 2.3.6 depends on its answer. Fortunately, it has been pointed out that the estimation error variance is robust to most errors likely to be made in semivariogram model selection and parameterization (Brooker, 1986).

The selection and fitting of a model by visual inspection of the experimental semivariogram is usually sufficient (David, 1977). Automatic curve fitting procedures, such as least squares techniques, are not recommended, unless some modifications are included to allow for the flexibility of giving more weight to semivariogram values that result from more pairs of sample points (Vieira *et al.*, 1983).

The adequacy of the chosen model and its parameters may, to some extent, be judged by a technique called cross-validation (Delhomme, 1978). This technique can be used to evaluate alternative semivariogram models (Warrick *et al.*, 1986; Hevesi *et al.*, 1990). The procedure involves deleting a sample from the data set of one ReV. Then kriging or cokriging (section 2.3.6) are used to estimate the value of that ReV at the location of the deleted sample, using the remaining samples and the chosen semivariogram model and parameters. Differences between estimated and measured values are summarized using the cross-validation statistics (Aboufirassi and Mariño, 1984; Cooper and Istok, 1988; Hevesi *et al.*, 1990): average kriging (or cokriging) error (*AKE*), mean squared error (*MSE*), and standardized error variance (*SMSE*).

A model is considered to ensure unbiased estimates if the *AKE* is close to zero

$$AKE = \frac{1}{n_k} \sum_{i=1}^{n_k} z_k^*(x_i) - z_k(x_i) \qquad [33]$$

where: $z_k^*(x_i)$ = estimated value of ReV $z_k(x)$ at location x_i

$z_k(x_i)$ = measured value of ReV $z_k(x)$ at location x_i

n_k = number of estimated values

A model is considered accurate if its calculated *MSE* is minimum

$$MSE = \frac{1}{n_k} \sum_{i=1}^{n_k} [z_k^*(x_i) - z_k(x_i)]^2 \qquad [34]$$

As a practical rule, the *MSE* should be less than the variance of the sample values (Cooper and Istok, 1988). If the *MSE* is less than the sample variance, the kriging (or cokriging) estimate is better than the estimate provided by the mean of all sample values.

The *SMSE* indicates the consistency of the calculated estimation error variances with the observed *MSE*. Model validity is satisfied if the *SMSE* result is within the interval $1 \pm 2\sqrt{2/n}$ (Delhomme, 1978)

$$SMSE = \frac{1}{n_k - 1} \sum_{i=1}^{n_k} \frac{[z_k^*(x_i) - z_k(x_i)]^2}{\sigma_{CK}^2} \qquad [35]$$

where: σ_{CK}^2 = calculated kriging or cokriging estimation error variance for $z_k^*(x_i)$

Recently, a maximum likelihood approach, which treats the cross-validation errors as gaussian, has been proposed to automatically fit the model parameters (Samper and Neuman, 1989). This approach still requires further analysis and testing before it is fully operational.

2.3.6 Kriging and cokriging

Kriging and cokriging are local estimation techniques which provide the best linear estimator of a particular ReV at a point where it is unknown (Journel and Huijbregts, 1978). This limitation to the class of linear estimators is quite natural since it means that only a knowledge of the second-order moments of the RF, the covariance or the semivariogram, is required. A review of kriging followed by a review of cokriging is presented in this section. This section only deals with ordinary point kriging and cokriging, the ones applied for point estimation under the assumptions of second order stationarity and the intrinsic hypothesis.

Kriging

Let $z(x)$ be a certain ReV unknown at a point x_0. Let this ReV be available at n sample points, $\{x_1, \ldots, x_n\}$, around that point x_0. A linear estimator $z^*(x_0)$ of the unknown and true value $z(x_0)$ is a linear combination of the n sample values (David, 1977; Journel and Huijbregts, 1978)

$$z^*(x_0) = \sum_{i=1}^{n} \lambda_i z(x_i) \qquad [36]$$

where: λ_i = weight assigned to a measured value of the ReV at sample point x_i

$z(x_i)$ = measured value of the ReV at sample point x_i

In kriging, the weights take account of the known spatial dependence expressed in the semivariogram and the geometric relationship among the sample points (Warrick *et al.*, 1986). The n weights λ_i are calculated to ensure that the estimator is unbiased and that the kriging estimation error variance is minimal (Journel and Huijbregts, 1978; Rendu, 1978). The estimator $z^*(x_0)$ is then said to be optimal. The non-bias condition means that the expected value of estimation errors is zero. The estimation error is the difference between the estimator and the true but unknown value of the ReV at location x_0

$$E[z(x_0) - z^*(x_0)] = 0 \qquad [37]$$

To assure this condition, it is enough to impose the following constraint (David, 1977; Journel and Huijbregts, 1978)

$$\sum_{i=1}^{n} \lambda_i = 1 \qquad [38]$$

The kriging estimation error variance, $\sigma^2_{OK}(x_0)$, is the expected value of the square of the difference between the estimator and the true but unknown value of the ReV at location x_0

$$\sigma^2_{OK}(x_0) = E\{[z(x_0) - z^*(x_0)]^2\} \quad [39]$$

This equation can be shown (Burguess and Webster, 1980; Cuenca and Amegee, 1987; Cooper and Istok, 1988) to be

$$\sigma^2_{OK}(x_0) = -\sum_{i=1}^{n}\sum_{j=1}^{n}\lambda_i\lambda_j\gamma(h_{ij}) + 2\sum_{j=1}^{n}\lambda_j\gamma(h_{0j}) \quad [40]$$

where: $\gamma(h_{ij})$ = model semivariogram value for distance vector h_{ij} which separates two sample points, x_i and x_j

$\gamma(h_{0j})$ = model semivariogram value for distance vector h_{0j} which separates a sample point, x_j, from the unknown point, x_0

The problem now is to find those weights λ_i which minimize the kriging estimation error variance under the constraint imposed by equation [38]. To minimize a function of these weights, the derivatives of the function with respect to the weights should set equal to zero. However, when there is a constraint (equation [38]), the Lagrange principle states that the following expression should be minimized

$$M = \sigma^2_{OK}(x_0) + 2\mu\left(\sum_{i=1}^{n}\lambda_i - 1\right) \quad [41]$$

where: μ = a new unknown, the Lagrange multiplier

Therefore, to minimize equation [40], it is necessary to take the derivatives of expression [41] with respect to all unknowns (the weights λ_i and μ) and set them equal to zero (David, 1977; Journel and Huijbregts, 1978; Cuenca and Amegee, 1987)

$$\begin{aligned} \frac{\partial M}{\partial \lambda_i} &= 2\gamma(h_{oj}) - 2\sum_{i=1}^{n}\lambda_i\gamma(h_{ji}) - 2\mu = 0 \\ \frac{\partial M}{\partial \mu} &= \sum_{i=1}^{n}\lambda_i - 1 = 0 \end{aligned} \qquad [42]$$

Rearrangement of this set of equations provides a system of $n+1$ linear equations with $n+1$ unknowns, the n weights λ_i and the Lagrange multiplier μ. This system is known as the kriging system of equations

$$\begin{aligned} &\sum_{i=1}^{n}\lambda_i\gamma(h_{ji}) + \mu = \gamma(h_{oj}) \qquad j = 1,\ldots,n \\ &\sum_{i=1}^{n}\lambda_i = 1 \end{aligned} \qquad [43]$$

The minimized kriging estimation error variance, also known as the kriging variance, is written as

$$\sigma^2_{OK}(x_0) = \sum_{i=1}^{n}\lambda_i\gamma(h_{io}) + \mu \qquad [44]$$

The kriging standard deviation is the square root of the kriging variance. Equation [44] shows that the accuracy of the kriging estimation depends on the semivariogram model fit to the experimental semivariogram. Errors in this model may lead to serious errors in the kriging variance. Fortunately, as pointed out in the previous section, the kriging variance is robust to most errors likely to be made in semivariogram model selection and parameterization (Brooker, 1986). Finally, it

is necessary to note that the kriging system of equations has an unique solution if and only if the semivariogram models are strictly positive definite (David, 1977; Journel and Huijbregts, 1978).

Cokriging

One of the most complete derivations of the cokriging system of equations is done by Journel and Huijbregts (1978) and, in matrix form, by Myers (1982) for a generic number of variables defined in a three-dimensional space. However, most practical applications only deal with one- or two-dimensional samples and two cross-correlated variables. Consequently, this section is limited to this situation which is fully discussed by Vieira *et al.* (1983).

Let $z_1(x)$ and $z_2(x)$ be two ReV's. Let n_1 and n_2 be the number of sample points in which those ReV have been measured, respectively. It is assumed that the ReV $z_1(x)$ is under-sampled with respect to the other ReV, $z_2(x)$, i.e. the ReV $z_2(x)$ has been measured at the same sample points where ReV $z_1(x)$ has been measured plus at a set of additional sample points. Finally, it is necessary to restate that the application of cokriging requires the modeling of direct-semivariograms for each variable separately as well as the modeling of cross-semivariograms (Warrick *et al.*, 1986).

Let x_0 be a point at which the ReV $z_1(x)$ is to be estimated. A linear estimator $z_1^*(x_0)$ of the true value $z_1(x_0)$ is given by the following expression (Smyth, 1988)

$$z_1^*(x_0) = \sum_{i=1}^{n_1} \lambda_{1i} z_1(x_i) + \sum_{j=1}^{n_2} \lambda_{2j} z_2(x_j) \qquad [45]$$

where: $\lambda_{1\ell}$ = weight assigned to a measured value of ReV $z_1(x)$ at sample point x_ℓ

λ_{2j} = weight assigned to a measured value of ReV $z_2(x)$ at sample point x_j

As in kriging, in cokriging the weights take account of the known spatial dependence expressed in the direct- and cross-semivariograms and the geometric relationship among the sample points (Warrick *et al.*, 1986). The n_1 weights $\lambda_{1\ell}$ and the n_2 weights λ_{2j} are calculated to ensure that the estimator is unbiased and that the cokriging estimation error variance is minimal (Journel and Huijbregts, 1978; Vieira *et al.*, 1983). The estimator $z_1^*(x_0)$ is then said to be optimal. The non-bias condition means that the expected value of estimation errors is zero. The estimation error is the difference between the estimator and the true but unknown value of the ReV $z_1(x)$ at location x_0

$$E[z_1(x_0) - z_1^*(x_0)] = 0 \qquad [46]$$

To assure this condition, it is enough to impose the following constraints (Vieira *et al.*, 1983; Aboufirassi and Mariño, 1984)

$$\sum_{\ell=1}^{n_1} \lambda_{1\ell} = 1$$

$$\sum_{j=1}^{n_2} \lambda_{2j} = 0 \qquad [47]$$

The cokriging estimation error variance, $\sigma^2_{CK}(x_0)$, is the expected value of the square of the difference between the estimator and the true but unknown value of the ReV $z_1(x)$ at location x_0

$$\sigma^2_{CK}(x_0) = E\{[z_1(x_0) - z_1^*(x_0)]^2\} \qquad [48]$$

The problem now is to find those weights λ_{1i} and λ_{2j} which minimize the cokriging estimation error variance under the constraint imposed by equation [47]. As done for kriging, Lagrangian multiplier techniques are used (Vieira *et al.*, 1983). The result is a linear system of $n_1 + n_2 + 2$ linear equations with $n_1 + n_2 + 2$ unknowns, the n_1 weights λ_{1i}, the n_2 weights λ_{2j} and the Lagrange multipliers μ_1 and μ_2 (David, 1977; Aboufirassi and Mariño, 1984; Smyth, 1988). This system is known as the cokriging system of equations

$$\begin{aligned}
&\sum_{i=1}^{n_1} \lambda_{1i}\gamma_{11}(h_{mi}) - \sum_{j=1}^{n_2} \lambda_{2j}\gamma_{12}(h_{mj}) - \mu_1 = \gamma_{11}(h_{0m}) \qquad m = 1, \ldots, n \\
&-\sum_{i=1}^{n_1} \lambda_{1i}\gamma_{12}(h_{qi}) - \sum_{j=1}^{n_2} \lambda_{2j}\gamma_{22}(h_{qj}) - \mu_2 = \gamma_{12}(h_{0q}) \qquad q = 1, \ldots, n \\
&\sum_{i=1}^{n_1} \lambda_{1i} = 1 \\
&\sum_{j=1}^{n_2} \lambda_{2j} = 0
\end{aligned} \qquad [49]$$

where: $\gamma_{11}(h_{mi})$ = direct-semivariogram model value for ReV $z_1(x)$ for distance vector h_{mi} which separates sample points, x_m and x_i

$\gamma_{11}(h_{0m})$ = direct-semivariogram model value for ReV $z_1(x)$ for distance vector h_{0m} which separates the unknown point x_0 from sample point x_m

$\gamma_{22}(h_{qj})$ = direct-semivariogram model value for ReV $z_2(x)$ for distance vector h_{qj} which separates sample points, x_q and x_j

$\gamma_{12}(h_{mj})$ = cross-semivariogram model value for distance vector h_{mj} which separates sample points, x_m and x_j

$\gamma_{12}(h_{0q})$ = cross-semivariogram model value for distance vector h_{0q} which separates the unknown point x_0 from sample point x_q

The minimized cokriging estimation error variance, also known as the cokriging variance, is then defined (Smyth, 1988) as

$$\sigma^2_{CK}(x_0) = -\sum_{i=1}^{n_1} \lambda_{1i}\gamma_{11}(h_{0i}) + \sum_{j=1}^{n_2} \lambda_{2j}\gamma_{12}(h_{0j}) + \mu_1 \qquad [50]$$

The cokriging standard deviation is the square root of the cokriging variance. Equation [50] shows that the accuracy of the cokriging estimation depends on the semivariogram models fit to the experimental direct- and cross-semivariograms. Errors in these models may lead to serious errors in the cokriging variance. Finally, it is necessary to note that the kriging system of equations has an unique solution if and only if the semivariogram models are strictly positive definite (David, 1977; Journel and Huijbregts, 1978).

3 MATERIAL AND METHODS

This chapter describes the procedures followed to perform this study. This chapter is divided in four sections. The first section presents a brief description of the general climatic characteristics of Oregon. The second and third sections discuss the two main data bases used in this study, the meteorological data base and the elevation data base. The last section presents the geostatistical procedures used in this study.

3.1 General description of Oregon

The state of Oregon is located on the Pacific Coast of the United States. It is approximately rectangular in shape with dimensions of about 650 *km* by 450 *km*. The north-south Coast and Cascade mountain ranges located in the western half of the state determine the main climatic characteristics. In this study, the nine major climatic regions recognized in Oregon (Redmond, 1985) were grouped into six regions (Figure 4) in an attempt to have enough weather stations within each region for the geostatistical analysis.

The six regions included in this study were denominated as: 1) Coast; 2) Willamette Valley; 3) Southern Valleys; 4) North Central; 5) South Central; and 6) East. West of the Cascade Mountains, i.e. in regions 1, 2 and 3, the climate is generally humid with an annual total precipitation of about 1000 mm (Cuenca and Amegee, 1987). East of the Cascade Mountains, in regions 4, 5 and 6, the general climatic conditions range from semiarid to arid with annual precipitation of about 250 mm or less. Two of the six climatic regions, regions 1 and 3, were excluded

from further analysis due to the lack of enough stations to perform an adequate geostatistical analysis and significant correlation between elevation and local ET_r. Section 4.1 discusses these reasons in more detail.

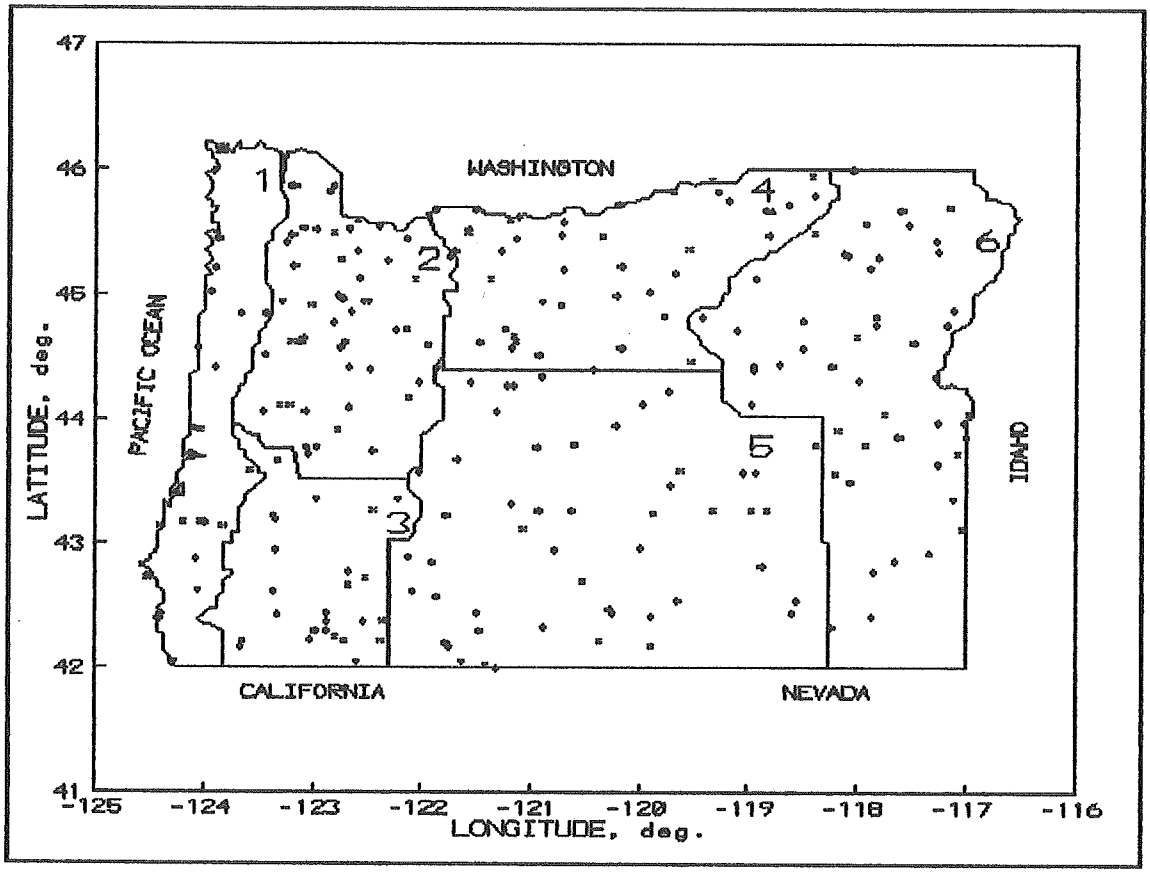

FIGURE 4. Distribution of primary weather stations within the six climatic regions of Oregon: 1) Coast: 27 stations; 2) Willamette Valley: 57 stations; 3) Southern Valleys: 25 stations; 4) North Central: 41 stations; 5) South Central: 52 stations; 6) East: 49 stations.

3.2 Computation of local estimates of ET_r

Estimates of local ET_r were computed at each of the weather stations available at this study using the FAO Blaney-Criddle method with USDA adjustments described in section 2.2.1. The choice of this method is discussed in that section. Application of the method required three types of data: 1) primary weather data, constituted by air temperature values; 2) secondary weather data, constituted by additional meteorological parameters; and 3) aridity factors to account for the aridity of the station surroundings.

Primary weather data

The primary weather data base was made up of monthly averages of maximum and minimum daily air temperature values recorded at 251 primary weather stations throughout Oregon for a period of 10 to 88 years. This data base was provided by the State Climatologist (Climatic Research Institute, Oregon State University). Long-term monthly averages of daily mean air temperature were computed from this data base and used as input into equation [3] (section 2.2.1). Appendix A lists all primary weather stations within the six climatic regions, including information about their longitude and latitude coordinates, the elevation of the station site and the number of years of record. Information on longitude, latitude and elevation of the weather stations was taken from Redmond (1985). Figure 4 shows the distribution of these stations within the different climatic regions. The number of primary weather stations was 27, 57, 25, 41, 52 and 49, respectively, for regions 1 to 6.

Secondary weather data

The additional meteorological parameters required to compute local values of ET_r (section 2.2.1) were the following: a) long-term monthly average of daily minimum air relative humidity (RH_{min}), %; b) long-term monthly average of daily ratio of actual to maximum possible sunshine hours (n/N), dimensionless; and c) long-term monthly average of daily daytime wind speed at 2 m height (U_{day}), $m\ s^{-1}$. These parameters were available from a number of different sources for a limited number of weather stations. The selection of the data source was based on the length of recorded data and ease of obtaining and processing the information. Appendix B shows a list of the secondary data stations, the original units in which they recorded the secondary weather parameters, and the years of record.

For RH_{min}, 21 weather stations were identified. Some of them provided dew point temperature. In this case, the following empirical relationship was used to estimate RH_{min} from dew point and air temperature values (Cuenca, 1989)

$$RH_{min} = 100 \left[\frac{112 - 0.1T_{max} + T_{dp}}{112 + 0.9T_{max}} \right]^8 \qquad [51]$$

where: T_{max} = long-term monthly average of daily maximum air temperature, $^{\circ}C$.

T_{dp} = long-term monthly average of daily dew point temperature, $^{\circ}C$.

For n/N, 25 weather stations were identified. With the exception of the station at Portland Airport, values of n/N were derived from either values of daytime cloud cover or values of incoming short-wave solar radiation. In those stations recording cloud cover, the following relationship (Doorenbos and Pruitt, 1977) was utilized to estimate n/N

Daytime cloudiness (tenths)	0	1	2	3	4	5	6	7	8	9	10
n/N	0.95	0.85	0.80	0.75	0.65	0.55	0.50	0.40	0.30	0.15	0.00

In those stations recording incoming short-wave solar radiation, the following equation (Doorenbos and Pruitt, 1977) was used to estimate n/N

$$\frac{n}{N} = \frac{R_s}{0.5 \quad R_a} - 0.5 \qquad [52]$$

where: R_s = long-term monthly average of daily total incoming short-wave solar radiation in equivalent depth of evaporation, $mm\ d^{-1}$,

R_a = long-term monthly average of atmospheric solar radiation in equivalent depth of evaporation, $mm\ d^{-1}$, published in Doorenbos and Pruitt (1977).

For U_{day}, 32 weather stations were identified. Some of them recorded total daily wind run values. These values were transformed to daytime wind speed under the assumption of daytime wind speed being two times nighttime wind speed (Doorenbos and Pruitt, 1977). Some of the stations recorded wind values at a height other than 2 m. In these cases, the log-wind law was used to adjust the wind speed values to a 2 m height (Doorenbos and Pruitt, 1977)

$$U_{day} = U_{zd} \left(\frac{2.0}{z}\right)^{0.2} \qquad [53]$$

where: U_{zd} = long-term monthly averages of daily daytime wind speed at height z, $m\ s^{-1}$.

Once RH_{min} , n/N and U_{day} were determined at the 21, 25, and 32 weather stations, respectively, it was required to extrapolate these values to the 251 primary weather stations. For this procedure, Oregon was divided in three zones: 1) Coast; 2) Willamette and Southern Valleys; 3) East of the Cascades. Stations with secondary data in each of these zones were used to extrapolate the secondary parameters to the primary weather stations in the same zone. The inverse squared distance technique was employed. The formula used is given by the following expression (Isaaks and Srivastava, 1989)

$$Y = \frac{\sum_{i=0}^{i=c}(y_i/h_i^w)}{\sum_{i=0}^{i=c}(1/h_i^w)} \qquad [54]$$

where Y = extrapolated secondary weather parameter at a desired location (primary weather station)

h_i = distance from the extrapolation point to a point where the secondary weather parameter is known

y_i = value of the known secondary weather parameter

w = weighting power factor, in this case, set to 2

c = number of secondary weather stations used in the extrapolation

Aridity factors

Descriptive information of the primary weather station locations and theirs surroundings was obtained through a personal visit with Clint Jensen (National Weather Service, Portland). This information included type of ground under the temperature sensor, obstructions near the station location, area characteristics and other general remarks. Aridity factors, in percent, were subjectively determined for the site, area and

region, based on that information. Cumulative aridity rates were computed using equation [8], described in section 2.2.1. Site, area, region and cumulative aridity factors for each primary weather station are listed in Appendix C.

Local estimates of ET_r

The meteorological and aridity data bases previously described were used as input to equation [3] (section 2.2.1) to compute local values of long-term monthly averages of daily ET_r ($mm\ d^{-1}$) for each month of the year and for each primary weather station. In addition, for each station, these monthly values were multiplied by the number of days in the month and the resulting values were summed to produce values of total annual or cumulative ET_r (mm). The monthly and cumulative values of local ET_r for each primary weather station are listed in Appendix D.

For each primary weather station, longitude and latitude coordinates were transformed to horizontal (easting) and vertical (northing) distances (km) from an arbitrary reference point located at 125.00° W longitude and 42.00° N latitude. Universal Transverse Mercator (UTM) coordinates were computed for each station and subtracted from the UTM coordinates for that reference point. The subroutine GSCUTM of the STATPAC package (Grundy and Miesch, 1988) was used to perform these computations.

3.3 Elevation data

In this study, elevation values were available from two different data sources. The first data source (Redmond, 1985) provided the elevation of the sites at which the primary weather stations were located. Those values, in *m* above sea level, are listed in Appendix A.

The second data source was the digital elevation model (DEM) produced by the Defense Mapping Agency and distributed by the U.S. Geological Survey. In this data base, elevation values, in *m* above sea level, are given at points separated by 3 arc-seconds, i.e. approximately by 100 *m* in the North-South direction and 70 *m* in the East-West direction. Each 1° longitude x 1° latitude block contains 1,442,401 data points. Oregon is covered by 35 of those blocks. In this work, points were selected every 156 arc-seconds (every 159 arc-seconds for each fourth point) in the North-South direction. In the East-West direction, points were selected every 225 arc-seconds. In this manner, additional elevation values were available on a grid of approximately 5 *km* per side. The total number of elevation points provided by these two data sources within each region is listed below.

Region	Weather stns.	5-*km* grid	Total
1	27	948	975
2	57	1360	1417
3	25	898	923
4	41	1504	1545
5	52	3181	3233
6	49	2525	2574

Longitude and latitude coordinates for each elevation point were transformed to UTM coordinates using the subroutine GSCUTM. Later, these UTM coordinates were subtracted from those of the arbitrary ref-

erence point located at 125.00° W longitude and 42.00° N latitude. In this manner, easting and northing distances (*km*) to that reference point were available for each elevation point.

Contour maps of elevation were developed for regions 2, 4, 5 and 6 (Figure 5) using the commercial package SURFER v. 4.0. The mapping scale was 1:2,700,000. The chosen interval width was 200 *m* as a compromise between constraints of that mapping scale and map accuracy. The main features of elevation within those climatic regions can be observed in those maps. In region 2, note the main floor of the Willamette Valley in the West and the Cascade Mountains ranging from North to South in the East. In region 4, a gradual increase in elevation is observed from the Columbia River to the Blue Mountains. In region 5, the central plateau and a series of ridges in the South can be noticed. In region 6, the main features of elevation are the Wallowa Mountains in the North and the Eastern side of the Blue Mountains in the West.

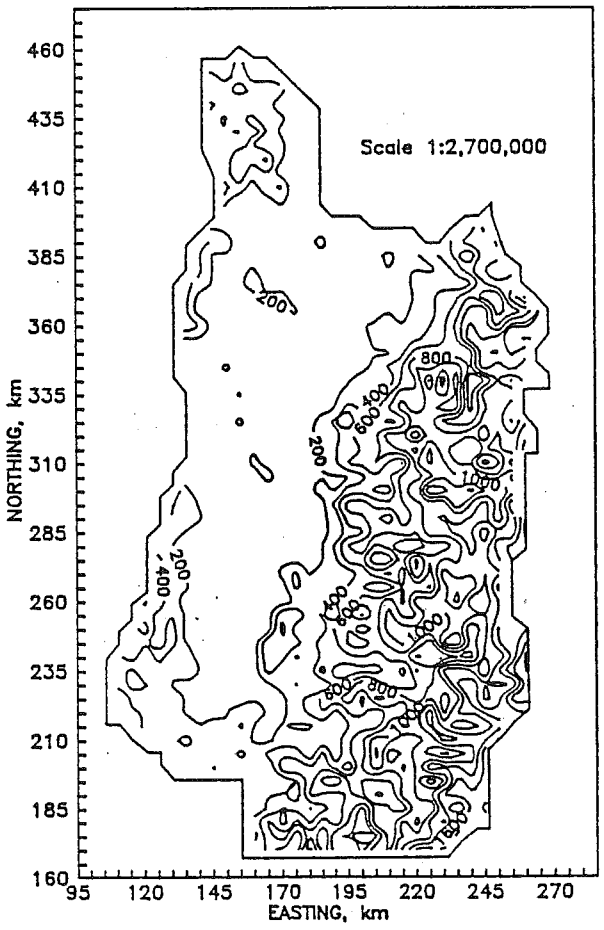

FIGURE 5. Contour maps of elevation, *m*, for Oregon. Region 2.

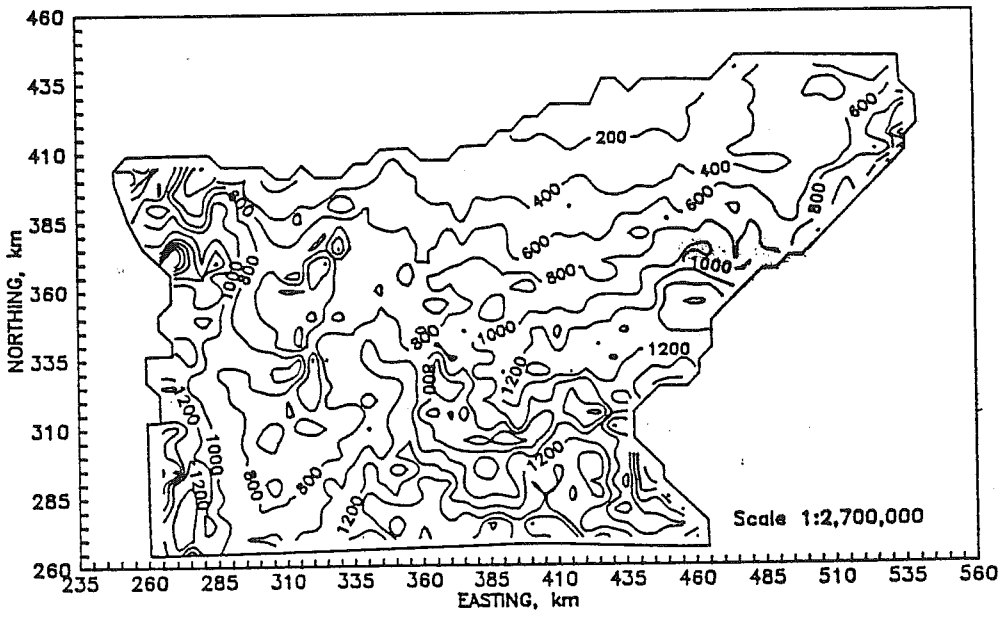

FIGURE 5. (continued). Region 4.

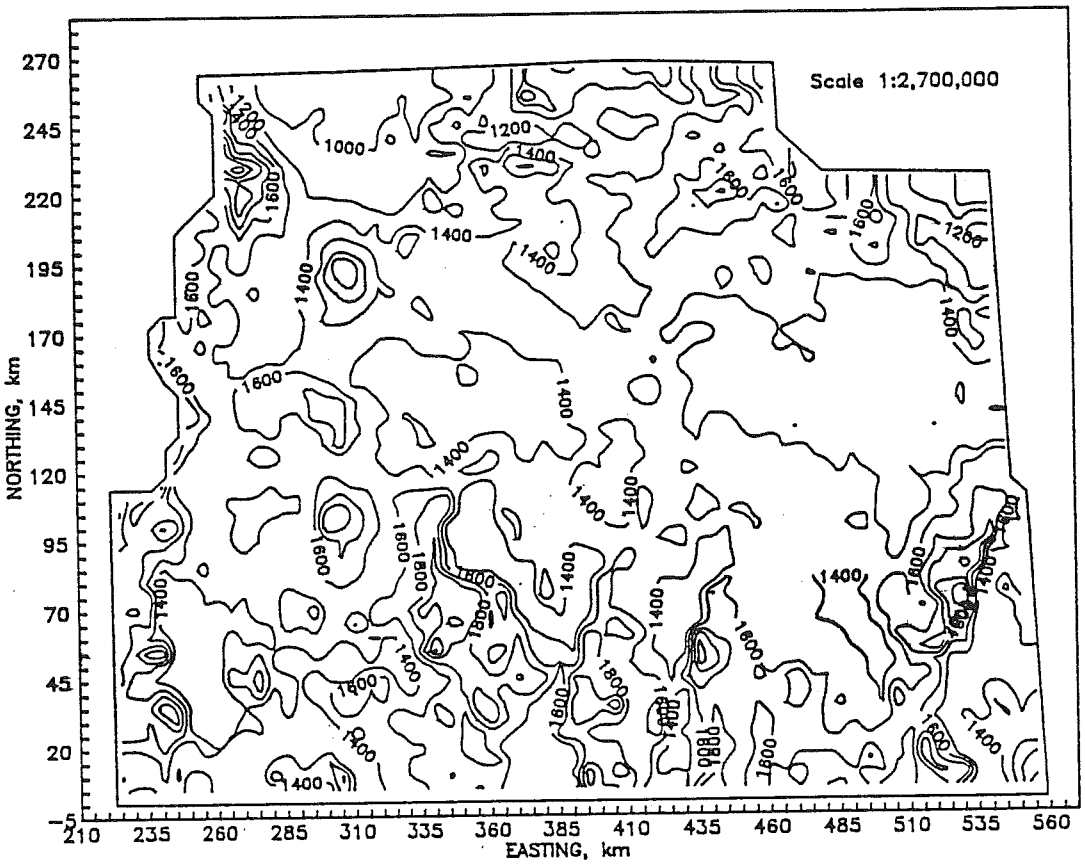

FIGURE 5. (continued). Region 5.

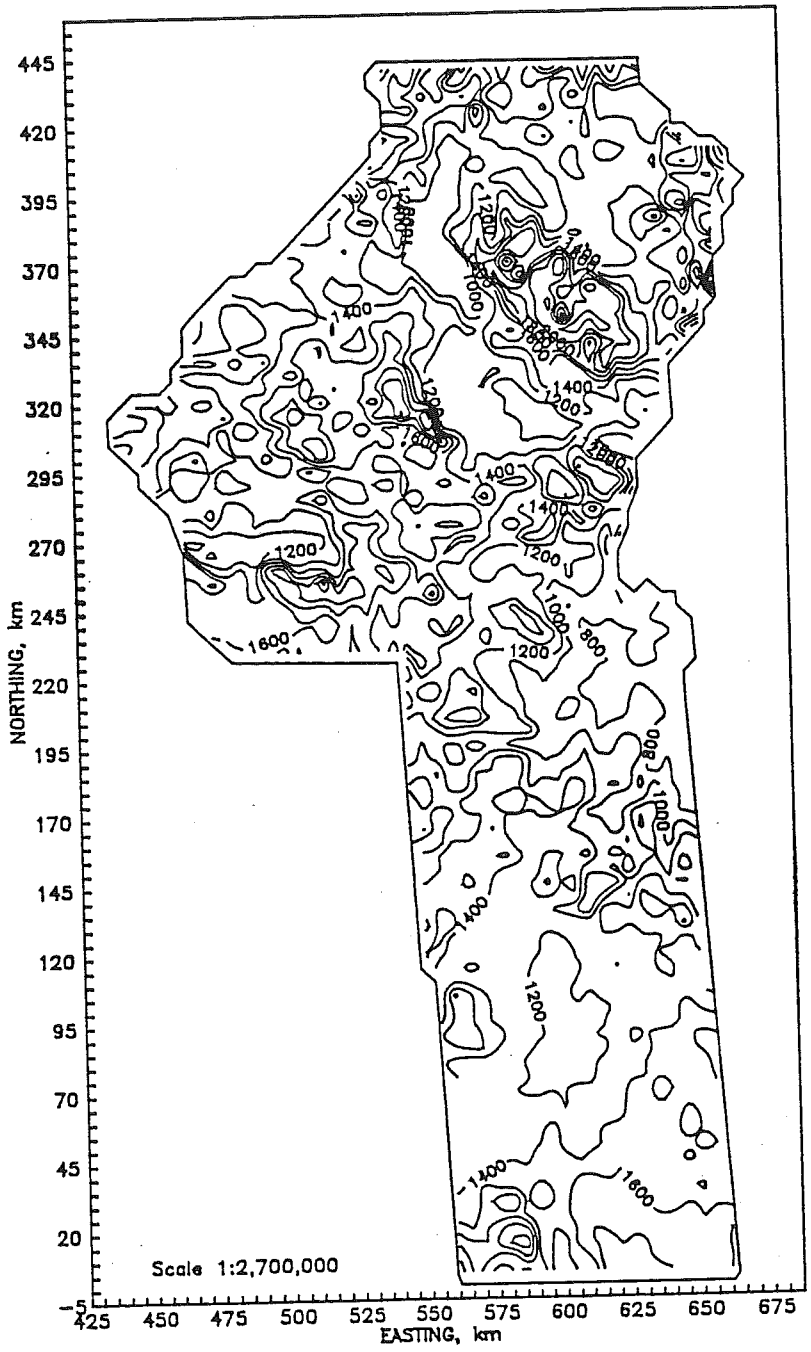

FIGURE 5. (continued). Region 6.

3.4 Geostatistical analysis

The geostatistical analysis performed in this work involved several steps. First a brief outline of these steps is provided. Next these steps are described in detail.

3.4.1 Outline of geostatistical analysis

In this project, each combination of region and month constituted a study case. For each of the cases, the geostatistical analysis performed involved several steps which are described below.

1. Preliminary analysis of the data sets. Some classical statistics were computed for both data sets, ET_r and elevation. Section 3.4.2 describes this step.
2. Semivariogram modeling. Three experimental semivariograms were computed for each case: direct-semivariogram for ET_r, direct-semivariogram for elevation and cross-semivariogram. These experimental semivariograms were plotted against distance and model semivariograms were fit. Semivariogram modeling is discussed in section 3.4.3.
3. Cross-validation. The fit models were tested using the procedure described in section 2.3.5.3. Section 3.4.4 deals with this cross-validation procedure.
4. Kriging and cokriging. The interpolation techniques of kriging and cokriging were used in conjunction with the previously fit semivariogram models to estimate ET_r at locations

where it is unknown. Kriging and cokriging standard deviations were computed at each of those locations. Kriging and cokriging results are compared for each case study. This step is described in section 3.4.5.

5. Mapping of ET_r and errors. Contour maps of cokriged ET_r estimates and cokriging standard deviations were performed. Section 3.4.6 discusses this last step.

3.4.2 Preliminary analysis

In this preliminary analysis and in the following geostatistical analysis, units for elevation were *dam* (decameters) and units for cumulative ET_r were *mm (100)*$^{-1}$. These units were chosen to avoid dealing with large numbers in the computations performed.

Several classical statistics were computed for the values of monthly and cumulative ET_r and elevation. These statistics included sample maxima, minima, averages, variances and coefficients of variation. Computation of these statistics provided the opportunity to get acquainted with the data set and anticipate some possible problems in the geostatistical analysis.

One of the assumptions of the geostatistical theory presented in section 2.3 is the normality of the distributions of the sample data values. To check this assumption normal, probability plots were computed for each case for both variables. A normal probability plot is a cumulative frequency plot scaled so that a normal distribution plots as a straight line (Devore and Peck, 1986).

Likewise, sample covariances and correlation coefficients between the values of ET_r and elevation of the station sites were computed for each case. Under the second-order stationary hypothesis, a sample covariance is equal to the value of the cross-covariance function (equation [16], section 2.3.3) at distance 0. As pointed out in section 2.3, the gain in accuracy due to cokriging depends, among other factors, upon the degree of correlation between the two variables involved (Ahmed and De Marsily, 1987; Hoeksema *et al.*, 1989). The statistical significance of the respective sample correlation coefficients was tested using a *t*-test (Neter *et al.*, 1983). In this test, the following null hypothesis, H_o , is tested against an alternative hypothesis, H_a

$$H_o: \quad \rho_{kk'} = 0 \qquad [55]$$

$$H_a: \quad \rho_{kk'} \neq 0$$

where $\rho_{kk'}$ = point to point correlation coefficient between two RF's, as defined in equation [23] (section 2.3.4), and estimated by the sample correlation coefficient, $r_{kk'}$.

In the test, the following statistic, t^*, is computed (Nester *et al.*, 1983).

$$t^* = \frac{r_{kk'}\sqrt{n-2}}{\sqrt{1-r_{kk'}^2}} \qquad [56]$$

where n = sample size.

This statistic is checked against the value of the t distribution (Neter *et al.*, 1983) with $n-2$ degrees of freedom and $1-\alpha/2$ probability level, where α is the significance level (usually taken as 0.05). If t^* is less than or equal to the t value, the null hypothesis is not rejected, otherwise the alternative hypothesis is accepted.

After this preliminary analysis of the data sets, regions 1 and 3 were excluded from further analysis. Section 4.1 explains the reasons for this decision. These preliminary analyses also motivated the exclusion of January and December in all regions. Therefore, the geostatistical analysis described in the next sections was performed for a total of 44 study cases, 11 cases per each one of the regions (2, 4, 5 and 6) remaining in the study. These 11 cases included the months of February to November and the cumulative ET_r case.

3.4.3 Semivariogram modeling

For each of the 44 study cases analyzed in this project, it was required to model a direct-semivariogram for ET_r, a direct-semivariogram for elevation, and a cross-semivariogram. For the 11 cases studied within a single region, the same model of direct-semivariogram for elevation was used. Therefore, a total of 44 direct-semivariograms for ET_r, 4 direct-semivariograms for elevation, and 44 cross-semivariograms were modeled.

The first step to model semivariograms was the computation of experimental semivariograms. The experimental direct-semivariogram values for both ET_r and elevation were computed using equation [24]. The experimental cross-semivariogram values were computed using equation [25]. Experimental direct-semivariograms for ET_r were computed using the local ET_r values available at the weather stations. Experimental direct-semivariograms for elevation were computed using the values of elevation available at the weather stations and the 5-*km* grid. Experimental cross-semivariograms were computed using the values of ET_r and elevation available at the weather stations.

The relatively small sample size for ET_r within each region precluded the computation of anisotropic experimental direct-semivariograms for ET_r and experimental cross-semivariograms unless very wide angle and distance classes were used. A loss of directional resolution could result from this situation. Therefore, isotropy was assumed and isotropic experimental direct-semivariograms for ET_r and cross-semivariograms were computed.

Likewise, the ET_r values were not aligned in a regular manner. Therefore, it was necessary to group these data into several distance intervals (Journel and Huijbregts, 1978). Three factors (Journel and Huijbregts, 1978; Clark, 1979) were considered to select an appropriate distance interval width for each experimental direct-semivariogram for ET_r and experimental cross-semivariogram. These factors were: 1) experimental semivariogram values, in general, are not valid for distances greater than half the maximum distance between sample pairs; 2) each experimental semivariogram value should be computed using at least 30 to 50 sample pairs in order to be statistically reliable; and 3) the higher the number of points in the semivariogram graph, the easier it is to characterize the underlying shape of the theoretical semivariogram function. Based on these factors, experimental semivariogram values were computed for 20, 15, 15 and 20 different distance intervals for regions 2, 4, 5 and 6, respectively up to a distance equal to one-half the maximum distance between sample pairs within each region.

The experimental direct-semivariograms for ET_r were computed using the package Geo-EAS, a geostatistical software developed by the Environmental Protection Agency (EPA), in cooperation with the Applied Earth Sciences Department at Stanford University and the Computer Sciences Corporation (Englund and Sparks, 1988). This package is a collection of interactive software tools for performing univariate two-dimensional geostatistical analyses of regionalized variables. The experimental cross-semivariograms were computed using the program VARIO

(Cooper *et al.*, 1988). This program is part of the Geostatistical Analysis Package (GAP), which is being developed by the Civil Engineering Department at Oregon State University and the Water Resources Division of the U.S. Geological Survey at Mercury, Nevada. The GAP package allows uni-, two-, and three-dimensional geostatistical analysis of one or more regionalized variables.

In the case of experimental direct-semivariograms for elevation, the large sample size allowed the computation of valid anisotropic semivariograms. For each region, five possible directions were considered: no direction (isotropic case), 0° (E-W direction), 45° (NE-SW direction), 90° (N-S direction), and 135° (NW-SE direction). For each of these directions, a tolerance angle of 22.5° was used, except for the isotropic case (180° tolerance angle). Because most of the sample values of elevation were aligned in a regular grid of about 5 *km*, this value was taken as the width of the distance intervals. Experimental semivariogram values were computed up to a distance approximately equal to one-half the maximum distance between sample pairs within each region.

The large sample sizes for elevation prevented the use of the two geostatistical packages mentioned previously to compute experimental semivariograms. For this reason, the Water Resources Engineering Team of the Agricultural Engineering Department at Oregon State University developed its own subroutine, VARIOWRT, in Quick BASIC v. 4.5. This subroutine was written to analyze the specific elevation data set and it has not yet been tested for any other data sets. The source code of this subroutine is listed in Appendix E.

Once the experimental semivariograms were computed, theoretical models were fit visually. The shape of the experimental semivariograms was checked against the models described in section 2.3.5.2. The appropriate model was selected based on that shape and the parameters of the model were estimated visually. In general, for a given semivariogram the corresponding sample variance (or covariance in the case of cross-semivariograms) was used as initial guess of the sum of

the nugget effect and the sill (or sills if nested structures were selected) of the model (Clark, 1979). A cross-validation procedure (sections 2.3.5.3 and 3.4.4) was performed to check the validity of the model. The estimated parameters of the model were then modified in a "trial-and-error" procedure until adequate cross-validation statistics were obtained. In the case of cross-semivariograms, PDC curves (equation [30], section 2.3.5.2) were also required to check the positive definite condition of the models. PDC curves were computed using the cross-validated models for direct-semivariograms of ET_r and elevation.

3.4.4 Cross-validation

Cross-validation is a technique used to test the validity of the parameters of the model semivariogram fit to the experimental values. In this technique, a sample is deleted from the data set of one ReV and kriging or cokriging are used to estimate the value of that ReV at the location of the deleted sample. This estimation is done using the remaining samples and the selected semivariogram model and parameters. Differences between estimated and measured values are summarized using the cross-validation statistics described in section 2.3.5.3.

Those cross-validation statistics must meet several criteria in order to accept a particular semivariogram model as adequate. The cross-validation criteria for the direct-semivariograms for ET_r and the cross-semivariograms are listed in Table 4. The cross-validation criteria for the direct-semivariograms for elevation are listed in Table 5. In the case of the cross-semivariograms, it was also required to check the positive definiteness of the models. For this, PDC curves (equation [30], section 2.3.5.2) were computed in each case using the

direct-semivariogram models for ET_r and elevation. The values and slopes of the cross-semivariogram models were compared with the values and slopes of these PDC curves as indicated in section 2.3.5.2.

TABLE 4. Cross-validation criteria for the direct-semivariograms for ET_r and the cross-semivariograms.

Region	*n*	*AKE*	*MSE*[1]	*SMSE*
2	57	0	$MSE < s^2_{sp}$	1 ± 0.3746
4	41	0	$MSE < s^2_{sp}$	1 ± 0.4417
5	52	0	$MSE < s^2_{sp}$	1 ± 0.3922
6	49	0	$MSE < s^2_{sp}$	1 ± 0.4041

[1] s^2_{sp} represents the sample variance of ET_r values for each of the 44 study cases.

TABLE 5. Cross-validation criteria for the direct-semivariograms for elevation.

Region	*n*	*AKE*	*MSE*[1]	*SMSE*
2	1417	0	$MSE < 2200.37$	1 ± 0.0751
4	1545	0	$MSE < 1482.78$	1 ± 0.0720
5	3233	0	$MSE < 525.37$	1 ± 0.0497
6	2574	0	$MSE < 1057.75$	1 ± 0.0557

[1] Values given in this column correspond to the sample variances (dam^2) of elevation in each of the four regions under study.

In any local estimation technique, such as kriging and cokriging, an important consideration is the choice of a search strategy. This search strategy can be defined during the cross-validation step. The search

strategy controls the sample points that are included in the estimation procedure. Two reasons exist to limit the size of the search neighborhood in practice (Isaaks and Srivastava, 1989). First, the amount of computations required to solve for the ordinary kriging and cokriging weights (section 2.3.6) is proportional to the cube of the number of sample points retained. If this number is doubled, the number of calculations is increased eight fold. Second, the aptness of a stationary random function model becomes more questionable as the distance between the sample points and the point being estimated increases. Unfortunately, there is not yet a definite rule applicable to all situations (Burguess and Webster, 1980; Vieira *et al.*, 1983) and common sense combined with a great deal of arbitrariness is usually involved in selecting the size of the search neighborhood.

Likewise, some sample points may cluster in certain directions around the point being estimated. This clustering may have adverse effects on the estimation results. These effects may be reduced if the search neighborhood is divided into quadrants and the number of sample points is limited in each quadrant (Isaaks and Srivastava, 1989). This study adhered to this quadrant search neighborhood approach. In a previous study on the application of geostatistics to estimate ET_r, Cuenca and Amegee (1987) suggested that eight was an optimum search neighborhood size. A closer look to the spatial configuration of the sample points for ET_r within each region showed that a search neighborhood including a maximum of 16 sample points could ensure most of the estimates be computed using a minimum of eight sample values. Consequently, a quadrant search neighborhood approach with a maximum of four sample points per quadrant was used during the cross-validation of direct-semivariogram models for ET_r. A search neighborhood radius equal to the semivariogram range of the model being cross-validated was also defined. In this way, sample points located at a larger distance from the point being estimated than the range were not included in the estimation.

In the case of elevation, the number of sample points within the search neighborhood became more critical. Preliminary cross-validation tests in region 2 showed that a maximum of 16 sample points per quadrant search would be appropriate. It was assumed that this search strategy could be applied in the other three regions analyzed (4, 5 and 6) since the sample density of the elevation data was similar in the four regions. In the case of cross-semivariograms, it was necessary to define two search strategies, one for each of the two variables. The search strategies previously described were used.

The cross-validation for the direct-semivariograms for ET_r was performed using the Geo-EAS package. The cross-validation for the direct-semivariograms for elevation and the cross-semivariograms was carried out with the aid of the subroutine XVAL-6 included in the GAP package.

3.4.5 Kriging and cokriging

Once the different semivariogram models were cross-validated, they were used to estimate values of ET_r by applying the kriging and cokriging interpolation techniques described in section 2.3.6. In all 44 study cases, both kriging and cokriging estimates were computed at a grid interval of about 5 *km*, at exactly the same points where elevation values were available. The search strategies used are described in the previous section. Kriging and cokriging variances were determined for each estimation point as indicated in section 2.3.6 and the square roots of these variances computed. Maxima, minima and averages for the corresponding kriging and cokriging standard deviations were determined and compared for each case. Kriging and cokriging computations were performed using the program COKRIG6 included in the GAP package.

3.4.6 Mapping of ET_r estimates and errors

The last step performed in this project was the mapping of ET_r estimates and standard deviations of the estimation errors. The commercial computer program SURFER v. 4.0 was used. Two groups of maps were made.

First, maps of kriged and cokriged cumulative ET_r estimates and kriging and cokriging standard deviations of cumulative ET_r were produced for each of the four regions analyzed at a scale of 1:2,700,000. These maps allowed a graphical comparison of kriging and cokriging. Cumulative ET_r was selected for this comparison because of the higher signal-to-noise ratio of this variable compared with monthly ET_r values. Second, maps of cokriged monthly ET_r estimates for all months and maps of cokriging standard deviations for the months of July and October were produced at the same scale as the first group of maps. Maps of cokriging standard deviations for July and October allowed the comparison of the errors obtained in a warm and a cold month with those obtained for the whole year (cumulative ET_r). The geographic coordinates of these maps were the easting and northing distances (km) to an arbitrary reference point located at 125.00° W longitude and 42.00° N latitude.

The contour interval widths of the cumulative and monthly ET_r maps were selected according two criteria: 1) the chosen interval width was higher than the corresponding average kriging or cokriging standard deviations; and 2) a number of about 10 to 12 contour intervals was considered the maximum possible under the constraints imposed by the selected mapping scale. This second criteria was used to select appropriate contour interval widths for the maps of kriging and cokriging standard deviations.

4 RESULTS AND DISCUSSION

This section discusses the results of the geostatistical analysis performed in this project. The first section presents the preliminary analysis results. The second section deals with the semivariogram modeling. The third and last section presents the kriged and cokriged estimates of ET_r and the errors associated with those estimates.

4.1 Preliminary analysis

Table 6 shows the sample maximum, minimum, mean, variance and coefficient of variation values for ET_r for the six climatic regions of Oregon. Note that most of the values of ET_r for the months of January and December were zero, particularly in the three regions east of the Cascades. This situation lead to the exclusion of these two months from the geostatistical analysis.

TABLE 6. Statistics for monthly and cumulative ET_r sample values. Region 1 (sample size = 27).

Month	Minimum[1] *mm d^{-1}*	Maximum[1] *mm d^{-1}*	Mean[1] *mm d^{-1}*	Variance[2] *mm^2 d^{-2}*	Coefficient of variation *%*
January	0.21	0.57	0.41	0.009	23.75
February	0.65	0.92	0.79	0.003	7.44
March	1.28	1.58	1.44	0.006	5.24
April	2.21	2.70	2.42	0.015	5.10
May	2.77	3.62	3.21	0.045	6.62
June	3.09	4.08	3.53	0.048	6.23
July	3.06	4.40	3.68	0.077	7.55
August	2.60	3.72	3.11	0.056	7.60
September	2.36	3.17	2.74	0.028	6.06
October	1.70	2.05	1.90	0.011	5.50
November	0.56	0.88	0.73	0.006	10.46
December	0.20	0.53	0.37	0.006	21.53
Cumulative	6.66	8.31	7.42	0.117	4.60

[1] For cumulative ET_r, *mm (100)$^{-1}$* [2] For cumulative ET_r, *mm^2 (100)$^{-2}$*

TABLE 6. (continued). Region 2 (sample size = 57).

Month	Minimum[1] *mm d^{-1}*	Maximum[1] *mm d^{-1}*	Mean[1] *mm d^{-1}*	Variance[2] *mm^2 d^{-2}*	Coefficient of variation *%*
January	0.00	0.43	0.23	0.008	39.24
February	0.14	1.12	0.77	0.027	21.58
March	0.58	2.03	1.52	0.070	17.42
April	1.41	3.46	2.84	0.137	13.04
May	2.44	4.66	3.92	0.158	10.16
June	3.40	5.14	4.66	0.117	7.34
July	4.33	6.11	5.28	0.134	6.94
August	3.40	5.07	4.46	0.104	7.23
September	2.38	3.83	3.46	0.073	7.79
October	1.24	2.37	2.04	0.036	9.22
November	0.10	0.82	0.59	0.014	20.26
December	0.00	0.39	0.18	0.007	47.01
Cumulative	5.94	10.53	9.14	0.681	9.03

[1] For cumulative ET_r , *mm (100)$^{-1}$* [2] For cumulative ET_r , *mm^2 (100)$^{-2}$*

TABLE 6. (continued). Region 3 (sample size = 25).

Month	Minimum[1] *mm d^{-1}*	Maximum[1] *mm d^{-1}*	Mean[1] *mm d^{-1}*	Variance[2] *mm^2 d^{-2}*	Coefficient of variation *%*
January	0.00	0.41	0.23	0.014	51.29
February	0.25	1.04	0.80	0.051	28.42
March	0.80	1.95	1.50	0.113	22.44
April	1.92	3.82	2.98	0.321	19.03
May	3.08	5.19	4.18	0.418	15.46
June	4.04	6.34	5.15	0.500	13.72
July	5.10	7.19	6.14	0.399	10.30
August	4.23	6.09	5.13	0.328	11.17
September	2.98	4.48	3.88	0.157	10.21
October	1.79	2.81	2.32	0.071	11.51
November	0.23	0.80	0.61	0.021	23.86
December	0.00	0.29	0.14	0.007	62.21
Cumulative	7.64	12.07	10.10	1.735	13.05

[1] For cumulative ET_r, *mm (100)$^{-1}$* [2] For cumulative ET_r, *mm^2 (100)$^{-2}$*

TABLE 6. (continued). Region 4 (sample size = 41).

Month	Minimum[1] *mm d^{-1}*	Maximum[1] *mm d^{-1}*	Mean[1] *mm d^{-1}*	Variance[2] *mm^2 d^{-2}*	Coefficient of variation *%*
January	0.00	0.21	0.02	0.002	192.40
February	0.00	0.94	0.60	0.024	26.17
March	0.58	2.17	1.55	0.069	16.93
April	1.81	4.38	3.24	0.213	14.23
May	3.07	6.22	4.59	0.356	13.01
June	3.65	7.28	5.50	0.406	11.59
July	5.32	7.92	6.46	0.373	9.45
August	4.51	7.21	5.38	0.365	11.22
September	3.19	4.72	3.88	0.146	9.84
October	1.39	2.79	2.27	0.059	10.73
November	0.12	0.78	0.51	0.014	22.69
December	0.00	0.16	0.03	0.002	128.58
Cumulative	7.26	13.51	10.40	1.328	11.08

[1] For cumulative ET_r, *mm (100)$^{-1}$* [2] For cumulative ET_r, *mm^2 (100)$^{-2}$*

TABLE 6. (continued). Region 5 (sample size = 52).

Month	Minimum[1] *mm d^{-1}*	Maximum[1] *mm d^{-1}*	Mean[1] *mm d^{-1}*	Variance[2] *mm^2 d^{-2}*	Coefficient of variation *%*
January	0.00	0.12	0.01	0.001	288.89
February	0.00	0.76	0.40	0.027	40.80
March	0.49	1.50	1.12	0.043	18.40
April	1.47	3.11	2.46	0.107	13.33
May	2.49	4.29	3.66	0.127	9.74
June	3.50	5.30	4.61	0.138	8.06
July	4.75	6.32	5.49	0.166	7.43
August	3.68	5.12	4.41	0.131	8.21
September	2.78	4.00	3.29	0.094	9.28
October	1.61	2.47	2.09	0.049	10.61
November	0.22	0.72	0.44	0.012	25.23
December	0.00	0.15	0.01	0.001	374.15
Cumulative	6.57	10.14	8.56	0.639	9.34

[1] For cumulative ET_r, *mm (100)$^{-1}$* [2] For cumulative ET_r, *mm^2 (100)$^{-2}$*

TABLE 6. (continued). Region 6 (sample size = 49).

Month	Minimum[1] *mm d^{-1}*	Maximum[1] *mm d^{-1}*	Mean[1] *mm d^{-1}*	Variance[2] *mm^2 d^{-2}*	Coefficient of variation *%*
January	0.00	0.00	0.00		
February	0.00	0.68	0.35	0.037	54.72
March	0.46	1.86	1.28	0.111	26.09
April	1.73	4.24	3.00	0.313	18.63
May	3.00	5.64	4.19	0.391	14.93
June	3.83	7.02	5.23	0.590	14.70
July	4.83	7.73	6.29	0.461	10.80
August	3.75	6.11	5.08	0.247	9.77
September	2.59	4.56	3.70	0.180	11.49
October	1.43	3.00	2.22	0.145	17.11
November	0.10	0.75	0.43	0.027	37.95
December	0.00	0.03	0.00	0.000	404.15
Cumulative	6.95	12.28	9.71	1.812	13.86

[1] For cumulative ET_r, *mm (100)$^{-1}$* [2] For cumulative ET_r, *mm^2 (100)$^{-2}$*

Figure 6 shows the normal probability plots for the values of ET_r for August (region 2) and cumulative ET_r (region 5). These normal probability plots are typical examples of the normal probability plots for all cases analyzed in this study. These plots showed an approximate fit to a normal distribution. These results agree with previous research which indicated a normal probability distribution for ET_r (Nixon *et al.*, 1972; Cuenca, 1989). Normal probability plots for region 3, in general, did not support the hypothesis of normality of the distribution. Devore and Peck (1986) commented that with small sample sizes (region 3 has only 25 stations), the sampling variability can be so much that substantial departures from linearity can be observed even when the distribution is normal.

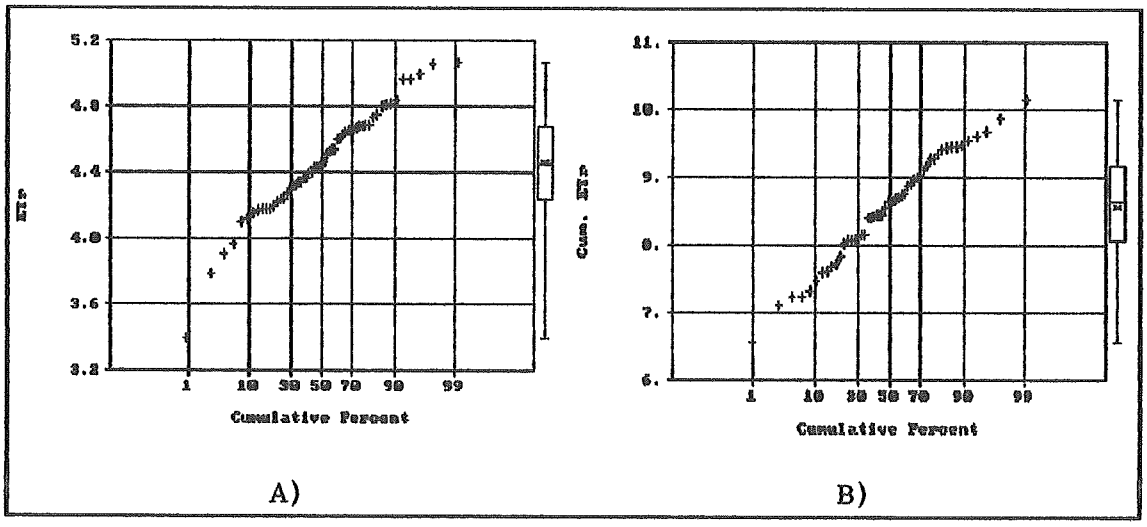

FIGURE 6. Normal probability plots for ET_r. A) August ET_r, *mm* d^{-1}, region 2. B) Cumulative ET_r, *mm* $(100)^{-1}$, region 5.

Table 7 shows the sample statistics for the elevation values at the weather stations and for all elevation values. Figure 7 shows the normal probability plot of elevation data for region 4. The shape of these plots was very similar for all regions. It can be noticed that there is some departure from linearity for low values of elevation. However, there was an overall fit to a normal distribution. Consequently, no transformations of the original sample values of both variables, ET_r and elevation, were performed due to the apparent normality of their respective distributions for all study cases.

TABLE 7. Statistics for weather station elevations and all elevation sample values.

	Region	Sample size	Minimum *dam*	Maximum *dam*	Mean *dam*	Variance dam^2	Coeff. var. %
Station elevation	1	27	0.30	35.40	5.83	71.45	144.99
	2	57	0.60	144.80	23.83	783.34	117.45
	3	25	8.80	141.40	58.95	1630.76	68.50
	4	41	3.00	181.10	56.21	1298.68	64.11
	5	52	86.60	197.50	131.71	390.97	15.01
	6	49	61.00	150.60	99.24	556.38	23.77
All elevations	1	975	0.00	141.10	28.84	562.80	82.26
	2	1417	0.60	210.20	52.70	2200.37	89.01
	3	923	5.70	208.30	77.20	1646.72	52.57
	4	1545	2.20	219.80	80.23	1482.78	48.00
	5	3233	82.70	260.80	148.71	525.37	15.41
	6	2574	43.70	257.00	133.39	1057.75	24.38

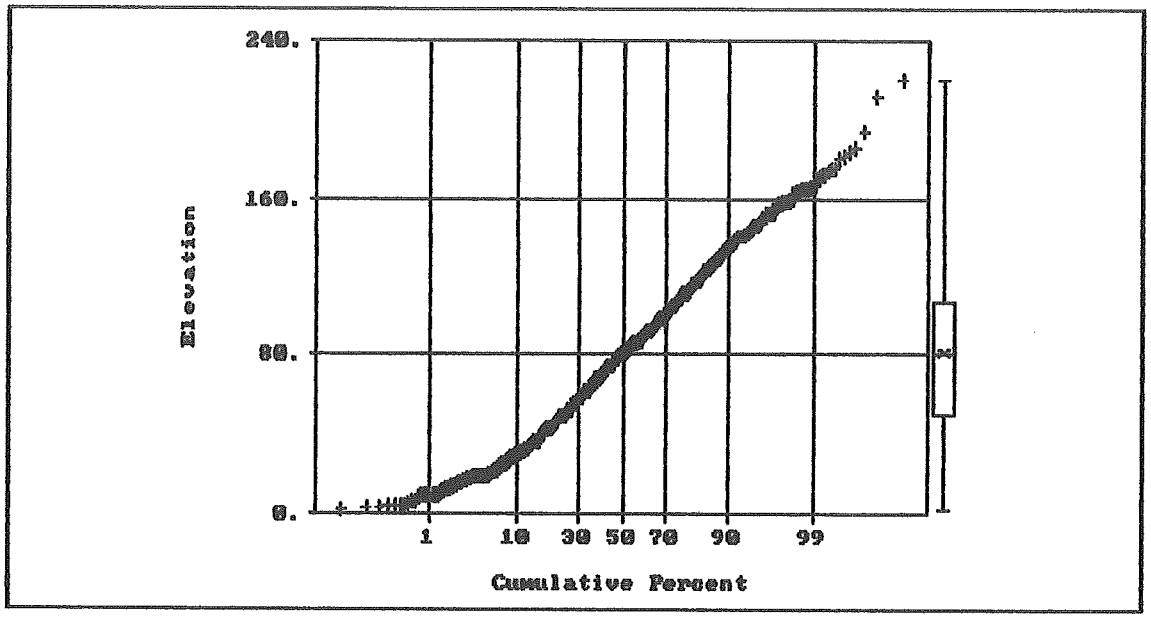

FIGURE 7. Normal probability plot for elevation, *dam*, at region 4.

Table 8 shows the results of the cross-statistics for ET_r and weather station elevation values. This table also indicates whether the respective correlation coefficients were statistically significant. For region 1, in no case were the correlation coefficients significant, with the exception of February. This situation lead to the exclusion of region 1 from further analyses. Two reasons may be presented to explain this situation. First is that most of the weather stations in this region were located at sites with an elevation lower than 50-70 *m*. The second reason is that, in the coastal areas, the influence of maritime conditions is especially important. It has been pointed out that evapotranspiration rates during summertime are greatly reduced by advective cooling from the ocean which is greatly influenced by the distance from the ocean (Nixon *et al.*, 1972).

TABLE 8. Cross-statistics of ET_r and elevation at the weather stations. Regions 1 and 2 (sample sizes are 27 and 57, respectively).

Month	Region 1			Region 2		
	Covar.[1] *dam mm d^{-1}*	Correl. coeff.	Signif.	Covar.[1] *dam mm d^{-1}*	Correl. coeff.	Signif.
January	-0.249	-0.3064	No	-2.009	-0.7924	Yes
February	-0.274	-0.5494	Yes	-4.202	-0.9083	Yes
March	-0.243	-0.3806	No	-6.708	-0.9039	Yes
April	-0.193	-0.1848	No	-9.502	-0.9176	Yes
May	0.026	0.0143	No	-9.873	-0.8863	Yes
June	0.461	0.2483	No	-8.386	-0.8772	Yes
July	0.699	0.2971	No	-6.596	-0.6434	Yes
August	0.435	0.2177	No	-6.974	-0.7725	Yes
September	0.148	0.1055	No	-6.450	-0.8553	Yes
October	-0.027	-0.0304	No	-4.498	-0.8525	Yes
November	-0.228	-0.3514	No	-2.958	-0.8908	Yes
December	-0.243	-0.3639	No	-1.737	-0.7496	Yes
Cumulative	0.104	0.0360	No	-21.269	-0.9207	Yes

[1] For cumulative ET_r, *dam mm (100)$^{-1}$*

TABLE 8. (continued). Regions 3 and 4 (sample sizes are 25 and 41, respectively).

Month	Region 3			Region 4		
	Covar.[1] *dam mm d^{-1}*	Correl. coeff.	Signif.	Covar.[1] *dam mm d^{-1}*	Correl. coeff.	Signif.
January	-3.978	-0.8425	Yes	-0.093	-0.0601	No
February	-7.933	-0.8683	Yes	-3.204	-0.5707	Yes
March	-9.682	-0.7148	Yes	-8.216	-0.8664	Yes
April	-13.136	-0.5737	Yes	-15.578	-0.9369	Yes
May	-11.016	-0.4220	Yes	-19.797	-0.9211	Yes
June	-10.305	-0.3609	No	-20.474	-0.8920	Yes
July	-9.108	-0.3569	No	-17.936	-0.8154	Yes
August	-6.361	-0.2750	No	-16.425	-0.7547	Yes
September	-5.852	-0.3661	No	-11.505	-0.8369	Yes
October	-5.170	-0.4801	Yes	-6.351	-0.7242	Yes
November	-4.665	-0.7890	Yes	-1.761	-0.4188	Yes
December	-2.664	-0.7617	Yes	-0.560	-0.3512	Yes
Cumulative	-27.278	-0.5128	Yes	-37.203	-0.8960	Yes

[1] For cumulative ET_r, *dam mm (100)$^{-1}$*

TABLE 8. (continued). Regions 5 and 6 (sample sizes are 52 and 49, respectively).

Month	Region 5			Region 6		
	Covar.[1] *dam mm d^{-1}*	Correl. coeff.	Signif.	Covar.[1] *dam mm d^{-1}*	Correl. coeff.	Signif.
January	-0.291	-0.5754	Yes	N.A.	N.A.	No
February	-1.906	-0.5860	Yes	-2.600	-0.5746	Yes
March	-2.984	-0.7303	Yes	-5.640	-0.7187	Yes
April	-4.689	-0.7243	Yes	-9.620	-0.7290	Yes
May	-4.652	-0.6602	Yes	-10.536	-0.7141	Yes
June	-4.882	-0.6644	Yes	-11.924	-0.6580	Yes
July	-4.706	-0.5835	Yes	-11.630	-0.7261	Yes
August	-3.746	-0.5229	Yes	-9.028	-0.7708	Yes
September	-2.717	-0.4493	Yes	-6.973	-0.6958	Yes
October	-2.090	-0.4760	Yes	-4.674	-0.5211	Yes
November	-1.145	-0.5233	Yes	-2.051	-0.5288	Yes
December	-0.245	-0.4915	Yes	-0.020	-0.1486	No
Cumulative	-10.366	-0.6559	Yes	-22.774	-0.7173	Yes

[1] For cumulative ET_r, *dam mm (100)$^{-1}$*

In the other five regions, the correlation coefficients between ET_r and elevation were negative which indicate an inverse correlation between both variables. In regions 2, 4, 5 and 6, these correlation coefficients were significant for all cases. The highest correlation coefficients were obtained in region 2.

In region 3, this correlation was not statistically significant for the months of June to September. The correlation for the cumulative ET_r case was significant. However, this correlation was not strong and it was the lowest of all regions. In region 3, an experimental isotropic direct-semivariogram for cumulative ET_r was computed for ten distance intervals up to half the maximum distance between sample pairs. In none of these distance intervals were more than 30 sample pairs available (Table 9). This same situation would have happened for the

monthly ET_r direct-semivariograms and for the cross-semivariograms as the same stations (i.e. same sample points) were used. As discussed in section 2.3.5.1, the less the number of sample pairs used to compute a single experimental semivariogram value, the less reliable this value is (Clark, 1979). Journel and Huijbregts (1978) indicated that a minimum of 30 to 50 sample pairs should be used to compute an experimental semivariogram value. In the previous work of Nuss (1989) on the application of geostatistics to estimate ET_r for various climates in Oregon, he also commented on the difficulty of modeling valid semivariograms within this region due to the lack of enough sample pairs. Difficult modeling of direct-semivariograms for ET_r and cross-semivariograms could be anticipated in addition to a likely lack of improvement in the cokriged estimates due to no significant or poor correlation between ET_r and elevation. Consequently, region 3 was also excluded from further analysis.

TABLE 9. Experimental semivariogram values for cumulative ET_r, region 3.

Interval	Average distance *km*	Number of pairs	Semivariogram values $mm^2\ (100)^{-2}$
1	7.4	8	0.252
2	15.1	12	0.510
3	23.8	17	0.883
4	33.7	20	1.464
5	42.5	25	2.614
6	52.1	28	2.547
7	60.6	23	1.438
8	70.9	27	1.434
9	80.5	18	0.803
10	90.3	19	0.897

4.2 Semivariogram modeling and cross-validation

4.2.1 Direct-semivariograms for ET_r

Appendix F lists the experimental values of the isotropic direct-semivariograms for ET_r for all study cases. Almost all experimental values were computed using a minimum of 30 sample pairs. Note that in all regions the first three points were computed with less than 30 sample pairs. This situation may be the consequence of the average distance between weather stations which is approximately between 25 and 40 *km*.

In general, the experimental isotropic direct-semivariograms for the different regions and months progressively increased with the distance and exhibited a more or less random fluctuation around a constant value beyond a certain distance (Figure 8). Due to the relatively high amount of scatter exhibited by the experimental semivariograms, in general, no obvious theoretical models seemed to fit the sample values in a straightforward manner. At this point, the application of geostatistics becomes somewhat a subjective procedure where the experience, the knowledge and the biases of the modeler are factors to be considered. Fortunately, it has been indicated that the kriging and cokriging variances are robust to most errors likely to be made in semivariogram model selection and parameterization (Brooker, 1986).

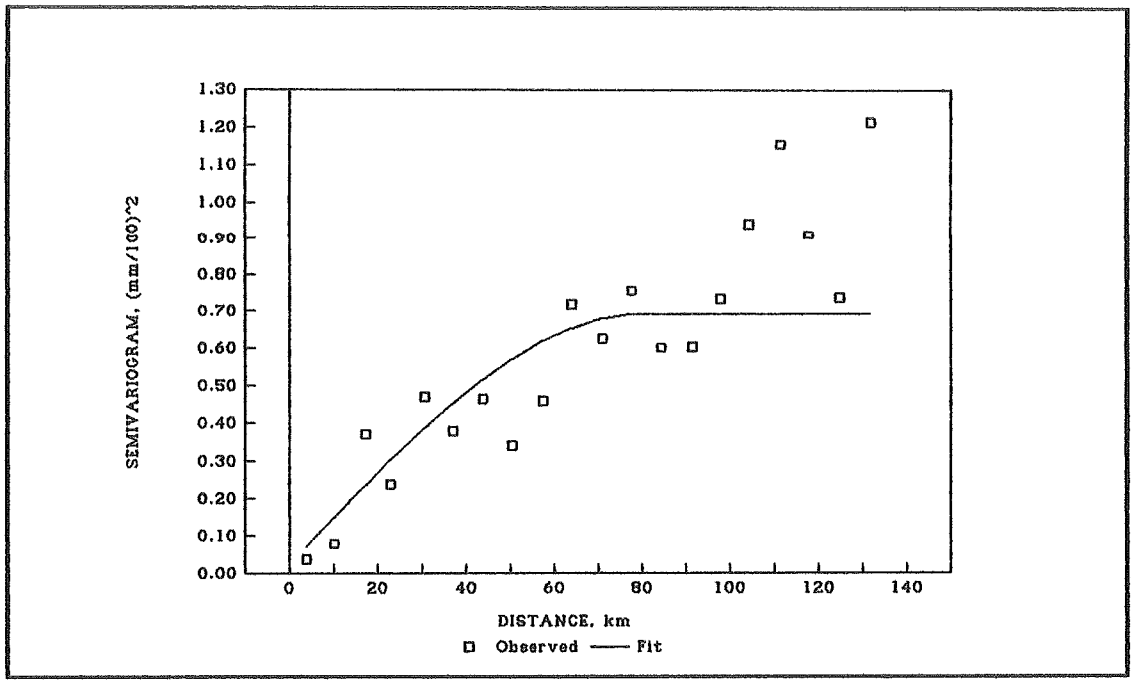

FIGURE 8. Model direct-semivariogram for cumulative ET_r. Region 2.

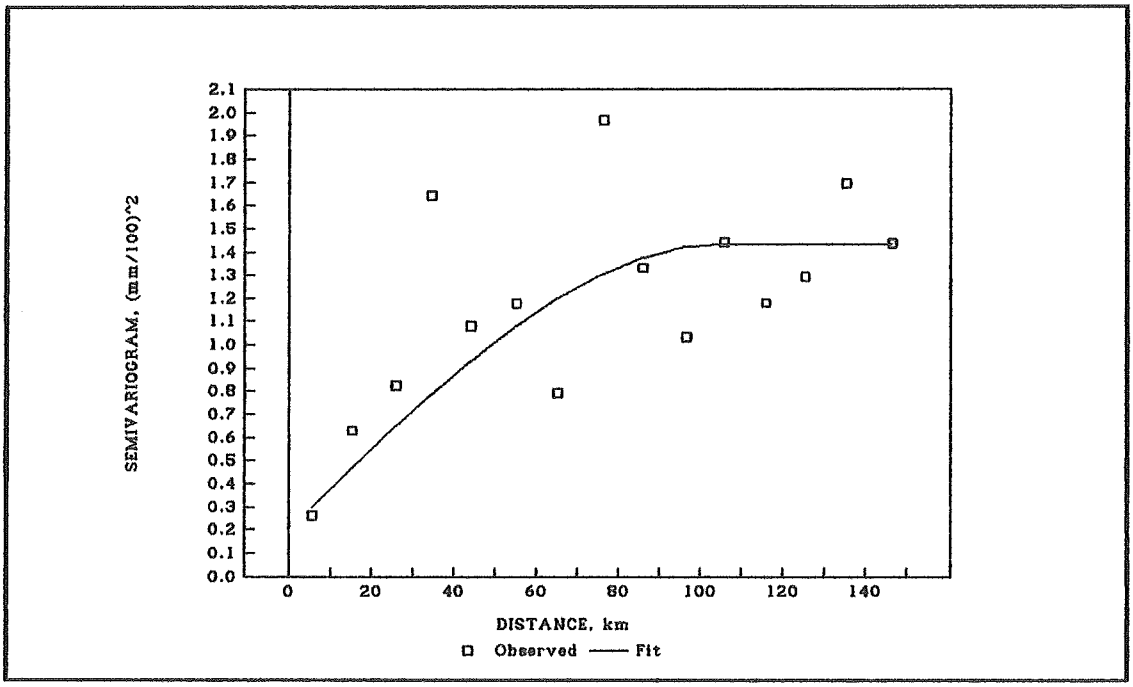

FIGURE 8. (continued). Region 4.

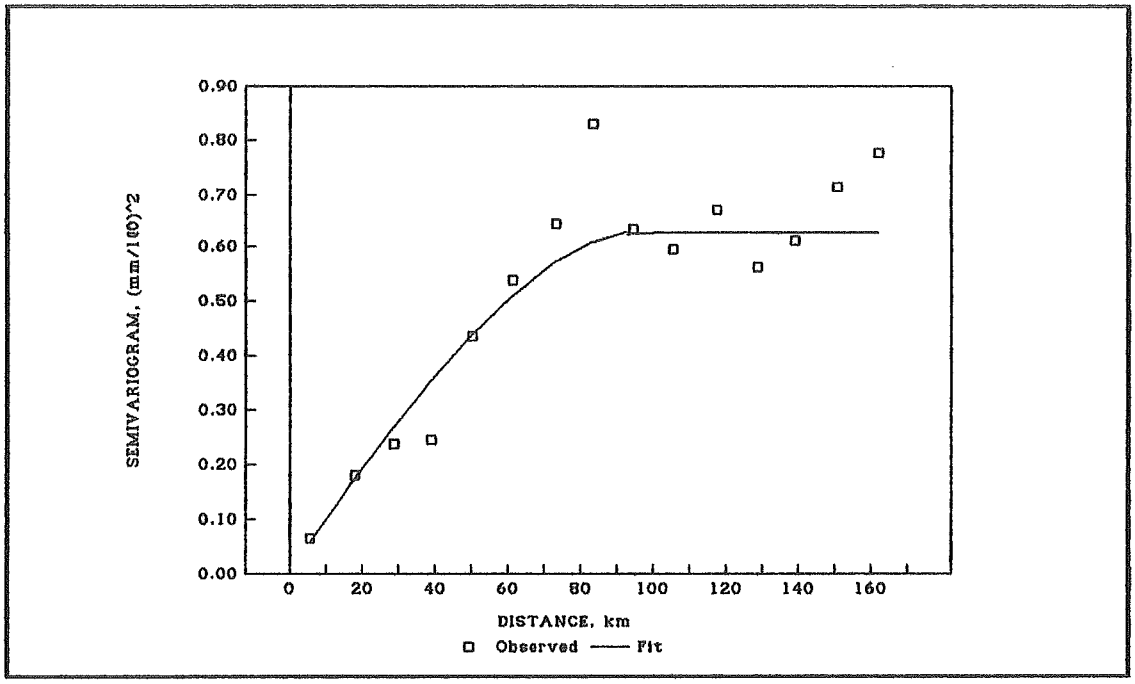

FIGURE 8. (continued). Region 5.

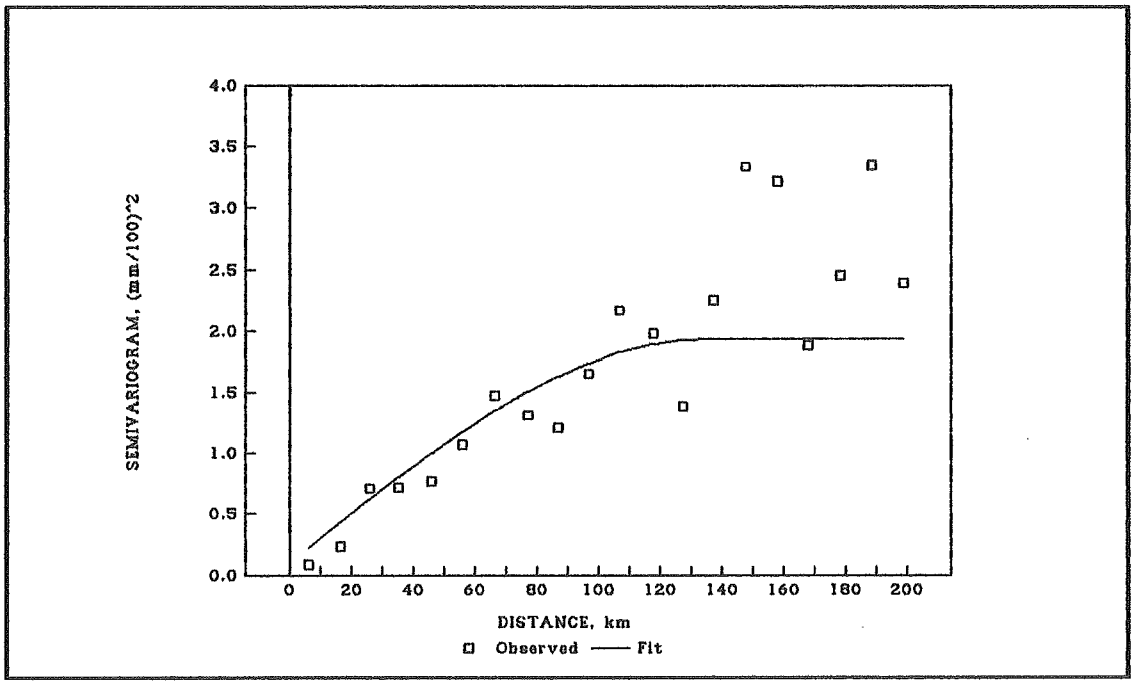

FIGURE 8. (continued). Region 6.

One of the most common semivariogram models used in hydrology (an other disciplines) is the spherical model. This model has been successfully applied to study the spatial variability of ET_r (Cuenca and Amegee, 1987; Nuss, 1989). Therefore, it was decided to use this theoretical model to characterize the spatial variability of ET_r. Cross-validation results (Table 10) indicated the aptness of this model. No nested structures other than nugget effects were evident in the experimental semivariograms.

TABLE 10. Spherical models for direct-semivariograms for ET_r and cross-validation statistics. Region 2.

Month	Nugget[1] $mm^2\ d^{-2}$	Sill[1] $mm^2\ d^{-2}$	Range km	AKE [2] $mm\ d^{-1}$	MSE [1] $mm^2\ d^{-2}$	Samp. var.[1] $mm^2\ d^{-2}$	$SMSE$ [1] $mm^2\ d^{-2}$
February	0.000	0.034	100	0.005	0.008	0.027	0.988
March	0.001	0.077	100	0.004	0.024	0.070	0.972
April	0.005	0.136	80	0.005	0.064	0.137	0.992
May	0.005	0.145	80	0.004	0.070	0.158	0.992
June	0.015	0.109	80	0.002	0.068	0.117	0.976
July	0.015	0.120	85	-0.003	0.065	0.134	0.976
August	0.016	0.089	70	-0.004	0.063	0.104	0.988
September	0.010	0.065	80	0.001	0.041	0.073	0.988
October	0.008	0.028	105	0.003	0.020	0.036	0.984
November	0.001	0.013	115	0.003	0.005	0.014	0.998
Cumulative	0.020	0.670	80	0.007	0.323	0.681	0.988

[1] For cumulative ET_r, $mm^2\ (100)^{-2}$ [2] For cumulative ET_r, $mm\ (100)^{-1}$

TABLE 10. (continued). Region 4.

Month	Nugget[1] $mm^2\ d^{-2}$	Sill[1] $mm^2\ d^{-2}$	Range km	AKE [2] $mm\ d^{-1}$	MSE [1] $mm^2\ d^{-2}$	Samp. var.[1] $mm^2\ d^{-2}$	$SMSE$ [1] $mm^2\ d^{-2}$
February	0.005	0.021	65	-0.003	0.019	0.024	0.990
March	0.007	0.066	75	-0.009	0.048	0.069	1.032
April	0.010	0.205	80	-0.014	0.118	0.213	1.024
May	0.018	0.301	100	-0.011	0.148	0.356	1.022
June	0.065	0.325	95	-0.012	0.217	0.406	0.978
July	0.040	0.334	100	-0.013	0.176	0.373	0.990
August	0.048	0.306	105	-0.009	0.162	0.365	0.914
September	0.025	0.114	100	-0.012	0.073	0.146	0.960
October	0.006	0.053	80	-0.014	0.036	0.059	1.030
November	0.002	0.010	80	-0.007	0.008	0.014	1.030
Cumulative	0.202	1.228	105	-0.022	0.738	1.328	1.012

[1] For cumulative ET_r, $mm^2\ (100)^{-2}$ [2] For cumulative ET_r, $mm\ (100)^{-1}$

TABLE 10. (continued). Region 5.

Month	Nugget[1] $mm^2\ d^{-2}$	Sill[1] $mm^2\ d^{-2}$	Range km	AKE [2] $mm\ d^{-1}$	MSE [1] $mm^2\ d^{-2}$	Samp. var.[1] $mm^2\ d^{-2}$	$SMSE$ [1] $mm^2\ d^{-2}$
February	0.001	0.028	95	-0.002	0.013	0.027	1.000
March	0.001	0.044	90	-0.002	0.024	0.043	1.014
April	0.019	0.088	100	0.000	0.065	0.107	1.008
May	0.010	0.111	100	0.001	0.062	0.127	0.990
June	0.005	0.132	100	-0.005	0.062	0.138	0.962
July	0.008	0.152	105	0.004	0.065	0.166	0.980
August	0.010	0.121	100	0.002	0.059	0.131	1.012
September	0.004	0.088	105	0.004	0.032	0.094	1.010
October	0.001	0.048	115	0.004	0.015	0.049	0.931
November	0.001	0.011	115	0.000	0.006	0.012	1.018
Cumulative	0.007	0.625	100	0.008	0.239	0.638	0.931

[1] For cumulative ET_r, $mm^2\ (100)^{-2}$ [2] For cumulative ET_r, $mm\ (100)^{-1}$

TABLE 10. (continued). Region 6.

Month	Nugget[1] $mm^2\ d^{-2}$	Sill[1] $mm^2\ d^{-2}$	Range km	AKE [2] $mm\ d^{-1}$	MSE [1] $mm^2\ d^{-2}$	Samp. var.[1] $mm^2\ d^{-2}$	$SMSE$ [1] $mm^2\ d^{-2}$
February	0.000	0.037	85	0.013	0.018	0.037	0.984
March	0.009	0.100	115	0.008	0.052	0.111	0.941
April	0.019	0.294	125	0.021	0.119	0.313	0.943
May	0.003	0.405	135	0.018	0.122	0.391	0.925
June	0.000	0.590	160	0.014	0.138	0.590	0.780
July	0.024	0.466	135	0.017	0.176	0.461	0.982
August	0.023	0.257	120	0.014	0.138	0.247	1.111
September	0.038	0.159	130	0.015	0.098	0.180	0.958
October	0.019	0.115	140	0.015	0.059	0.145	0.970
November	0.003	0.023	90	0.011	0.014	0.027	0.962
Cumulative	0.100	1.840	135	0.045	0.704	1.812	0.947

[1] For cumulative ET_r, $mm^2\ (100)^{-2}$ [2] For cumulative ET_r, $mm\ (100)^{-1}$

The nugget effect accounts for the variation of ET_r within the smallest sampling intervals and for the error of "measurement" or estimation of this variable at the sample points. It is known there are errors related to the estimation method used to compute local values of ET_r. As a consequence, it was not surprising there was evidence of nugget effect in most of the experimental semivariograms. However, in some cases a nugget effect equal to zero was assumed based on the cross-validation statistics.

Figure 8 shows the experimental and model semivariograms for cumulative ET_r for the four regions analyzed. Table 10 lists the parameters of the different spherical models fit to the experimental semivariograms and the cross-validation statistics for each of the 44 study cases. All models presented here showed adequate cross-validation statistics (Table 10) meeting the criteria outlined in Table 4. These cross-validation statistics results were used as the main criteria to accept a particular model as adequate.

Note that the nugget effect, in general, is higher for the warmer months of the year. However, this result may be artificial due to the fact that the relative magnitude of the ET_r values during those months is higher than during winter months. In general, the nugget effects shown in Table 10 are lower than those reported by Nuss (1989) in a previous study of the application of geostatistics on evapotranspiration analyses. He performed the study for similar climatic regions in Oregon, using three-year averages of local ET_r. This factor possibly lead to higher "measurement" errors in the sample values of ET_r and, therefore, to higher nugget effects.

The ranges of the semivariogram models also show some variation during the year (Table 10). For region 2, the ranges are smaller for the warmer months. In regions 4 and 6, the ranges are larger in the winter months. In region 5 the relative variation in range is smaller than in the other three regions, although the warmer months show slightly larger ranges. In the case of the cumulative ET_r, the ranges are similar to those for the warmer months. Recall that ET_r rates during the warmer months are the highest and have the greatest influence on the cumulative ET_r rates. Ranges of regions 2, 4 and 5 are, in general, relatively similar while region 6 shows higher range values. Ranges shown in Table 10 are, in general, similar to those from Nuss (1989) with the exception of region 2 in which ranges are higher.

4.2.2 Direct-semivariograms for elevation

Appendix G lists the experimental values of the isotropic direct-semivariograms for elevation. In region 5, some of the experimental values were computed using more than 100,000 sample pairs. In regions 2

and 4, the number of sample pairs use to compute the experimental values was lower than in regions 5 and 6. Still, more than 20,000 sample pairs were used for most of the experimental values. Figure 9 shows the experimental semivariograms for elevation computed for several directions for region 4. Anisotropy is evident. This phenomenon was also noticed in the other three regions, 2, 5 and 6, under study. The direction of the maximum spatial variability changed from region to region. Thus, for example, in region 2 the direction of maximum variability was W-E with N-S as the direction of minimum spatial variability. In the W-E direction, the elevation changes from the altitude of the Coastal Range down to the Valley floor and up again to the elevations of the Cascade Range (Figure 5). In region 4, however, the maximum spatial variability occurred in the N-S direction and the minimum in the W-E direction. In this region going N-S, the elevation changes from the elevation of the Columbia Gorge to the Blue Mountains (Figure 5).

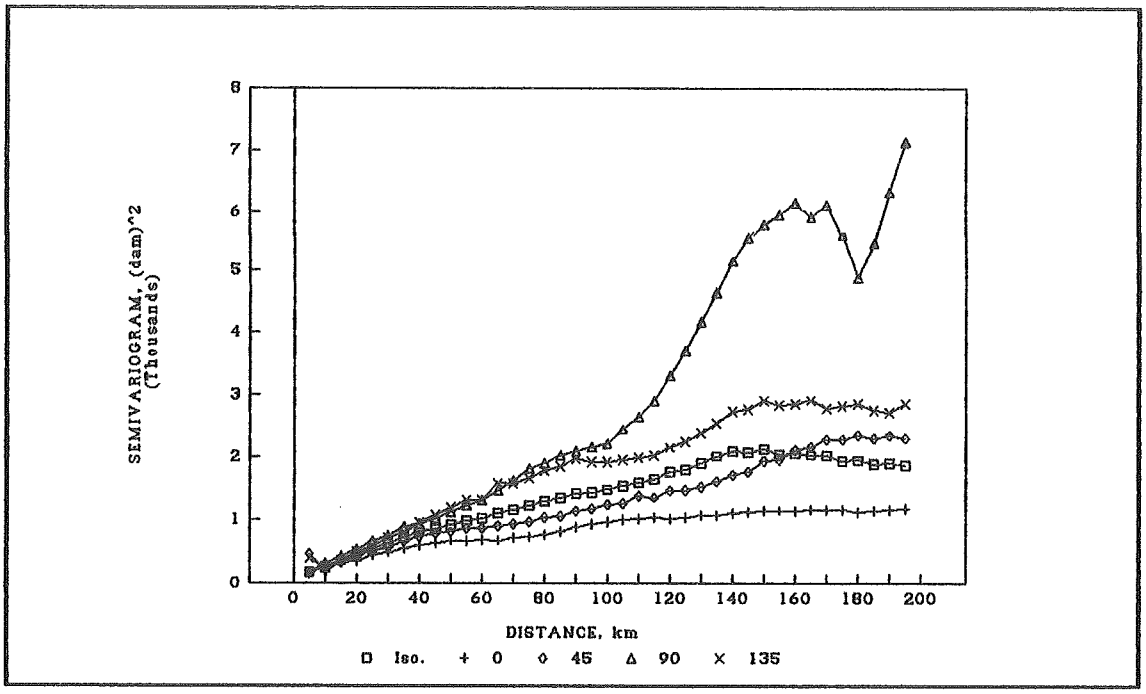

FIGURE 9. Anisotropic direct-semivariogram for elevation. Region 4.

In some cases, for example in the N-S direction in region 4 (Figure 9), a parabolic growth of the semivariogram was noticed. This is generally interpreted as an evidence of drift or non-stationarity (Myers, 1989). However, for distances shorter than approximately the maximum range modeled for the direct-semivariograms for ET_r within a particular region, stationarity of elevation could be reasonably assumed at least for the isotropic semivariogram. No drift was evident for the isotropic semivariograms, with the exception of region 5 (Figure 10). Two reasons may be used to justify semivariogram isotropy and the quasi-stationarity hypothesis (section 2.3.3) for those distances (Hevesi *et al.*, 1990). First, the convenience of a simplified semivariogram model. This simplification becomes critical during cross-validation because the identification of the large number of parameters required for the more sophisticated models is particularly difficult. Second, a model

consistency should be maintained between the two ReV's under study. The linear model of coregionalization (section 2.3.5.2) implies the existence of anisotropic structures for both correlated ReV's if one of them shows evidence of anisotropy. The small sample size did not allow development of evidence for anisotropy for ET_r. As a consequence, the use of an isotropic semivariogram model for elevation within the distances previously mentioned seemed more reasonable that proposing an unobservable anisotropic structure for ET_r.

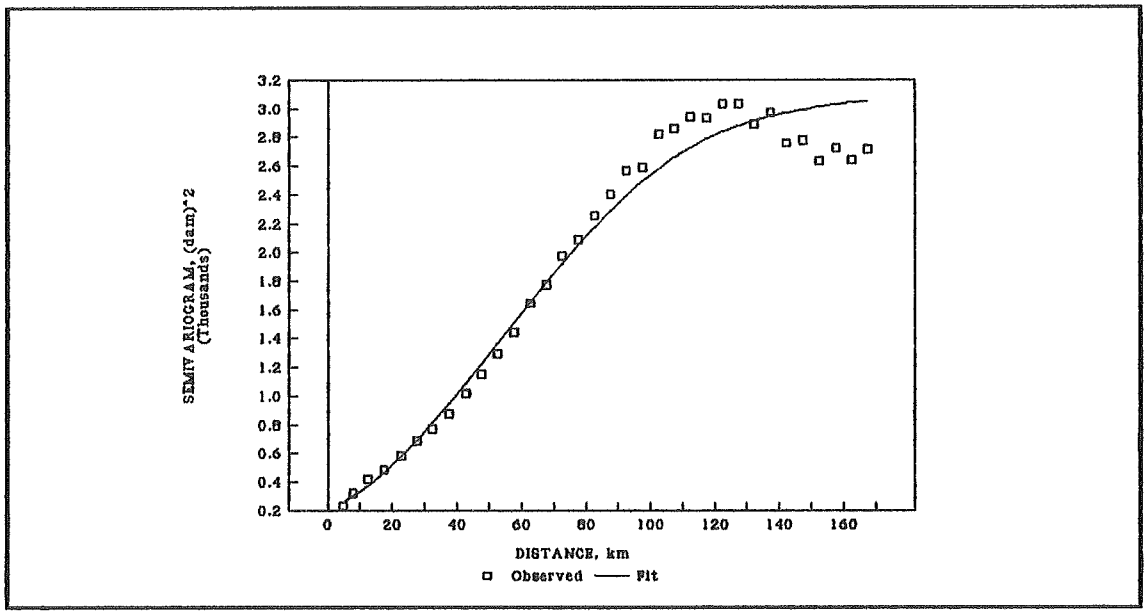

FIGURE 10. Model isotropic direct-semivariogram for elevation. Region 2.

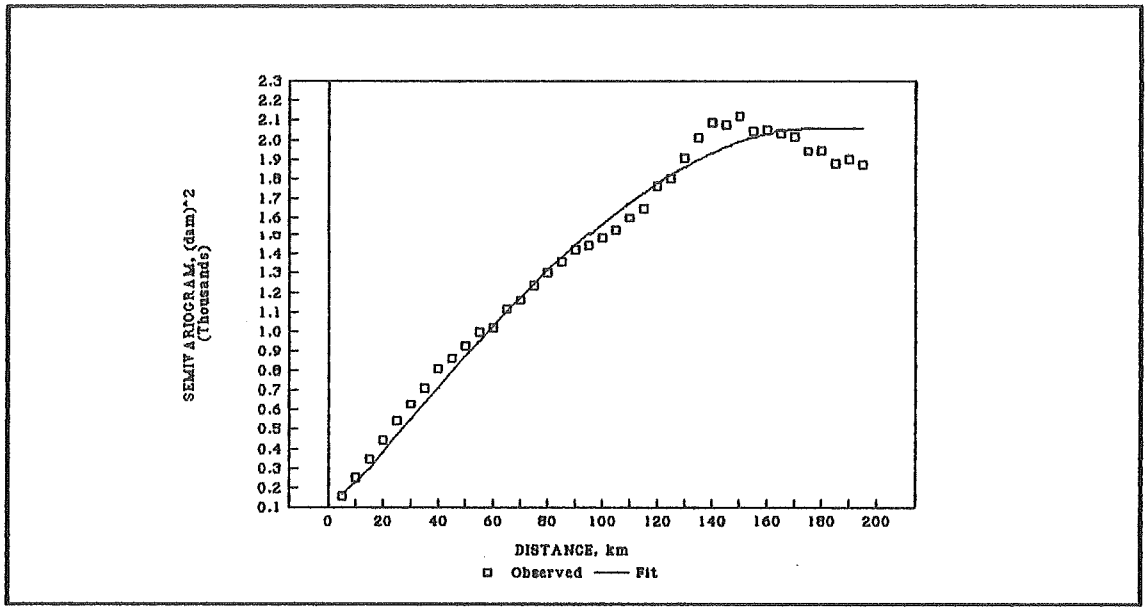

FIGURE 10. (continued). Region 4.

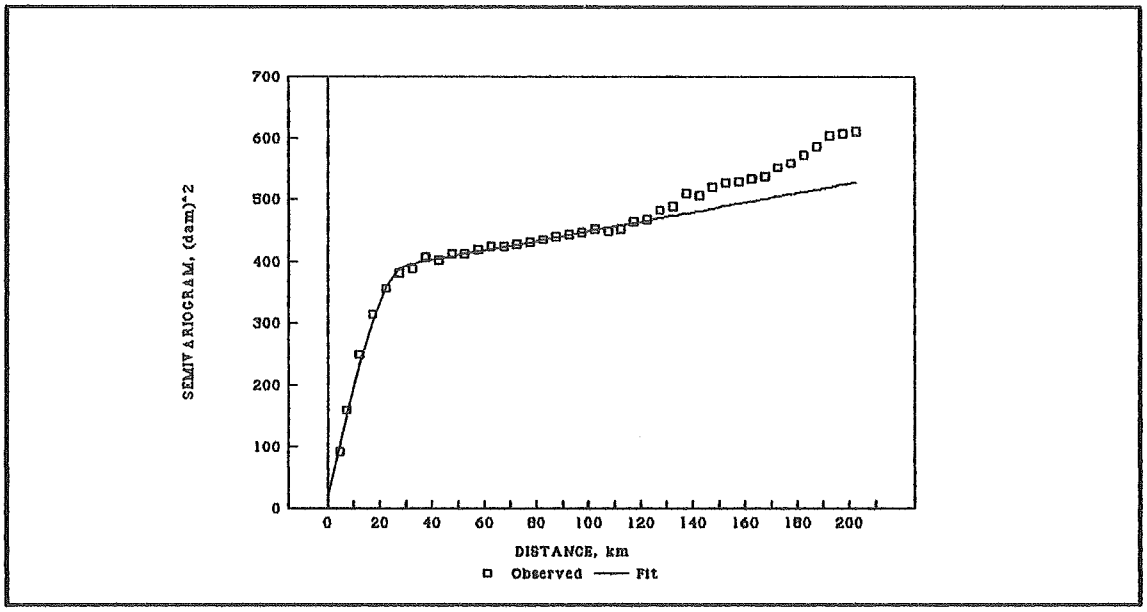

FIGURE 10. (continued). Region 5.

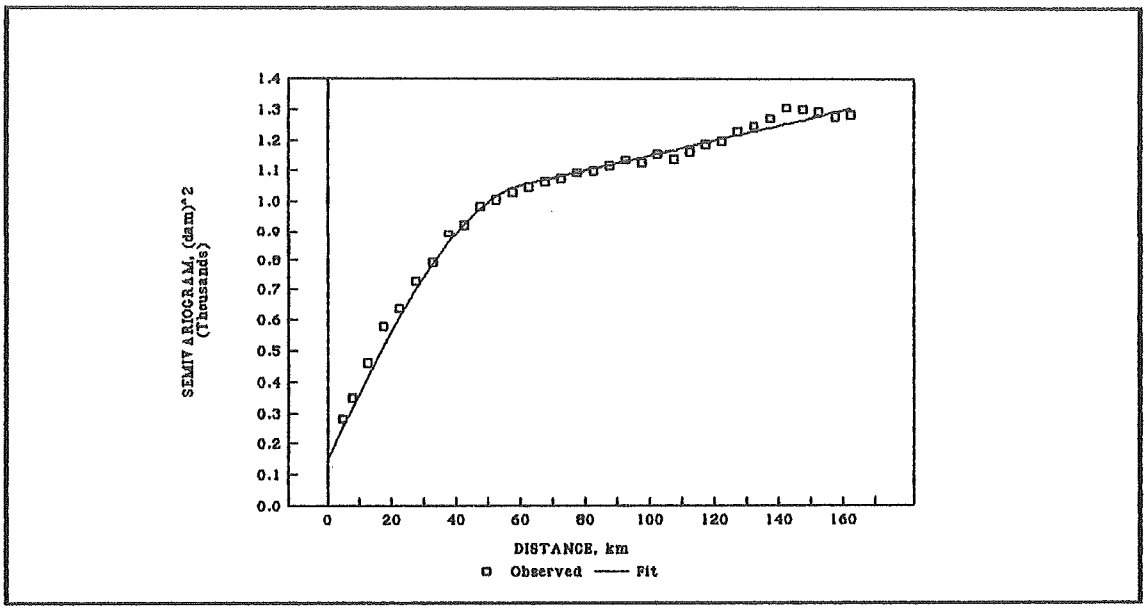

FIGURE 10. (continued). Region 6.

Table 11 lists the parameters of the fit isotropic direct-semivariogram models for elevation and the corresponding cross-validation statistics for the four regions under study. Figure 10 shows the experimental and fit semivariogram models for these four regions. With the exception of region 4, models with nested structures were fit. Nugget effects were also evident in these models. The elevation semivariogram in region 2 was fit by a model with two nested structures, a gaussian structure with a range of 85 *km* and a spherical structure with a range of 125 *km*. The range of the gaussian structure was very similar to the one observed for the direct-semivariogram for cumulative ET_r. In regions 5 and 6, the semivariogram model was made up of two nested structures, a spherical structure and a linear structure. Note the small range of the spherical structures, 30 and 60 *km*, for regions 5 and 6, respectively, compared with the range of the direct-

semivariograms for ET_r within the two regions. For region 4, the semivariogram was fit by a model with a spherical structure with a particularly large range of 175 *km*.

TABLE 11. Models of direct-semivariograms for elevation and cross-validation statistics.

		Gaussian		Spherical		Linear				
Reg	Nugget dam^2	Sill dam^2	Range *km*	Sill dam^2	Range *km*	Slope dam^2 km^{-1}	*AKE* *dam*	*MSE* dam^2	Samp. var. dam^2	*SMSE* dam^2
2	200	2000	85	890	125		0.073	260.41	2200.37	0.978
4	85			1975	175		0.014	156.47	1482.78	0.936
5	19			353	30	0.77	0.021	92.56	525.37	0.973
6	150			755	60	2.45	-0.033	249.47	1057.75	0.976

4.2.3 Cross-semivariograms

Appendix H lists the experimental values of the cross-semivariograms for each of the study cases. The number of sample pairs used to compute each experimental value was the same as in the case of direct-semivariograms for ET_r since the same sample points were used in the computations. Figure 11 shows the experimental and model cross-semivariograms for cumulative ET_r and elevation. This Figure also shows the PDC curve computed to check the positive definite condition. Most of the cases analyzed, with the exception of region 4, showed absolute experimental values for the cross-semivariogram smaller than the absolute values of the PDC curve for most of the distances computed.

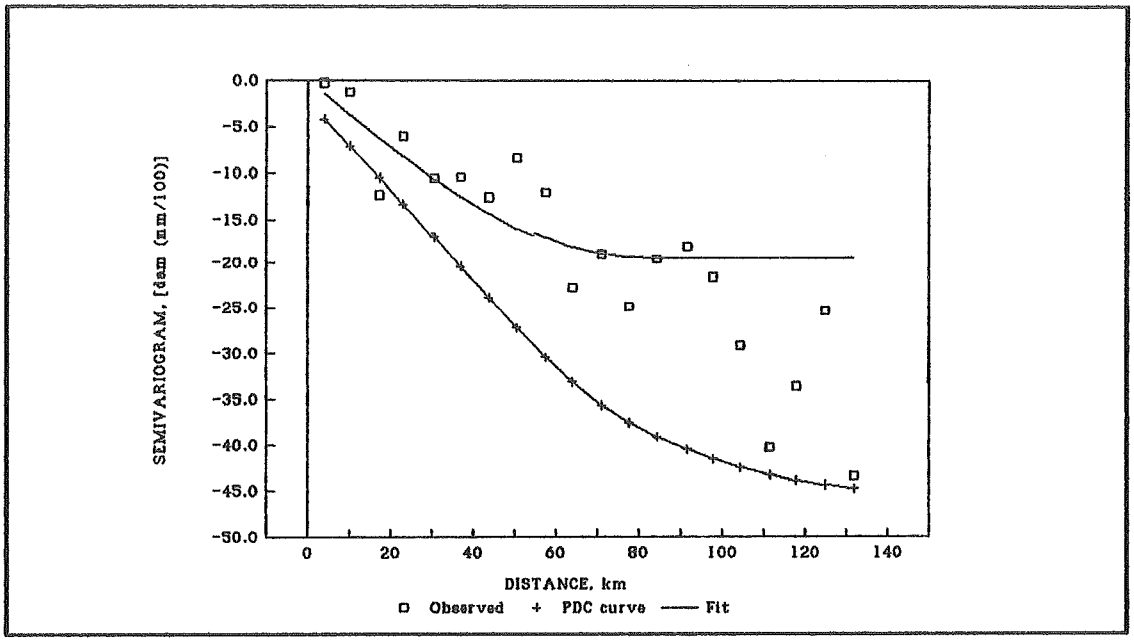

FIGURE 11. Cross-semivariogram models for cumulative ET_r and elevation. Region 2.

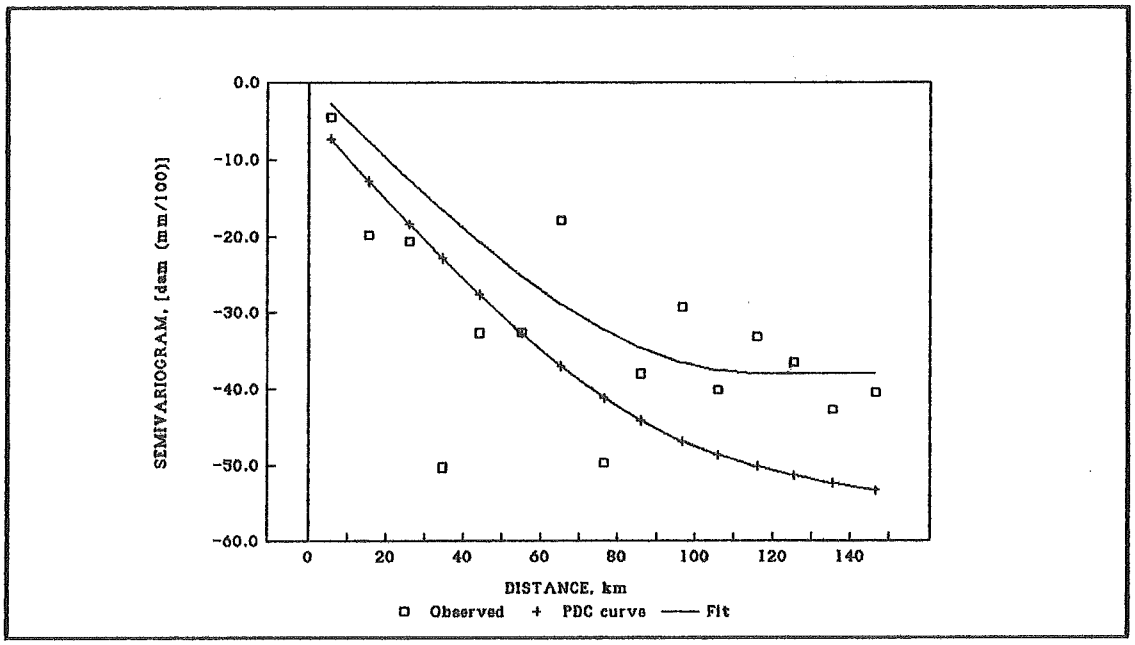

FIGURE 11. (continued). Region 4.

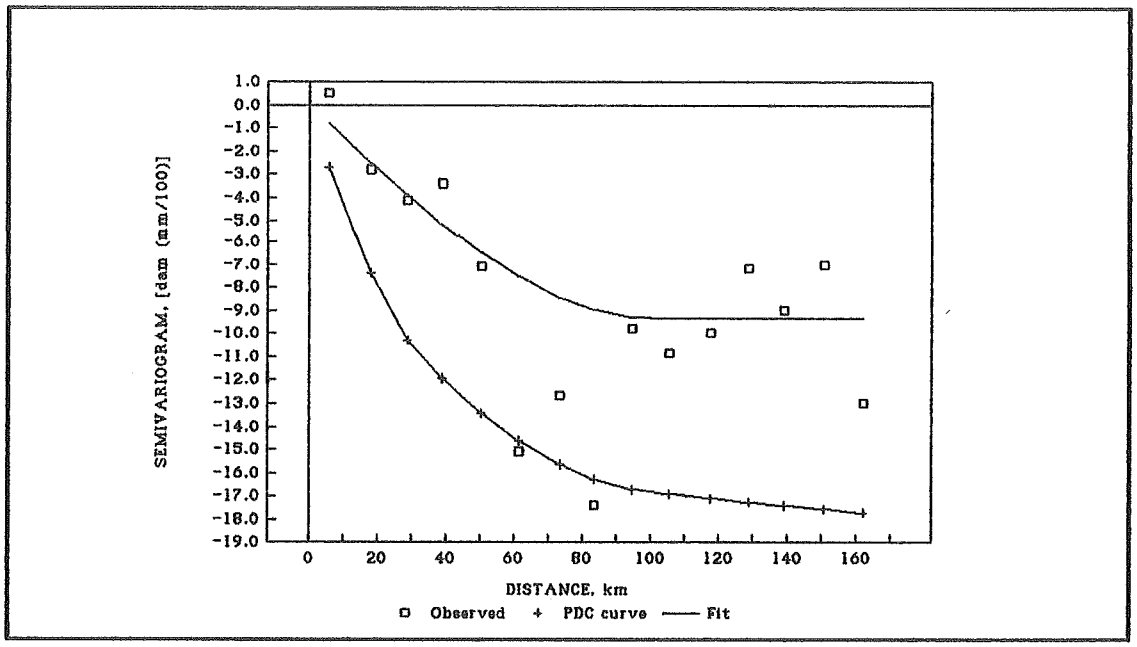

FIGURE 11. (continued). Region 5.

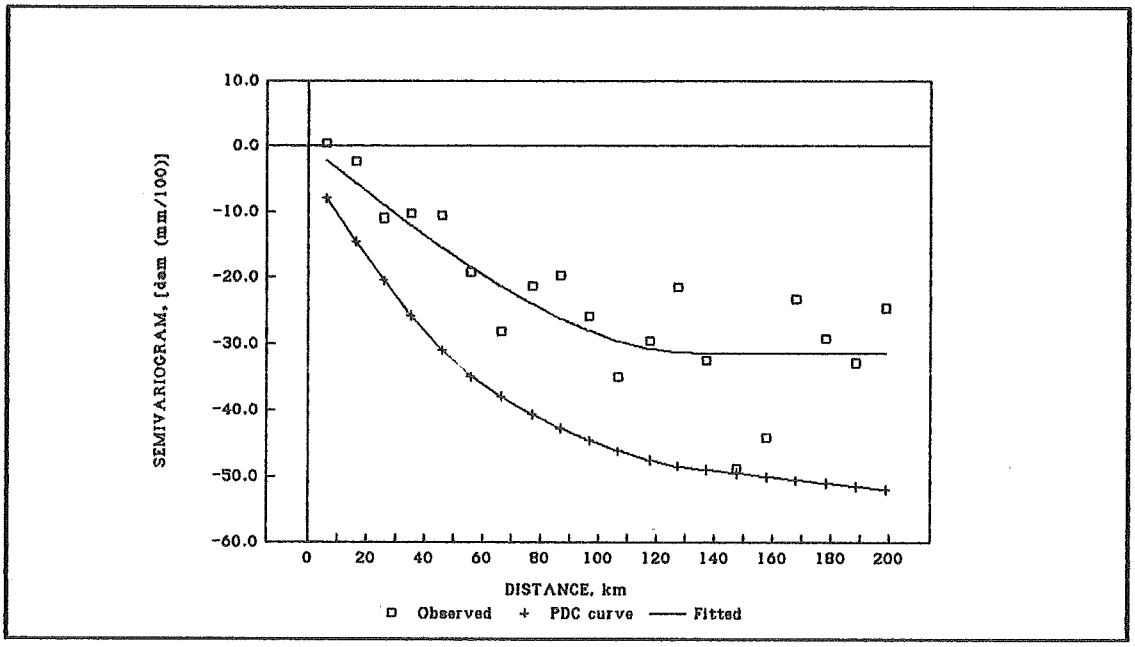

FIGURE 11. (continued). Region 6.

As in the case of the direct-semivariograms for ET_r, the experimental cross-semivariograms showed a high amount of scatter and, in general, no obvious theoretical models were evident. Recall that the linear model of coregionalization implies that any structure present in a cross-semivariogram must also appear in both direct-semivariograms. Spherical models were fit to both direct-semivariograms as discussed previously. For this reason, spherical models were selected to fit the experimental cross-semivariograms. In region 4, the modeling of cross-semivariograms was somewhat more difficult because of the problems related to the positive definite condition mentioned previously. In this case, the experimental values meeting the positive definite condition were considered more representative of the underlying theoretical cross-semivariogram. Validity of the selected models and parameters was based mainly on the cross-validation statistics.

Table 12 lists the parameters of the model semivariograms and the cross-validation statistics for all 44 study cases. There was no clear evidence of nugget effects. These were assumed equal to zero in all cases and this assumption was supported by the cross-validation statistics. In general, the ranges defined for the direct-semivariograms for ET_r seemed appropriate for the spherical models in the cross-semivariograms. However, in region 4 it was usually necessary to define larger ranges than those used for direct-semivariograms for ET_r. Notice that most of the experimental values of the cross-semivariograms in region 4 (Figure 11) meeting the positive definite condition are at distances close to or greater than the ranges of the direct-semivariograms for ET_r. Cross-validation results were used to support the selected ranges.

TABLE 12. Spherical models for cross-semivariograms and cross-validation statistics. Region 2.

Month	Nugget[1] *dam mm d^{-1}*	Sill[1] *dam mm d^{-1}*	Range *km*	*AKE*[2] *mm d^{-1}*	*MSE*[3] *mm^2 d^{-2}*	Samp. var.[3] *mm^2 d^{-2}*	*SMSE*[3] *mm^2 d^{-2}*
February	0.000	-5.04	100	0.007	0.003	0.027	0.999
March	0.000	-7.24	100	0.008	0.010	0.070	1.002
April	0.000	-8.46	80	0.011	0.030	0.137	1.027
May	0.000	-9.01	80	0.010	0.031	0.158	1.053
June	0.000	-8.61	80	0.008	0.030	0.117	0.992
July	0.000	-8.50	85	0.007	0.034	0.134	0.967
August	0.000	-6.89	70	0.007	0.035	0.104	1.072
September	0.000	-6.39	80	0.006	0.022	0.073	1.056
October	0.000	-4.85	105	0.006	0.012	0.036	0.968
November	0.000	-3.18	115	0.004	0.003	0.014	0.934
Cumulative	0.000	-19.40	80	0.019	0.138	0.681	1.052

[1] Cumulative ET_r, *dam mm (100)$^{-1}$* [2] Cumulative ET_r, *mm (100)$^{-1}$*
[3] Cumulative ET_r, *mm^2 (100)$^{-2}$*

TABLE 12. (continued). Region 4.

Month	Nugget[1] *dam mm d^{-1}*	Sill[1] *dam mm d^{-1}*	Range *km*	*AKE*[2] *mm d^{-1}*	*MSE*[3] *mm^2 d^{-2}*	Samp. var.[3] *mm^2 d^{-2}*	*SMSE*[3] *mm^2 d^{-2}*
February	0.000	-3.45	65	-0.029	0.009	0.024	1.030
March	0.000	-7.65	90	-0.052	0.019	0.069	0.978
April	0.000	-14.35	100	-0.085	0.048	0.213	0.979
May	0.000	-19.20	120	-0.083	0.060	0.356	0.947
June	0.000	-20.50	115	-0.110	0.104	0.406	0.921
July	0.000	-19.30	120	-0.084	0.108	0.373	1.067
August	0.000	-17.89	125	-0.071	0.127	0.365	1.125
September	0.000	-12.55	125	-0.063	0.047	0.146	1.088
October	0.000	-6.35	90	-0.047	0.017	0.059	0.940
November	0.000	-1.76	80	-0.016	0.004	0.014	0.680
Cumulative	0.000	-37.90	115	-0.202	0.345	1.328	0.969

[1] Cumulative ET_r, *dam mm (100)$^{-1}$* [2] Cumulative ET_r, *mm (100)$^{-1}$*
[3] Cumulative ET_r, *mm^2 (100)$^{-2}$*

TABLE 12. (continued). Region 5.

Month	Nugget[1] *dam* *mm d^{-1}*	Sill[1] *dam* *mm d^{-1}*	Range *km*	*AKE*[2] *mm d^{-1}*	*MSE*[3] *mm^2 d^{-2}*	Samp. var.[3] *mm^2 d^{-2}*	*SMSE*[3] *mm^2 d^{-2}*
February	0.000	-1.58	95	-0.034	0.013	0.027	1.161
March	0.000	-2.47	90	-0.059	0.020	0.043	1.107
April	0.000	-3.92	100	-0.116	0.057	0.107	1.186
May	0.000	-4.09	100	-0.101	0.053	0.127	1.119
June	0.000	-4.06	100	-0.094	0.057	0.138	1.137
July	0.000	-4.29	105	-0.086	0.060	0.166	1.101
August	0.000	-3.18	100	-0.064	0.060	0.131	1.133
September	0.000	-2.62	105	-0.045	0.032	0.094	1.111
October	0.000	-2.10	115	-0.033	0.014	0.049	1.000
November	0.000	-1.04	115	-0.020	0.006	0.012	1.110
Cumulative	0.000	-9.34	100	-0.200	0.227	0.638	1.170

[1] Cumulative ET_r, *dam mm (100)$^{-1}$* [2] Cumulative ET_r, *mm (100)$^{-1}$*
[3] Cumulative ET_r, *mm^2 (100)$^{-2}$*

TABLE 12. (continued). Region 6.

Month	Nugget[1] *dam* *mm d^{-1}*	Sill[1] *dam* *mm d^{-1}*	Range *km*	*AKE*[2] *mm d^{-1}*	*MSE*[3] *mm^2 d^{-2}*	Samp. var.[3] *mm^2 d^{-2}*	*SMSE*[3] *mm^2 d^{-2}*
February	0.000	-3.26	85	-0.009	0.013	0.037	1.063
March	0.000	-6.93	115	-0.036	0.037	0.111	0.939
April	0.000	-11.65	125	-0.044	0.086	0.313	0.929
May	0.000	-13.20	135	-0.040	0.088	0.391	0.966
June	0.000	-17.85	160	-0.052	0.100	0.590	0.838
July	0.000	-14.80	135	-0.059	0.126	0.461	0.970
August	0.000	-10.30	120	-0.049	0.102	0.247	1.084
September	0.000	-10.35	130	-0.070	0.070	0.180	0.916
October	0.000	-7.05	140	-0.026	0.045	0.145	0.904
November	0.000	-2.60	90	-0.010	0.011	0.027	0.942
Cumulative	0.000	-31.55	135	-0.125	0.487	1.812	0.940

[1] Cumulative ET_r, *dam mm (100)$^{-1}$* [2] Cumulative ET_r, *mm (100)$^{-1}$*
[3] Cumulative ET_r, *mm^2 (100)$^{-2}$*

4.3 Results of kriging and cokriging

In this section the results of applying the kriging and cokriging interpolation techniques to estimate ET_r at a grid interval of approximately 5 *km* are presented. Before commenting on these results, two clarifications are required. First, the results for cumulative ET_r are given in *mm* rather than in *mm (100)*$^{-1}$ because the first unit is more consistent with the standard units used in the scientific community. Second, despite the fact that the computer program used in this analysis provided kriging and cokriging variances, this section presents these results in terms of standard deviations in order to use the same units as for the estimates of ET_r.

Table 13 lists the maximum, minimum and average values of the kriged and cokriged estimates of ET_r for the four regions under study. The percent difference between kriged and cokriged estimates, based on the kriged estimates, is also provided. Minimum values for February are negative in regions 4 and 6. This may indicate some failure of the kriging and cokriging interpolation techniques when the values of the variable under study are very small. Recall that zero was the minimum experimental value of ET_r for that month in those regions (Table 6).

In general, no differences between kriging and cokriging were noticed for the maxima of the estimated values, with the exception of region 4 where a slight difference was observed. The minima and averages of the estimated values were consistently smaller for cokriging than kriging in all regions. This decrease was particularly noticeable for the minima of the estimated values in region 4, where a decrease of approximately 15 to 20 % was observed. For all regions, the decrease of the minima of the estimated values was larger than the decrease of the averages of the estimated values. In general, decreases in the average are small and within the accuracy of the Blaney-Criddle method used to

compute the local estimates of ET_r. These changes are higher for the cumulative ET_r values due to the additive effect of small but consistent errors.

TABLE 13. Comparison of kriged and cokriged ET_r estimates. Region 2.

Month	Maximum[1]		mm d^{-1}	Minimum[1]		mm d^{-1}	Average[1]		mm d^{-1}
	Krig.	Cokg.	Diff. %	Krig.	Cokg.	Diff. %	Krig.	Cokg.	Diff. %
February	1.07	1.05	-2.52	0.16	0.00	-100.14	0.74	0.66	-10.02
March	2.00	1.98	-1.10	0.63	0.41	-35.17	1.47	1.37	-7.28
April	3.40	3.37	-0.94	1.53	1.30	-14.94	2.79	2.63	-5.77
May	4.55	4.52	-0.55	2.58	2.38	-7.57	3.85	3.68	-4.48
June	5.06	5.09	0.67	3.68	3.34	-9.27	4.63	4.46	-3.60
July	5.98	5.96	-0.37	4.52	4.20	-7.18	5.28	5.14	-2.76
August	5.01	4.97	-0.74	3.64	3.30	-9.42	4.43	4.29	-3.21
September	3.77	3.81	1.01	2.60	2.35	-9.58	3.43	3.32	-3.45
October	2.26	2.23	-1.11	1.47	1.31	-11.28	2.02	1.95	-3.33
November	0.77	0.74	-2.77	0.16	0.08	-51.03	0.56	0.52	-7.15
Cumulative	1031	1021	-0.97	621	571	-8.08	904	867	-4.07

[1] For cumulative ET_r, *mm*

TABLE 13. (continued). Region 4.

Month	Maximum[1]		mm d^{-1}	Minimum[1]		mm d^{-1}	Average[1]		mm d^{-1}
	Krig.	Cokg.	Diff. %	Krig.	Cokg.	Diff. %	Krig.	Cokg.	Diff. %
February	0.84	0.82	-2.65	0.13	-0.09	-167.39	0.61	0.54	-12.58
March	2.12	2.04	-3.50	0.73	0.50	-31.73	1.56	1.43	-8.00
April	4.33	4.24	-2.03	1.95	1.65	-15.55	3.22	3.03	-5.77
May	6.11	5.94	-2.83	3.28	2.86	-12.95	4.54	4.34	-4.41
June	6.98	6.66	-4.49	4.18	3.31	-20.85	5.46	5.19	-4.94
July	7.71	7.56	-2.00	5.58	4.69	-15.99	6.39	6.18	-3.20
August	6.89	6.69	-2.92	4.58	3.64	-20.48	5.33	5.15	-3.41
September	4.60	4.49	-2.28	3.39	2.82	-16.95	3.84	3.70	-3.69
October	2.74	2.69	-2.11	1.52	1.31	-13.72	2.28	2.19	-4.31
November	0.70	0.70	-0.45	0.20	0.12	-36.92	0.52	0.49	-5.29
Cumulative	1299	1245	-4.16	808	650	-19.56	1032	983	-4.74

[1] For cumulative ET_r, *mm*

TABLE 13. (continued). Region 5.

Month	Maximum[1] mm d^{-1} Krig.	Cokg.	Diff. %	Minimum[1] mm d^{-1} Krig.	Cokg.	Diff. %	Average[1] mm d^{-1} Krig.	Cokg.	Diff. %
February	0.74	0.76	1.91	0.05	0.02	-48.05	0.39	0.34	-13.91
March	1.49	1.50	0.54	0.53	0.49	-6.89	1.11	1.01	-8.83
April	2.99	2.96	-1.01	1.69	1.48	-11.99	2.43	2.25	-7.47
May	4.24	4.23	-0.26	2.64	2.54	-3.68	3.64	3.48	-4.44
June	5.26	5.29	0.44	3.57	3.48	-2.44	4.59	4.45	-3.15
July	6.20	6.24	0.52	4.76	4.44	-6.66	5.43	5.28	-2.63
August	4.98	4.97	-0.34	3.69	3.51	-4.96	4.37	4.26	-2.43
September	3.91	3.90	-0.38	2.74	2.58	-5.56	3.24	3.16	-2.44
October	2.46	2.47	0.57	1.63	1.51	-7.59	2.08	2.02	-2.87
November	0.67	0.68	0.92	0.25	0.20	-18.71	0.43	0.40	-7.55
Cumulative	999	1003	0.43	662	622	-6.06	846	814	-3.87

[1] For cumulative ET_r, *mm*

TABLE 13. (continued). Region 6.

Month	Maximum[1] mm d^{-1} Krig.	Cokg.	Diff. %	Minimum[1] mm d^{-1} Krig.	Cokg.	Diff. %	Average[1] mm d^{-1} Krig.	Cokg.	Diff. %
February	0.67	0.67	0.45	-0.03	-0.14	-426.59	0.34	0.29	-13.92
March	1.79	1.80	0.45	0.56	0.34	-38.38	1.21	1.12	-7.13
April	4.08	4.09	0.27	1.91	1.62	-15.07	2.85	2.72	-4.50
May	5.47	5.49	0.29	3.05	2.66	-12.87	4.01	3.89	-3.12
June	6.83	6.85	0.28	3.87	3.46	-10.74	5.04	4.84	-3.91
July	7.63	7.62	-0.08	5.02	4.58	-8.90	6.09	5.94	-2.45
August	5.98	5.98	0.00	3.99	3.74	-6.22	4.95	4.83	-2.43
September	4.36	4.37	0.21	2.98	2.64	-11.28	3.58	3.45	-3.66
October	2.84	2.84	0.00	1.59	1.44	-9.46	2.16	2.08	-3.53
November	0.70	0.70	-0.04	0.13	0.03	-79.75	0.41	0.37	-9.60
Cumulative	1208	1211	0.25	718	624	-13.12	936	904	-3.47

[1] For cumulative ET_r, *mm*

Figure 12 shows the contour maps of kriged cumulative ET_r estimates. Figure 13 shows the contour maps of cokriged cumulative ET_r. In general, the kriged contours are very smooth as compared with the cokriged contours. The kriged contours follow roughly the main features of elevation of the different regions. However, the cokriged contours follow these elevation changes much more closely. The kriged and cokriged contours are relatively similar in areas of low elevation, for example, in the West and North areas of region 2 and the North area of region 4 (Figures 12 and 13). However, in areas of high elevation, the cokriged contours provided finer detail of the changes of ET_r as the elevation changes. Notice, for example, in region 5 the general trend of cokriged contours in the South Central area (Figure 13) which resembles closer the trend in elevation (Figure 5) while kriged contours do not follow it at all. Another example is in the North area of region 6, close to the mountainous group observed in Figure 5. Figures 14 to 17 show the cokriged contours of monthly ET_r for regions 2, 4, 5 and 6. In general, the cokriged contours of monthly ET_r follow the same pattern as cokriged contours of cumulative ET_r. In all cases ET_r decreases as elevation increases as expected due to the negative correlation between both variables.

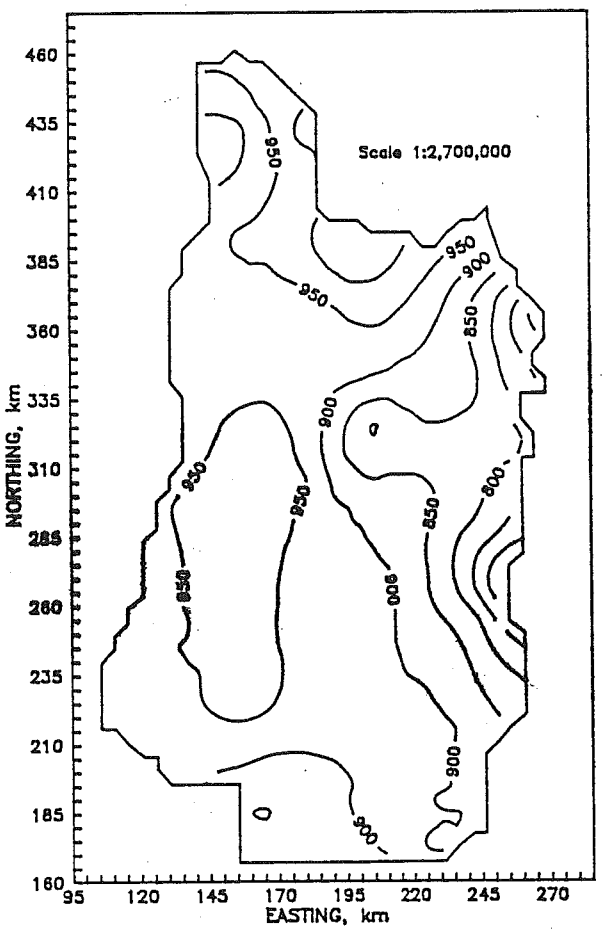

FIGURE 12. Contour maps of kriged cumulative ET_r, *mm*. Region 2.

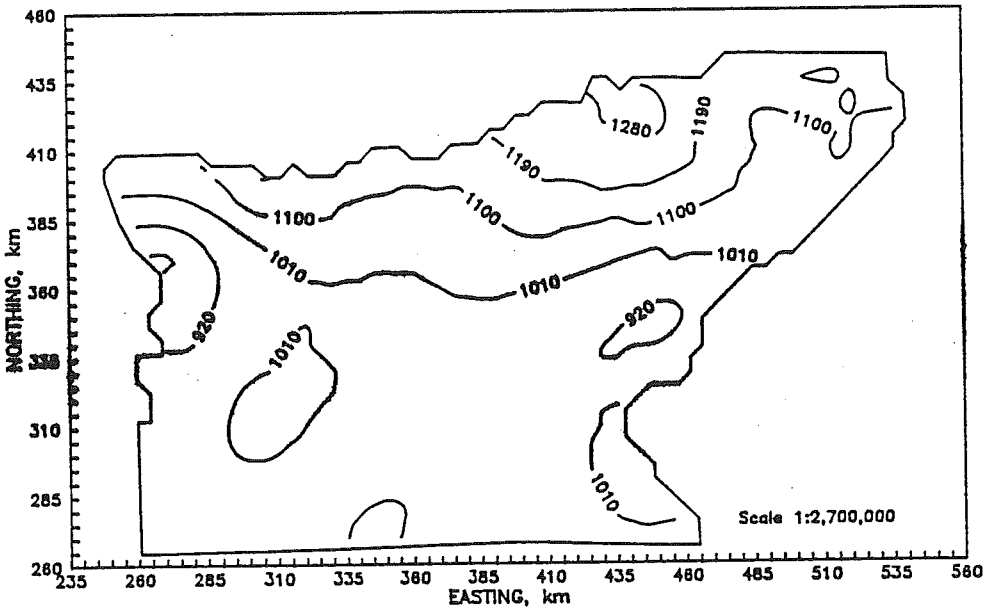

FIGURE 12. (continued). Region 4.

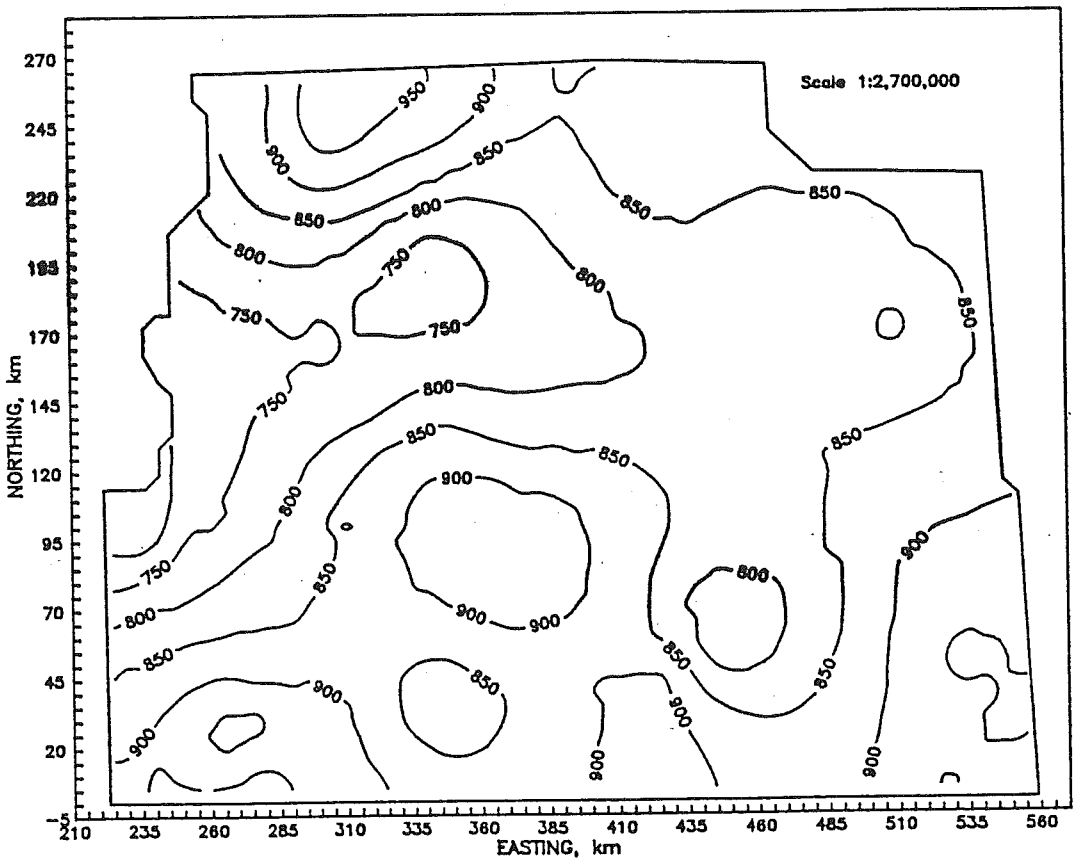

FIGURE 12. (continued). Region 5.

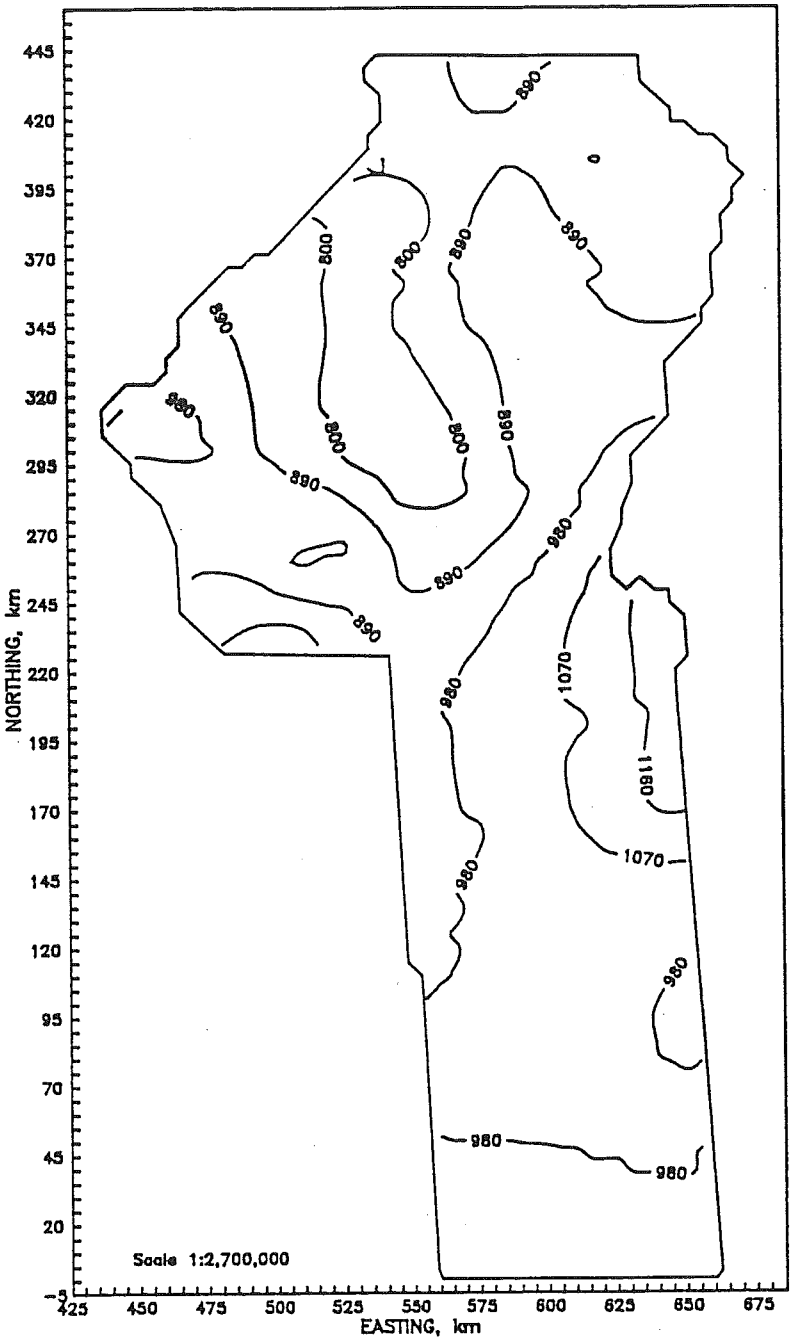

FIGURE 12. (continued). Region 6.

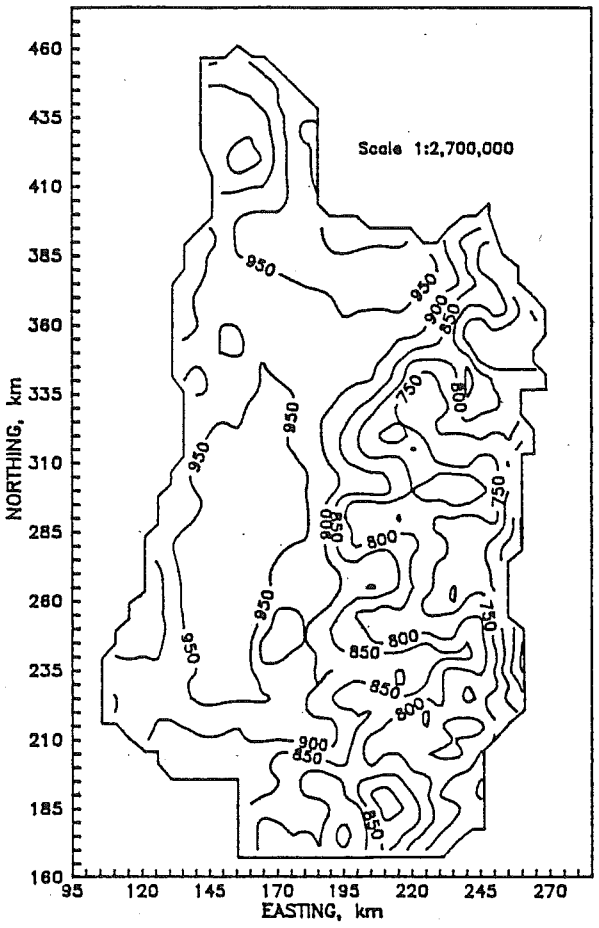

FIGURE 13. Contour maps of cokriged cumulative ET_r, *mm*. Region 2.

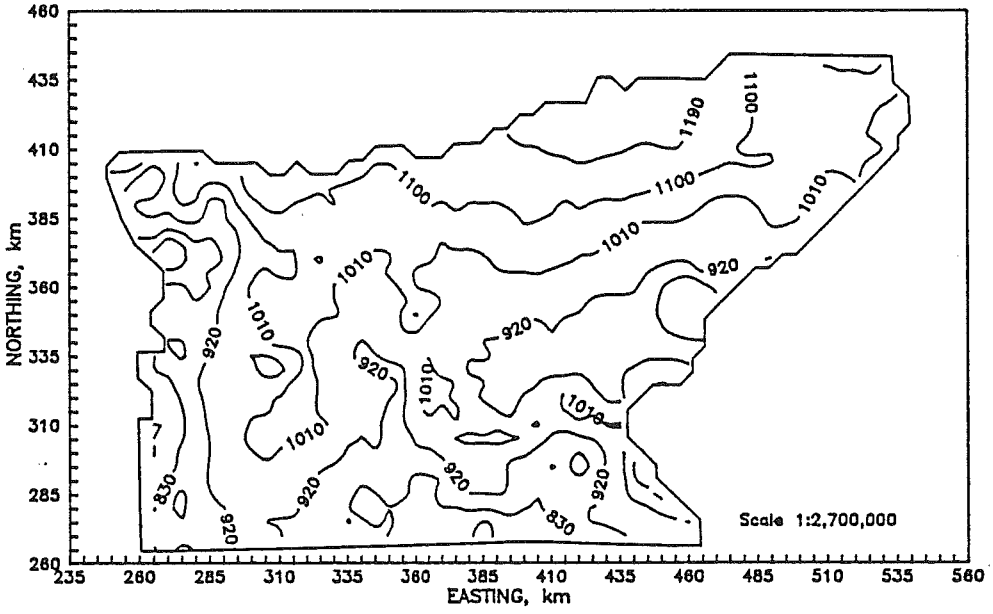

FIGURE 13. (continued). Region 4.

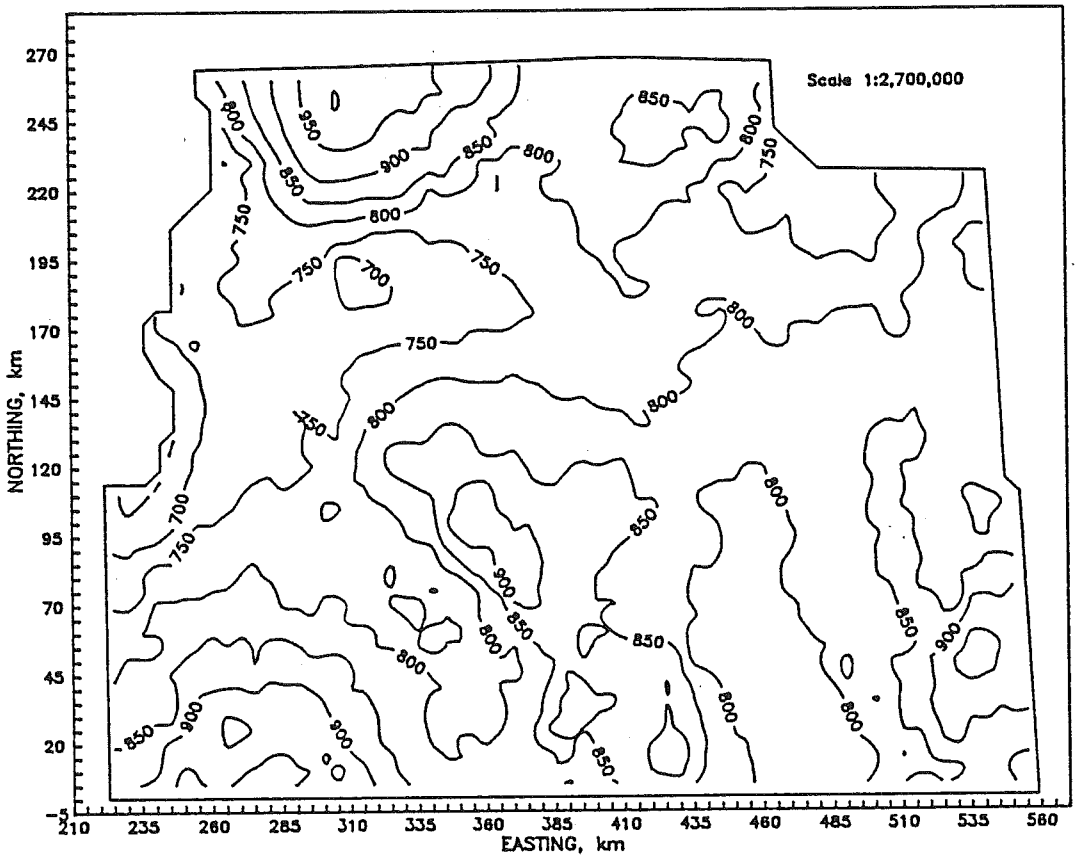

FIGURE 13. (continued). Region 5.

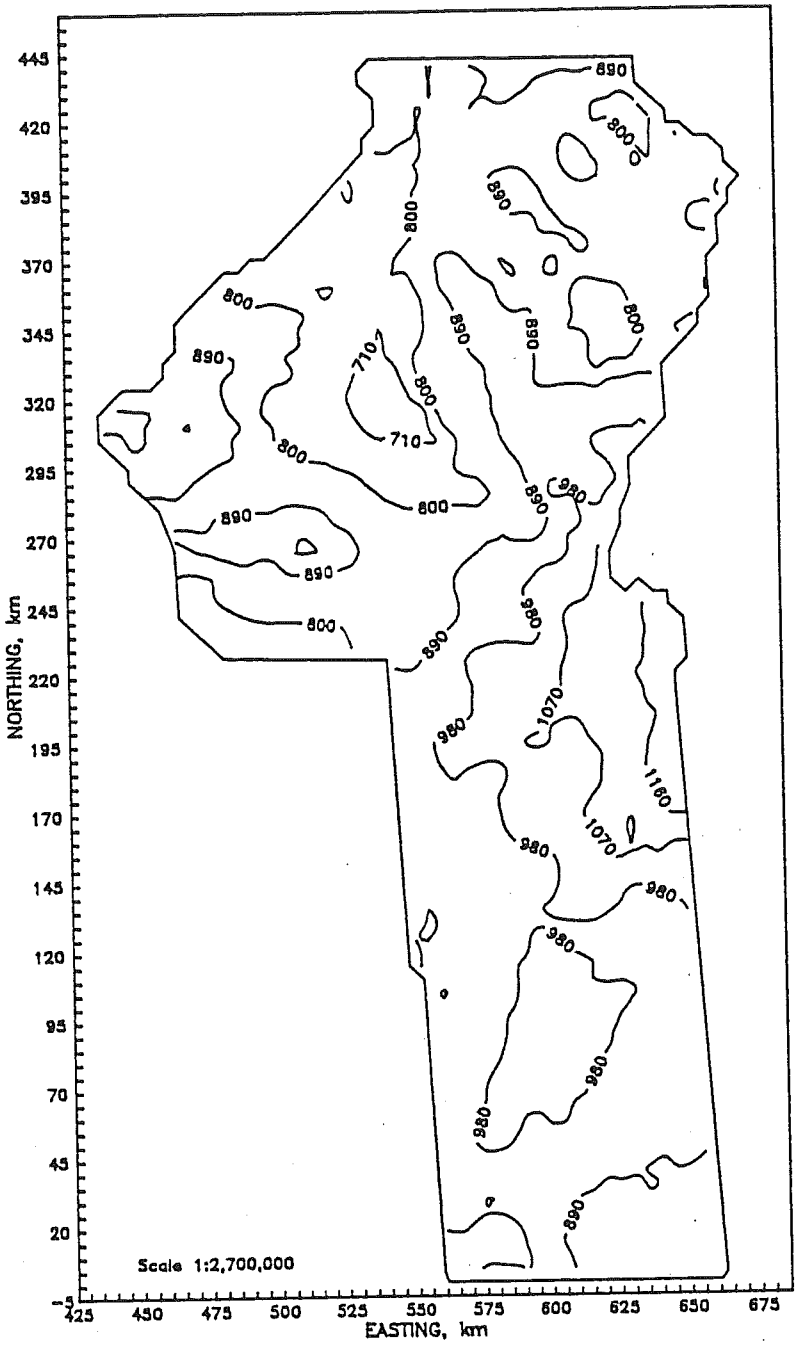

FIGURE 13. (continued). Region 6.

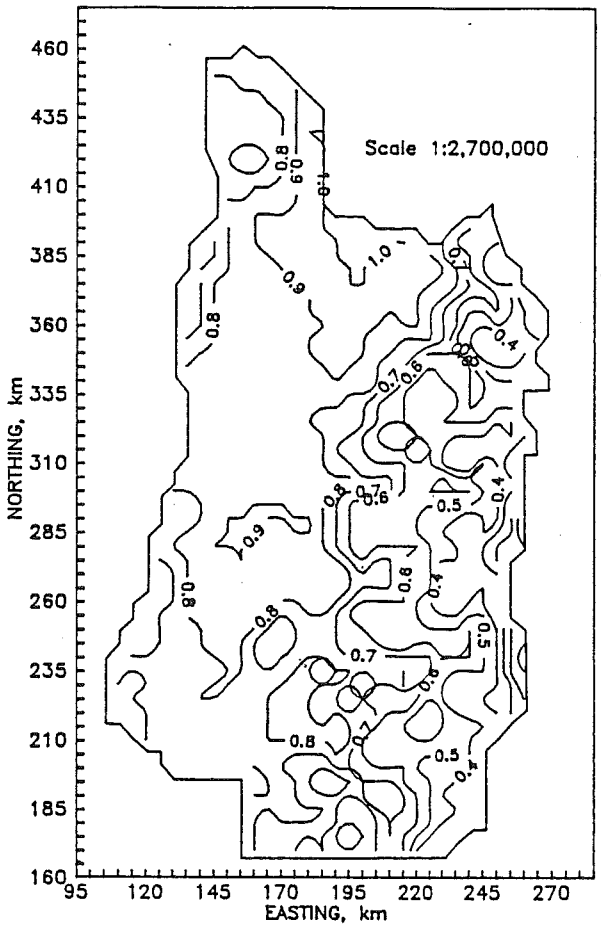

FIGURE 14. Contour maps of cokriged monthly ET_r, $mm\ d^{-1}$, for region 2. February.

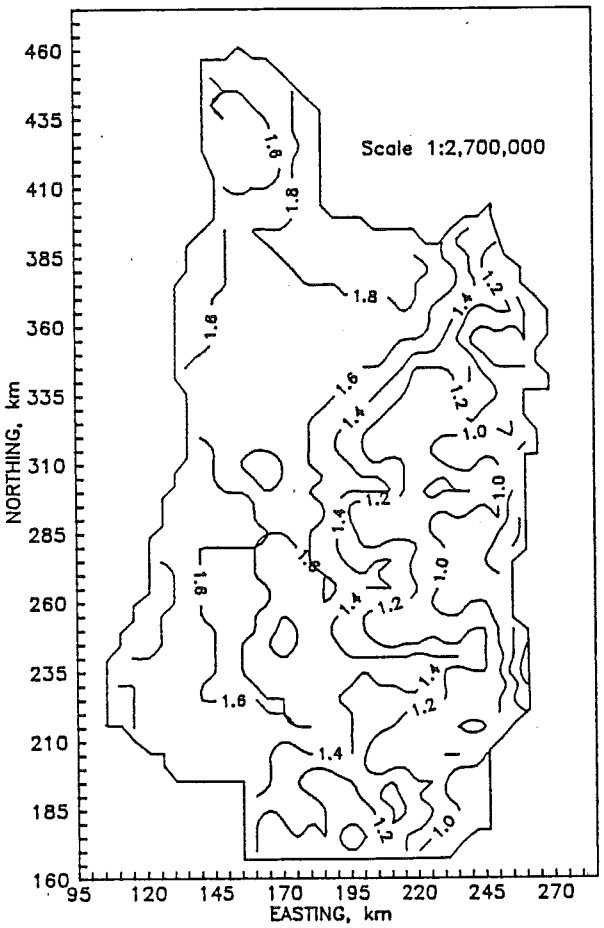

FIGURE 14. (continued). March.

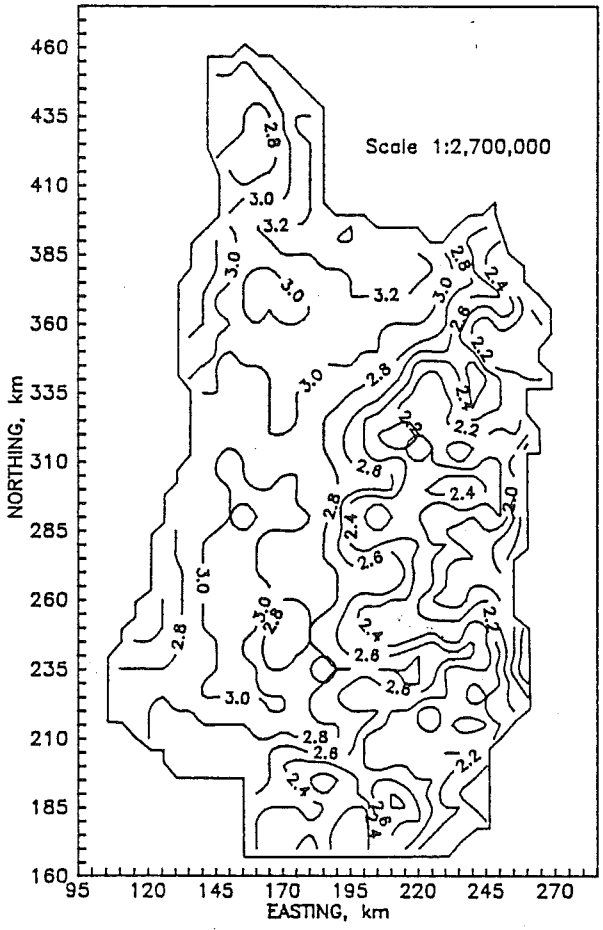

FIGURE 14. (continued). April.

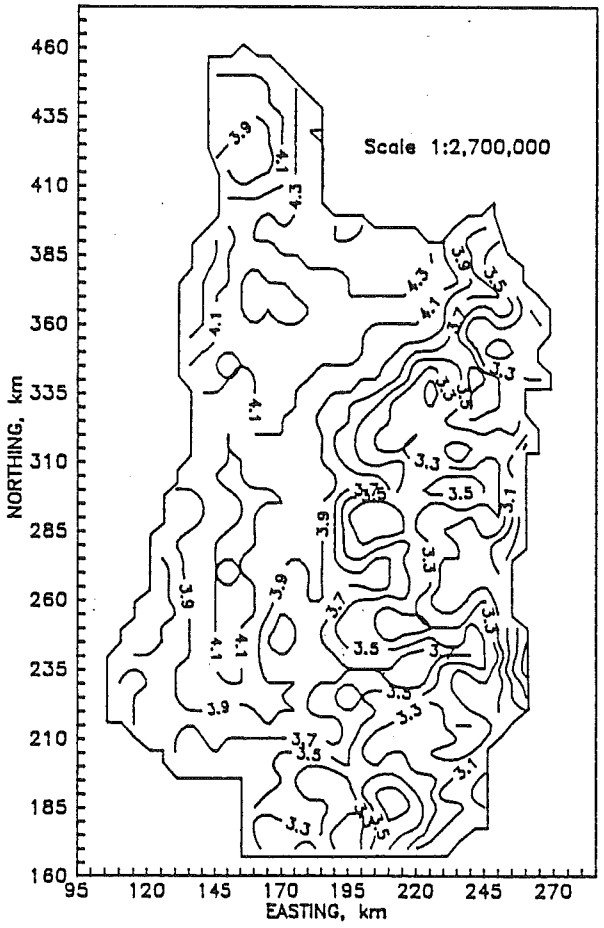

FIGURE 14. (continued). May.

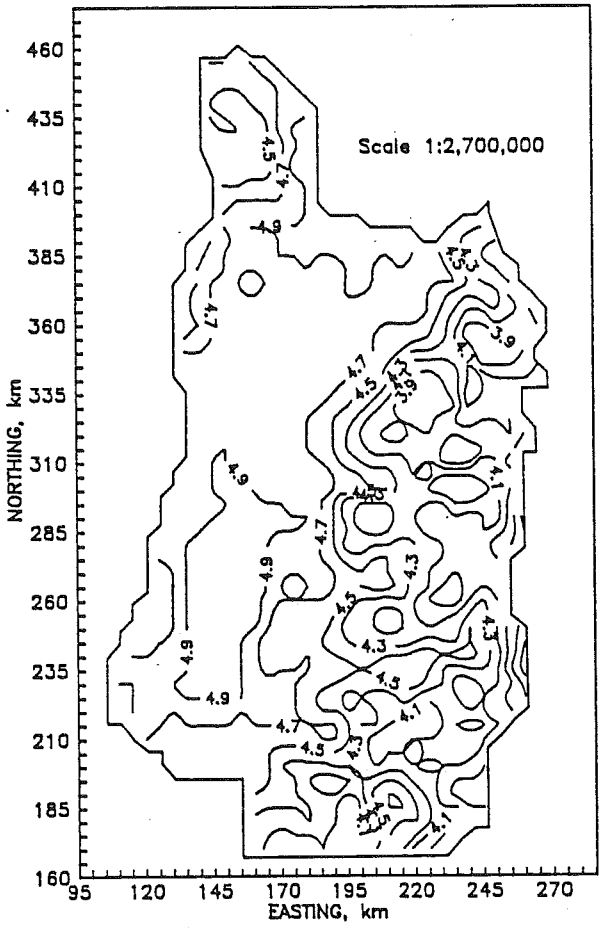

FIGURE 14. (continued). June.

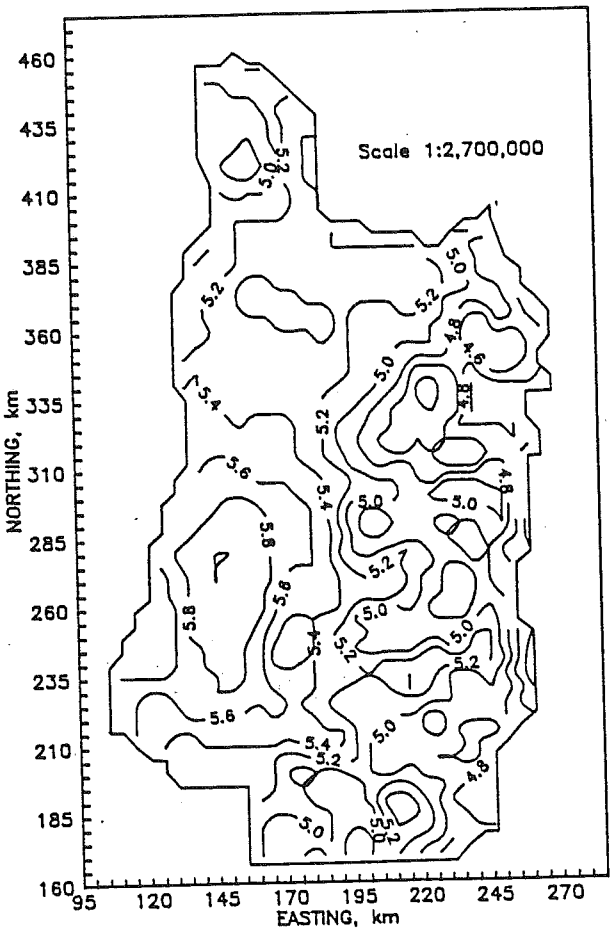

FIGURE 14. (continued). July.

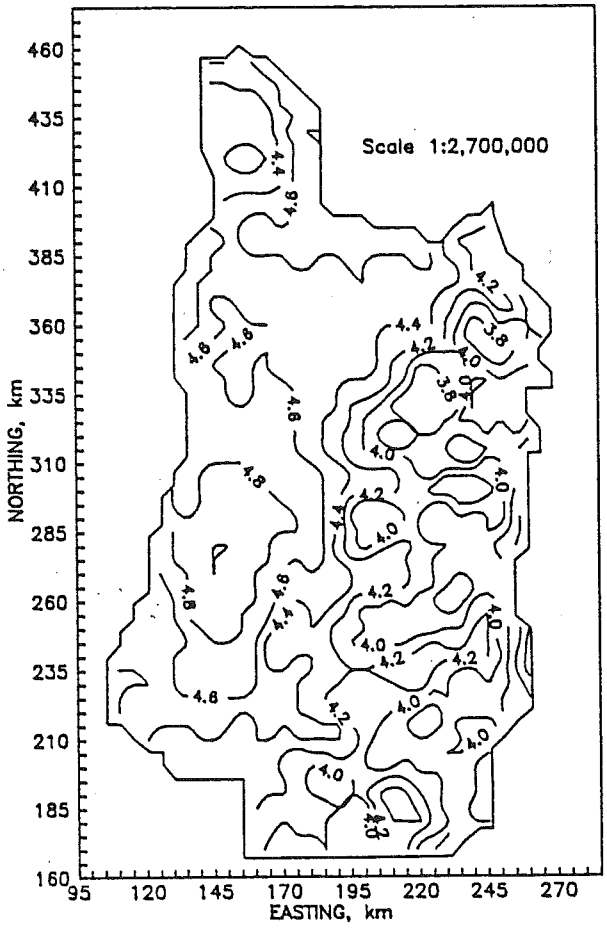

FIGURE 14. (continued). August.

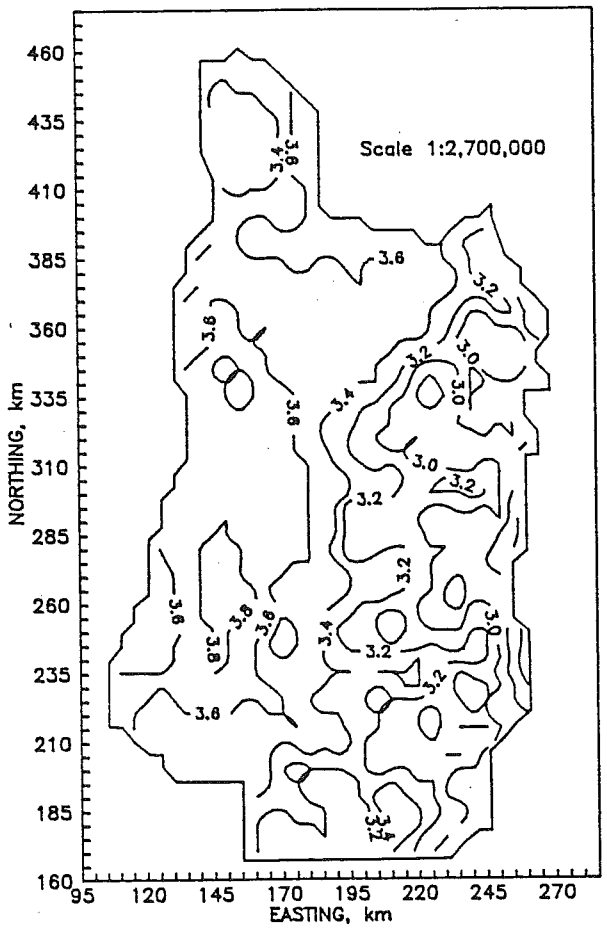

FIGURE 14. (continued). September.

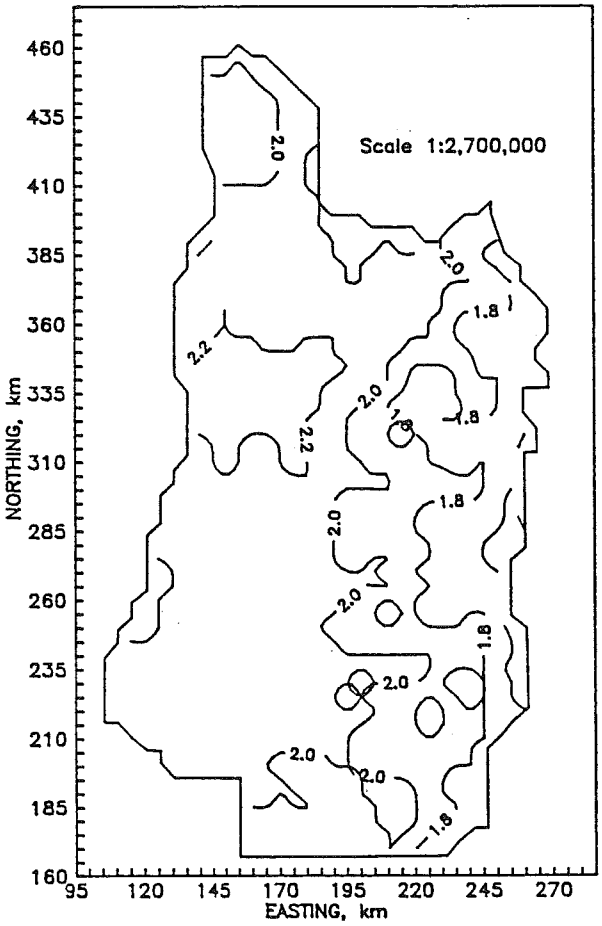

FIGURE 14. (continued). October.

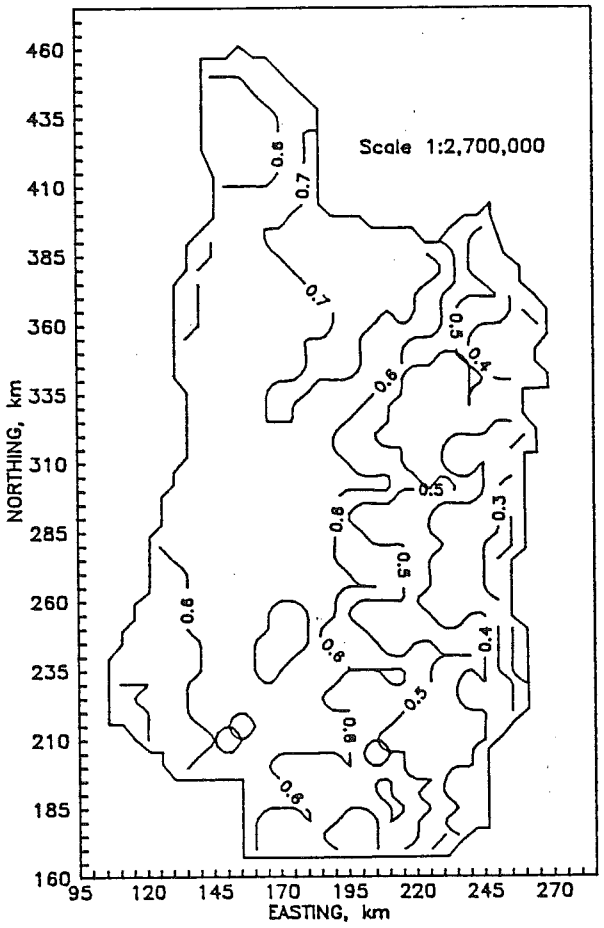

FIGURE 14. (continued). November.

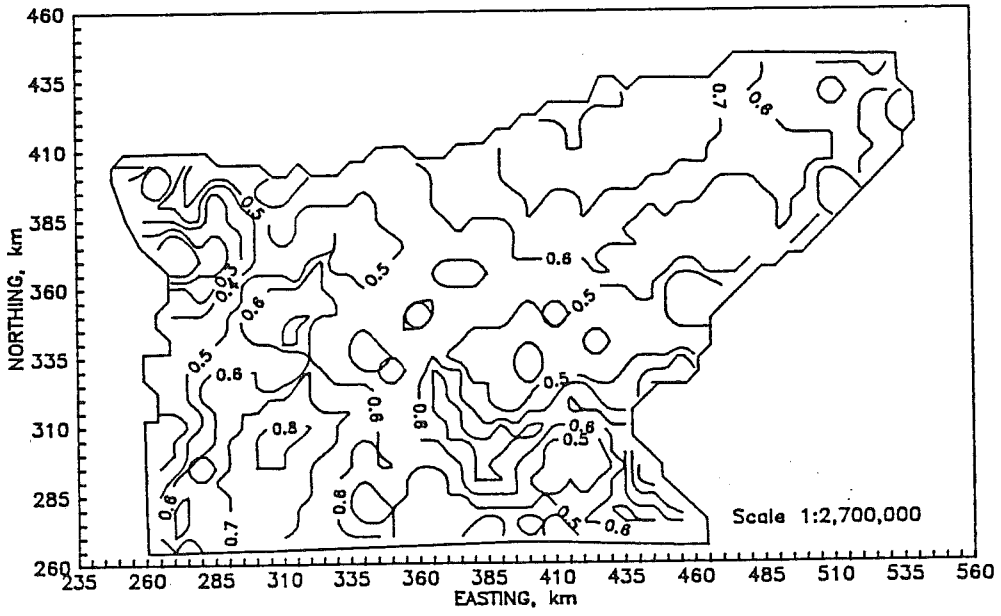

FIGURE 15. Contour maps of cokriged monthly ET_r, $mm\ d^{-1}$, for region 4. February.

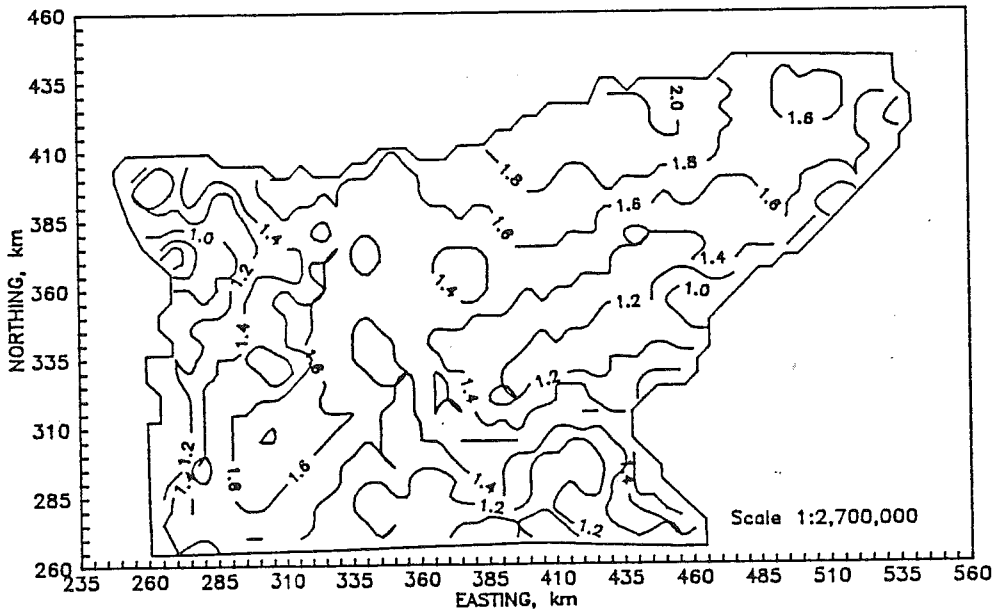

FIGURE 15. (continued). March.

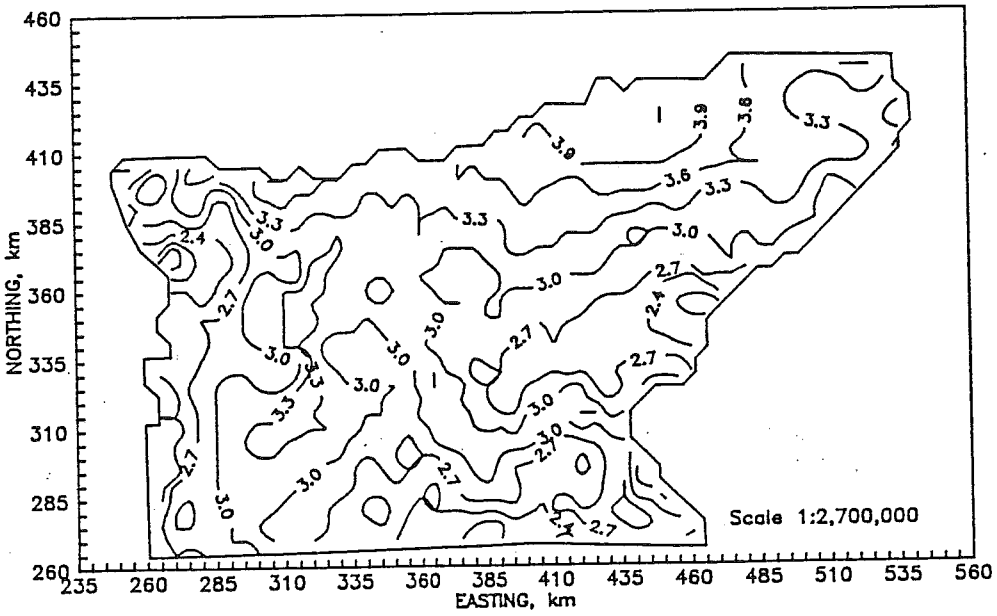

FIGURE 15. (continued). April.

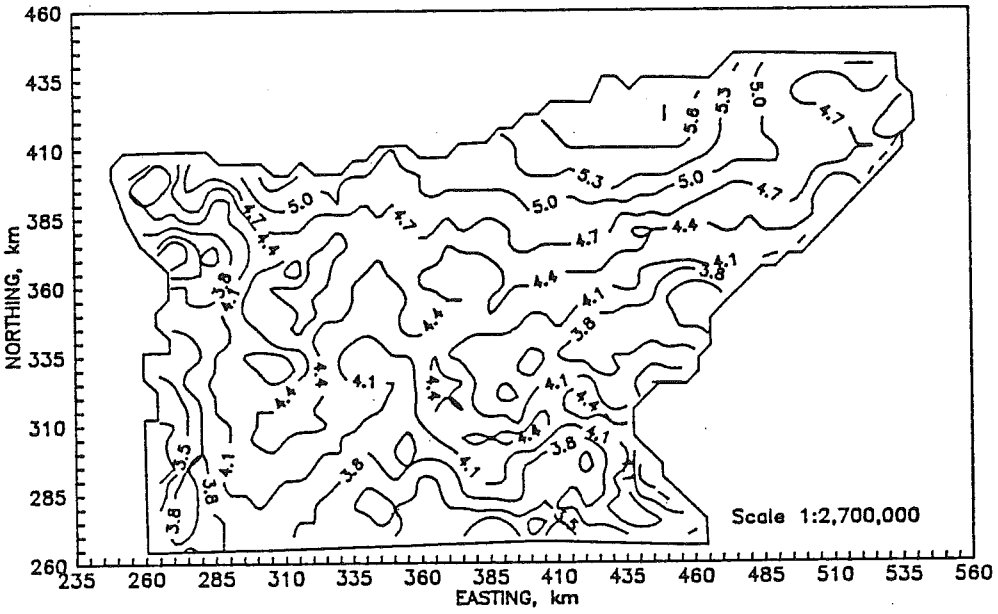

FIGURE 15. (continued). May.

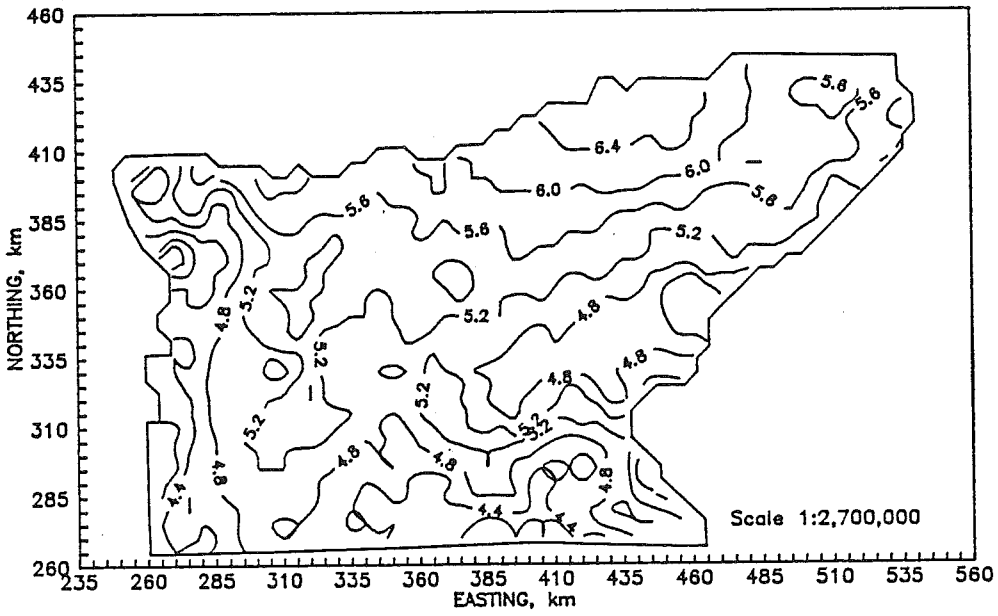

FIGURE 15. (continued). June.

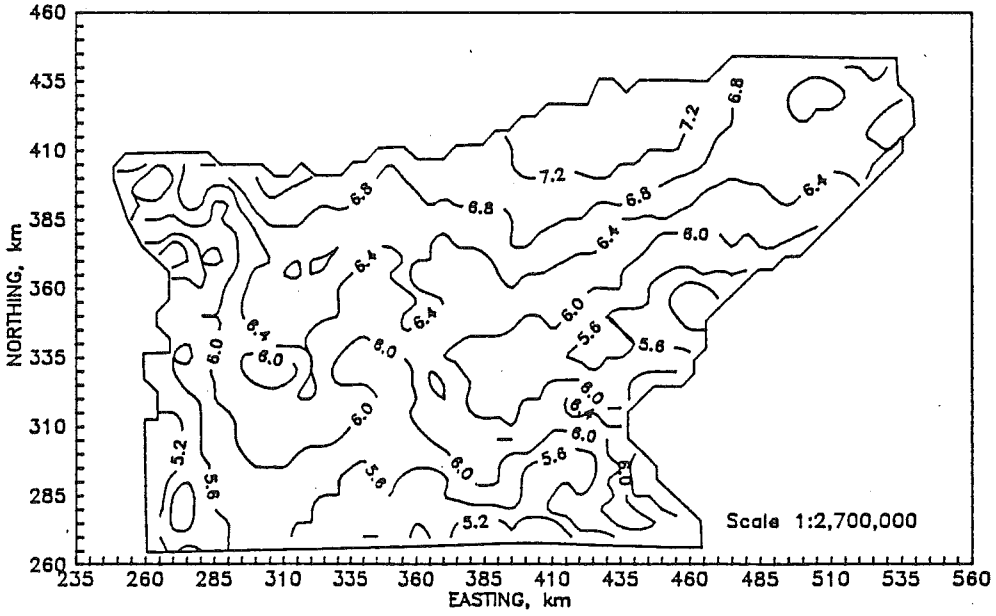

FIGURE 15. (continued). July.

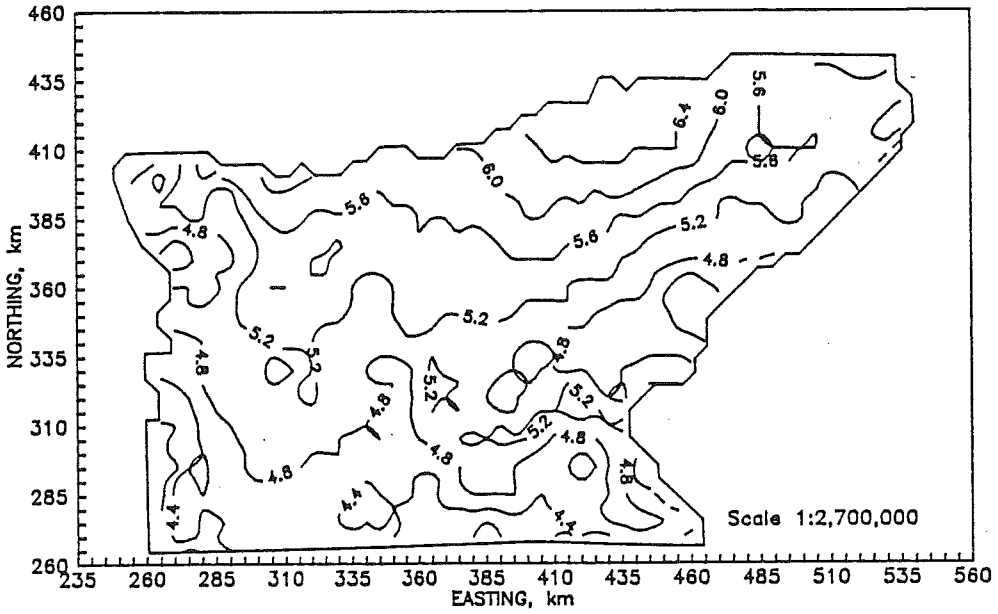

FIGURE 15. (continued). August.

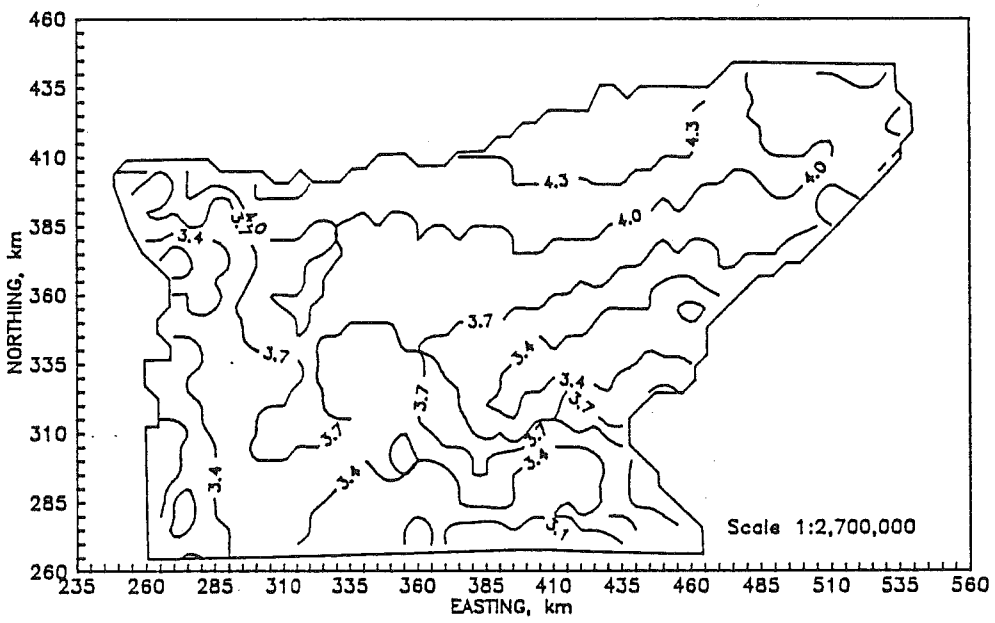

FIGURE 15. (continued). September.

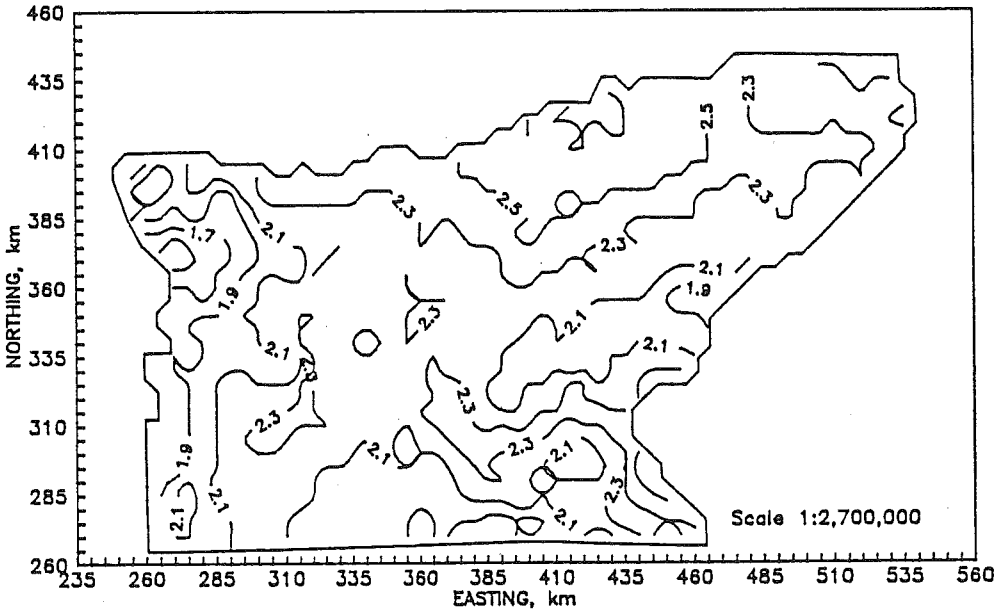

FIGURE 15. (continued). October.

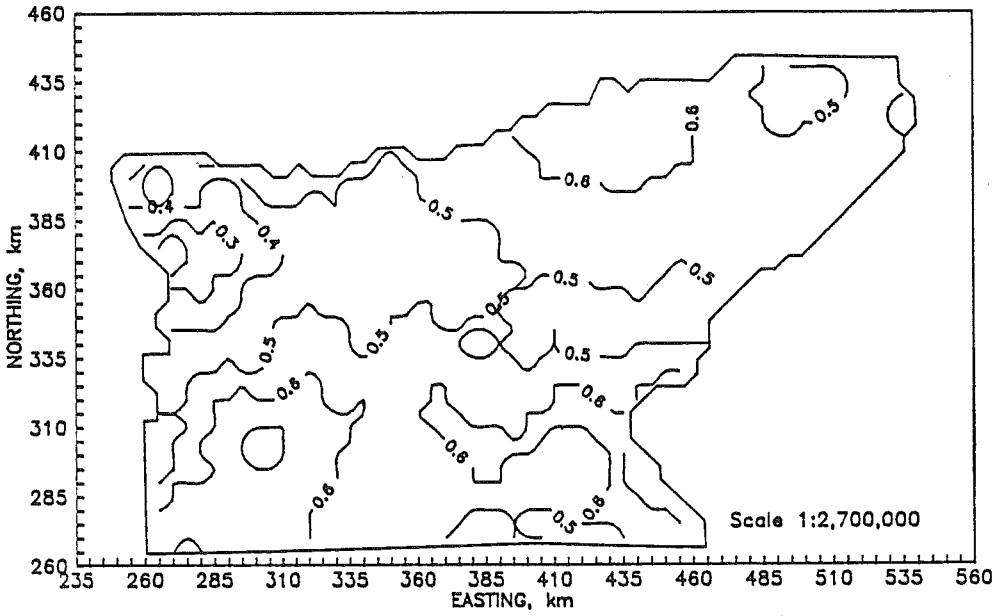

FIGURE 15. (continued). November.

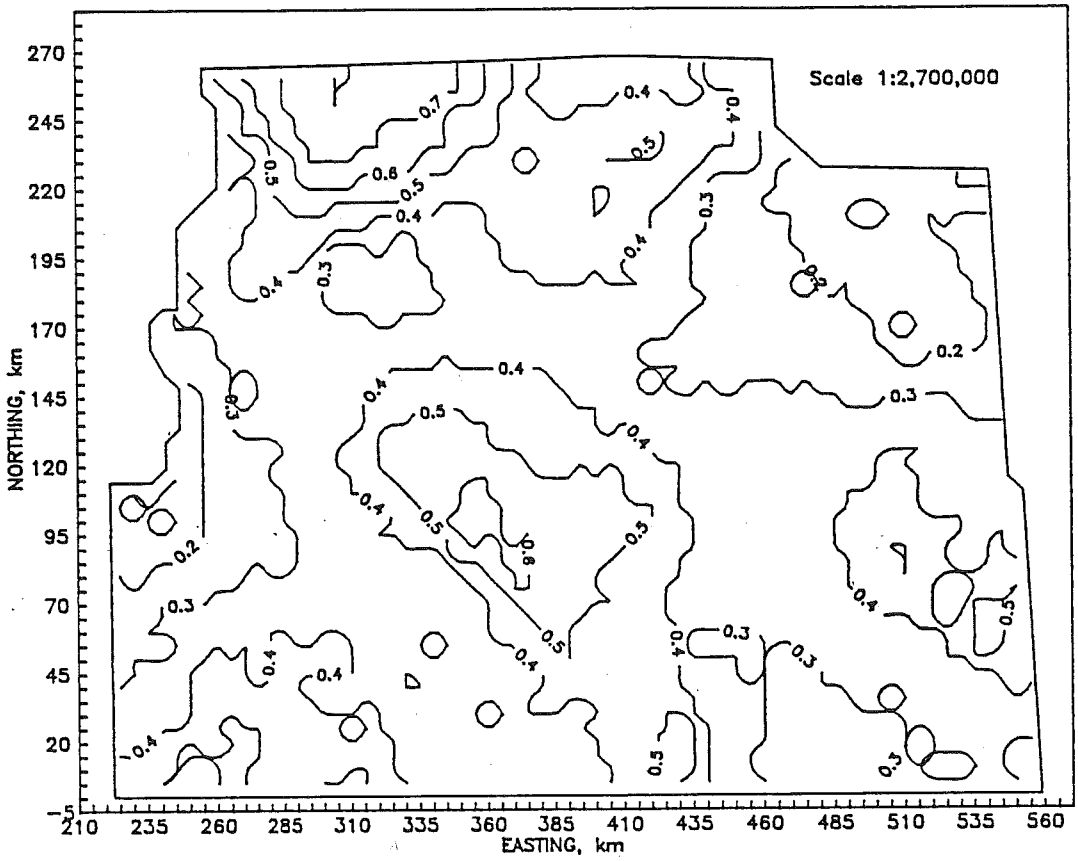

FIGURE 16. Contour maps of cokriged monthly ET_r, $mm\ d^{-1}$, for region 5. February.

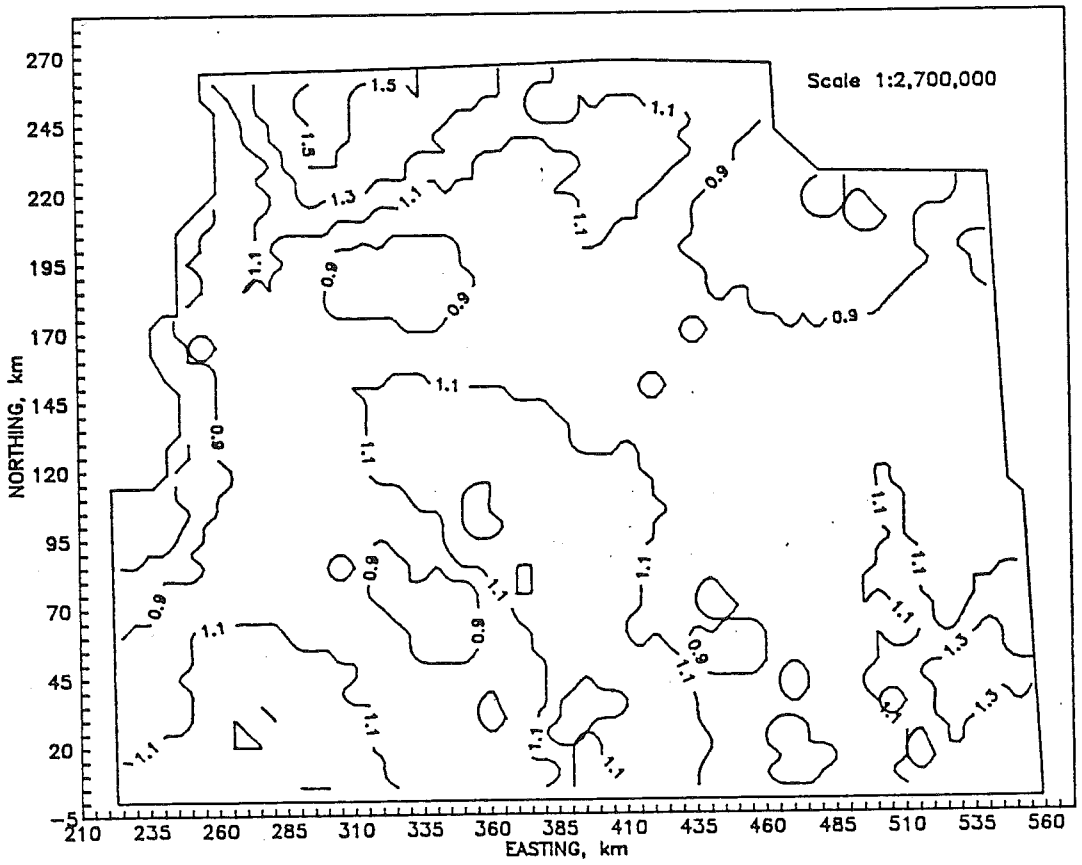

FIGURE 16. (continued). March.

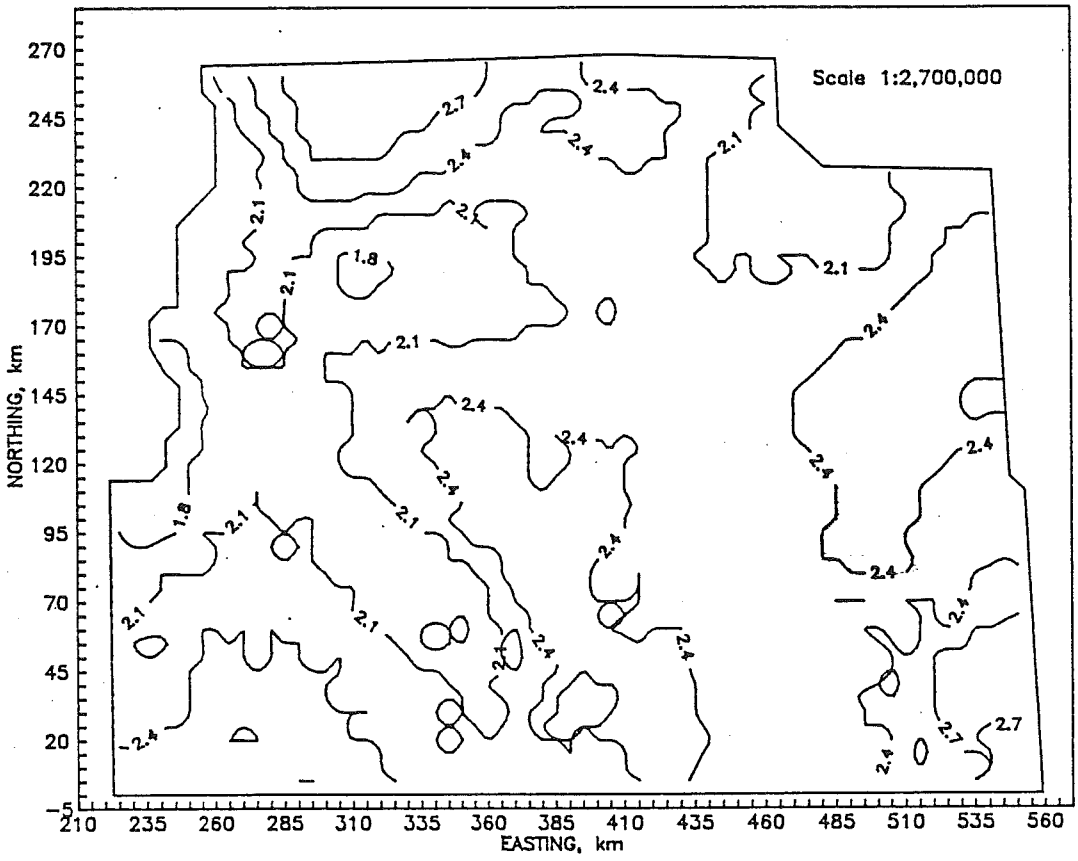

FIGURE 16. (continued). April.

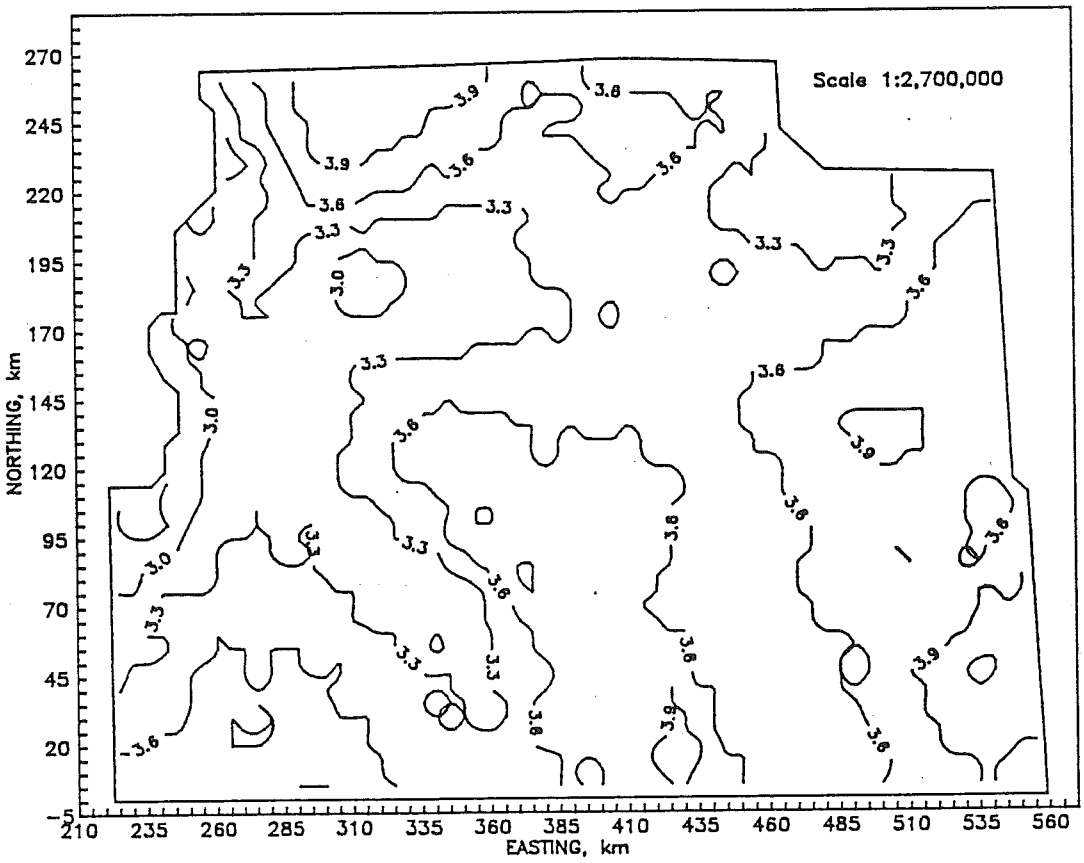

FIGURE 16. (continued). May.

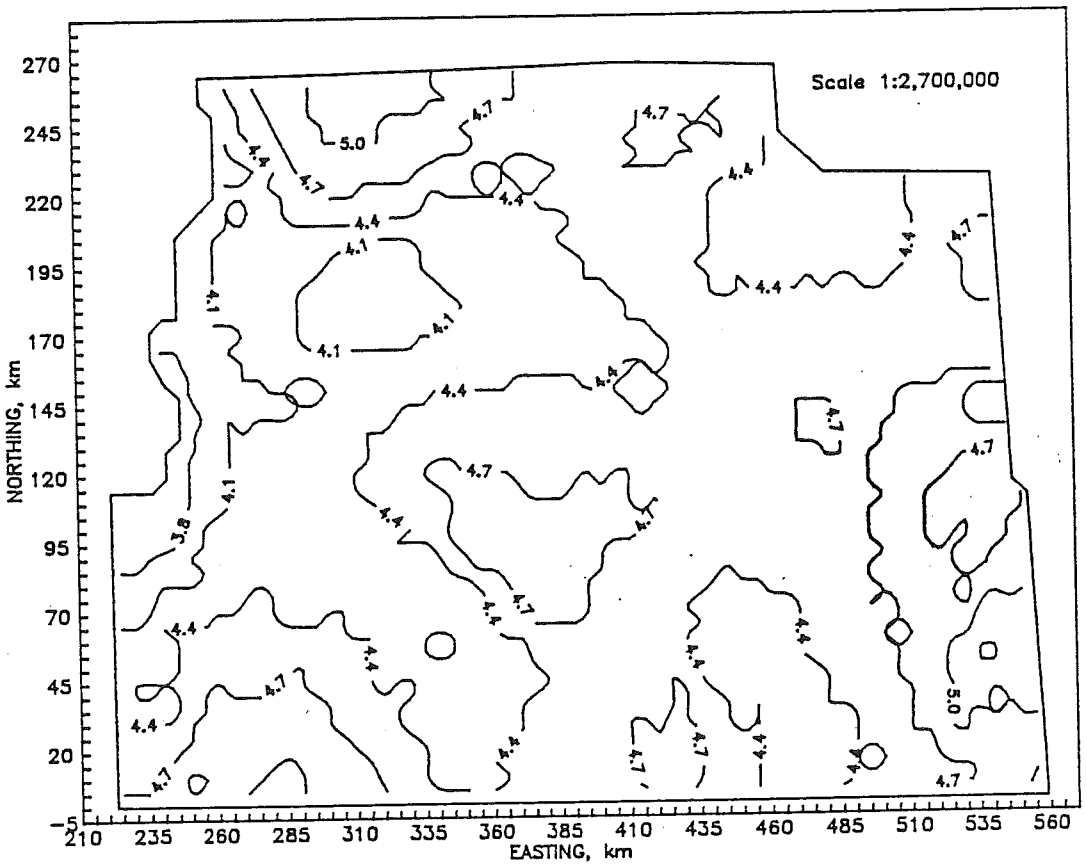

FIGURE 16. (continued). June.

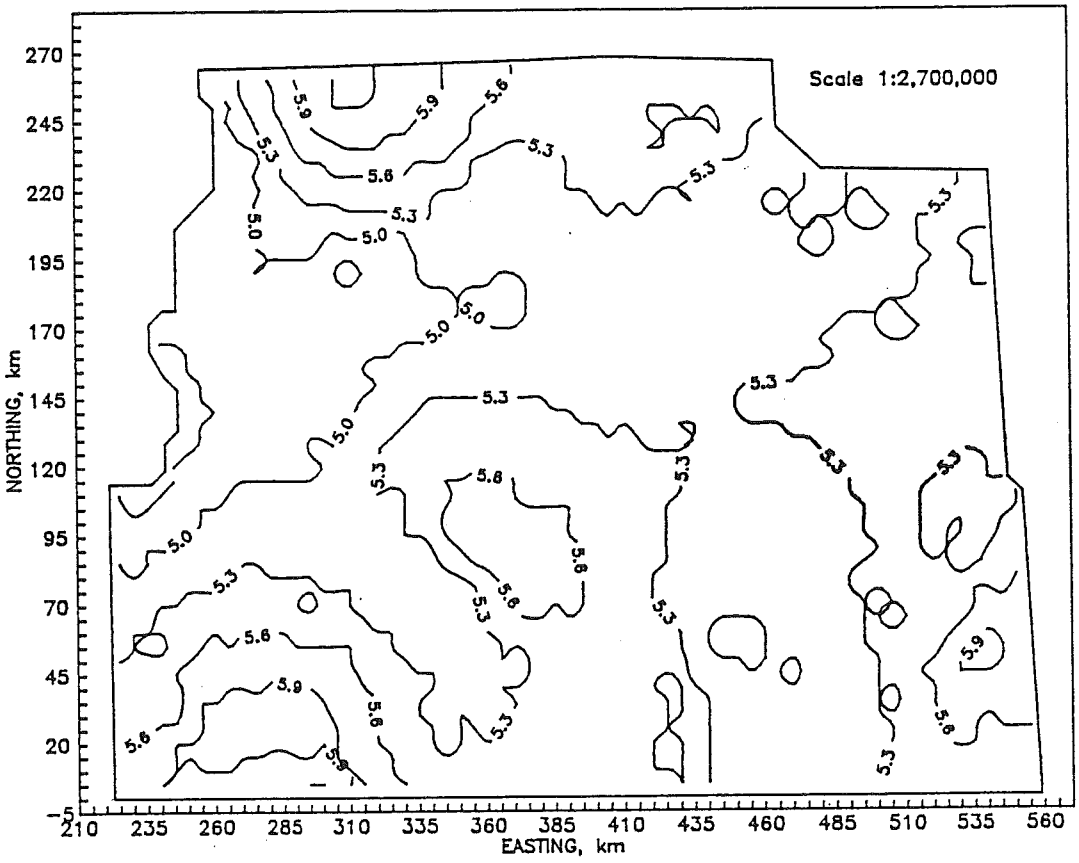

FIGURE 16. (continued). July.

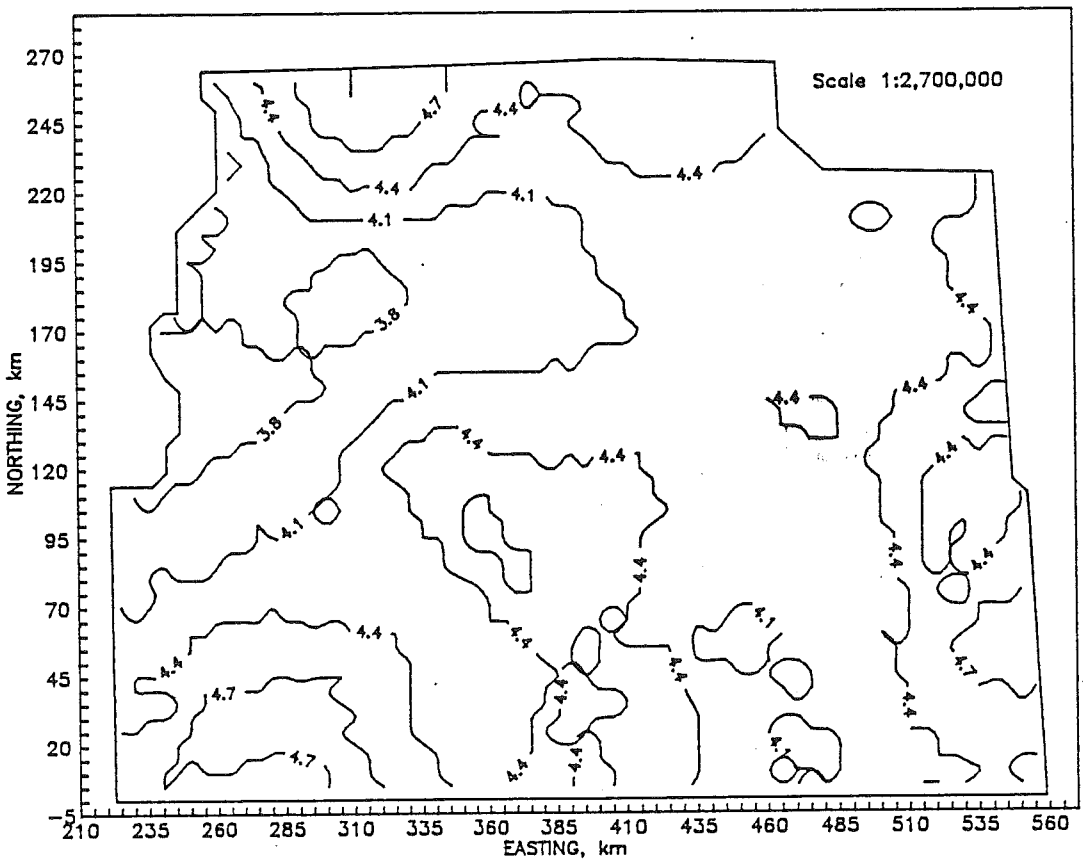

FIGURE 16. (continued). August.

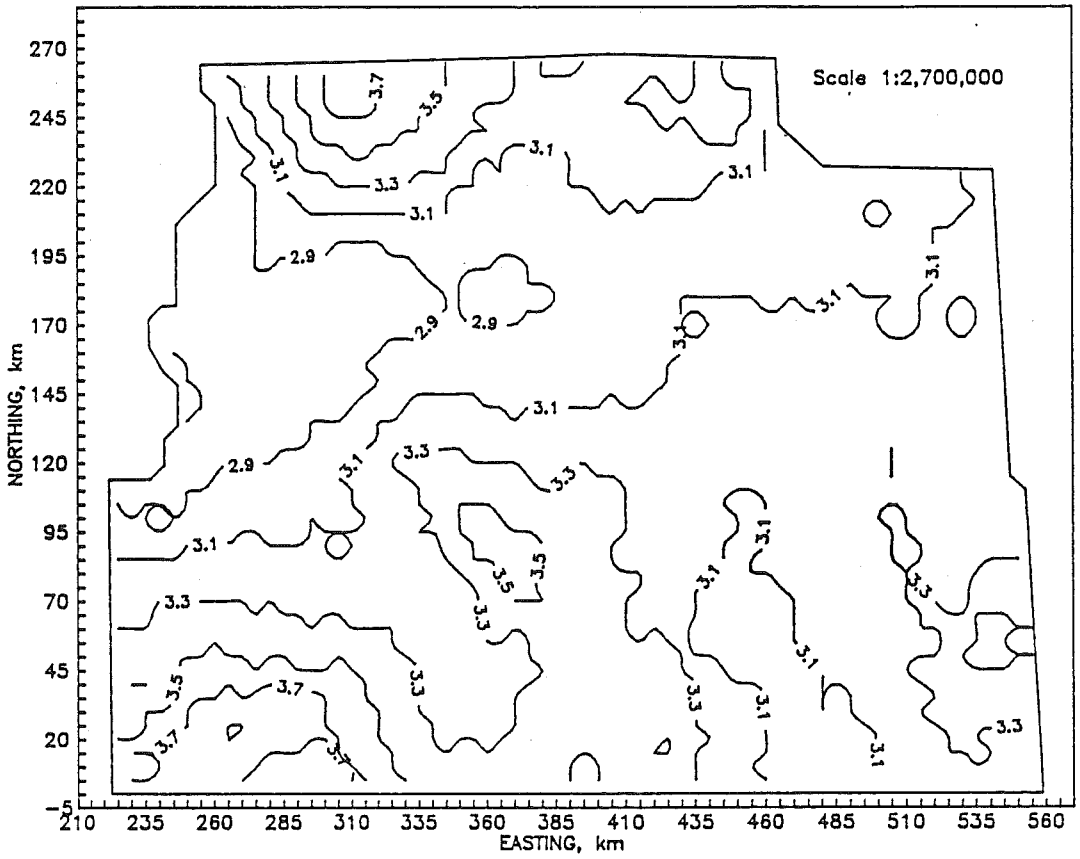

FIGURE 16. (continued). September.

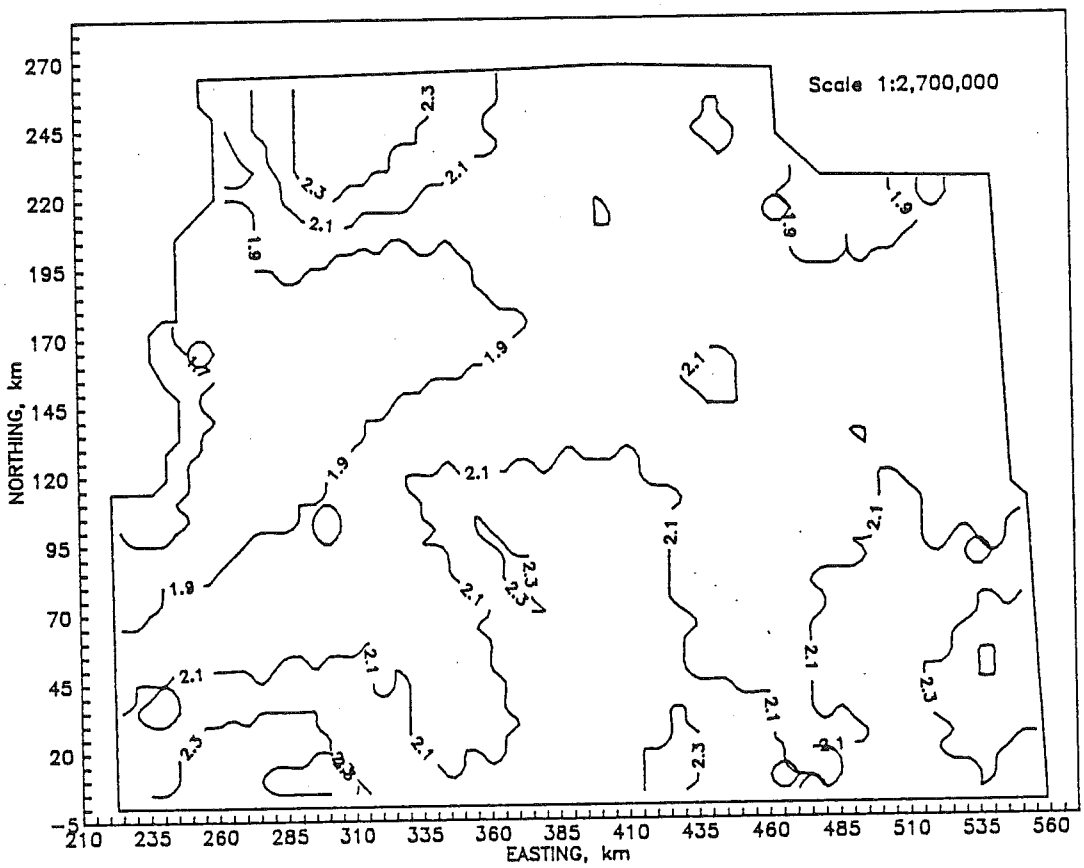

FIGURE 16. (continued). October.

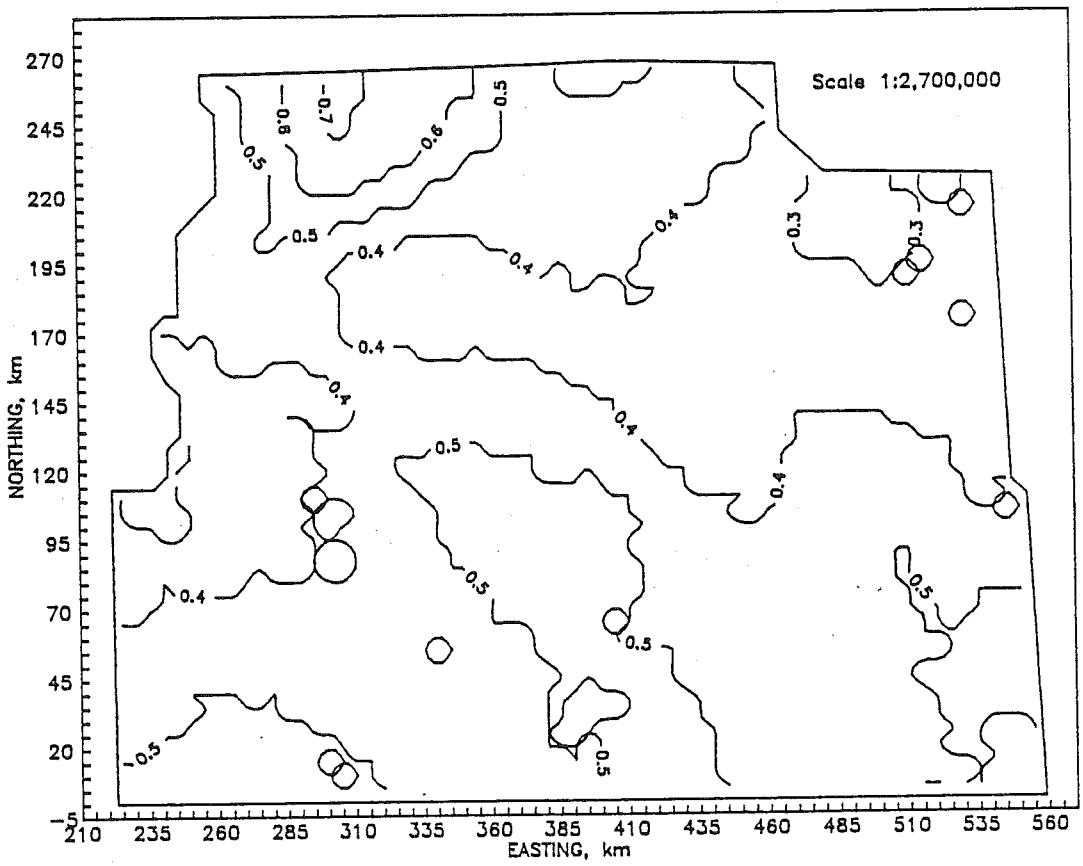

FIGURE 16. (continued). November.

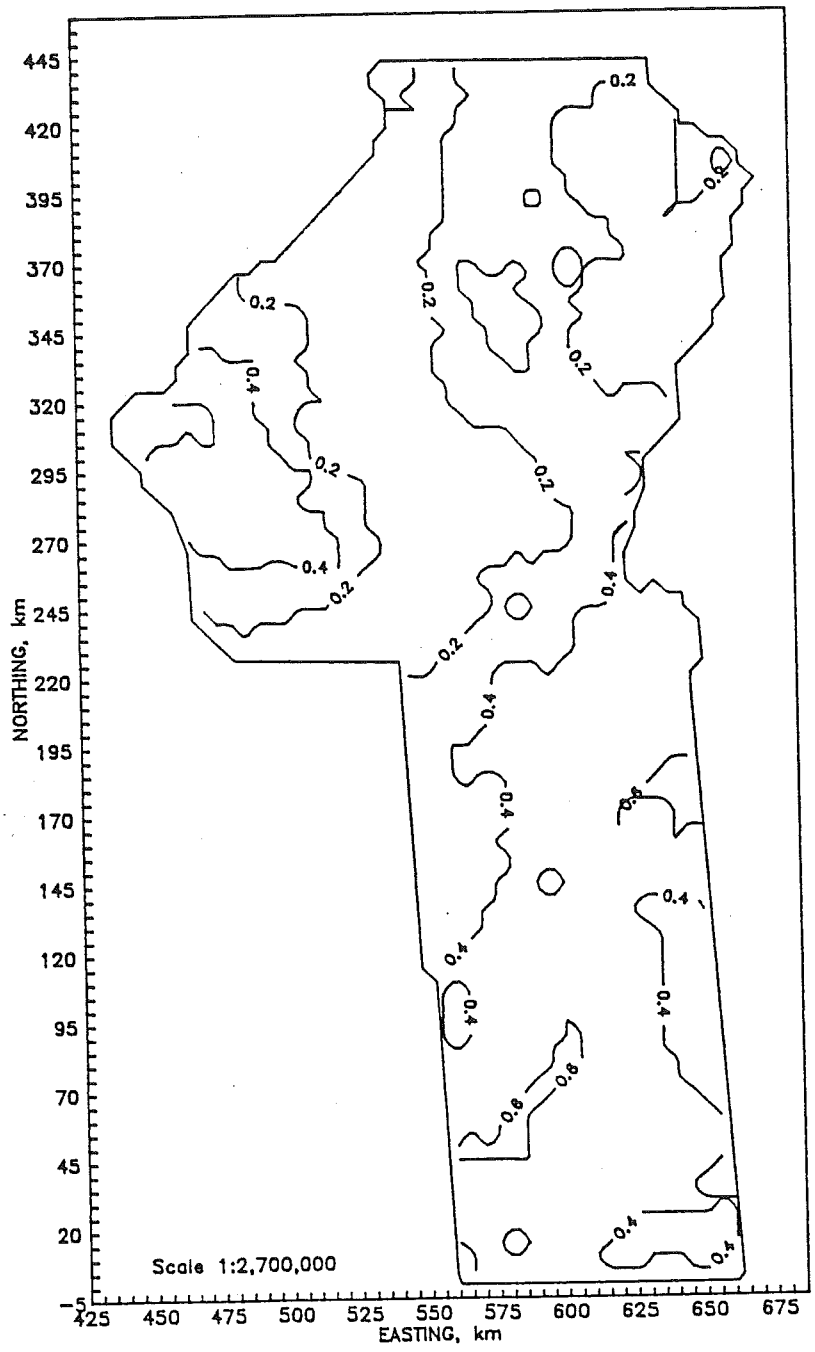

FIGURE 17. Contour maps of cokriged monthly ET_r, $mm\ d^{-1}$, for region 6. February.

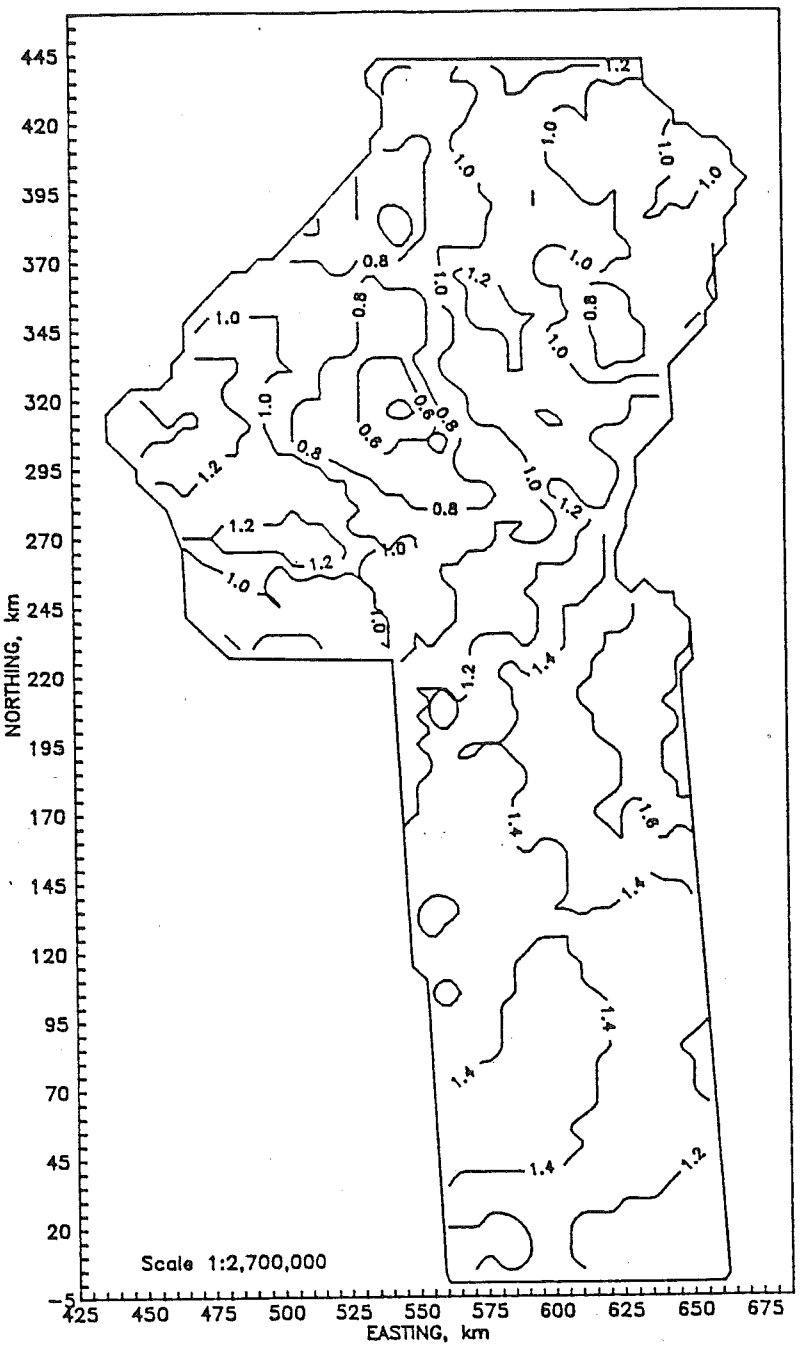

FIGURE 17. (continued). March.

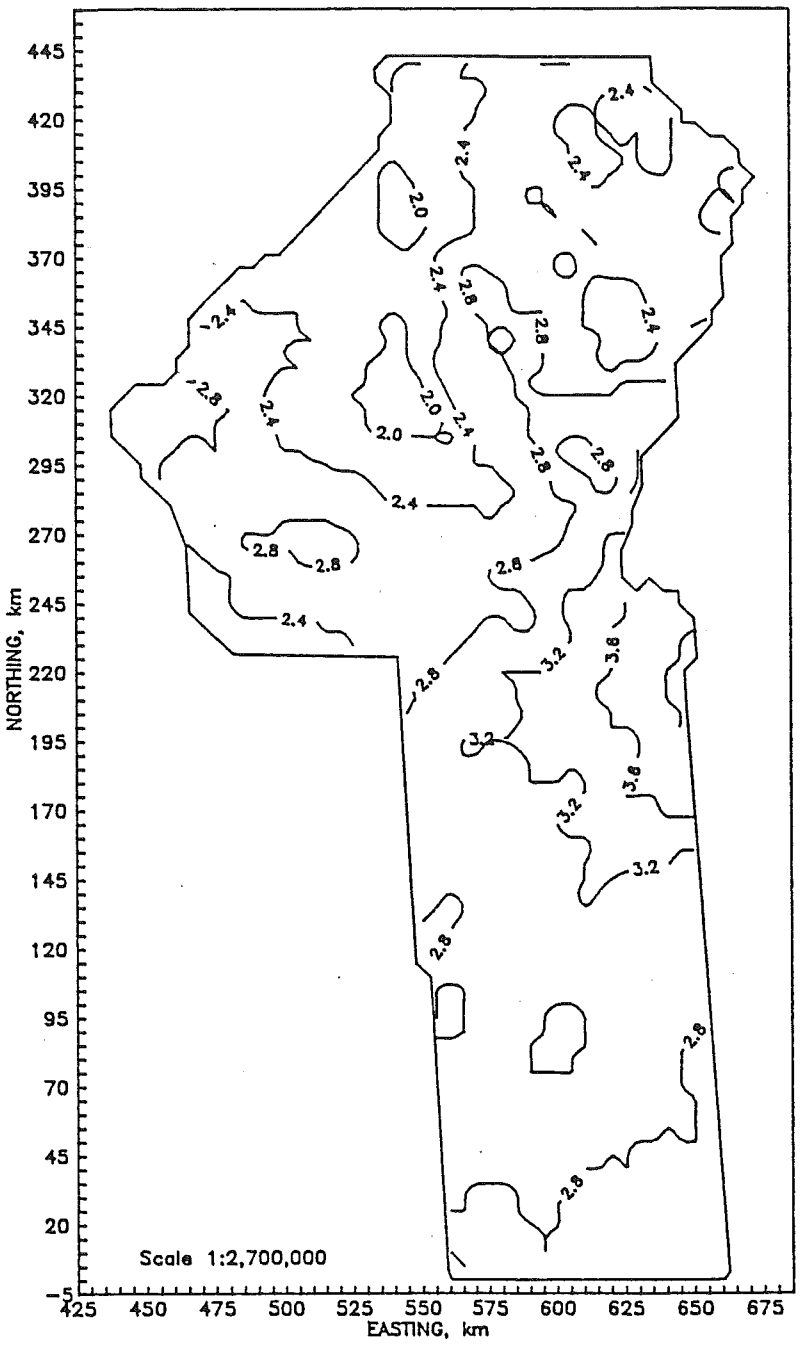

FIGURE 17. (continued). April.

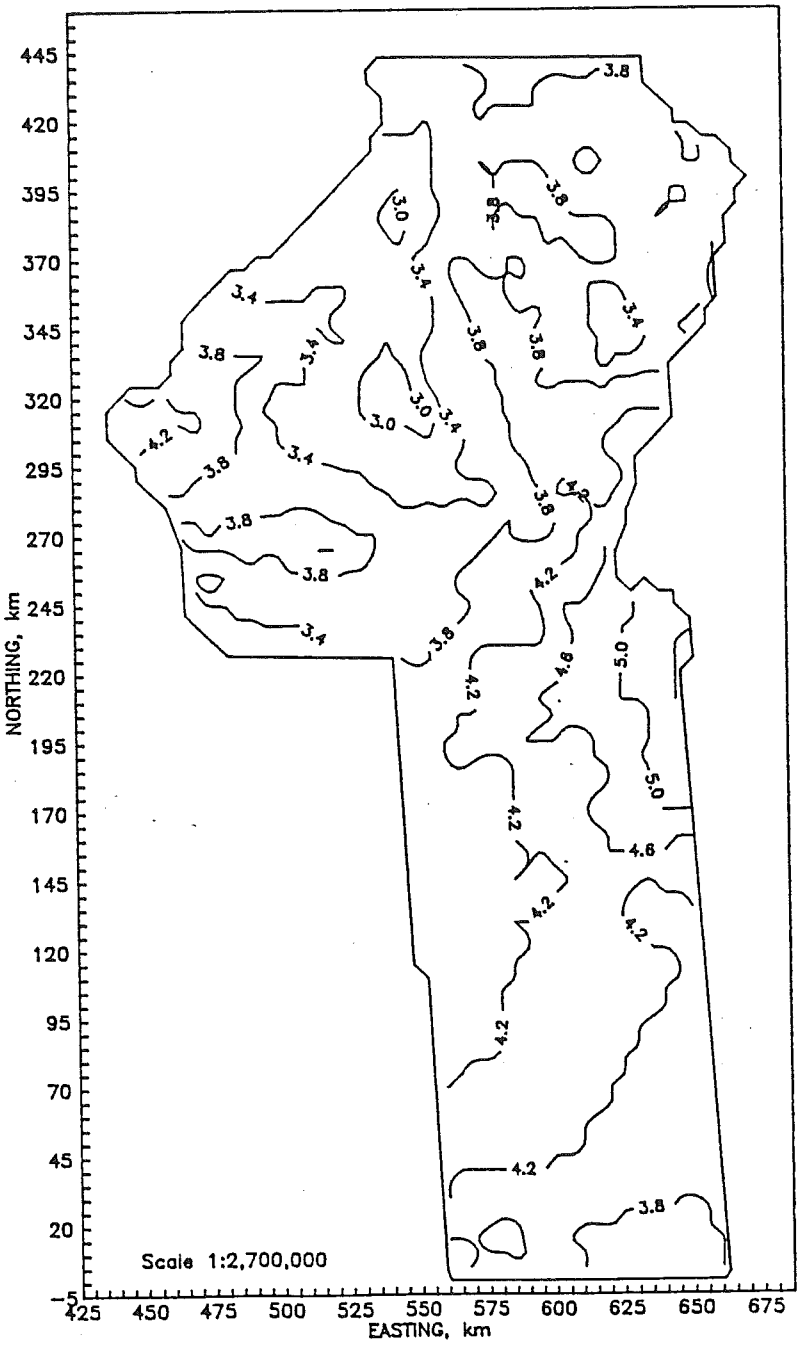

FIGURE 17. (continued). May.

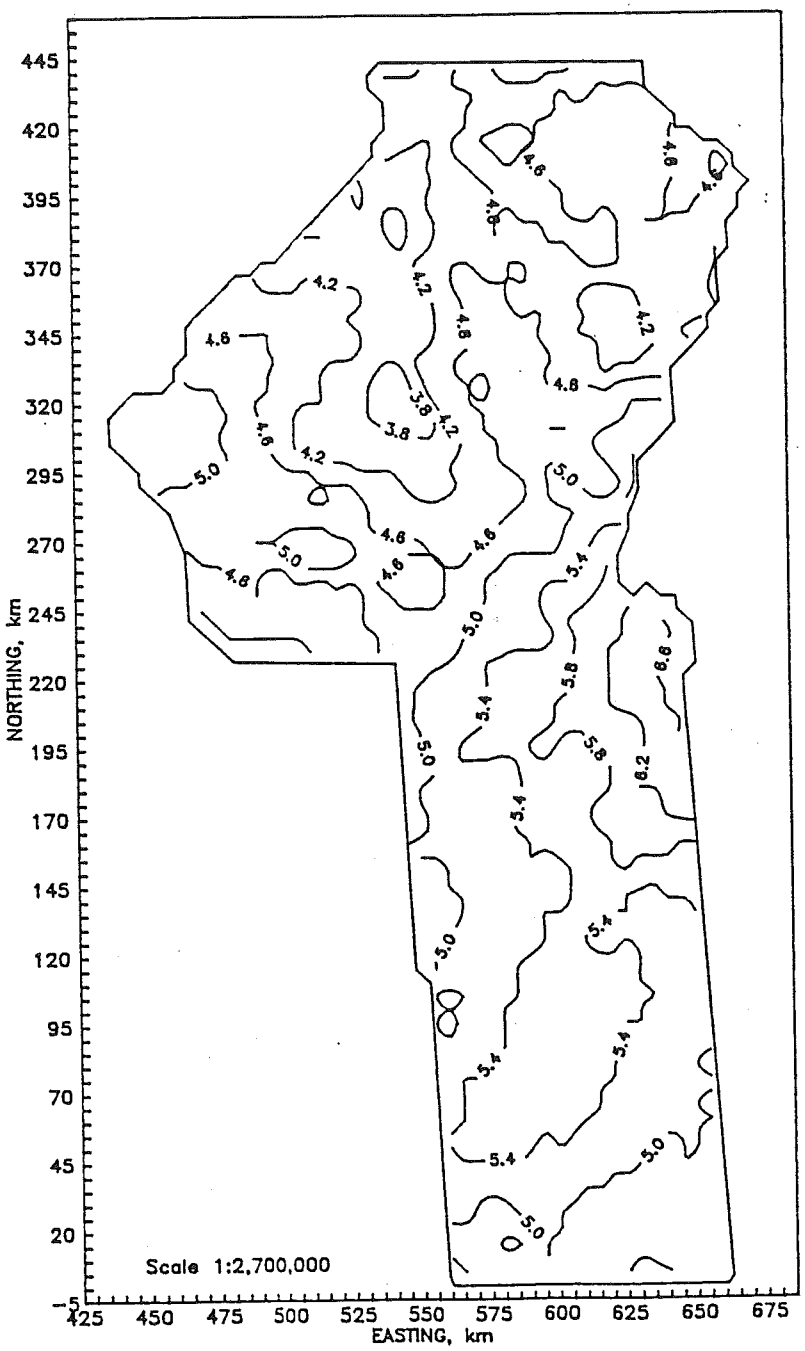

FIGURE 17. (continued). June.

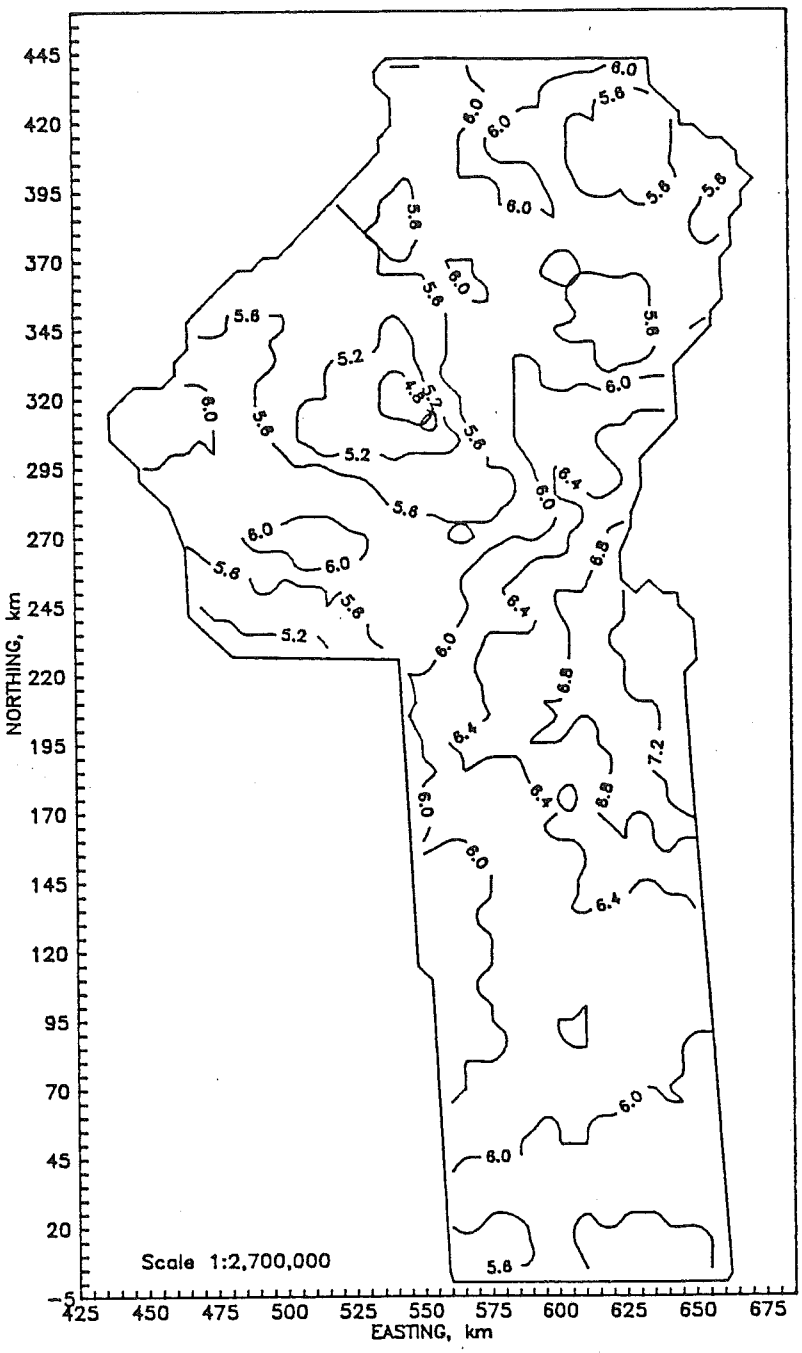

FIGURE 17. (continued). July.

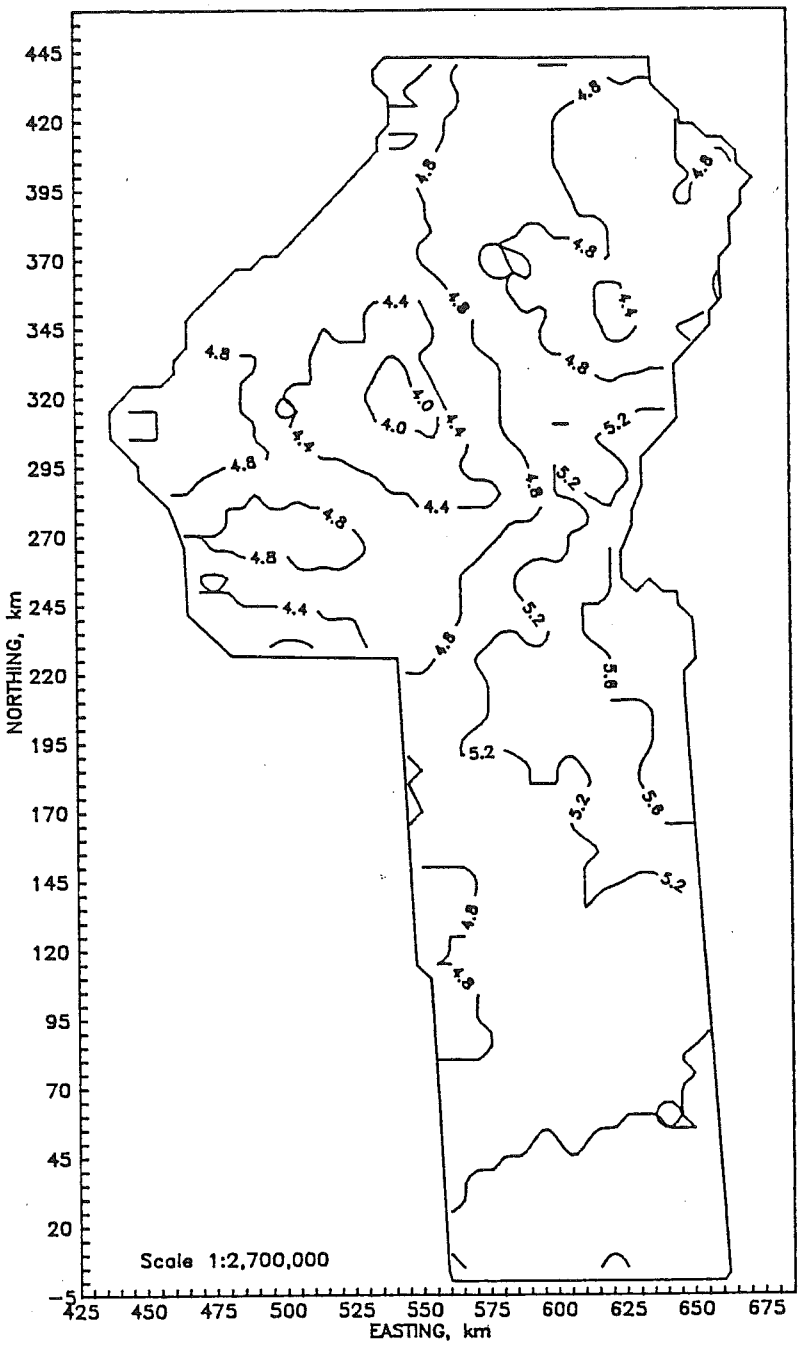

FIGURE 17. (continued). August.

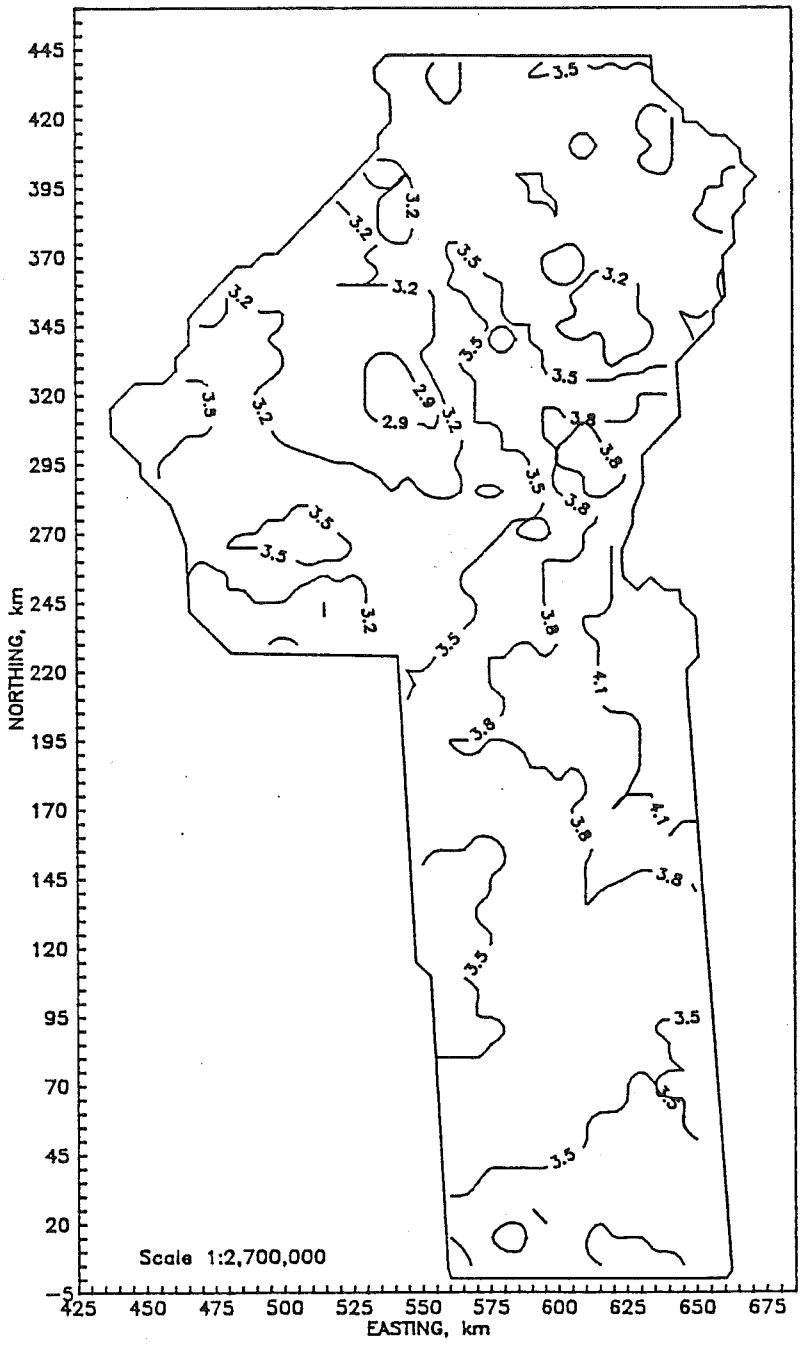

FIGURE 17. (continued). September.

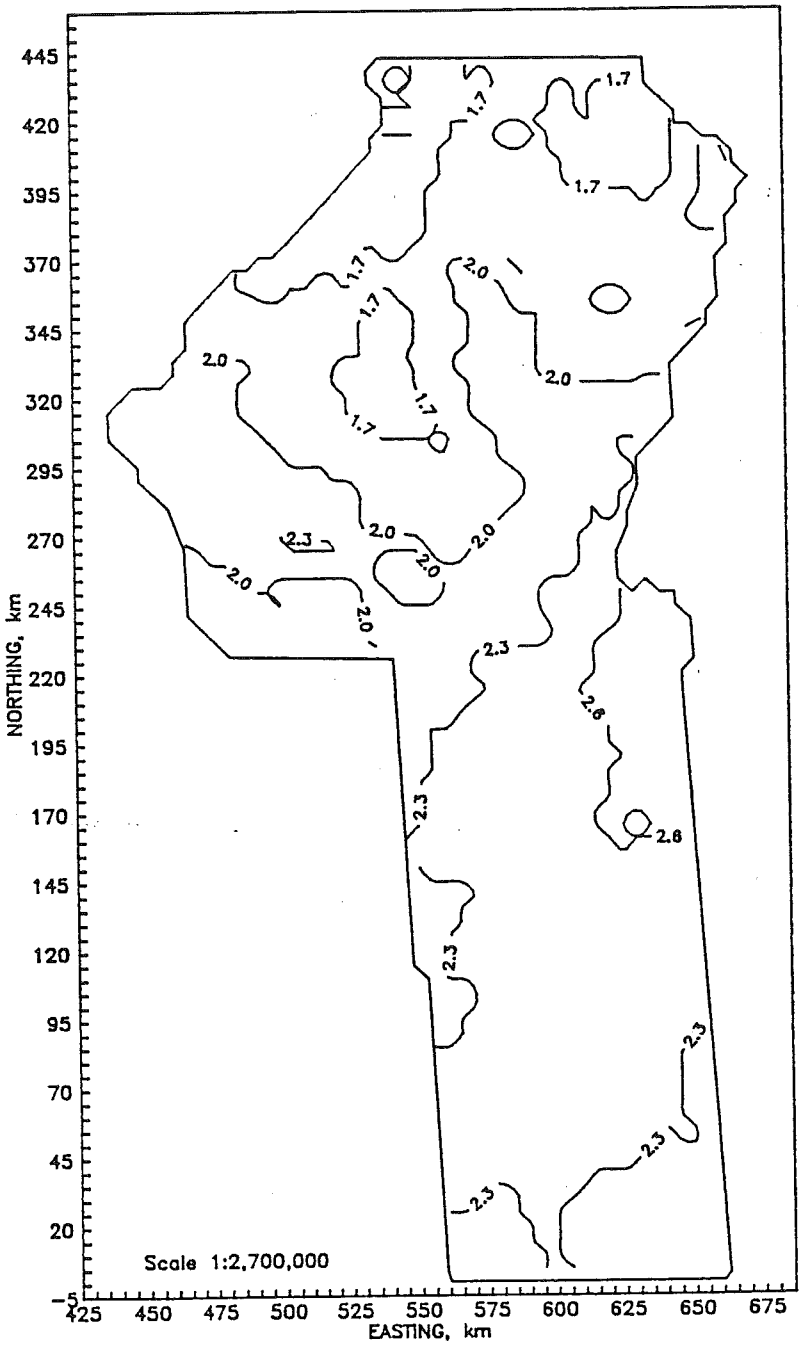

FIGURE 17. (continued). October.

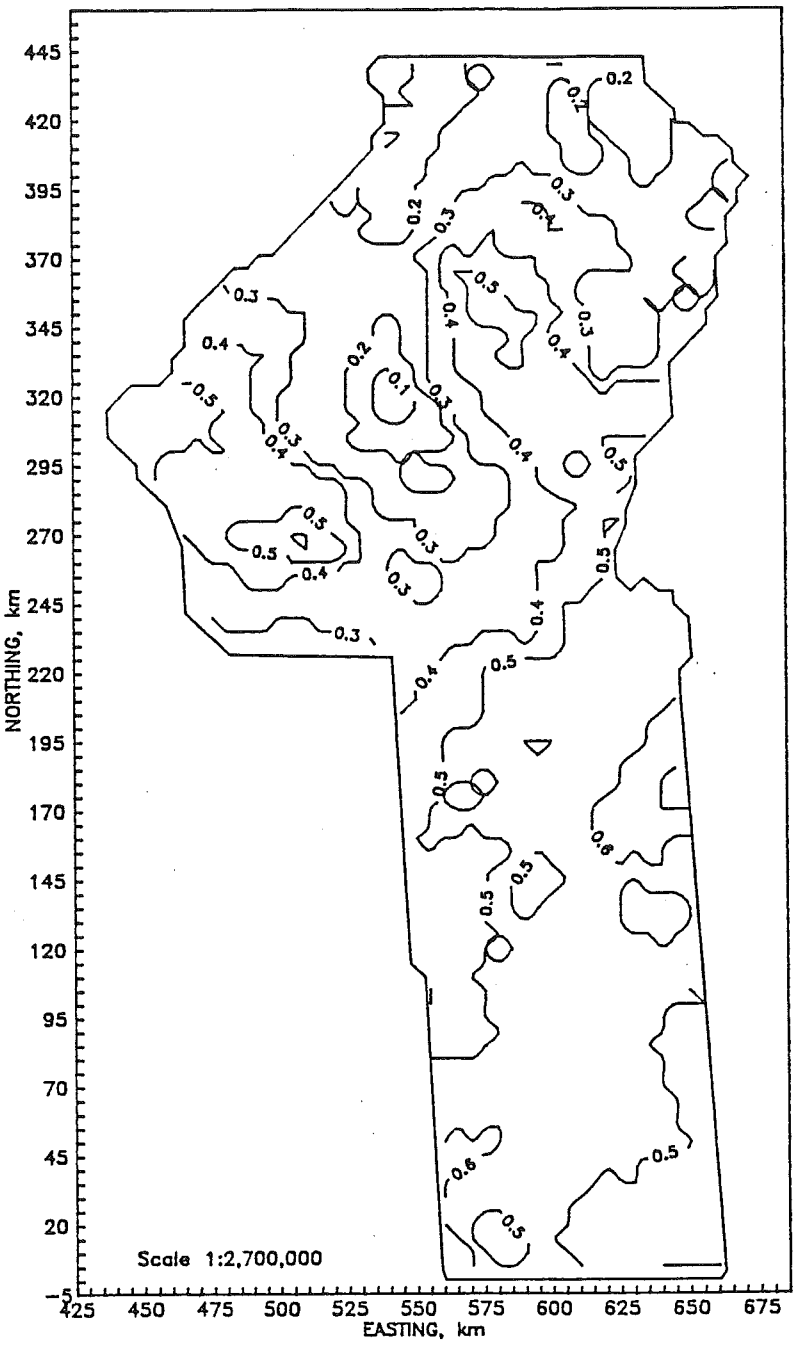

FIGURE 17. (continued). November.

Table 14 lists the maximum, minimum and average values of the kriging and cokriging standard deviations for the four regions under study. The percent difference between kriging and cokriging standard deviations, based on the kriging standard deviation, is also provided. In all regions, a consistent decrease in the maxima and averages of the estimation error standard deviations was noticed for cokriging in all study cases. No differences were observed for the minimum values. The minimum estimation errors could be expected in locations at lower elevation where the influence of elevation is less significant. In those locations, less differences could be expected between kriging and cokriging and maximum values of ET_r should be expected due to the inverse correlation between ET_r and elevation. This could also explain why no differences were observed for the maximum values of the kriged and cokriged ET_r estimates.

TABLE 14. Comparison of kriging and cokriging standard deviations. Region 2.

	Maximum[1]		*mm d^{-1}*	Minimum[1]		*mm d^{-1}*	Average[1]		*mm d^{-1}*
Month	Krig.	Cokg.	Diff. %	Krig.	Cokg.	Diff. %	Krig.	Cokg.	Diff. %
February	0.179	0.133	-26.00	0.019	0.019	-1.77	0.092	0.060	-34.71
March	0.273	0.211	-22.48	0.048	0.048	-1.11	0.143	0.103	-28.39
April	0.400	0.319	-20.18	0.097	0.095	-1.29	0.222	0.166	-25.49
May	0.412	0.322	-21.84	0.097	0.096	-1.46	0.229	0.165	-27.82
June	0.378	0.290	-23.27	0.152	0.143	-6.31	0.234	0.173	-26.08
July	0.389	0.314	-19.19	0.153	0.147	-3.74	0.236	0.188	-20.59
August	0.369	0.301	-18.25	0.156	0.148	-5.11	0.232	0.181	-22.13
September	0.295	0.234	-20.69	0.124	0.117	-5.28	0.184	0.143	-22.53
October	0.192	0.158	-17.53	0.104	0.099	-5.09	0.131	0.111	-15.10
November	0.111	0.090	-19.51	0.040	0.039	-2.60	0.065	0.052	-20.08
Cumulative	88	69	-22.13	20	20	-1.39	49	35	-28.48

[1] For cumulative ET_r, *mm*

TABLE 14. (continued). Region 4.

Month	Maximum[1] mm d^{-1} Krig.	Cokg.	Diff. %	Minimum[1] mm d^{-1} Krig.	Cokg.	Diff. %	Average[1] mm d^{-1} Krig.	Cokg.	Diff. %
February	0.191	0.137	-27.93	0.090	0.084	-7.15	0.130	0.095	-26.77
March	0.308	0.197	-36.08	0.116	0.109	-6.20	0.191	0.137	-28.16
April	0.516	0.317	-38.54	0.150	0.143	-4.57	0.301	0.209	-30.41
May	0.581	0.347	-40.28	0.194	0.180	-6.84	0.337	0.237	-29.48
June	0.669	0.412	-38.37	0.319	0.298	-6.68	0.436	0.329	-24.43
July	0.636	0.428	-32.78	0.262	0.249	-5.15	0.392	0.306	-21.85
August	0.613	0.444	-27.59	0.278	0.266	-4.22	0.389	0.321	-17.42
September	0.394	0.254	-35.39	0.195	0.184	-5.83	0.260	0.205	-21.08
October	0.272	0.188	-30.77	0.105	0.100	-5.31	0.168	0.128	-23.99
November	0.123	0.108	-12.34	0.057	0.056	-2.07	0.081	0.073	-9.61
Cumulative	123	77	-37.95	57	53	-6.84	79	59	-25.34

[1] For cumulative ET_r, *mm*

TABLE 14. (continued). Region 5.

Month	Maximum[1] mm d^{-1} Krig.	Cokg.	Diff. %	Minimum[1] mm d^{-1} Krig.	Cokg.	Diff. %	Average[1] mm d^{-1} Krig.	Cokg.	Diff. %
February	0.191	0.171	-10.46	0.045	0.044	-0.40	0.112	0.104	-6.75
March	0.249	0.211	-15.14	0.047	0.047	-0.74	0.141	0.123	-12.62
April	0.366	0.299	-18.21	0.169	0.167	-1.21	0.243	0.213	-12.36
May	0.386	0.319	-17.29	0.130	0.129	-0.78	0.236	0.209	-11.39
June	0.409	0.349	-14.68	0.098	0.098	-0.57	0.237	0.214	-9.59
July	0.436	0.377	-13.56	0.120	0.120	-0.55	0.255	0.233	-8.47
August	0.401	0.365	-9.08	0.130	0.130	-0.41	0.243	0.230	-5.46
September	0.330	0.302	-8.45	0.086	0.086	-0.32	0.192	0.182	-5.08
October	0.233	0.210	-9.65	0.046	0.046	-0.35	0.129	0.122	-5.81
November	0.116	0.105	-9.73	0.041	0.040	-0.43	0.070	0.066	-5.48
Cumulative	87	73	-17.11	14	14	-0.75	49	43	-11.77

[1] For cumulative ET_r, *mm*

TABLE 14. (continued). Region 6.

Month	Maximum[1]		mm d^{-1}	Minimum[1]		mm d^{-1}	Average[1]		mm d^{-1}
	Krig.	Cokg.	Diff. %	Krig.	Cokg.	Diff. %	Krig.	Cokg.	Diff. %
February	0.271	0.232	-14.54	0.026	0.026	-1.31	0.130	0.115	-10.97
March	0.393	0.295	-24.91	0.127	0.125	-1.56	0.215	0.191	-11.23
April	0.655	0.502	-23.32	0.191	0.188	-1.40	0.342	0.307	-10.41
May	0.730	0.573	-21.57	0.103	0.102	-0.75	0.345	0.308	-10.80
June	0.827	0.621	-24.94	0.077	0.076	-1.29	0.375	0.330	-12.21
July	0.802	0.618	-22.94	0.219	0.216	-1.35	0.408	0.367	-10.13
August	0.625	0.497	-20.47	0.203	0.200	-1.23	0.339	0.308	-9.01
September	0.515	0.356	-30.97	0.237	0.232	-1.88	0.313	0.278	-11.21
October	0.417	0.341	-18.33	0.171	0.169	-1.01	0.240	0.224	-6.70
November	0.226	0.197	-12.86	0.072	0.072	-1.16	0.119	0.109	-7.84
Cumulative	160	116	-27.12	44	44	-1.57	82	72	-11.81

[1] For cumulative ET_r, *mm*

The differences between kriging and cokriging standard deviations were larger for regions 2 and 4, where higher correlation coefficients between the two analyzed variables were noticed. In these two regions, averages of cokriging standard deviations generally were between 20 to 30 % lower than kriging standard deviations. In region 2, the highest decrease in the average was observed in February (35 %) and the lowest decrease was observed in October (15 %). The decrease for cumulative ET_r was 28 %. In region 4, the highest decrease in the average was observed in April (30 %) and the lowest decrease was observed in November (10 %). The decrease for cumulative ET_r was 25 %. In regions 5 and 6, the decrease due to cokriging was between 5 to 13 % in region 5 and between 7 to 12 % in region 6 for the average standard deviations. In region 5, the decrease in average ranged from 13 % for March to 5 % for September. The decrease for cumulative ET_r was 12 %. In region 6, the decrease in average ranged from 12 % for June and cumulative ET_r to 7 % in October.

These improvements due to cokriging are relatively low compared to those observed in a similar study performed in Nevada with total annual precipitation and elevation (Hevesi *et al.*, 1990). This may be due to the fact that evapotranspiration is modified by various factors, including biological ones, and has shorter spatial scale variations than precipitation. However, the original values of ET_r used in this project were themselves estimates. Thus, a higher "measurement" error may be expected in these values as compared with precipitation which was actually measured.

Figure 18 shows the contour maps of the kriging standard deviations of cumulative ET_r. Figure 19 shows the contour maps of the cokriging standard deviations of cumulative ET_r. For regions 2 and 4, there are important differences between kriging and cokriging. As indicated previously, the average cokriging standard deviation of cumulative ET_r decreased by about 25 to 28 % (Table 14) as compared with the average kriging standard deviation. Note in the maps the dense contouring of the kriging standard deviations and the large decrease of the contours in the vicinity of the weather stations. In cokriging, the standard deviations are very uniform and lower over each region, with the exception of the borders The decrease of the estimation errors in the vicinity of the weather stations was not as large as for kriging. This is particularly evident in region 4. Estimation errors increase at the borders for both kriging and cokriging, although these increases and the absolute values are still higher in kriging.

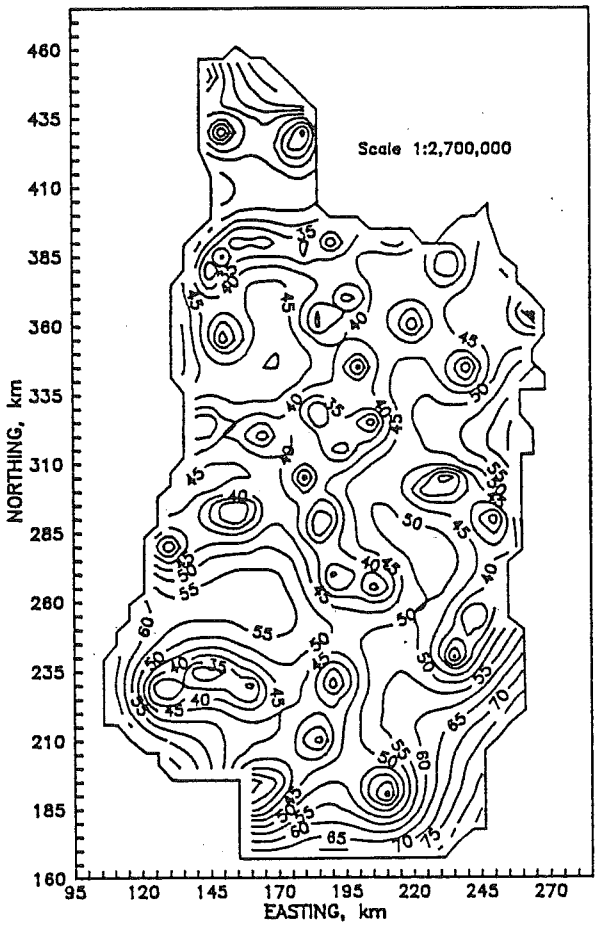

FIGURE 18. Contour maps of kriging standard deviation for cumulative ET_r, *mm*. Region 2.

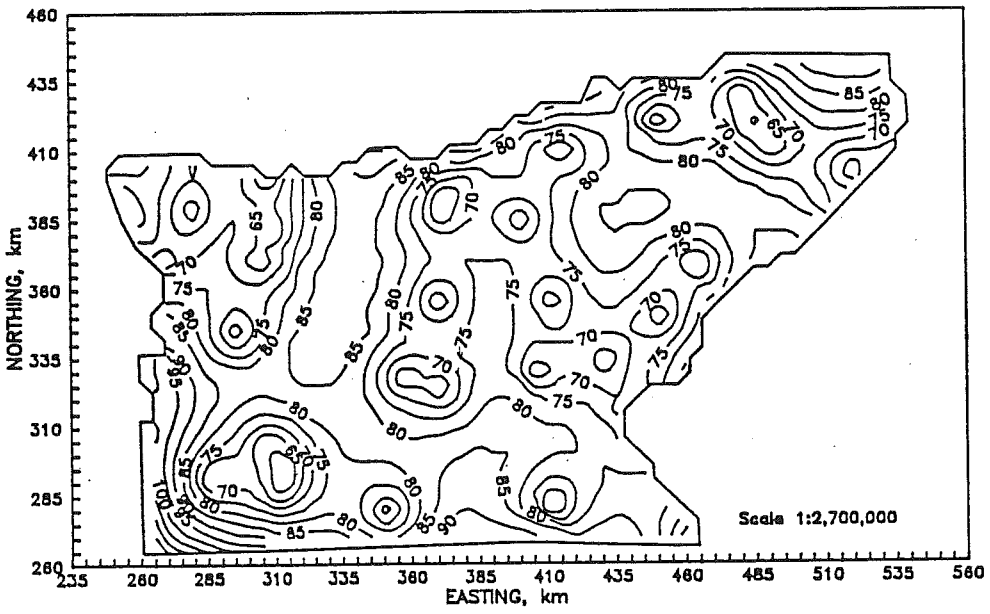

FIGURE 18. (continued). Region 4.

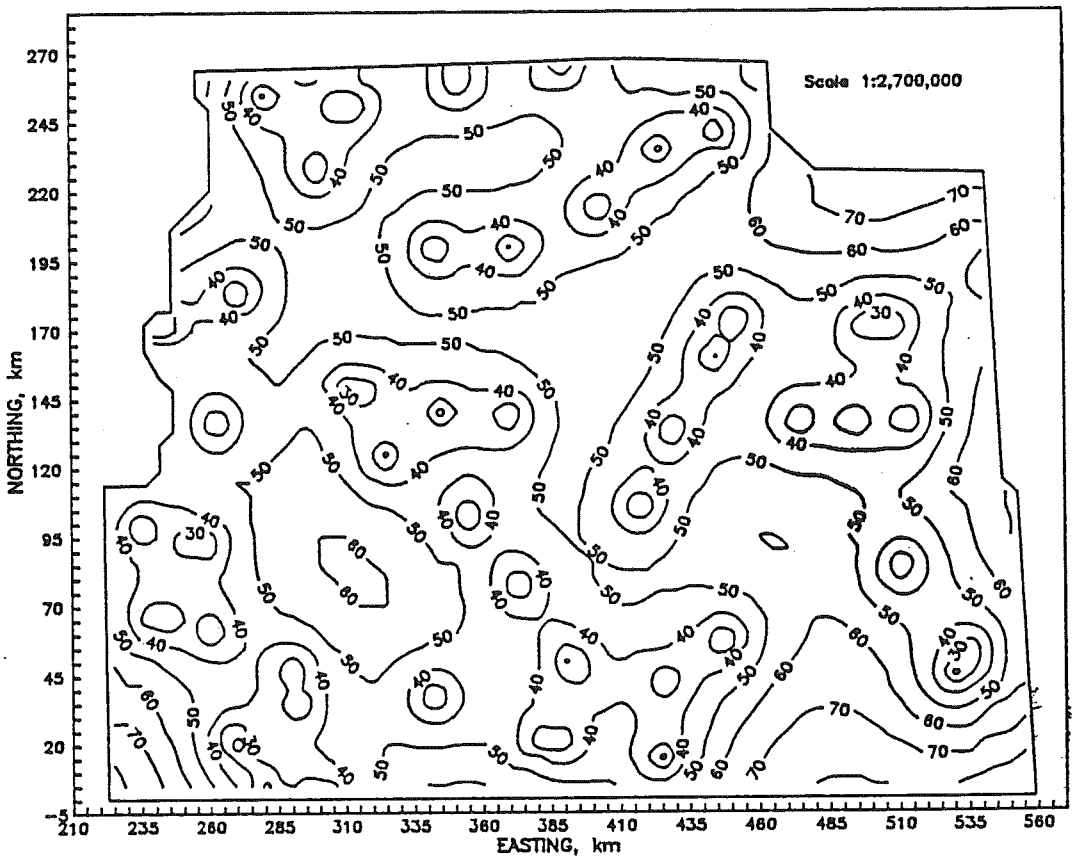

FIGURE 18. (continued). Region 5.

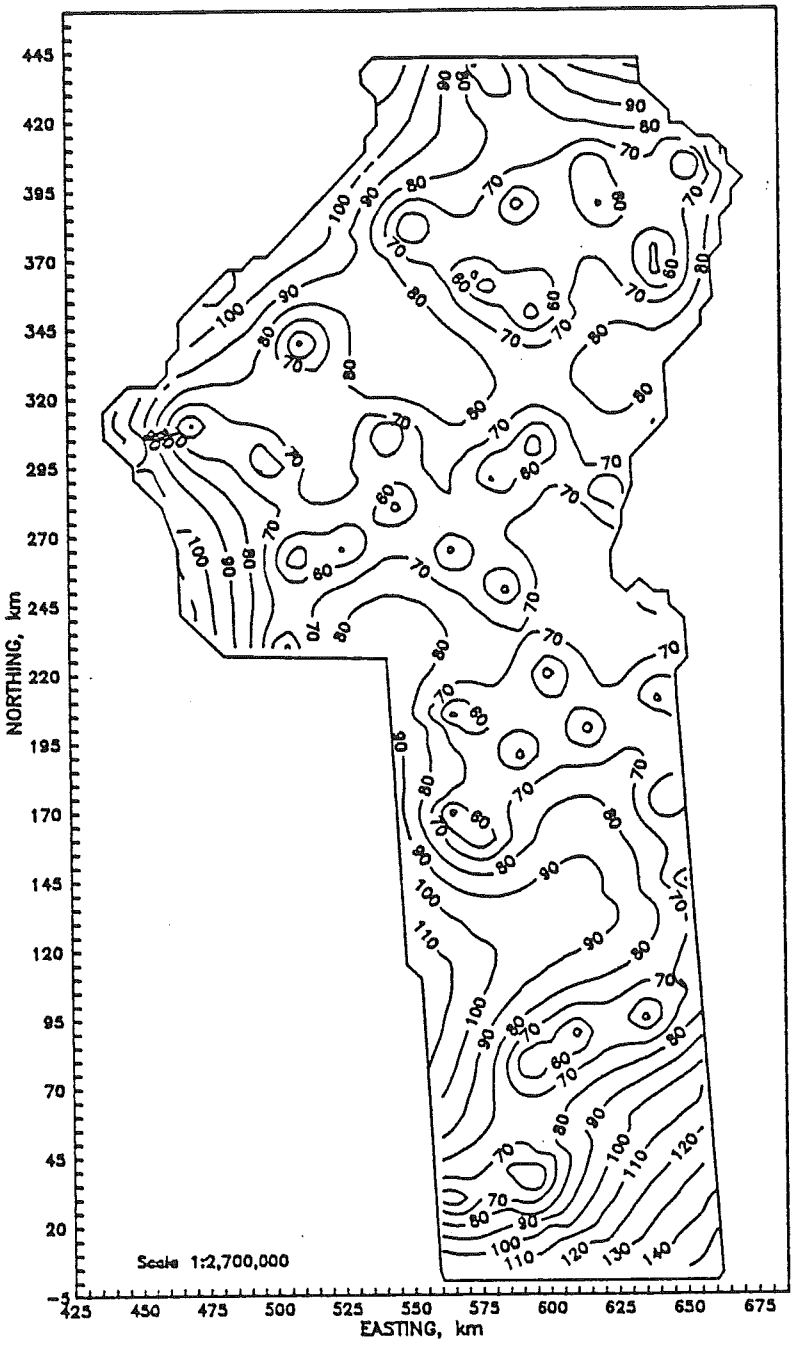

FIGURE 18. (continued). Region 6.

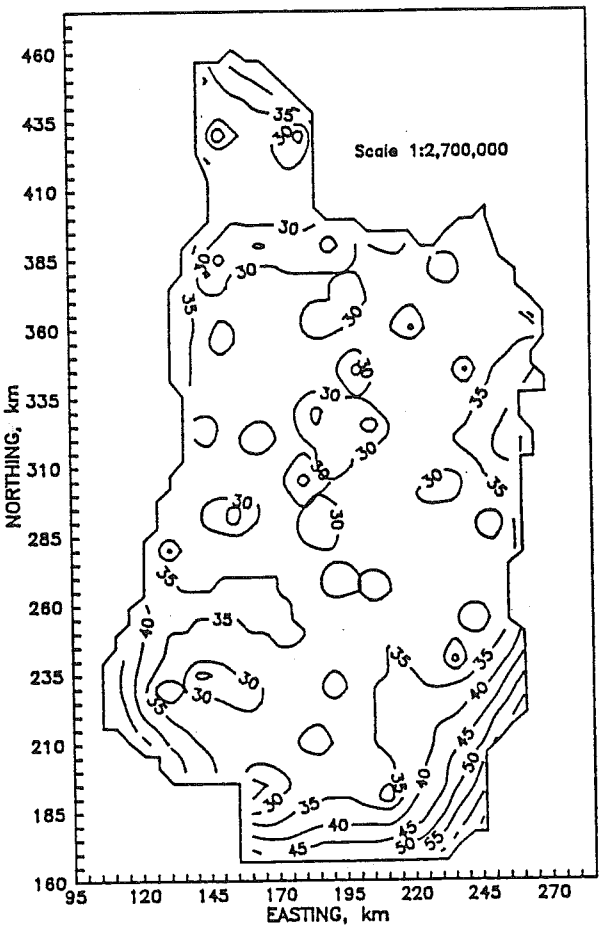

FIGURE 19. Contour maps of cokriging standard deviation for cumulative ET_r, *mm*. Region 2.

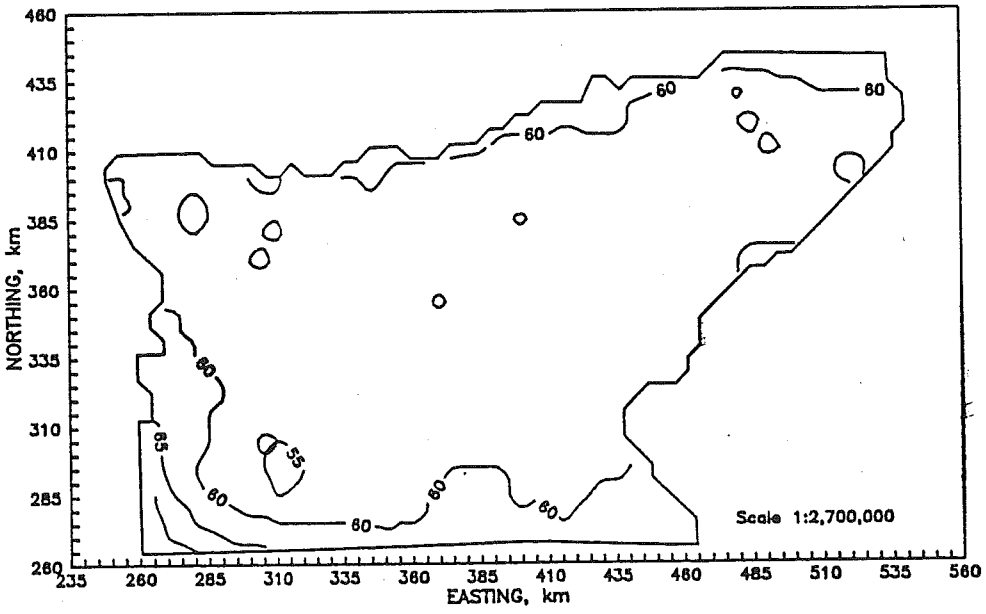

FIGURE 19. (continued). Region 4.

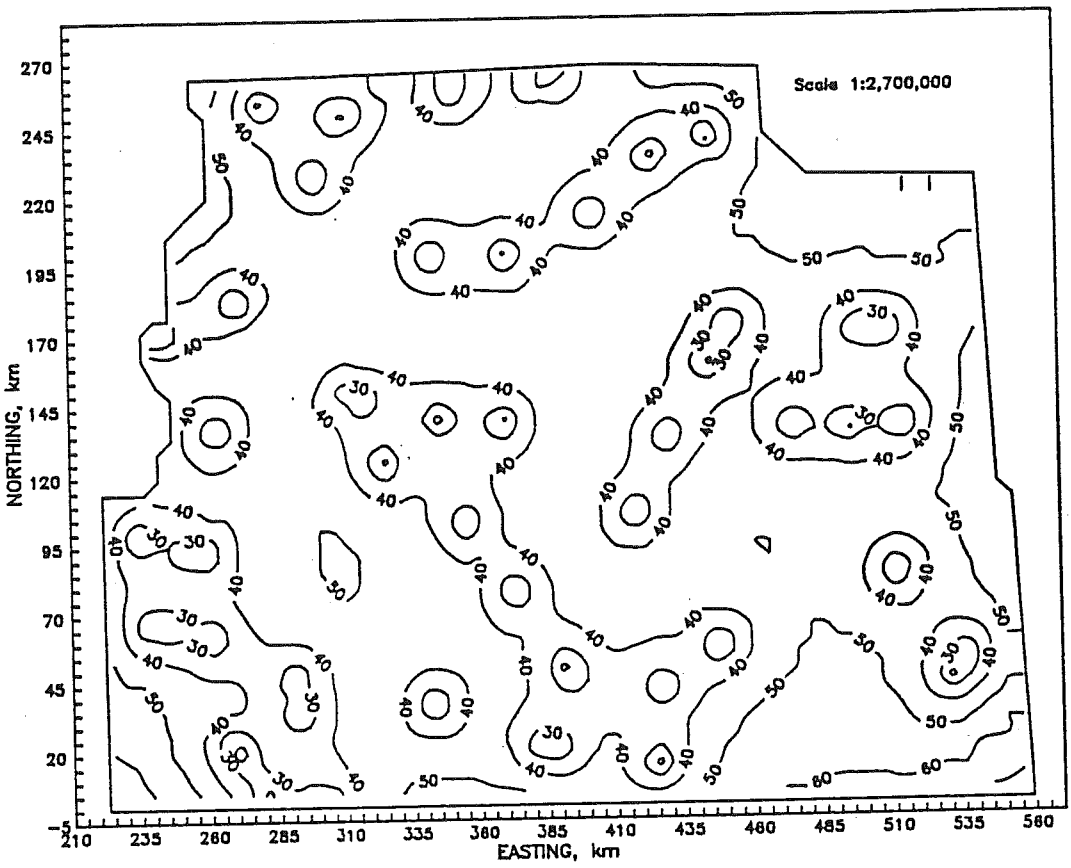

FIGURE 19. (continued). Region 5.

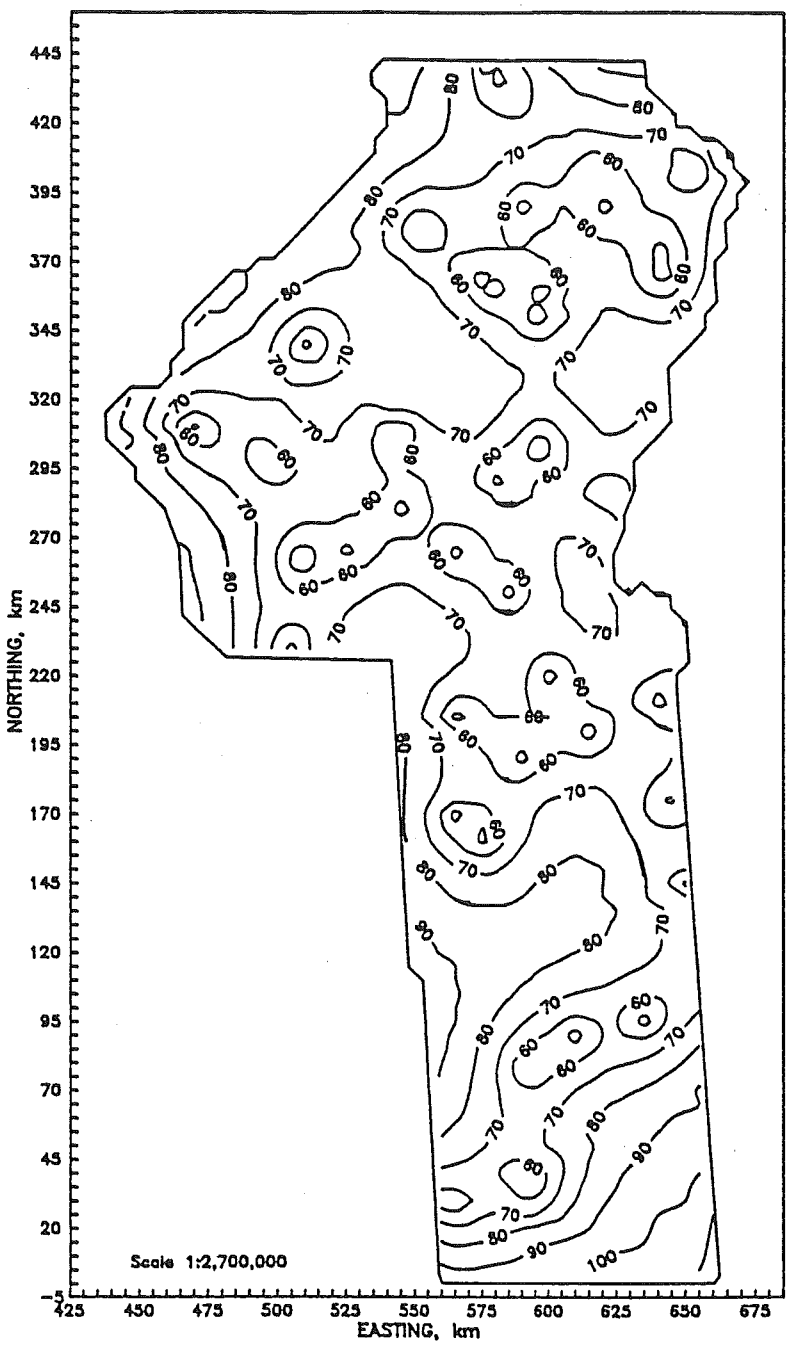

FIGURE 19. (continued). Region 6.

In regions 5 and 6, the average cokriging standard deviation of cumulative ET_r decreased by 12 % (Table 14) as compared with kriging standard deviations. Again, progressive increases in the estimation errors as the estimation points move away from the weather stations is observed for kriging. In cokriging, this effect is also noticed although not as pronounced. The gradual increase of the estimation errors in the borders is very similar for kriging and cokriging although the maximum values are smaller for cokriging. It can be concluded that cokriging did not perform in regions 5 and 6 as well as it did in regions 2 and 4. Recall that the correlation coefficient between ET_r and elevation was higher in these latter two regions than in regions 5 and 6 (Table 8). The fact that the correlation coefficients were higher in regions 2 and 4 may have be occurred simply because the spatial distribution of the weather stations was not totally random. Weather stations tend to be located close to populated areas and the population density in regions 5 and 6 is lower and more irregularly distributed. Likewise, the density of secondary weather stations (Appendix B) in these two regions was particularly low when compared with regions 2 and 4. Consequently, the values of the secondary weather parameters extrapolated to the primary weather stations (section 3.2) in regions 5 and 6 may not represent adequately their general climatic conditions.

Figures 20 to 23 show the contour maps of the cokriging standard deviations of July and October ET_r in regions 2, 4, 5 and 6. The shape of the contour lines is very similar to those observed for cumulative ET_r (Figure 19), with the exception of region 4. In this region, the contours appear to be intermediate to those observed for kriging and cokriging (Figure 19). Likely, this is due to the contour interval width selected to plot those maps. No alternative selection of contour interval width was done in order to be consistent with the criteria followed to select that width (section 3.4.6). In any case, the cokriging standard deviations were 22 to 24 % lower that kriging standard deviations (Table 14) for region 4.

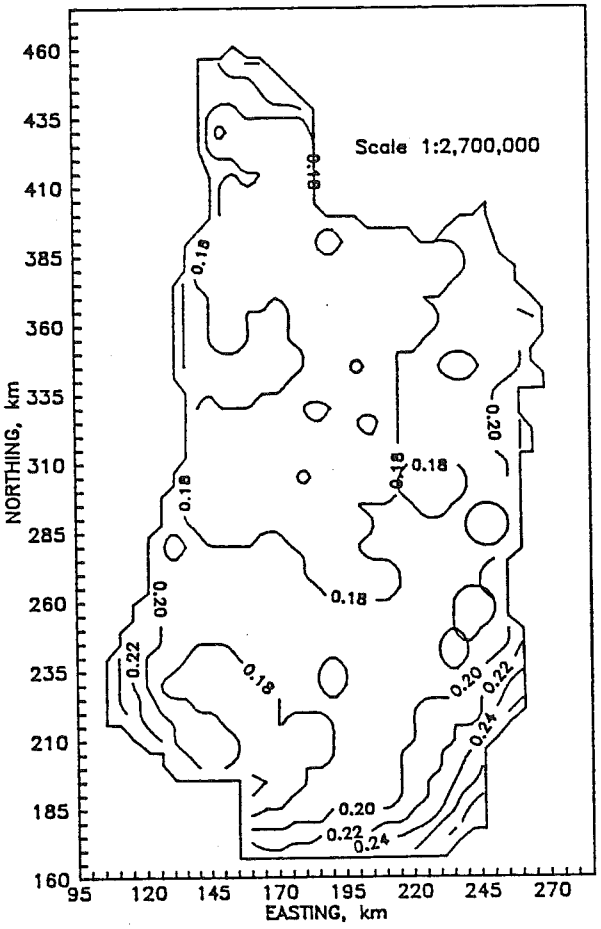

FIGURE 20. Contour maps of cokriging standard deviation for monthly ET_r, $mm\ d^{-1}$, for region 2. July.

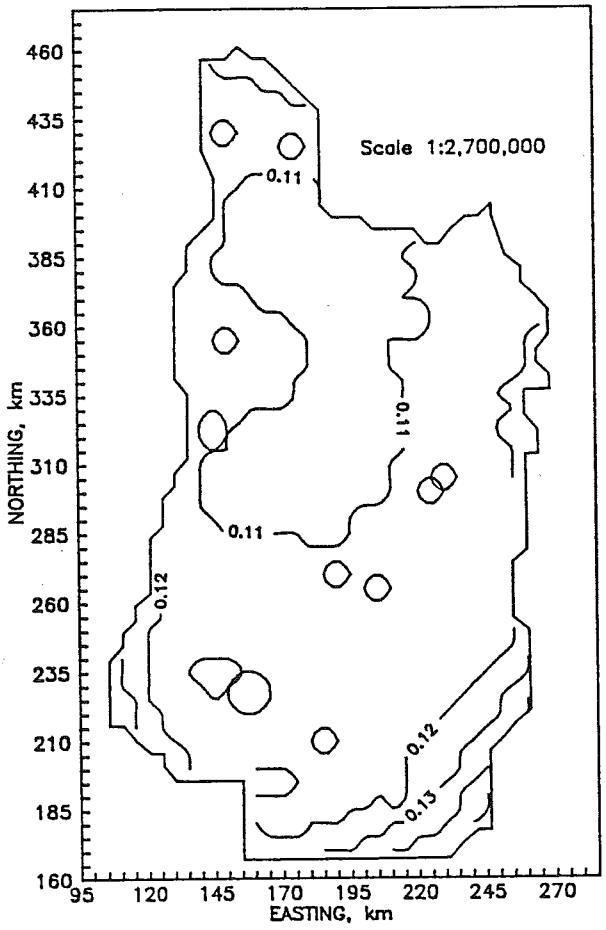

FIGURE 20. (continued). October.

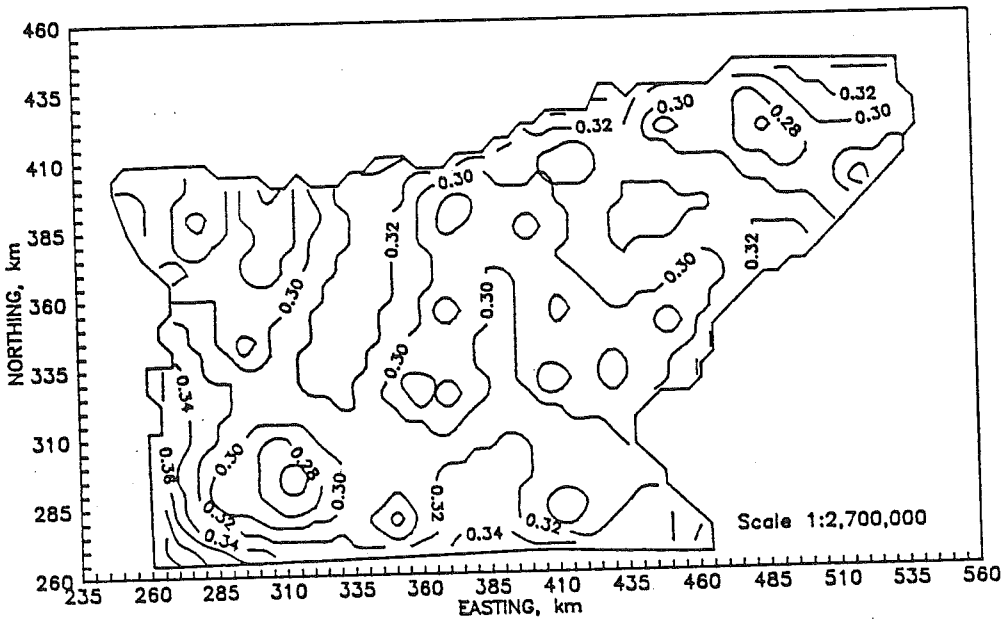

FIGURE 21. Contour maps of cokriging standard deviation for monthly ET_r, $mm\ d^{-1}$, for region 4. July.

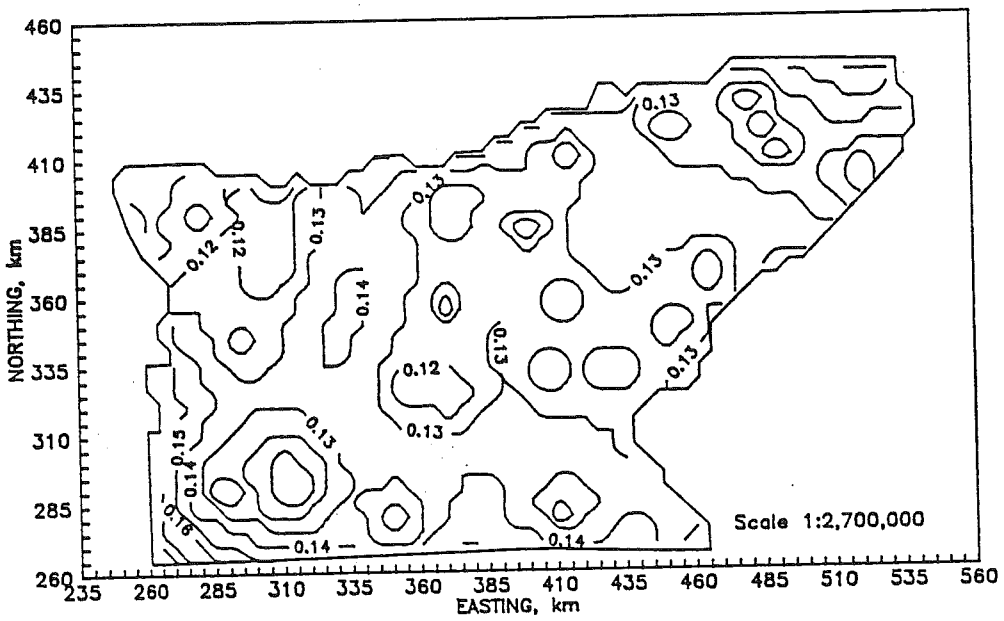

FIGURE 21. (continued). October.

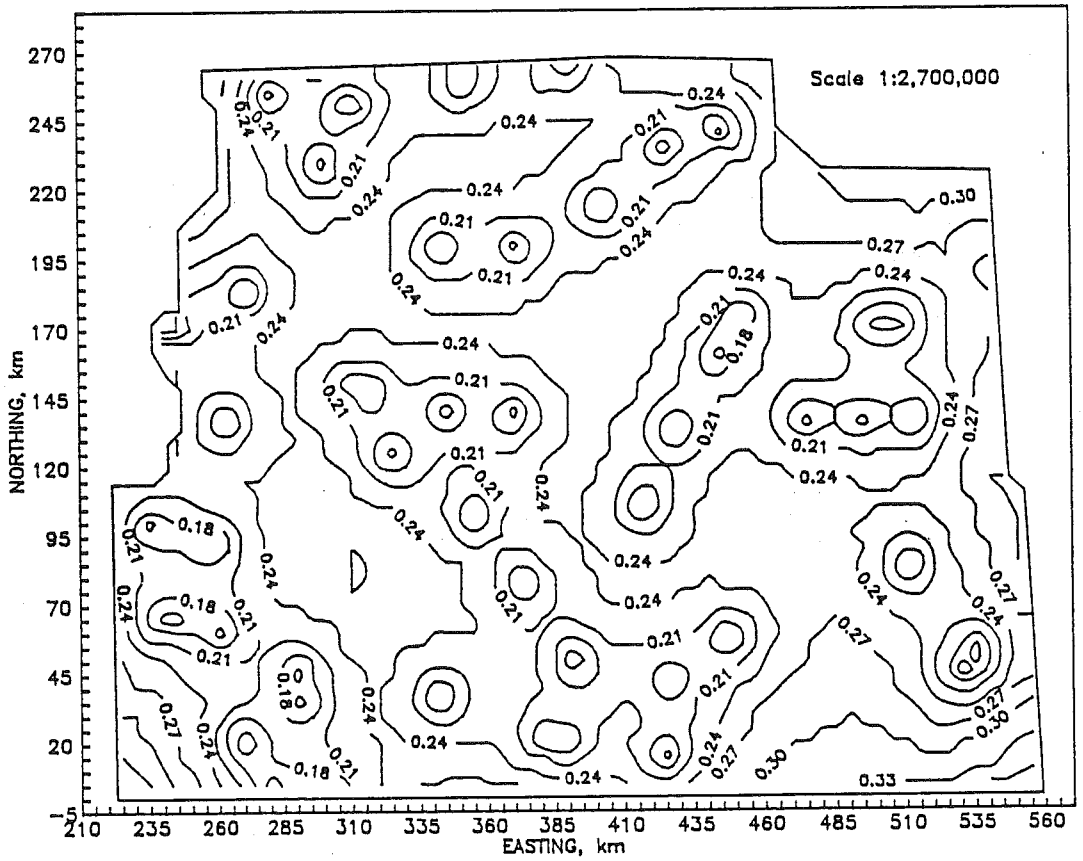

FIGURE 22. Contour maps of cokriging standard deviation for monthly ET_r, $mm\ d^{-1}$, for region 5. July.

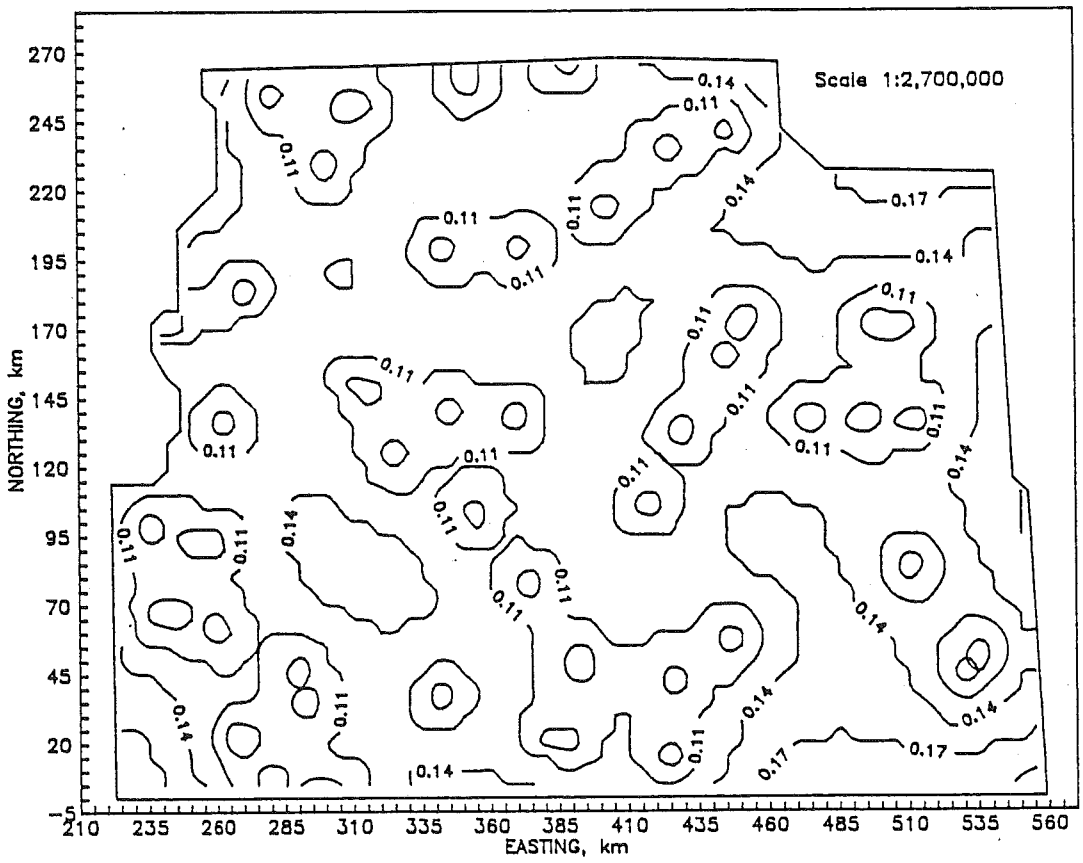

FIGURE 22. (continued). October.

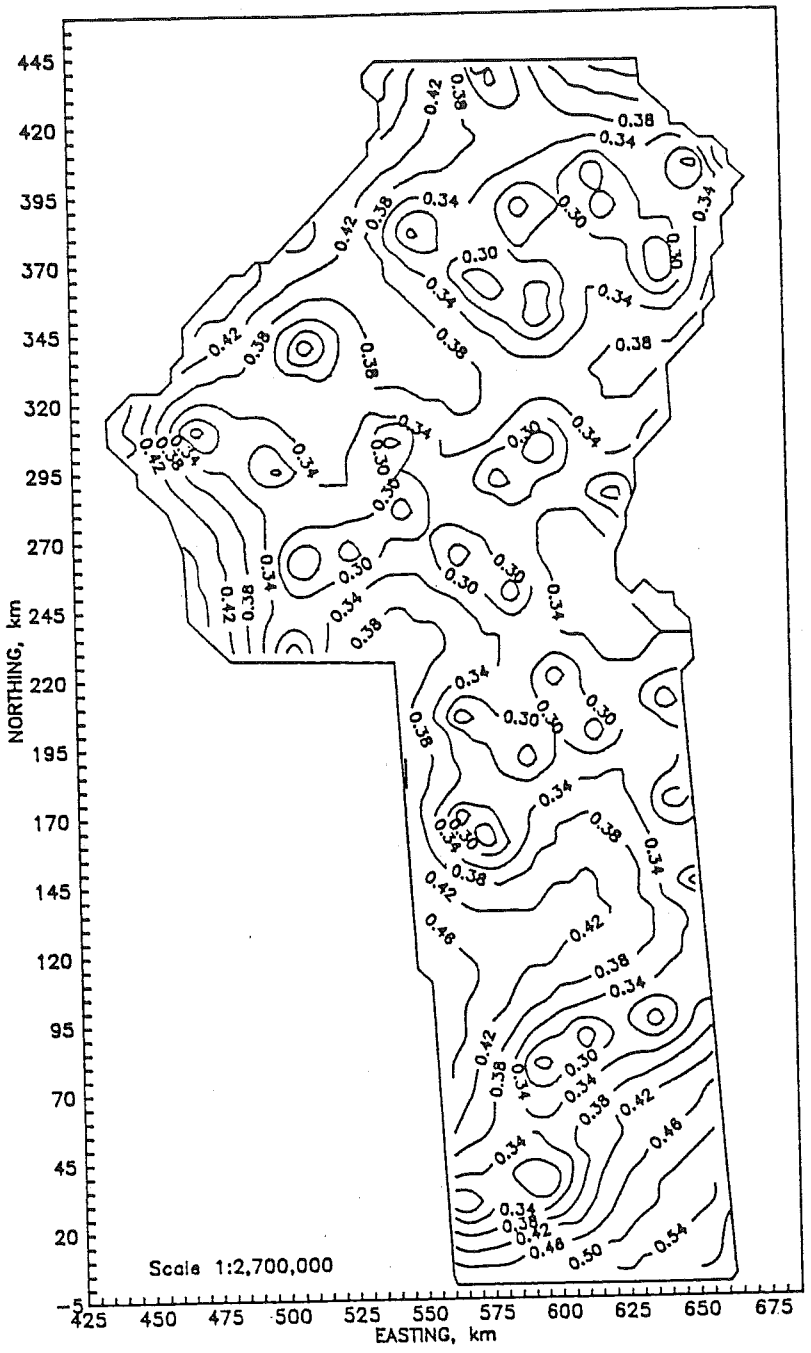

FIGURE 23. Contour maps of cokriging standard deviation for monthly ET_r, $mm\ d^{-1}$, for region 6. July.

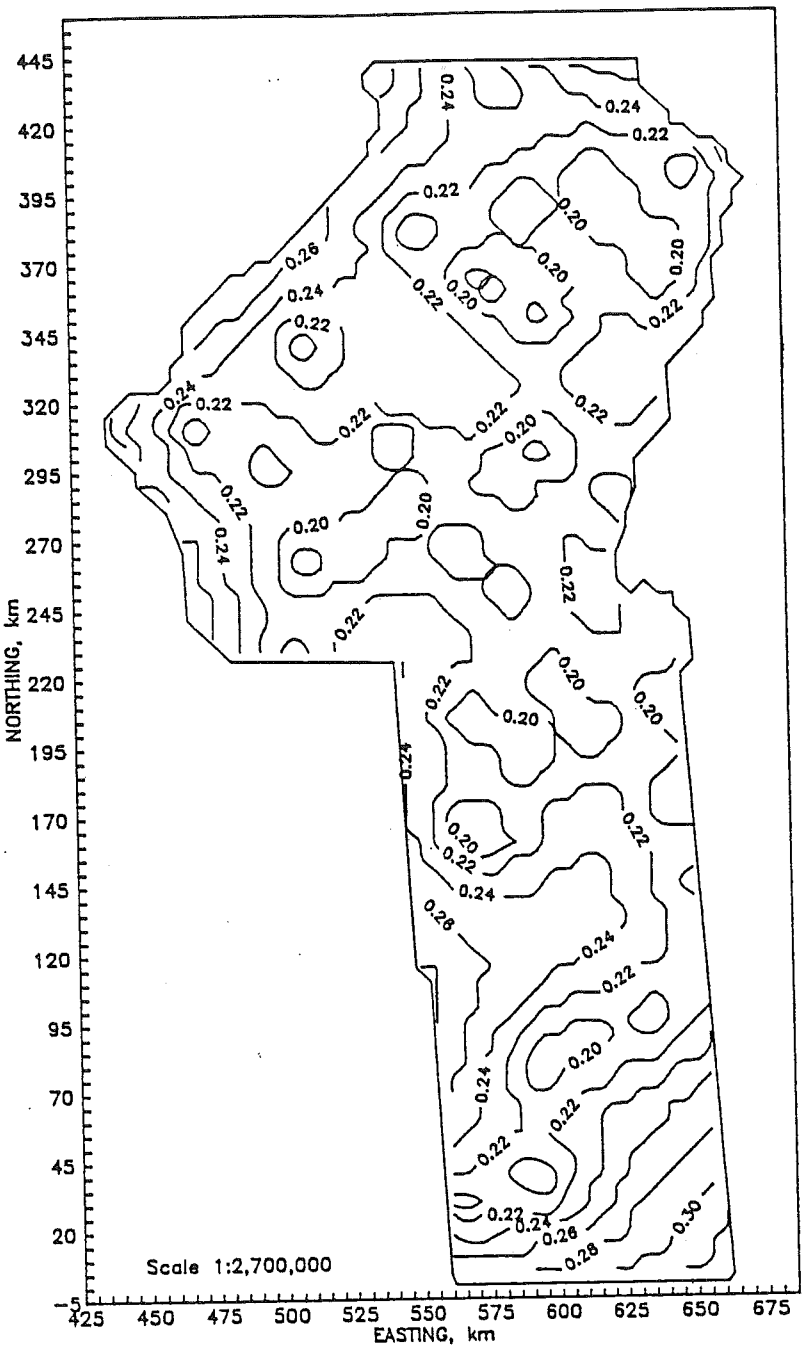

FIGURE 23. (continued). October.

5 CONCLUSIONS AND RECOMMENDATIONS

5.1 Summary

Weather data were collected at 199 weather stations over four different climatic regions in the state of Oregon for a period of 10 to 88 years. Two other climatic regions were recognized in Oregon but they were not included in this project because of the small number of stations and the lack of significant correlation between ET_r and elevation in those regions. The four regions analyzed were labeled Willamette Valley, North Central, South Central and East. Long-term monthly averages of daily ET_r and long-term averages of total annual (cumulative) ET_r rates were computed at the 199 weather stations using the FAO Blaney-Criddle method with USDA adjustments. This method was selected because of its compatibility with the weather data available throughout the climatic regions. Values of elevation above sea level at the weather station locations and at 5 *km* grid corners were also available.

For each region, a multivariate geostatistical analysis was performed for each month of the year and for the cumulative ET_r values. For each study case, direct-semivariograms were computed and modeled. In all cases, the model semivariogram was fit with a nugget effect and a spherical structure with diverse ranges depending on the month and region. Likewise, direct-semivariograms were computed and modeled for elevation. Different nested structures were fit to these semivariogram models. A nugget effect and a gaussian and spherical structures were fit to the Willamette Valley region. A nugget effect and a spherical structure was fit to the North Central region. A nugget effect and a spherical and linear structures were fit to the other two regions. Finally, cross-semivariograms for ET_r and elevation at the weather sta-

tions were computed and modeled for each case study. Spherical structures were fit to these models. Nugget effects were assumed to be zero for the cross-semivariograms. These models were tested by the cross-validation procedure. Cross-validation statistics, including the average kriging error, the mean squared error and the standardized mean squared error, were used to test for the validity of the models. Isotropy was assumed for all semivariograms in order to preserve model consistency although anisotropy was evident for elevation values.

The fit semivariogram values were used to estimate monthly and cumulative ET_r values on a 5 *km* grid by use of kriging and cokriging interpolation techniques. Comparisons of kriged and cokriged ET_r estimates shown relatively small but consistent differences between the methods in terms of maxima, minima and averages of the estimates. However, the contouring of the respective estimates for cumulative ET_r showed cokriging to be superior to kriging. Cokriging contours provided more detail of the changes of ET_r and followed closer the main changes in elevation of the different climatic regions. Contours of monthly ET_r were very similar to those for cumulative ET_r.

Comparisons of the kriging and cokriging estimation error standard deviations in terms of maximum, minimum and average values showed cokriging to be superior to kriging. The average cokriging estimation error standard deviation decreased by about 20 to 30 % in the Willamette Valley and North Central regions, while it decreased by 5 to 13 % in the other two regions. This difference between regions may be due to the lower correlation between ET_r and elevation observed in the South Central and East regions as compared with the other two regions. Contours of the kriging and cokriging standard deviations showed that cokriging reduced the estimation error around the weather stations and more uniform and constant errors were observed over each region. This reduction was more noticeable in the Willamette Valley and North Central regions. Errors at the region borders were higher for both kriging and cokriging although the maximum values were still lower for cokriging.

5.2 Conclusions

A general conclusion of this project was that multivariate geostatistics has proven to be successful in modeling the spatial variability of ET_r by including the effects of elevation. It was previously indicated that one of the appeals of geostatistics is its robustness which allows acceptable results even when some of the theoretical assumptions are not strictly enforced (David, 1977). Results of this project lead to similar conclusion: Geostatistical methods applied to the analysis of hydrological variables can be considered as robust operational tools.

One of the important aspects of hydrology which have traditionally received little attention is topography (Burges, 1986). This research showed that multivariate geostatistics can be an useful tool to predict changes in hydrological variables, such as evapotranspiration, as a function of altitude. Thus, more accurate estimates of ET_r have been computed and contoured by application of the multivariate spatial variability of ET_r in conjunction with elevation using cokriging interpolation techniques. The potential of a multivariate geostatistical approach to analyze the spatial variability of other hydrological variables, such as precipitation, as function of altitude has also been reported (Hevesi *et al.*, 1990). The usefulness of multivariate geostatistics for ET_r analysis varies between the different climatic regions analyzed. In regions with a high statistical correlation between available ET_r data and elevation, the benefits will be maximized. In other regions, the use of a multivariate geostatistical approach may be too costly due to the high computational requirements and low potential for improvement in accuracy of the ET_r estimates.

The results of this project indicated several further possible applications of multivariate geostatistics. In section 2.3.1, the potential of geostatistics for sampling network design was discussed. Errors associated with the estimation of ET_r using univariate geostatistics may

be used to optimize sample network design. Zones within a region in which more sampling sites (i.e. weather stations) are needed to further reduce the estimation errors can be identified. This research showed the improvement in the estimation errors using a multivariate geostatistical approach. The benefit of this approach in economical terms is evident compared with univariate geostatistics. The cost of using elevation data, which is readily available in digital form for most of the United States, is almost negligible compared with the costs of the installation, maintenance and operation of new weather stations. Because the most important decrease in the estimation errors due to multivariate geostatistics was observed for the maximum cokriging standard deviation values, this approach may allow a better identification of the locations where the installation of new weather stations is most critical.

In the analysis and design of water resource systems, the amount of ET_r to be expected on a probability basis is useful information. Historical records of meteorological parameters could be used to develop these different probability levels of evapotranspiration, assuming a normal distribution for this variable (Nixon *et al.*, 1972; Cuenca, 1989), for different locations on a monthly or cumulative basis. Application of the multivariate geostatistical tools described in section 2.3 (direct- and cross-semivariograms and the cokriging system of equations) in conjunction with elevation data would result in regional plots of monthly or cumulative ET_r for different probability levels.

Other possible applications of multivariate geostatistics for irrigation scheduling purposes over large geographic areas can be envisioned. Both direct- and cross-semivariogram functions could be developed for each month of the growing season. These functions could be used with the cokriging system of equations together with elevation and ET_r values corresponding to a previous irrigation period, e.g. seven days. Thus, contour maps of ET_r could be developed for that previous irrigation period. These maps could be used to predict crop water requirements if information on the crop of interest is available. This

scenario again raises the question about whether the semivariogram functions developed using long-term average values can be applied for shorter time periods.

Evapotranspiration is one of the components of the hydrological balance equation (section 1.1). The long-term estimates of evapotranspiration computed in this research could be used as input in the hydrological balance equation for various long-term regional studies, such as management of water resources and environmental assessments. Because of the reduced errors in the cokriged estimates of ET_r, an improvement in the uncertainty involved in this type of studies is to be expected. The importance of the reduced errors in ET_r is more clearly perceived when the additive nature of errors in successive years is considered. Better and more accurate predictions of hydrological events, such as runoff, could result from this type of analysis.

It is known that the phenomenon of evapotranspiration affects the thermodynamic and dynamic state of the atmosphere (André *et al.*, 1986). Global circulation models (GCMs) of the atmosphere have made possible an initial examination of these effects. However, the parameterization of evapotranspiration in the present GCM models is in general too simple and further improvements are required (André *et al.*, 1986; Eagleson, 1986). Multivariate geostatistics is a relatively simple method which can be applied with relatively readily available meteorological data. This approach could allow a better understanding of the spatial variability of evapotranspiration as affected by elevation. The more accurate cokriged estimates of evapotranspiration offer the potential to allow a spatial integration of evapotranspiration to GCM grids.

5.3 Recommendations

Several specific recommendations for future research can be made from the results of this project.

1. One of the problems to develop a valid and adequate spatial variability model of ET_r is the "measurement" error inherent in the local estimates of ET_r computed by using the FAO Blaney-Criddle method. The uncertainty of this method should be included in the modeling of semivariograms for ET_r and cross-semivariograms. Further research should be focused on this problem.

2. The accuracy of the cokriged estimates of ET_r at the edges of the different climatic regions is relatively questionable. The problem of the border effect has not been addressed correctly. It would be beneficial to develop a procedure which would systematically correct this problem. One alternative could be the use of locations from other regions situated in the neighborhood of the region being studied.

3. The direct-semivariograms for ET_r modeled and cross-validated in this project have been developed using long-term averages of ET_r. The feasibility of applying these models in different years should be tested. Previous work by Nuss (1989) showed a high variability between successive years in the model parameters. However, he used only three years of data in his analysis.

4. One of the main disadvantages of cokriging is the high computational efforts required. Other interpolation methods which combine geostatistical analysis with linear regression techniques should be tested and compared with cokriging. Assuming the cokriging estimates are the most accurate, this comparison could

be used to identify simpler regression techniques which can give estimates nearly as accurate as cokriging. The result would be the reduction of the cost of computer time in a routine procedure to contour ET_r at a regional scale.

5. The study of the spatial variability of several meteorological parameters, including relative humidity, wind speed, solar radiation and pan evaporation is recommended. At the present the weather data bases available preclude this research. The need to install more weather stations which record parameters of this type is stressed. The inclusion of the spatial variability and correlation of these parameters with ET_r in a geostatistical analysis could improve the accuracy of the estimates of ET_r.

6 BIBLIOGRAPHY

ABOUFIRASSI, M. and M. A. MARIÑO. 1984. Cokriging of aquifer transmissivities from field measurements of transmissivity and specific capacity. *Mathematical Geology.* 16 (1): 19-35.

AHMED, S. and G. MARSILY. 1987. Comparison of geostatistical methods for estimating transmissivity using data on transmissivity and specific capacity. *Water Resources Research.* 23 (9): 1717-1737.

ALLEN, R. G. 1986. A Penman for all seasons. *Journal of Irrigation and Drainage Engineering.* 112 (4): 348-368.

ALLEN, R. G. and C. E. BROCKWAY. 1982. *Consumptive irrigation requirements for crops in Idaho.* Final Technical Completion Report. Idaho Water and Energy Resources Research Institute. University of Idaho. Moscow.

ALLEN, R. G. and W. O. PRUITT. 1986. Rational use of the FAO Blaney-Criddle formula. *Journal of Irrigation and Drainage Engineering.* 112 (2): 139-155.

AMEGEE, K. Y. 1985. *Application of geostatistics to regional evapotranspiration.* Ph.D. Thesis. Oregon State University. Corvallis.

ANDRE, J. C., J. P. GOUTORBE and A. PERRIER. 1986. HAPEX-MOBILHY: A hydrologic atmospheric experiment for the study of water budget and evaporation flux at the climatic scale. *Bulletin of the American Meteorological Society.* 67 (2): 138-144.

ANDRE, J. C., J. P. GOUTORBE, A. PERRIER and OTHERS. 1988. Evaporation over land-surfaces: First results from HAPEX-MOBILHY special observing period. *Annales Geophysicae.* 6 (5): 477-492.

ARMSTRONG, M. and R. JABIN. 1981. Variogram models must be positive definite. *Mathematical Geology.* 13 (5): 455-459.

BASKETFIELD, D. L. 1986. *Irrigation requirements for selected Oregon locations.* M.S. Thesis. Oregon State University. Corvallis.

BOUFASSA, A. and M. ARMSTRONG. 1989. Comparison between different kriging estimators. *Mathematical Geology.* 21 (3): 331-345.

BROOKER, P. I. 1986. A parametric study of robustness of kriging variance as a function of range and relative nugget effect for a spherical semivariogram. *Mathematical Geology.* 18 (5): 477-488.

BRUTSAERT, W. 1982. *Evaporation in the Atmosphere.* Reidel. Dordrecht. 299 p.

BRUTSAERT, W. and J. A. MAWDSLEY. 1976. The applicability of planetary boundary layer theory to calculate regional evapotranspiration. *Water Resources Research.* 12 (5): 852-859.

BRUTSAERT, W. and H. STRICKER. 1979. An advection-aridity approach to estimate actual regional evapotranspiration. *Water Resources Research.* 15 (2): 443-450.

BURGES, S. J. 1986. Trends and directions in hydrology. *Water Resources Research.* 22 (9): 1S-5S.

BURGESS, T. M. and R. WEBSTER. 1980. Optimal interpolation and isarithmic mapping of soil properties: I. The semivariogram and punctual kriging. *Journal of Soil Science.* 31: 315-331.

BURMAN, R. D., R. H. CUENCA and A. WEISS. 1983. Techniques for estimating irrigation water requirements. *Advances in Irrigation.* v. 2: 335-394.

CHOUDHURY, B. J., S. B. IDSO and R. J. REGINATO. 1987. Analysis of an empirical model for soil heat flux under a growing wheat crop for estimating evaporation by an infrared-temperature based energy balance equation. *Agricultural and Forest Meteorology.* 39 (4): 283-297.

CLARK, I. 1979. *Practical geostatistics.* Applied Science. London. 129 p.

COOPER, R. M. and J. D. ISTOK. 1988. Geostatistics applied to groundwater contamination: 1. Methodology. *Journal of Environmental Engineering.* 114 (2): 270-286.

COOPER, R. M., J. D. ISTOK and L. FLINT. 1988. Three-dimensional cross-semivariogram calculations for hydrogeological data. *Ground Water.* 26: 638-646.

CUENCA, R. H. 1989. *Irrigation system design: An engineering approach.* Prentice Hall. Englewood Cliffs, NJ. 552 p.

CUENCA, R. H. and K. Y. AMEGEE. 1987. Analysis of evapotranspiration as a regionalized variable. *Advances in Irrigation.* v. 4: 181-220.

CUENCA, R. H., J. ERPENBECK and W. O. PRUITT. 1981. Advances in computation of regional evapotranspiration. *Proceedings of Water Forum '81 Specialty Conference.* San Francisco. American Society of Civil Engineering. 73-80.

DAVID, M. 1977. *Geostatistical ore reserve estimation.* Elsevier Scientific. Amsterdam. 364 p.

DELHOMME, J. P. 1978. Kriging in the hydrosciences. *Advances in Water Resources.* 1 (5): 251-266.

DELHOMME, J. P. 1979. Spatial variability and uncertainty in groundwater flow parameters: A geostatistical approach. *Water Resources Research.* 15 (2): 269-280.

DEVORE, J. and R. PECK. 1986. *Statistics: The exploration and analysis of data.* West Publishing. St. Paul, Minnesota. 699 p.

DOORENBOS, J. and W. O. PRUITT. 1977. *Guidelines for predicting crop water requirements.* FAO Irrigation and Drainage Paper 24. FAO. Rome. 144 p.

EAGLESON, P. S. 1986. The emergence of global-scale hydrology. *Water Resources Research.* 22 (9): 6S-14S.

ENGLUND, E. and A. SPARKS. 1988. *Geo-EAS (Geostatistical Environmental Assessment Software) user's guide.* U.S. Environmental Protection Agency. Las Vegas, Nevada. 173 p.

ERPENBECK, J. M. 1981. *A methodology to estimate crop water requirements in Washington State.* M.S. Thesis. Washington State University.

FREVERT, D. K., R. W. HILL and B. C. BRAATEN. 1983. Estimation of FAO evapotranspiration coefficients. *Journal of Irrigation and Drainage Engineering.* 109 (2): 265-270.

GRUNDY, W. D. and A. T. MIESCH. 1988. *Brief description of STATPAC and related statistical programs for the IBM Personal Computer.* U.S. Department of Interior, Geological Survey. 34 p.

GURNEY, R. J. and P. J. CAMILLO. 1984. Modelling daily evapotranspiration using remotely sensed data. *Journal of Hydrology.* 69: 305-324.

HATFIELD, J. L. 1985. Estimation of regional evapotranspiration. In: *Advances in Evapotranspiration.* American Society of Agricultural Engineering. St. Joseph, MI. 357-363.

HATFIELD, J. L. 1988a. Research priorities in ET: Evolving methods. *Transactions of the ASAE.* 31 (2): 490-495.

HATFIELD, J. L. 1988b. Large scale evapotranspiration from remotely sensed surface temperature. *National Conference on Irrigation and Drainage Engineering.* Lincoln, Nebraska. R.H. DeLynn (ed.). 502-509. American Society of Civil Engineering.

HENLEY, S. 1981. *Nonparametric geostatistics.* Elsevier Applied Science. London. 145 p.

HEVESI, J. A., A. L. FLINT and J. D. ISTOK. 1990. Precipitation estimation in mountainous terrain using multivariate geostatistics: 1. Structural analysis (in press).

HOEKSEMA, R. J., R. B. CLAPP, A. L. THOMAS, A. E. HUNLEY, N. D. FARROW and K. C. DEARSTONE. 1989. Cokriging model for estimation of water table elevation. *Water Resources Research.* 25 (3): 429-438.

HUGHES, J. P. and D. P. LETTENMAIER. 1981. Data requirements for kriging: Estimation and network design. *Water Resources Research.* 17 (6): 1641-1650.

ISAAKS, E. H., and R. M. SRIVASTAVA. 1989. *An introduction to applied geostatistics.* Oxford University. New York. 561 p.

JACKSON, R. D. 1985. Evaluating evapotranspiration at local and regional scales. *Proceedings of the IEEE.* 73 (6): 1086-1096.

JACKSON, P. D., J. L. HATFIELD, R. J. REGINATO, S. B. IDSO and P. J. PINTER Jr. 1983. Estimation of daily evapotranspiration from one-time-of day-measurements. *Agriculture and Water Management.* 7: 351-362.

JACKSON, R. D., P. J. PINTER Jr and R. J. REGINATO. 1985. Net radiation calculated from remote multispectral and ground station meteorological data. *Agricultural and Forest Meteorology.* 35: 153-164.

JENSEN, M. E. 1974. *Consumptive use of water and irrigation water requirements.* American Society of Civil Engineering Irrigation Division. 215 p.

JOURNEL, A. G. 1983. Nonparametric estimation of spatial distributions. *Mathematical Geology.* 15 (3): 445-468.

JOURNEL, A. G. 1984. The place of non-parametric geostatistics. In: *Geostatistics for Natural Resources Characterization* (Part I). G. Verly *et al.* (eds.). 122: 307-335. Reidel. Dordrecht.

JOURNEL, A. G. 1989. *Fundamentals of geostatistics in five lessons.* 28th International Geological Congress. American Geophysical Union. 40 p.

JOURNEL, A. G., and C. J. HUIJBREGTS. 1978. *Mining Geostatistics.* Academic Press. London. 600 p.

LOAICIGA, H. A. 1989. An optimization approach for groundwater quality monitoring network design. *Water Resources Research.* 25 (8): 1771-1782.

MANSUR MARQUES, J. P. 1985. *Ore reserve estimation: a summary of principles and methods.* Inter regional Training Course on Exploration Drilling and Ore Reserve Estimation for Uranium Deposits. Comissao Nacional de Energia Nuclear, Nuclebras, Brazil. 69 p.

MATHERON, G. 1963. Principles of Geostatistics. *Economic Geology.* 58: 1246-1266.

MCBRATNEY, A. B. and R. WEBSTER. 1983. Optimal interpolation and isarithmic mapping of soil properties: V. Coregionalization and multiple sampling strategy. *Journal of Soil Science.* 34: 137-162.

MCNAUGHTON, K. G. and T. W. SPRIGGS. 1986. A mixed-layer model for regional evaporation. *Boundary-Layer Meteorology.* 34: 243-262.

MORTON, F. I. 1983. Operational estimates of areal evapotranspiration and their significance to the science and practice of hydrology. *Journal of Hydrology.* 66: 1-76.

MORTON, F. I. 1985. The complementary relationship areal evapotranspiration model: How it works. In: *Advances in Evapotranspiration.* 377-384. American Society of Agricultural Engineering. St Joseph, MI.

MYERS, D. E. 1982. Matrix formulation of co-kriging. *Mathematical Geology.* 14 (3): 249-257.

MYERS, D. E. 1989. To be or not to be ... stationary?. That is the question. *Mathematical Geology.* 21 (3): 347-362.

NETER, J., W. WASSERMAN and M. H. KUTNER. 1983. *Applied linear regression models.* R.D. Irwin Publ. Homewood, Illinois. 547 p.

NIXON, P. R., G. P. LAWLESS and G. V. RICHARDSON. 1972. Coastal California evapotranspiration frequencies. *Journal of Irrigation and Drainage Division Proceedings of the American Society of Civil Engineering.* 98 (IR2): 185-191.

NUSS, J. L. 1989. *Analysis of evapotranspiration for various climatic regimes using geostatistics.* M.S. Thesis. Oregon State University. Corvallis.

PACIFIC NORTHWEST RIVER BASINS COMMISSION. 1968. *Climatological Handbook of the Columbia Basin States.* Vol. 3. Part A.

PENMAN, H. L. 1948. Natural evaporation from open water, bare soil and grass. *Proceedings of the Royal Society.* A193: 120-146.

PRICE, J. L. 1982. On the use of satellite data to infer surface ET at meteorological scales. *Journal of Applied Meteorology.* 21: 1111-1122.

PRUITT, W. O., E. FERERES, K. KAITA, and R. L. SNYDER. 1987. *Reference evapotranspiration (ETo) for California.* Bull. 1922. Agricultural Experiment Station. University of California, Davis. 14 p.

RAYMOND, L. H. and S. J. OWEN-JOYCE. 1986. Estimates of consumptive use and evapotranspiration in Palo Verde Valley, California. In: *Remote Sensing Applications for Consumptive use (evapotranspiration).* AWRA Monograph Series 6. 25-34.

REDMOND, K. T. 1985. *An inventory of climate data for the state of Oregon.* Report SCP-3. Climatic Research Institute. Oregon State University. Corvallis. 160 p.

REGINATO, R. J., R. D. JACKSON and P. J. PINTER Jr. 1985. Evapotranspiration calculated from remote multispectral and ground station meteorological data. *Remote Sensing of Environment.* 18: 75-89.

RENDU, J. M. 1978. *An introduction to geostatistical methods of mineral evaluation.* South African Institute of Mining and Metallurgy. Johannesburg. 84 p.

ROSE, C. W. and M. L. SHARMA. 1984. Summary and recommendations of the workshop on "Evapotranspiration from plant communities". *Agricultural Water Management.* 8: 325-342.

ROUHANI, S. 1985. Variance reduction analysis. *Water Resources Research.* 21 (6): 837-846.

SAMPER, F. J. and S. P. NEUMAN. 1989. Estimation of spatial covariance structures by adjoint state maximum likelihood cross validation: 1. Theory. *Water Resources Research.* 25 (3): 351-362.

SATTERLUND, D. R. and J. E. MEANS. 1979. *Solar radiation in the Pacific Northwest.* Bulletin 874. College of Agriculture Research Center. Washington State University.

SEGUIN, B. and B. ITIER. 1983. Using midday surface temperature to estimate daily evaporation from satellite thermal IR data. *International Journal of Remote Sensing.* 4: 371-383.

SHARMA, M. L. 1985. Estimating evapotranspiration. *Advances in Irrigation.* v. 3: 213-281.

SHUKLA, J. and Y. MINTZ. 1982. Influence of land-surface evapotranspiration on the Earth's climate. *Science.* 215: 1498-1501.

SMYTH, J. D. 1988. *Multivariate geostatistical analysis of groundwater contamination by pesticide and nitrate.* M.S. Thesis. Oregon State University. Corvallis.

THOM, A. S. and H. R. OLIVER. 1977. On Penman's equation for estimating regional evaporation. *Quarterly Journal of the Royal Meteorological Society.* 103: 345-357.

THOMPSON, N., I. A. BARRIE and M. AYLES. 1981. *The Meteorological Office rainfall and evaporation calculation system: MORECS.* Hydrological Memorandum 45. Meteorological Office. London. 69 p.

VIEIRA, S. R., J. L. HATFIELD, D. R. NIELSEN and J. W. BIGGAR. 1983. Geostatistical theory and application to variability of some agronomical properties. *Hilgardia.* 51(3): 1-75.

WARRICK, A. W., D. E. MYERS and D. R. NIELSEN. 1986. Geostatistical methods applied to soil science. In: *Methods of Soil Analysis,* Part 1. A. Klute (ed.). 53-82. American Society of Agronomy and Soil Science Society of America. Madison, WI.

WRIGHT, J. L. 1982. New evapotranspiration crop coefficients. *Journal of Irrigation and Drainage Division Proceedings of the American Society of Civil Engineering.* 108 (IR2): 57-74.

APPENDICES

APPENDIX A. Primary weather stations

List of the primary weather stations used in this study. Listed are the longitude and latitude, the elevation above sea level and the number of years of record for each station. Years of record vary for different months and they are listed as a range.

Reg	Stn ID	Station name	Lat. (*deg*)	Long. (*deg*)	Elev (*m*)	Years of record
1	318	Astoria Exp. Stn.	46.15	123.82	15	33-35
1	324	Astoria	46.18	123.83	61	28-30
1	328	Astoria AP	46.15	123.88	3	34-35
1	471	Bandon	43.15	124.40	6	42-47
1	1055	Brookings	42.05	124.28	21	56-57
1	1324	Canary	43.92	124.03	24	38-39
1	1360	Cape Blanco	42.83	124.57	58	26-28
1	1682	Cloverdale	45.22	123.90	24	45-47
1	1836	Coquille City	43.18	124.20	6	16
1	2370	Dora	43.17	124.00	274	17-19
1	2633	Elkton	43.60	123.58	37	43-50
1	3356	Gold Beach R. Stn.	42.40	124.42	15	50-54
1	3995	Honeyman St. Park	43.93	124.10	37	16-17
1	4133	Illahe	42.63	124.05	107	41-46
1	5375	Mc Kinley	43.18	124.03	43	12-14
1	6032	Newport	44.58	124.05	43	52-56
1	6073	North Bend AP	43.42	124.25	3	55-57
1	6366	Otis	45.03	123.93	46	38-40
1	6779	Port Orford	42.73	124.52	88	27-32
1	6784	Port Orford 2	42.75	124.50	15	21-25
1	6820	Powers	42.88	124.07	70	54-56
1	7082	Reedsport	43.70	124.12	18	42-45
1	7641	Seaside	45.98	123.92	3	55-57
1	7866	Sitkum	43.15	123.83	186	18-22
1	8481	Tidewater	44.42	123.90	15	43-46
1	8494	Tillamook	45.45	123.87	3	50-55
1	8833	Valsetz	44.85	123.67	354	42-48
2	78	Albany 1	44.65	123.10	64	32-33
2	82	Albany 2	44.62	123.12	67	11-13
2	595	Beaverton	45.50	122.82	67	14-16
2	652	Belknap Springs	44.30	122.03	655	25-28
2	897	Bonneville Dam	45.63	121.95	18	49-51
2	1433	Cascadia	44.40	122.48	262	47-54
2	1552	Cherry Grove	45.42	123.25	238	45-46
2	1643	Clatskanie	46.10	123.28	27	52-53
2	1862	Corvallis O.S.U.	44.63	123.20	70	56-57

Reg	Stn ID	Station name	Lat. (*deg*)	Long. (*deg*)	Elev (*m*)	Years of record
2	1877	Corvallis W. B.	44.52	123.45	180	24-25
2	1897	Cottage Grove	43.78	123.07	198	56-57
2	1902	Cottage Grove Dam	43.72	123.05	253	46
2	2112	Dallas	44.95	123.28	88	48-51
2	2277	Detroit	44.73	122.15	485	35-37
2	2292	Detroit Dam	44.72	122.25	372	33-34
2	2374	Dorena Dam	43.78	122.97	250	36-38
2	2693	Estacada	45.27	122.32	125	55-57
2	2707	Eugene	44.07	123.08	137	14-15
2	2709	Eugene AP	44.12	123.22	110	40-42
2	2800	Falls City	44.85	123.45	183	27-30
2	2805	Falls City 2	44.85	123.43	134	26-27
2	2867	Fernridge Dam	44.12	123.30	149	43-45
2	2997	Forest Grove	45.53	123.10	55	55-57
2	3047	Foster Dam	44.42	122.67	168	18-19
2	3402	Government Camp	45.30	121.75	1213	36-37
2	3770	Hwks. Portland W.B.	45.45	122.15	229	56-57
2	3908	Hillsboro	45.52	122.98	49	55-57
2	4603	La Comb 1	44.58	122.75	204	29-31
2	4606	La Comb 3	44.62	122.72	158	12-15
2	4811	Leaburg	44.10	122.68	207	52-54
2	5050	Lookout P. Dam	43.92	122.77	216	32-33
2	5221	Marion Forks	44.60	121.95	756	38-40
2	5362	Mc Kenzie Bridge	44.18	122.12	451	42-55
2	5384	Mc Minnville	45.23	123.18	46	50-53
2	5677	Molalla	45.13	122.57	122	27-28
2	6151	N. Willamette E.S.	45.28	122.75	46	24-25
2	6173	Noti	44.07	123.47	137	23-24
2	6213	Oakridge	43.75	122.45	390	50-55
2	6334	Oregon City	45.35	122.60	52	38-40
2	6749	Portland KGW-TV	45.52	122.68	49	13-15
2	6751	Portland AP	45.60	122.60	6	40-42
2	6761	Portland W.B.	45.53	122.67	9	25
2	7466	Saint Helens	45.87	122.82	30	11-12
2	7500	Salem	44.92	123.02	61	40-42
2	7559	Santiam Pass	44.42	121.87	1448	18-29
2	7586	Scogginns Dam	45.48	123.20	110	11-13
2	7631	Scotts Mills	44.95	122.53	707	31-32
2	7809	Silver Creek F.	44.87	122.65	411	45-49
2	7823	Silverton	45.00	122.77	125	23-26
2	7827	Silverton 4	44.97	122.73	311	11-12
2	8095	Stayton	44.78	122.82	131	34-36
2	8221	Sundown Ranch	44.95	122.50	732	22-24
2	8466	Three Lynx	45.12	122.07	341	55-56
2	8634	Troutdale	45.55	122.40	9	30-33
2	8879	Vernonia	45.87	123.20	256	26-28

Reg	Stn ID	Station name	Lat. (*deg*)	Long. (*deg*)	Elev (*m*)	Years of record
2	8884	Vernonia 2	45.87	123.18	192	20-21
2	9051	Warren	45.82	122.85	24	24-26
3	304	Ashland	42.22	122.72	543	87-88
3	1448	Cave Junction	42.17	123.67	390	25-26
3	2406	Drain	43.67	123.32	88	49-52
3	2928	Fish Lake	42.38	122.35	1414	23-30
3	3445	Grants Pass	42.43	123.32	283	85-88
3	4060	Howard P. Dam	42.22	122.37	1393	27-28
3	4126	Idleyld Park	43.37	122.97	329	26-28
3	4216	Jacksonville	42.30	122.98	500	21-30
3	4420	Kerby	42.22	123.65	387	10-11
3	4635	Lake Creek	42.37	122.53	533	30-35
3	4835	Lemolo Lake	43.37	122.22	1244	10
3	5055	Lost Creek Dam	42.67	122.68	482	17-18
3	5424	Medford Exp. Stn.	42.30	122.87	445	48-51
3	5429	Medford AP	42.37	122.87	399	60-63
3	5656	Modoc Orchard	42.45	122.88	372	49-51
3	6907	Prospect	42.73	122.52	756	77-81
3	7169	Riddle	42.95	123.35	207	68-74
3	7326	Roseburg AP	43.23	123.37	155	17-18
3	7331	Roseburg	43.20	123.35	143	21-23
3	7391	Ruch	42.23	123.03	472	24-25
3	7698	Sexton Summit	42.62	123.37	1170	39-41
3	7850	Siskiyou Summit	42.05	122.60	1369	12-13
3	8338	Talent	42.25	122.80	472	42-44
3	8536	Toketee Falls	43.28	122.45	628	34-35
3	8588	Trail	42.78	122.67	564	15-18
4	197	Antelope	44.92	120.72	817	55-57
4	265	Arlington	45.72	120.20	88	53-57
4	753	Big Eddy	45.62	121.12	40	25-27
4	858	Boardman	45.83	119.70	91	15-17
4	1407	Cascade Locks	45.68	121.88	30	22-23
4	1765	Condon	45.23	120.18	863	54-56
4	2168	Dayville	44.47	119.53	719	39-44
4	2440	Dufur	45.45	121.13	405	54-57
4	2564	Echo	45.75	119.18	201	38-40
4	3038	Fossil	45.00	120.22	808	37-45
4	3121	Friend	45.35	121.27	744	33-35
4	3542	Grizzly	44.52	120.93	1109	37-40
4	3644	Hardman	45.17	119.68	1091	12-13
4	3737	Hay Creek	44.95	120.90	896	13-15
4	3827	Heppner	45.37	119.55	576	58-67
4	3847	Hermiston	45.82	119.28	189	56-57
4	4003	Hood River E.S	45.68	121.52	152	55-57
4	4411	Kent	45.20	120.70	829	49-57
4	4479	Kinzua	45.03	119.92	1052	10-12

Reg	Stn ID	Station name	Lat. (*deg*)	Long. (*deg*)	Elev (*m*)	Years of record
4	5139	Madras	44.63	121.13	680	52-57
4	5142	Madras 2	44.67	121.15	744	18-20
4	5515	Metolius	44.58	121.18	762	39-42
4	5545	Mikkalo	45.47	120.35	472	33-37
4	5593	Milton Freewater	45.95	118.42	296	67-71
4	5641	Mitchell	44.58	120.18	808	46-50
4	5707	Montgomery Ranch	44.62	121.48	579	17-19
4	5734	Moro	45.48	120.72	570	55-57
4	6464	Parkdale	45.52	121.58	521	36-38
4	6468	Parkdale 2	45.50	121.58	576	11-13
4	6532	Pelton Dam	44.73	121.23	430	27-30
4	6540	Pendleton Exp. Stn.	45.72	118.63	454	39-41
4	6541	Pendleton R. Park	45.67	118.80	321	20-22
4	6546	Pendleton AP	45.68	118.85	454	39-40
4	6634	Pilot Rock	45.48	118.82	524	72-76
4	6655	Pine Grove	45.12	121.37	677	17-19
4	8009	Spray	44.83	119.78	530	19-20
4	8407	The Dalles	45.60	121.20	30	47-50
4	8530	Timberline Lodge	45.35	121.70	1811	11-13
4	8734	Umatilla	45.92	119.35	82	32-34
4	9068	Wasco	45.58	120.70	384	23
4	9216	Weston	45.80	118.40	640	50-52
5	36	Adel	42.18	119.90	1396	20-27
5	118	Alkali Lake	42.97	120.00	1320	25-27
5	188	Andrews	42.45	118.60	1268	10-12
5	189	Andrews Weston M.	42.55	118.55	1457	17-19
5	501	Barnes Station	43.95	120.22	1210	26
5	694	Bend	44.07	121.32	1113	57
5	1067	Brothers	43.80	120.60	1414	28-29
5	1176	Burns	43.58	119.05	1262	34-35
5	1415	Cascade Summit	43.58	122.03	1475	15-17
5	1546	Chemult	43.23	121.78	1451	44-50
5	1571	Chiloquin	42.58	121.87	1277	55-62
5	1946	Crater Lake	42.90	122.13	1975	53-55
5	2415	Drewsey	43.80	118.38	1073	15-18
5	3022	Forth Klamath	42.62	122.08	1268	11-13
5	3095	Fremont	43.33	121.17	1375	47-53
5	3659	Harney B. E.S	43.58	118.93	1262	23-24
5	3692	Hart Mountain Ref.	42.55	119.65	1713	45-49
5	4506	Klamath Falls	42.20	121.78	1250	83-87
5	4511	Klamath F. Agr. Stn.	42.17	121.75	1247	22-24
5	4632	Lake	43.27	120.63	1314	27-29
5	4670	Lakeview	42.22	120.37	1457	53-57
5	5162	Malheur Ref. Hdq.	43.28	118.83	1253	24-28
5	5170	Malin	42.02	121.42	1234	15-16
5	5174	Malin 5	42.00	121.32	1411	19-20

Reg	Stn ID	Station name	Lat. (*deg*)	Long. (*deg*)	Elev (*m*)	Years of record
5	5505	Merrill	42.05	121.63	1244	15-19
5	6243	Ochoco	44.40	120.43	1213	47-51
5	6251	Odell Lake	43.58	122.03	1460	24-28
5	6302	OO Ranch	43.28	119.32	1262	20-28
5	6426	Paisley	42.70	120.53	1329	53-56
5	6500	Paulina	44.13	119.97	1122	26
5	6662	Pine Mountain	43.78	120.95	1902	10-13
5	6717	Plush	42.42	119.90	1375	16-19
5	6853	P Ranch Refuge	42.82	118.88	1280	29-32
5	6883	Prineville	44.35	120.90	866	55-57
5	6982	Rager	44.23	119.73	1219	11-13
5	7052	Redmond	44.27	121.22	917	47-49
5	7062	Redmond AP	44.27	121.15	933	36-39
5	7354	Round Grove	42.33	120.88	1490	50-54
5	7533	Sand Creek	42.85	121.90	1426	16-17
5	7817	Silver Lake	43.12	121.07	1335	17-19
5	7857	Sisters	44.30	121.55	969	24-29
5	8007	Sprague River	42.45	121.50	1329	26-32
5	8029	Squaw Butte E.S	43.48	119.72	1420	43-49
5	8173	Summer Lake	42.95	120.78	1277	30-31
5	8250	Suntex	43.60	119.63	1314	24-26
5	8420	The Poplars	43.27	120.93	1317	23-27
5	8812	Valley Falls	42.48	120.28	1320	32-35
5	8818	Valley Falls 3	42.45	120.25	1396	12-17
5	8924	Voltage	43.28	118.97	1253	19-21
5	8948	Wagontire	43.25	119.88	1442	21-24
5	9316	Wickiup Dam	43.68	121.68	1329	44-47
5	9604	Yonna	42.30	121.48	1274	15-18
6	41	Adrian	43.73	117.07	680	40-42
6	356	Austin	44.58	118.50	1283	53-64
6	412	Baker AP	44.83	117.82	1027	44-45
6	417	Baker KBKR	44.77	117.83	1049	32-34
6	723	Beulah	43.92	118.17	997	31-46
6	1174	Burns Junction	42.78	117.85	1198	14-16
6	1352	Canyon City	44.40	118.95	972	13-15
6	1926	Cove 1	45.30	117.80	951	54-56
6	2135	Danner	42.93	117.33	1289	46-56
6	2482	Durkee	44.62	117.48	847	25-28
6	2597	Elgin	45.57	117.92	811	41-49
6	2672	Enterprise	45.43	117.27	1155	47-50
6	2678	Enterprise 20	45.70	117.15	1000	18-19
6	3430	Granite	44.80	118.50	1506	18-20
6	3604	Halfway	44.88	117.12	814	43-46
6	3666	Harper	43.87	117.62	765	33-34
6	4098	Huntington	44.35	117.27	649	53-57
6	4175	Ironside	44.32	117.98	1195	22-29

Reg	Stn ID	Station name	Lat. (*deg*)	Long. (*deg*)	Elev (*m*)	Years of record
6	4291	John Day	44.43	118.95	933	34-35
6	4329	Joseph	45.35	117.25	1280	21-23
6	4357	Juntura	43.80	117.93	863	21-23
6	4615	La Grande	45.33	118.12	856	63-65
6	4622	La Grande KTVR	45.32	118.08	841	20-23
6	5020	Long Creek	44.72	119.10	1134	27-31
6	5160	Malheur B. E.S	43.98	117.02	680	44-46
6	5258	Mason Dam	44.67	118.00	1189	18-19
6	5335	Mc Dermitt	42.42	117.87	1359	29-32
6	5396	Meacham	45.50	118.40	1234	28-31
6	5610	Minam	45.68	117.60	1100	20-30
6	5711	Monument	44.82	119.42	610	25-27
6	6179	Nyssa	43.87	117.00	664	48-50
6	6294	Ontario	44.05	116.97	655	39-43
6	6405	Owyhee Dam	43.65	117.25	732	50-53
6	6845	Prairie City	44.45	118.72	1079	10-12
6	7160	Richland	44.77	117.17	677	33-39
6	7208	Riverside	43.50	118.07	914	30-34
6	7277	Rocksville	43.37	117.12	1119	20-25
6	7310	Rome	42.87	117.65	1039	31-36
6	7675	Seneca	44.13	118.97	1420	45-52
6	7736	Sheaville	43.12	117.03	1408	36-40
6	8726	Ukiah	45.13	118.93	1024	57-62
6	8746	Union Exp. Stn.	45.22	117.88	844	73-74
6	8780	Unity	44.43	118.23	1228	33-49
6	8797	Vale	43.98	117.25	683	51-54
6	8985	Walla Walla	46.00	118.05	732	33-36
6	8997	Wallowa	45.56	117.53	890	79-84
6	9046	Warm Springs Res.	43.57	118.20	1018	34-44
6	9176	Westfall	44.05	117.75	957	19-25
6	9290	Whitehorse Ranch	42.33	118.23	1280	16-22

APPENDIX B. Secondary weather stations

List of secondary weather stations. For each secondary weather parameter, the data source, the original variable and the years of record are listed. Years of record are given as a range as they vary for different months. Data sources are listed at the end of the table. All stations but Coos Bay, Boise and Mountain Home also were primary weather stations.

		Min. rel. humidity			Sunshine			Windspeed		
Stn ID	Station name	Data source	Orig. variab.	Years record	Data source	Orig. variab.	Years record	Data source	Orig. variab.	Years record
328	Astoria AP[1]	ODD	Min. rel. hum. %	16	PNSR	Solar rad. *cal cm^{-2}d^{-1}*	5-10	DHA	Avg. windsp. *knots x 10*	31
	Coos Bay[1]				ASSR	Solar rad. *kW h m^{-2}*	7			
6073	North Bend AP[1]	DHA	Avg. rel. hum. %	31				DHA	Avg. windsp. *knots x 10*	31
1862	Corvallis O.S.U.[2]				PNSR	Solar rad. *cal cm^{-2}d^{-1}*	5-10	WRPE	Mon. windrun *mi*	3-21
1902	Cottage Grove Dam[2]							WRPE	Mon. windrun *mi*	12-13
2292	Detroit Dam[2]							WRPE	Mon. windrun *mi*	3-22
2709	Eugene AP[2]	ODD	Min. rel. hum. %	10-12	ASSR	Solar rad. *kW h m^{-2}*	9	DHA	Avg. windsp. *knots x 10*	36
5050	Lookout P. Dam[2]							WRPE	Mon. windrun *mi*	8-22
5429	Medford AP[2]	ODD	Min. rel. hum. %	20-21	PNSR	Solar rad. *cal cm^{-2}d^{-1}*	5-10	DHA	Avg. windsp. *knots x 10*	36
6151	N. Willamette E.S[2]							WRPE	Mon. windrun *mi*	15-22
6751	Portland AP[2]	ODD	Min. rel. hum. %	20-21	ODD	Sunshine ratio	23	DHA	Avg. windsp. *knots x 10*	37
7326	Roseburg AP[2]	DHA	Avg. rel. hum. %	17	DHA	Hourly cloud cover	17	DHA	Avg. windsp. *knots x 10*	17
7500	Salem[2]	ODD	Min. rel. hum. %	20-21	ODD	Daytime cloud cover	23	DHA	Avg. windsp. *knots x 10*	38

		Min. rel. humidity			Sunshine			Windspeed		
Stn ID	Station name	Data source	Orig. variab.	Years record	Data source	Orig. variab.	Years record	Data source	Orig. variab.	Years record
7698	Sexton Summit[2]	DHA	Avg. rel. hum. %	31	ODD	Daytime cloud cover	22-23	DHA	Avg. windsp. *knots x 10*	31
412	Baker AP[3]	DHA	Avg. rel. hum. %	17	DHA	Hourly cloud cover	17	DHA	Avg. windsp. *knots x 10*	17
694	Bend[3]				ASSR	Solar rad. *kW h m^{-2}*	7			
858	Boardman[3]	CHDD	Dewp. temp. *°F*	2-5	CHDD	Solar rad. *cal cm^{-2}d^{-1}*	5	CHDD	Daily windrun *mi*	2-5
	Boise, ID[3]	DHA	Avg. rel. hum. %	36	DHA	Hourly cloud cover	36	DHA	Avg. windsp. *knots x 10*	36
1176	Burns[3]	DHA	Avg. rel. hum. %	33	ODD	Daytime cloud cover	7-8	DHA	Avg. windsp. *knots x 10*	33
3847	Hermiston[3]	CHDD	Dewp. temp. *°F*	1-9	CHDD	Solar rad. *cal cm^{-2}d^{-1}*	9	CHDD	Daily windrun *mi*	8-9
4511	Klamath F. Agr. Stn.[3]	DHA	Avg. rel. hum. %	23	DHA	Hourly cloud cover	23	DHA	Avg. windsp. *knots x 10*	23
4615	La Grande[3]	PNHH	Min. rel. hum. %	6	ASSR	Solar rad. *kW h m^{-2}*	7	PNHH	Avg. windsp. *mph*	6
5142	Madras 2[3]							WRPE	Mon. windrun *mi*	4-14
5162	Malheur Ref. Hdq.[3]							WRPE	Mon. windrun *mi*	4-17
5396	Meacham[3]	PNHH	Min. rel. hum. %	10	PNSR	Solar rad. *cal cm^{-2}d^{-1}*	5-10	PNHH	Avg. windsp. *mph*	10
5734	Moro[3]							WRPE	Mon. windrun *mi*	17-22
	Mountain Home, ID[3]				PNSR	Solar rad. *cal cm^{-2}d^{-1}*	5-10			
6294	Ontario[3]	PNHH	Min. rel. hum. %	7	PNSR	Solar rad. *cal cm^{-2}d^{-1}*	5-10	PNHH	Avg. windsp. *mph*	7
6546	Pendleton AP[3]	ODD	Min. rel. hum. %	20-21	ODD	Daytime cloud cover	23	DHA	Avg. windsp. *knots x 10*	46
7062	Redmond AP[3]	DHA	Avg. rel. hum. %	36	DHA	Hourly cloud cover	36	DHA	Avg. windsp. *knots x 10*	36
8173	Summer Lake[3]							WRPE	Mon. windrun *mi*	21-22

		Min. rel. humidity			Sunshine			Windspeed		
Stn ID	Station name	Data source	Orig. variab.	Years record	Data source	Orig. variab.	Years record	Data source	Orig. variab.	Years record
8407	The Dalles[3]	DHA	Avg. rel. hum. %	17	DHA	Hourly cloud cover	17	DHA	Avg. windsp. *knots x 10*	17
8985	Walla Walla[3]	DHA	Avg. rel. hum. %	18	DHA	Hourly cloud cover	18	DHA	Avg. windsp. *knots x 10*	18
9046	Warm Springs Res.[3]							WRPE	Mon. windrun *mi*	6-9
9290	Whitehorse Ranch[3]				ASSR	Solar rad. $kW\ h\ m^{-2}$	7			
9316	Wickiup Dam[3]							WRPE	Mon. windrun *mi*	9-22

[1] Coast region [2] Willamette Valley and Southern Valleys regions
[3] East of the Cascades regions

Code	Data source	Provided by
ODD	Digital daily data base	State Climatologist
DHA	Digital hourly airport data base	State Climatologist
CHDD	Hermiston digital daily data base	Mr. Chaur-Fong Chen, Agr. Engr., Oregon State University
PNHH	Pacific NW published data base	Pacific NW River Basins Commission (1968)
PNSR	Pacific NW published solar radiation data base	Satterlund and Means (1979)
ASSR	Atmospheric Sciences solar radiation data base	Dr. Rao, Atm. Sci., Oregon State University
WRPE	Windrun (pan evaporimeter height) data base	State Climatologist

APPENDIX C. Aridity factors

List of the aridity factors used to compute local estimates of ET_r for each primary weather station.

			Aridity (%)			
Reg	Stn ID	Station name	Site	Area	Region	Cumulative
1	318	Astoria Exp. Stn.	30	30	0	27
1	324	Astoria	30	30	0	27
1	328	Astoria AP	30	30	0	27
1	471	Bandon	90	10	10	42
1	1055	Brookings	10	10	0	9
1	1324	Canary	50	10	0	25
1	1360	Cape Blanco	30	10	10	18
1	1682	Cloverdale	10	10	10	10
1	1836	Coquille City	10	10	10	10
1	2370	Dora	20	30	20	25
1	2633	Elkton	20	30	20	25
1	3356	Gold Beach R. Stn.	20	30	20	25
1	3995	Honeyman St. Park	20	20	20	20
1	4133	Illahe	20	30	20	25
1	5375	Mc Kinley	50	40	30	43
1	6032	Newport	50	10	20	27
1	6073	North Bend AP	20	20	20	20
1	6366	Otis	20	30	20	25
1	6779	Port Orford	50	20	10	31
1	6784	Port Orford 2	20	20	10	19
1	6820	Powers	20	40	30	31
1	7082	Reedsport	50	10	10	26
1	7641	Seaside	60	10	10	30
1	7866	Sitkum	50	10	10	26
1	8481	Tidewater	20	30	20	25
1	8494	Tillamook	20	40	30	31
1	8833	Valsetz	60	40	10	45
2	78	Albany 1	10	10	10	10
2	82	Albany 2	10	10	10	10
2	595	Beaverton	30	20	20	24
2	652	Belknap Springs	70	10	60	39
2	897	Bonneville Dam	10	10	10	10
2	1433	Cascadia	0	0	0	0
2	1552	Cherry Grove	40	20	20	28
2	1643	Clatskanie	10	0	0	4

			Aridity (%)			
Reg	Stn ID	Station name	Site	Area	Region	Cumulative
2	1862	Corvallis O.S.U.	10	10	10	10
2	1877	Corvallis W.B.	10	10	10	10
2	1897	Cottage Grove	10	20	20	16
2	1902	Cottage Grove Dam	90	20	20	48
2	2112	Dallas	80	20	30	45
2	2277	Detroit	50	30	20	37
2	2292	Detroit Dam	80	30	20	49
2	2374	Dorena Dam	20	40	20	30
2	2693	Estacada	80	40	30	55
2	2707	Eugene	10	10	10	10
2	2709	Eugene AP	10	10	10	10
2	2800	Falls City	10	40	30	27
2	2805	Falls City 2	10	40	30	27
2	2867	Fernridge Dam	80	10	10	38
2	2997	Forest Grove	20	40	30	31
2	3047	Foster Dam	80	40	30	55
2	3402	Government Camp	20	10	10	14
2	3770	Hwks. Portland W.B.	90	10	40	45
2	3908	Hillsboro	80	30	20	49
2	4603	La Comb 1	20	50	40	37
2	4606	La Comb 3	20	50	40	37
2	4811	Leaburg	70	50	30	56
2	5050	Lookout P. Dam	20	40	30	31
2	5221	Marion Forks	20	30	30	26
2	5362	Mc Kenzie Bridge	90	50	40	65
2	5384	Mc Minnville	20	30	20	25
2	5677	Molalla	50	30	20	37
2	6151	N. Willamette E.S	80	40	20	54
2	6173	Noti	20	30	10	24
2	6213	Oakridge	20	50	40	37
2	6334	Oregon City	50	20	20	32
2	6749	Portland KGW-TV	70	60	30	61
2	6751	Portland AP	80	60	30	65
2	6761	Portland W.B.	50	60	30	53
2	7466	Saint Helens	20	40	20	30
2	7500	Salem	20	10	10	14
2	7559	Santiam Pass	80	40	50	57
2	7586	Scogginns Dam	80	30	20	49
2	7631	Scotts Mills	20	40	30	31
2	7809	Silver Creek F.	20	30	20	25
2	7823	Silverton	80	50	40	61
2	7827	Silverton 4	50	50	40	49
2	8095	Stayton	20	30	20	25
2	8221	Sundown Ranch	50	30	20	37
2	8466	Three Lynx	60	20	30	37

			Aridity (%)			
Reg	Stn ID	Station name	Site	Area	Region	Cumulative
2	8634	Troutdale	80	20	20	44
2	8879	Vernonia	60	40	20	46
2	8884	Vernonia 2	50	40	20	42
2	9051	Warren	50	40	30	43
3	304	Ashland	30	50	50	42
3	1448	Cave Junction	10	30	30	22
3	2406	Drain	20	40	30	31
3	2928	Fish Lake	50	20	30	33
3	3445	Grants Pass	80	50	60	63
3	4060	Howard P. Dam	80	20	30	45
3	4126	Idleyld Park	20	40	30	31
3	4216	Jacksonville	50	50	40	49
3	4420	Kerby	80	80	70	79
3	4635	Lake Creek	50	50	40	49
3	4835	Lemolo Lake	90	10	10	42
3	5055	Lost Creek Dam	80	40	30	55
3	5424	Medford Exp. Stn.	20	30	40	27
3	5429	Medford AP	90	40	40	60
3	5656	Modoc Orchard	50	50	40	49
3	6907	Prospect	90	40	60	62
3	7169	Riddle	20	40	30	31
3	7326	Roseburg AP	50	60	70	57
3	7331	Roseburg	60	60	70	61
3	7391	Ruch	20	30	40	27
3	7698	Sexton Summit	20	50	60	39
3	7850	Siskiyou Summit	50	40	60	46
3	8338	Talent	50	40	40	44
3	8536	Toketee Falls	80	30	40	51
3	8588	Trail	50	50	60	51
4	197	Antelope	100	50	50	70
4	265	Arlington	30	50	30	40
4	753	Big Eddy	50	50	50	50
4	858	Boardman	10	20	20	16
4	1407	Cascade Locks	50	30	30	38
4	1765	Condon	10	70	80	47
4	2168	Dayville	80	80	70	79
4	2440	Dufur	80	30	20	49
4	2564	Echo	50	20	20	32
4	3038	Fossil	20	40	30	31
4	3121	Friend	50	50	60	51
4	3542	Grizzly	20	30	20	25
4	3644	Hardman	50	50	40	49
4	3737	Hay Creek	50	70	60	61
4	3827	Heppner	80	90	80	85
4	3847	Hermiston	10	40	30	27

			Aridity (%)			
Reg	Stn ID	Station name	Site	Area	Region	Cumulative
4	4003	Hood River E.S	70	20	30	41
4	4411	Kent	60	70	60	65
4	4479	Kinzua	50	90	80	73
4	5139	Madras	60	50	50	54
4	5142	Madras 2	80	50	50	62
4	5515	Metolius	20	70	90	52
4	5545	Mikkalo	60	50	30	52
4	5593	Milton Freewater	80	50	40	61
4	5641	Mitchell	90	80	70	83
4	5707	Montgomery Ranch	50	70	70	62
4	5734	Moro	80	70	80	75
4	6464	Parkdale	20	30	30	26
4	6468	Parkdale 2	50	30	30	38
4	6532	Pelton Dam	80	30	40	51
4	6540	Pendleton Exp. Stn.	60	80	70	71
4	6541	Pendleton R. Park	20	80	70	55
4	6546	Pendleton AP	20	80	70	55
4	6634	Pilot Rock	60	80	70	71
4	6655	Pine Grove	60	70	60	65
4	8009	Spray	50	70	70	62
4	8407	The Dalles	60	50	40	53
4	8530	Timberline Lodge	20	10	10	14
4	8734	Umatilla	50	40	50	45
4	9068	Wasco	50	70	80	63
4	9216	Weston	50	50	60	51
5	36	Adel	100	80	100	90
5	118	Alkali Lake	100	50	80	73
5	188	Andrews	100	100	100	100
5	189	Andrews Weston M.	100	100	100	100
5	501	Barnes Station	90	80	80	84
5	694	Bend	70	70	90	72
5	1067	Brothers	90	90	90	90
5	1176	Burns	70	70	80	71
5	1415	Cascade Summit	50	30	30	38
5	1546	Chemult	80	60	60	68
5	1571	Chiloquin	10	50	50	34
5	1946	Crater Lake	10	20	30	17
5	2415	Drewsey	80	40	30	55
5	3022	Forth Klamath	10	50	50	34
5	3095	Fremont	80	50	60	63
5	3659	Harney B. E.S	50	70	60	61
5	3692	Hart Mountain Ref.	80	80	70	79
5	4506	Klamath Falls	50	60	50	55
5	4511	Klamath F. Agr. Stn.	70	60	50	63
5	4632	Lake	50	80	80	68

			Aridity (%)			
Reg	Stn ID	Station name	Site	Area	Region	Cumulative
5	4670	Lakeview	60	80	100	74
5	5162	Malheur Ref. Hdq.	80	30	40	51
5	5170	Malin	80	40	50	57
5	5174	Malin 5	50	40	50	45
5	5505	Merrill	50	80	70	67
5	6243	Ochoco	20	40	50	33
5	6251	Odell Lake	20	30	50	28
5	6302	OO Ranch	60	50	70	56
5	6426	Paisley	20	60	70	45
5	6500	Paulina	60	50	60	55
5	6662	Pine Mountain	90	70	80	79
5	6717	Plush	50	80	80	68
5	6853	P Ranch Refuge	20	80	70	55
5	6883	Prineville	60	50	50	54
5	6982	Rager	50	50	60	51
5	7052	Redmond	20	60	70	45
5	7062	Redmond AP	70	60	70	65
5	7354	Round Grove	60	50	60	55
5	7533	Sand Creek	50	40	40	44
5	7817	Silver Lake	50	30	60	41
5	7857	Sisters	80	60	60	68
5	8007	Sprague River	80	20	50	47
5	8029	Squaw Butte E.S	80	80	80	80
5	8173	Summer Lake	60	30	80	47
5	8250	Suntex	20	70	80	51
5	8420	The Poplars	20	40	60	34
5	8812	Valley Falls	60	80	100	74
5	8818	Valley Falls 3	50	80	100	70
5	8924	Voltage	50	80	90	69
5	8948	Wagontire	60	50	80	57
5	9316	Wickiup Dam	80	30	60	53
5	9604	Yonna	50	20	50	35
6	41	Adrian	80	70	60	73
6	356	Austin	30	30	20	29
6	412	Baker AP	30	10	20	19
6	417	Baker KBKR	30	10	20	19
6	723	Beulah	10	50	90	38
6	1174	Burns Junction	90	100	100	96
6	1352	Canyon City	30	10	10	18
6	1926	Cove 1	50	20	10	31
6	2135	Danner	80	60	60	68
6	2482	Durkee	50	50	50	50
6	2597	Elgin	20	20	20	20
6	2672	Enterprise	20	30	20	25
6	2678	Enterprise 20	20	40	20	30

			Aridity (%)			
Reg	Stn ID	Station name	Site	Area	Region	Cumulative
6	3430	Granite	50	50	90	54
6	3604	Halfway	20	40	30	31
6	3666	Harper	50	70	60	61
6	4098	Huntington	80	60	70	69
6	4175	Ironside	20	40	30	31
6	4291	John Day	80	40	30	55
6	4329	Joseph	50	30	20	37
6	4357	Juntura	70	60	50	63
6	4615	La Grande	60	40	30	47
6	4622	La Grande KTVR	50	40	30	43
6	5020	Long Creek	20	50	30	36
6	5160	Malheur B. E.S	70	30	40	47
6	5258	Mason Dam	90	40	40	60
6	5335	Mc Dermitt	80	90	90	86
6	5396	Meacham	50	30	30	38
6	5610	Minam	50	50	40	49
6	5711	Monument	50	70	70	62
6	6179	Nyssa	20	60	70	45
6	6294	Ontario	80	50	40	61
6	6405	Owyhee Dam	60	30	70	46
6	6845	Prairie City	50	40	30	43
6	7160	Richland	60	40	30	47
6	7208	Riverside	90	50	90	70
6	7277	Rocksville	20	60	80	46
6	7310	Rome	80	40	80	60
6	7675	Seneca	70	50	30	56
6	7736	Sheaville	50	70	80	63
6	8726	Ukiah	20	40	40	32
6	8746	Union Exp. Stn.	20	20	20	20
6	8780	Unity	90	40	20	58
6	8797	Vale	80	40	50	57
6	8985	Walla Walla	20	40	40	32
6	8997	Wallowa	50	40	20	42
6	9046	Warm Springs Res.	50	70	80	63
6	9176	Westfall	60	70	80	67
6	9290	Whitehorse Ranch	20	70	80	51

APPENDIX D. Local values of ET_r

Values of local estimates of long-term monthly averages of daily ET_r, *mm* d^{-1}, and cumulative ET_r, *mm*, for each primary weather station.

Reg	Stn ID	Jan	Feb	Mar	Apr	May	Jun	Jul	Aug	Sep	Oct	Nov	Dec	Cum
1	318	0.25	0.79	1.47	2.53	3.49	3.40	3.68	3.22	2.79	1.75	0.63	0.30	742
1	324	0.27	0.77	1.51	2.70	3.62	3.47	3.75	3.28	2.81	1.81	0.63	0.34	762
1	328	0.30	0.81	1.50	2.48	3.43	3.38	3.66	3.22	2.73	1.71	0.63	0.31	737
1	471	0.50	0.80	1.38	2.26	2.89	3.33	3.30	2.70	2.44	1.86	0.80	0.42	692
1	1055	0.57	0.86	1.49	2.48	3.18	3.52	3.53	3.01	2.79	2.02	0.88	0.53	758
1	1324	0.40	0.73	1.33	2.30	3.01	3.59	3.69	3.05	2.72	1.92	0.75	0.34	727
1	1360	0.52	0.80	1.34	2.21	2.77	3.09	3.06	2.60	2.36	1.81	0.81	0.46	666
1	1682	0.38	0.92	1.58	2.58	3.49	3.44	3.75	3.26	2.87	1.88	0.73	0.38	771
1	1836	0.45	0.80	1.44	2.36	3.10	3.60	3.78	3.19	2.78	1.95	0.75	0.36	750
1	2370	0.45	0.81	1.48	2.43	3.24	3.82	3.99	3.35	2.93	2.05	0.75	0.36	783
1	2633	0.35	0.74	1.45	2.55	3.39	4.04	4.30	3.55	3.01	2.00	0.70	0.28	805
1	3356	0.56	0.85	1.45	2.38	3.05	3.41	3.45	2.91	2.65	1.96	0.85	0.52	733
1	3995	0.42	0.76	1.39	2.31	3.04	3.54	3.65	3.00	2.70	1.90	0.71	0.29	724
1	4133	0.35	0.74	1.50	2.64	3.54	4.08	4.40	3.72	3.17	2.05	0.72	0.32	831
1	5375	0.40	0.74	1.47	2.49	3.13	3.61	3.69	3.07	2.74	2.01	0.74	0.36	746
1	6032	0.42	0.80	1.41	2.32	3.05	3.31	3.40	2.83	2.54	1.81	0.73	0.36	701
1	6073	0.49	0.80	1.41	2.36	3.07	3.54	3.58	2.99	2.65	1.95	0.82	0.42	735
1	6366	0.31	0.79	1.44	2.39	3.24	3.39	3.61	3.10	2.71	1.77	0.64	0.28	722
1	6779	0.55	0.82	1.44	2.43	3.06	3.43	3.46	2.89	2.59	1.94	0.84	0.51	731
1	6784	0.53	0.84	1.44	2.33	3.03	3.49	3.58	3.03	2.72	1.95	0.82	0.46	739
1	6820	0.42	0.76	1.40	2.45	3.21	3.73	3.90	3.26	2.84	1.99	0.75	0.37	765
1	7082	0.41	0.76	1.36	2.33	3.06	3.56	3.66	3.03	2.72	1.96	0.75	0.35	731
1	7641	0.37	0.89	1.58	2.58	3.51	3.36	3.58	3.17	2.77	1.82	0.70	0.39	754
1	7866	0.33	0.69	1.28	2.35	3.16	3.70	3.87	3.22	2.79	1.90	0.68	0.32	741
1	8481	0.37	0.80	1.47	2.49	3.32	3.72	3.96	3.32	2.93	1.98	0.73	0.30	775
1	8494	0.35	0.87	1.52	2.48	3.34	3.26	3.44	2.98	2.63	1.75	0.68	0.36	722
1	8833	0.21	0.65	1.30	2.24	3.19	3.44	3.75	3.11	2.61	1.70	0.56	0.20	701
2	78	0.23	0.84	1.56	3.16	4.18	5.01	6.11	5.06	3.82	2.10	0.63	0.21	1005
2	82	0.25	0.87	1.51	2.85	4.02	4.92	5.95	5.00	3.73	2.02	0.66	0.17	976
2	595	0.31	0.93	1.83	3.17	4.30	4.90	5.30	4.69	3.61	2.08	0.65	0.25	978
2	652	0.01	0.51	1.16	2.33	3.44	4.47	5.21	4.27	3.23	1.84	0.39	0.00	821
2	897	0.19	0.79	1.71	3.25	4.46	5.06	5.66	4.96	3.82	2.19	0.65	0.22	1007
2	1433	0.18	0.73	1.44	2.85	3.87	4.76	5.53	4.65	3.52	1.99	0.55	0.12	922
2	1552	0.18	0.73	1.49	2.81	3.95	4.53	5.13	4.46	3.54	2.05	0.58	0.18	905
2	1643	0.24	0.81	1.66	3.08	4.23	4.73	5.21	4.68	3.62	2.01	0.59	0.24	950
2	1862	0.22	0.84	1.51	2.98	4.04	4.90	6.00	5.07	3.81	2.07	0.62	0.18	985
2	1877	0.19	0.76	1.48	2.79	3.84	4.80	5.74	4.83	3.66	2.02	0.56	0.10	940
2	1897	0.27	0.79	1.40	2.66	3.61	4.46	5.24	4.32	3.35	1.98	0.61	0.16	881
2	1902	0.23	0.76	1.31	2.52	3.48	4.33	5.03	4.12	3.24	1.93	0.59	0.14	845

Reg	Stn ID	Jan	Feb	Mar	Apr	May	Jun	Jul	Aug	Sep	Oct	Nov	Dec	Cum
2	2112	0.25	0.78	1.57	2.88	4.02	4.75	5.27	4.45	3.54	2.21	0.63	0.20	933
2	2277	0.04	0.55	1.18	2.49	3.63	4.41	5.10	4.24	3.20	1.85	0.45	0.02	830
2	2292	0.18	0.69	1.32	2.51	3.61	4.47	5.13	4.34	3.35	2.07	0.56	0.11	866
2	2374	0.25	0.76	1.32	2.53	3.49	4.38	5.09	4.18	3.28	1.92	0.58	0.14	853
2	2693	0.30	0.86	1.70	3.03	4.08	4.61	5.00	4.24	3.32	2.04	0.64	0.25	918
2	2707	0.26	0.72	1.60	3.16	4.15	5.06	5.87	4.73	3.78	2.22	0.56	0.17	986
2	2709	0.24	0.74	1.56	3.01	4.06	5.06	5.94	4.80	3.83	2.10	0.55	0.14	978
2	2800	0.22	0.72	1.48	2.91	3.97	4.63	5.44	4.61	3.63	2.15	0.60	0.19	933
2	2805	0.22	0.78	1.51	2.75	3.81	4.69	5.42	4.66	3.54	2.08	0.60	0.14	922
2	2867	0.23	0.72	1.51	2.91	3.96	4.90	5.64	4.54	3.70	2.14	0.55	0.12	944
2	2997	0.27	0.84	1.73	3.16	4.34	4.90	5.37	4.69	3.62	2.10	0.63	0.24	974
2	3047	0.27	0.85	1.58	2.78	3.79	4.61	5.26	4.30	3.32	2.09	0.63	0.17	905
2	3402	0.00	0.27	0.76	1.75	2.86	3.64	4.40	3.79	2.78	1.46	0.20	0.00	670
2	3770	0.27	0.82	1.65	3.03	4.16	4.66	5.07	4.37	3.43	2.10	0.64	0.24	929
2	3908	0.28	0.87	1.74	3.15	4.27	4.79	5.19	4.43	3.45	2.07	0.63	0.26	950
2	4603	0.23	0.79	1.47	2.81	3.86	4.64	5.47	4.54	3.54	2.09	0.63	0.17	924
2	4606	0.24	0.80	1.57	2.81	3.80	4.64	5.26	4.43	3.40	2.07	0.59	0.17	909
2	4811	0.28	0.80	1.52	2.82	3.78	4.59	5.27	4.22	3.39	2.10	0.61	0.16	902
2	5050	0.30	0.85	1.52	2.75	3.67	4.56	5.29	4.34	3.45	2.15	0.66	0.20	908
2	5221	0.00	0.40	0.99	2.19	3.35	4.33	5.10	4.18	3.02	1.64	0.30	0.00	780
2	5362	0.10	0.63	1.38	2.73	3.78	4.61	5.25	4.19	3.28	1.97	0.47	0.03	868
2	5384	0.26	0.81	1.65	3.04	4.16	4.80	5.35	4.60	3.56	2.14	0.63	0.22	953
2	5677	0.31	0.85	1.59	2.93	4.02	4.67	5.11	4.40	3.47	2.06	0.66	0.24	925
2	6151	0.27	0.84	1.65	2.86	3.92	4.56	4.85	4.17	3.25	1.96	0.61	0.21	890
2	6173	0.26	0.76	1.55	2.87	3.90	4.86	5.59	4.53	3.56	2.08	0.56	0.12	936
2	6213	0.22	0.76	1.45	2.79	3.80	4.68	5.52	4.51	3.58	2.15	0.59	0.12	921
2	6334	0.35	0.96	1.81	3.25	4.40	4.98	5.34	4.64	3.64	2.15	0.70	0.29	992
2	6749	0.41	1.05	2.03	3.41	4.50	5.08	5.36	4.68	3.71	2.32	0.76	0.32	1026
2	6751	0.34	0.99	1.91	3.30	4.47	5.01	5.39	4.65	3.60	2.21	0.73	0.31	1005
2	6761	0.43	1.12	1.98	3.46	4.66	5.12	5.56	4.81	3.79	2.37	0.82	0.39	1053
2	7466	0.30	0.98	2.00	3.38	4.52	5.14	5.50	4.96	3.74	2.20	0.66	0.25	1027
2	7500	0.31	0.80	1.64	2.97	4.10	4.99	5.54	4.82	3.71	2.28	0.66	0.23	979
2	7559	0.00	0.14	0.58	1.41	2.44	3.40	4.33	3.40	2.38	1.24	0.10	0.00	594
2	7586	0.26	0.78	1.65	2.93	4.00	4.64	5.07	4.43	3.51	2.09	0.63	0.22	923
2	7631	0.22	0.65	1.23	2.29	3.33	4.09	4.63	3.97	3.07	1.90	0.50	0.13	794
2	7809	0.19	0.67	1.36	2.61	3.69	4.38	4.97	4.18	3.24	1.94	0.52	0.13	852
2	7823	0.27	0.82	1.65	2.82	3.91	4.69	5.10	4.39	3.43	2.23	0.65	0.18	920
2	7827	0.25	0.71	1.41	2.80	3.80	4.60	5.19	4.37	3.46	2.19	0.58	0.21	903
2	8095	0.30	0.84	1.63	2.95	4.04	4.86	5.46	4.67	3.59	2.22	0.67	0.21	960
2	8221	0.16	0.55	1.18	2.35	3.37	3.92	4.58	3.91	3.10	1.90	0.58	0.15	787
2	8466	0.15	0.66	1.43	2.80	3.90	4.55	5.08	4.32	3.34	1.99	0.53	0.12	882
2	8634	0.33	0.99	1.89	3.33	4.44	5.08	5.47	4.75	3.66	2.21	0.75	0.30	1013
2	8879	0.19	0.71	1.48	2.83	3.90	4.31	4.74	4.10	3.25	1.88	0.54	0.19	859
2	8884	0.17	0.74	1.58	2.72	3.83	4.38	4.71	4.15	3.14	1.82	0.51	0.14	852
2	9051	0.28	0.88	1.71	3.08	4.35	4.82	5.30	4.63	3.60	2.08	0.65	0.27	966
3	304	0.25	0.97	1.87	3.61	4.92	6.05	6.88	5.81	4.29	2.54	0.69	0.13	1161
3	1448	0.36	0.93	1.58	2.97	4.34	5.32	6.40	5.46	4.17	2.48	0.74	0.24	1069

Reg	Stn ID	Jan	Feb	Mar	Apr	May	Jun	Jul	Aug	Sep	Oct	Nov	Dec	Cum
3	2406	0.32	0.87	1.51	2.83	3.80	4.67	5.51	4.51	3.54	2.13	0.66	0.20	933
3	2928	0.00	0.25	0.89	2.27	3.55	4.51	5.58	4.72	3.56	1.91	0.38	0.00	845
3	3445	0.41	0.91	1.59	3.06	4.26	5.12	6.18	5.13	4.01	2.55	0.79	0.29	1048
3	4060	0.00	0.37	0.95	2.17	3.54	4.72	5.56	4.71	3.37	1.91	0.27	0.00	843
3	4126	0.24	0.81	1.42	2.65	3.65	4.57	5.49	4.52	3.48	2.03	0.58	0.12	903
3	4216	0.18	1.01	1.44	3.52	4.84	5.12	6.38	5.14	3.95	2.81	0.71	0.25	1080
3	4420	0.37	0.85	1.52	2.96	3.89	4.80	5.76	4.78	3.64	2.49	0.80	0.24	980
3	4635	0.24	0.91	1.75	3.48	4.60	5.57	6.50	5.45	4.16	2.48	0.69	0.13	1098
3	4835	0.04	0.39	0.99	1.99	3.08	4.16	5.10	4.23	2.98	1.79	0.23	0.00	764
3	5055	0.27	0.88	1.60	3.03	4.34	5.44	6.38	5.39	3.99	2.44	0.64	0.14	1055
3	5424	0.23	1.00	1.94	3.81	5.19	6.34	7.14	6.09	4.48	2.51	0.66	0.13	1207
3	5429	0.23	1.02	1.95	3.76	5.12	6.34	7.19	6.03	4.43	2.59	0.68	0.11	1205
3	5656	0.25	0.99	1.90	3.75	4.96	6.09	6.98	5.86	4.37	2.59	0.68	0.14	1178
3	6907	0.18	0.73	1.41	2.78	3.95	4.86	5.85	4.83	3.66	2.24	0.60	0.09	953
3	7169	0.39	0.90	1.54	2.90	3.94	4.84	5.95	4.95	3.84	2.34	0.76	0.27	996
3	7326	0.29	0.83	1.44	2.81	3.69	4.52	5.73	4.62	3.61	2.09	0.61	0.22	930
3	7331	0.30	0.85	1.50	2.70	3.73	4.68	5.69	4.70	3.60	2.14	0.63	0.18	938
3	7391	0.30	1.04	1.90	3.58	5.11	6.27	7.04	6.05	4.47	2.62	0.70	0.16	1198
3	7698	0.27	0.50	0.80	1.92	3.10	4.04	5.28	4.47	3.59	2.18	0.61	0.17	823
3	7850	0.00	0.46	1.21	2.64	3.93	4.73	5.99	5.11	3.97	2.25	0.45	0.00	940
3	8338	0.22	0.95	1.93	3.82	5.16	6.30	7.14	6.00	4.35	2.51	0.66	0.13	1196
3	8536	0.14	0.67	1.30	2.62	3.78	4.82	5.77	4.68	3.53	1.99	0.48	0.03	911
3	8588	0.22	0.81	1.44	2.85	4.09	4.98	5.99	4.96	3.93	2.32	0.64	0.11	988
4	197	0.00	0.59	1.43	2.98	4.24	5.16	6.17	5.07	3.68	2.29	0.54	0.00	982
4	265	0.01	0.79	1.95	4.03	5.73	6.75	7.63	6.70	4.67	2.74	0.61	0.05	1273
4	753	0.00	0.55	1.74	3.92	5.53	6.35	7.56	6.29	4.67	2.48	0.53	0.07	1213
4	858	0.00	0.87	2.17	4.38	6.22	7.28	7.92	7.21	4.72	2.79	0.63	0.01	1351
4	1407	0.08	0.67	1.76	3.78	5.11	5.80	6.88	5.80	4.35	2.48	0.63	0.16	1146
4	1765	0.00	0.48	1.37	2.94	4.30	5.24	6.28	5.33	3.75	2.20	0.42	0.00	988
4	2168	0.07	0.71	1.50	3.11	4.24	5.17	6.03	4.84	3.61	2.42	0.66	0.06	990
4	2440	0.00	0.51	1.51	3.29	4.80	5.68	6.75	5.61	4.06	2.13	0.40	0.00	1062
4	2564	0.00	0.65	1.71	3.62	5.11	5.96	6.62	5.60	3.99	2.34	0.49	0.03	1104
4	3038	0.00	0.62	1.31	2.88	4.25	5.10	6.09	5.16	3.56	2.12	0.56	0.00	967
4	3121	0.00	0.39	1.21	2.81	4.19	5.10	6.36	5.21	3.78	1.95	0.30	0.00	957
4	3542	0.00	0.59	1.25	2.63	3.76	4.76	5.74	4.77	3.47	2.07	0.53	0.01	904
4	3644	0.00	0.49	1.11	2.34	3.72	4.80	5.54	4.73	3.31	1.99	0.43	0.00	870
4	3737	0.01	0.54	1.60	3.21	4.25	5.06	6.03	4.86	3.61	2.28	0.52	0.02	978
4	3827	0.09	0.66	1.58	3.12	4.30	5.14	5.74	4.70	3.87	2.34	0.57	0.01	981
4	3847	0.00	0.57	1.68	3.51	4.98	5.88	6.44	5.51	3.84	2.18	0.43	0.00	1070
4	4003	0.00	0.59	1.61	3.45	4.96	5.77	6.75	5.65	4.07	2.19	0.47	0.02	1086
4	4411	0.00	0.48	1.39	2.98	4.38	5.32	6.37	5.36	3.79	2.26	0.42	0.00	1001
4	4479	0.00	0.41	1.28	2.74	3.82	4.69	5.56	4.51	3.27	2.17	0.49	0.00	885
4	5139	0.07	0.72	1.56	3.08	4.10	4.96	5.80	4.63	3.45	2.08	0.61	0.08	951
4	5142	0.06	0.69	1.53	3.02	4.04	4.91	5.72	4.64	3.48	2.12	0.57	0.06	942
4	5515	0.05	0.72	1.50	2.96	4.01	4.87	5.70	4.60	3.44	2.07	0.61	0.07	935
4	5545	0.00	0.73	1.70	3.44	4.97	6.04	7.01	6.10	4.24	2.56	0.52	0.00	1140
4	5593	0.00	0.61	1.79	3.56	4.92	5.93	7.13	5.86	4.14	2.42	0.54	0.03	1129

Reg	Stn ID	Jan	Feb	Mar	Apr	May	Jun	Jul	Aug	Sep	Oct	Nov	Dec	Cum
4	5641	0.05	0.64	1.47	3.01	4.12	5.12	6.01	4.84	3.57	2.34	0.57	0.03	971
4	5707	0.07	0.70	1.71	3.29	4.27	4.97	5.86	4.65	3.53	2.31	0.67	0.12	982
4	5734	0.00	0.51	1.49	3.18	4.65	5.49	6.43	5.43	3.82	2.26	0.42	0.00	1030
4	6464	0.00	0.42	1.36	3.18	4.57	5.37	6.45	5.36	3.88	2.01	0.37	0.00	1008
4	6468	0.00	0.44	1.33	2.90	4.37	5.27	6.30	5.17	3.66	1.92	0.33	0.00	969
4	6532	0.21	0.94	1.89	3.55	4.67	5.73	6.60	5.38	4.01	2.44	0.78	0.16	1110
4	6540	0.01	0.65	1.75	3.35	4.75	5.91	6.68	5.54	3.94	2.36	0.55	0.07	1087
4	6541	0.00	0.58	1.70	3.53	4.89	5.75	6.66	5.44	4.07	2.42	0.55	0.11	1091
4	6546	0.00	0.68	1.70	3.39	4.87	5.97	6.96	5.84	4.17	2.41	0.56	0.05	1119
4	6634	0.00	0.56	1.55	3.16	4.45	5.42	6.53	5.37	3.85	2.29	0.54	0.01	1031
4	6655	0.00	0.58	1.52	3.03	4.40	5.33	6.34	5.27	3.60	2.07	0.43	0.00	996
4	8009	0.11	0.82	1.69	3.37	4.69	5.90	6.89	5.66	4.15	2.57	0.69	0.08	1119
4	8407	0.03	0.67	1.83	3.93	5.59	6.53	7.67	6.33	4.59	2.48	0.56	0.07	1231
4	8530	0.00	0.00	0.58	1.81	3.07	3.65	5.32	4.57	3.19	1.39	0.12	0.00	726
4	8734	0.00	0.62	1.75	3.71	5.22	6.05	6.70	5.72	4.00	2.34	0.49	0.02	1119
4	9068	0.00	0.53	1.63	3.51	4.97	5.74	6.82	5.77	4.13	2.44	0.47	0.01	1101
4	9216	0.00	0.44	1.54	3.26	4.55	5.40	6.73	5.61	4.02	2.29	0.51	0.00	1050
5	36	0.01	0.56	1.29	2.65	4.13	4.96	5.71	4.60	3.48	2.40	0.59	0.00	928
5	118	0.00	0.52	1.18	2.49	3.81	4.81	5.51	4.49	3.26	2.14	0.49	0.00	877
5	188	0.00	0.32	1.41	3.11	4.29	5.16	5.90	4.67	3.42	2.43	0.50	0.00	954
5	189	0.00	0.49	1.30	2.81	4.12	5.30	5.95	4.92	3.55	2.47	0.54	0.00	961
5	501	0.00	0.49	1.16	2.40	3.61	4.62	5.33	4.24	3.10	2.10	0.44	0.00	840
5	694	0.08	0.67	1.50	2.85	3.94	4.86	5.59	4.43	3.36	2.40	0.64	0.07	928
5	1067	0.00	0.42	1.05	2.18	3.30	4.31	5.00	3.87	2.84	1.96	0.37	0.00	773
5	1176	0.00	0.21	0.88	2.30	3.53	4.58	5.35	4.34	3.14	2.05	0.32	0.00	817
5	1415	0.00	0.24	0.92	2.00	3.06	3.88	4.83	3.82	2.78	1.70	0.38	0.00	722
5	1546	0.00	0.27	0.94	2.04	3.20	4.09	4.81	3.68	2.78	1.75	0.34	0.00	731
5	1571	0.00	0.34	1.09	2.38	3.55	4.49	5.54	4.45	3.38	1.99	0.40	0.00	844
5	1946	0.00	0.06	0.49	1.47	2.49	3.50	4.75	3.92	2.92	1.62	0.24	0.00	657
5	2415	0.00	0.29	1.21	2.75	3.94	5.06	5.87	4.74	3.26	2.02	0.30	0.00	900
5	3022	0.00	0.29	1.01	2.31	3.41	4.33	5.36	4.21	3.35	2.01	0.44	0.00	817
5	3095	0.00	0.35	1.09	2.21	3.31	4.18	4.93	3.82	2.82	1.81	0.37	0.00	761
5	3659	0.00	0.00	0.85	2.45	3.54	4.33	5.17	4.15	2.99	1.90	0.22	0.00	784
5	3692	0.00	0.24	0.79	2.06	3.24	4.08	4.84	3.93	2.94	1.98	0.35	0.00	748
5	4506	0.00	0.50	1.33	2.81	4.08	5.09	6.32	5.12	4.00	2.45	0.56	0.00	986
5	4511	0.00	0.52	1.25	2.66	3.82	4.81	6.01	4.82	3.81	2.37	0.49	0.00	934
5	4632	0.00	0.39	1.08	2.32	3.53	4.43	5.31	4.13	3.02	1.96	0.42	0.00	813
5	4670	0.00	0.33	1.12	2.52	3.74	4.62	5.54	4.44	3.38	2.18	0.46	0.00	866
5	5162	0.00	0.35	1.02	2.43	3.88	4.83	5.43	4.46	3.22	1.98	0.34	0.00	854
5	5170	0.00	0.41	1.36	2.82	3.99	4.80	5.88	4.55	3.51	2.25	0.46	0.00	918
5	5174	0.00	0.56	1.22	2.51	3.89	4.97	6.02	4.98	3.82	2.34	0.51	0.00	942
5	5505	0.00	0.42	1.17	2.51	3.66	4.54	5.52	4.30	3.59	2.25	0.53	0.00	871
5	6243	0.00	0.29	1.04	2.48	3.65	4.58	5.50	4.54	3.33	1.92	0.30	0.00	845
5	6251	0.00	0.30	0.83	1.80	2.91	3.93	4.83	3.82	2.82	1.61	0.38	0.00	710
5	6302	0.00	0.33	0.99	2.39	3.78	4.76	5.33	4.42	3.16	2.00	0.37	0.00	842
5	6426	0.00	0.59	1.33	2.82	4.03	4.92	5.90	4.83	3.65	2.34	0.57	0.00	947
5	6500	0.00	0.48	1.20	2.54	3.76	4.79	5.62	4.53	3.24	2.04	0.44	0.00	875

Reg	Stn ID	Jan	Feb	Mar	Apr	May	Jun	Jul	Aug	Sep	Oct	Nov	Dec	Cum
5	6662	0.00	0.22	0.76	1.68	2.97	4.01	5.05	3.90	2.95	1.80	0.30	0.00	723
5	6717	0.00	0.44	1.21	2.89	3.96	4.75	5.72	4.57	3.50	2.25	0.50	0.00	911
5	6853	0.00	0.52	1.24	2.72	4.03	4.96	5.49	4.51	3.37	2.19	0.52	0.00	903
5	6883	0.07	0.70	1.47	2.93	4.05	4.95	5.84	4.62	3.45	2.22	0.62	0.06	946
5	6982	0.00	0.46	1.09	2.37	3.72	4.81	5.72	4.76	3.45	2.15	0.48	0.00	887
5	7052	0.12	0.76	1.49	2.99	4.12	5.13	6.32	5.05	3.89	2.46	0.72	0.15	1014
5	7062	0.08	0.71	1.39	2.75	3.90	5.02	6.17	4.92	3.69	2.35	0.63	0.06	968
5	7354	0.00	0.36	1.02	2.25	3.35	4.26	5.29	4.26	3.24	2.04	0.43	0.00	810
5	7533	0.00	0.16	0.94	2.17	3.31	4.16	5.14	4.01	3.06	1.84	0.30	0.00	768
5	7817	0.00	0.53	1.22	2.40	3.68	4.69	5.42	4.53	3.28	2.05	0.47	0.00	864
5	7857	0.06	0.66	1.40	2.57	3.67	4.79	5.57	4.46	3.29	2.17	0.53	0.00	891
5	8007	0.00	0.40	1.12	2.36	3.58	4.68	5.71	4.59	3.43	2.08	0.41	0.00	867
5	8029	0.00	0.21	0.89	2.25	3.48	4.45	5.22	4.29	3.17	2.13	0.33	0.00	808
5	8173	0.04	0.65	1.36	2.70	3.99	5.03	5.91	4.81	3.55	2.29	0.58	0.01	945
5	8250	0.00	0.21	0.91	2.31	3.50	4.51	5.20	4.30	3.09	1.93	0.27	0.00	802
5	8420	0.00	0.47	1.14	2.48	3.65	4.51	5.37	4.34	3.16	1.92	0.43	0.00	840
5	8812	0.00	0.45	1.22	2.65	3.79	4.57	5.36	4.30	3.22	2.18	0.48	0.00	863
5	8818	0.00	0.54	1.18	2.52	3.78	4.73	5.69	4.57	3.51	2.28	0.50	0.00	895
5	8924	0.00	0.25	1.01	2.58	3.93	4.57	5.32	4.29	3.23	2.07	0.37	0.00	845
5	8948	0.00	0.30	0.94	2.17	3.46	4.51	5.26	4.31	3.15	1.99	0.28	0.00	807
5	9316	0.00	0.38	1.06	2.16	3.31	4.21	4.89	3.83	2.80	1.77	0.44	0.00	760
5	9604	0.00	0.36	1.24	2.71	3.87	4.86	6.26	5.09	3.89	2.30	0.45	0.00	949
6	41	0.00	0.60	1.78	3.85	5.22	6.40	7.51	5.83	4.36	2.84	0.67	0.00	1194
6	356	0.00	0.00	0.74	2.31	3.37	4.32	5.48	4.39	3.10	1.67	0.15	0.00	782
6	412	0.00	0.20	1.07	2.78	3.97	4.89	6.25	5.07	3.77	2.03	0.36	0.00	930
6	417	0.00	0.29	1.12	2.90	4.05	5.02	6.48	5.26	4.05	2.25	0.47	0.00	975
6	723	0.00	0.35	1.29	3.12	4.27	5.36	6.52	5.27	3.89	2.40	0.47	0.00	1007
6	1174	0.00	0.55	1.50	3.22	4.37	5.69	6.18	4.94	3.64	2.50	0.50	0.00	1011
6	1352	0.00	0.52	1.37	3.26	4.32	5.16	6.58	5.42	4.11	2.47	0.63	0.02	1035
6	1926	0.00	0.40	1.23	2.86	3.92	4.71	6.01	4.96	3.58	2.09	0.50	0.00	925
6	2135	0.00	0.36	1.34	3.06	4.21	5.33	6.22	4.98	3.62	2.40	0.47	0.00	978
6	2482	0.00	0.34	1.22	2.94	4.19	5.14	6.52	5.19	3.87	2.20	0.44	0.00	980
6	2597	0.00	0.39	1.21	2.87	4.05	4.87	6.21	5.22	3.65	1.96	0.39	0.00	943
6	2672	0.00	0.11	0.94	2.55	3.73	4.53	5.72	4.67	3.34	1.77	0.21	0.00	844
6	2678	0.00	0.26	1.12	2.61	3.83	4.79	5.80	4.93	3.31	1.70	0.22	0.00	874
6	3430	0.00	0.00	0.46	1.89	3.00	3.88	4.91	3.92	2.92	1.61	0.10	0.00	695
6	3604	0.00	0.14	1.16	3.04	4.22	5.15	6.37	5.19	3.79	2.11	0.37	0.00	965
6	3666	0.00	0.38	1.52	3.48	4.65	5.85	6.77	5.23	3.82	2.46	0.48	0.00	1059
6	4098	0.00	0.48	1.70	3.90	5.30	6.59	7.73	6.11	4.53	2.82	0.58	0.00	1215
6	4175	0.00	0.18	1.13	2.83	4.04	5.18	6.59	5.39	3.84	2.17	0.32	0.00	969
6	4291	0.00	0.53	1.31	2.84	4.01	5.12	6.10	4.95	3.65	2.28	0.55	0.00	958
6	4329	0.00	0.04	0.89	2.58	3.71	4.39	5.72	4.68	3.44	1.93	0.27	0.00	846
6	4357	0.00	0.55	1.53	3.33	4.53	5.74	6.73	5.42	3.95	2.55	0.58	0.00	1067
6	4615	0.00	0.47	1.35	3.12	4.04	4.80	6.04	4.97	3.66	2.26	0.59	0.03	958
6	4622	0.00	0.54	1.38	2.95	4.00	4.90	5.92	5.02	3.60	2.15	0.54	0.00	947
6	5020	0.00	0.49	1.16	2.53	3.66	4.71	5.68	4.78	3.35	2.04	0.42	0.00	881
6	5160	0.00	0.46	1.79	4.18	5.53	6.88	7.46	5.84	4.34	2.71	0.50	0.00	1213

Reg	Stn ID	Jan	Feb	Mar	Apr	May	Jun	Jul	Aug	Sep	Oct	Nov	Dec	Cum
6	5258	0.00	0.05	0.89	2.40	3.54	4.47	5.48	4.44	3.24	1.90	0.27	0.00	817
6	5335	0.00	0.54	1.40	2.95	4.20	5.31	5.88	4.72	3.55	2.46	0.55	0.00	964
6	5396	0.00	0.05	0.48	1.73	3.00	3.83	5.61	4.65	3.15	1.43	0.11	0.00	736
6	5610	0.00	0.07	0.79	2.20	3.33	4.22	5.26	4.41	3.00	1.51	0.11	0.00	762
6	5711	0.00	0.66	1.51	3.09	4.33	5.43	6.32	5.29	3.73	2.28	0.57	0.00	1015
6	6179	0.00	0.52	1.79	4.09	5.45	6.79	7.59	6.02	4.40	2.76	0.59	0.00	1223
6	6294	0.00	0.49	1.86	4.24	5.64	7.02	7.57	5.84	4.30	2.71	0.51	0.00	1228
6	6405	0.00	0.68	1.84	3.85	5.14	6.35	7.32	5.90	4.56	3.00	0.75	0.02	1204
6	6845	0.00	0.36	1.38	3.19	4.27	5.28	6.56	5.27	3.84	2.49	0.59	0.00	1016
6	7160	0.00	0.51	1.54	3.52	4.75	5.76	6.95	5.64	4.26	2.52	0.61	0.00	1102
6	7208	0.00	0.40	1.39	3.08	4.12	5.29	6.11	4.95	3.51	2.30	0.48	0.00	967
6	7277	0.00	0.47	1.41	3.03	4.33	5.58	6.55	5.26	3.79	2.27	0.52	0.00	1015
6	7310	0.00	0.56	1.47	3.21	4.55	5.69	6.49	5.19	3.78	2.46	0.55	0.00	1038
6	7675	0.00	0.00	0.66	2.10	3.13	4.10	4.83	3.75	2.59	1.55	0.14	0.00	699
6	7736	0.00	0.29	1.20	2.83	4.09	5.29	6.38	5.08	3.70	2.37	0.45	0.00	969
6	8726	0.00	0.17	0.98	2.46	3.54	4.45	5.49	4.51	3.13	1.77	0.27	0.00	819
6	8746	0.00	0.43	1.29	2.95	3.96	4.75	6.00	4.98	3.60	2.08	0.53	0.00	935
6	8780	0.00	0.09	0.96	2.50	3.64	4.53	5.68	4.48	3.29	1.95	0.25	0.00	838
6	8797	0.00	0.46	1.77	3.99	5.31	6.66	7.38	5.71	4.19	2.69	0.53	0.00	1183
6	8985	0.00	0.32	1.28	2.75	4.04	5.08	6.34	5.22	3.57	1.77	0.20	0.00	935
6	8997	0.00	0.16	1.13	2.75	3.87	4.71	5.86	4.79	3.38	1.85	0.28	0.00	881
6	9046	0.00	0.33	1.32	3.13	4.07	5.11	6.17	5.03	3.73	2.50	0.49	0.00	975
6	9176	0.00	0.41	1.46	3.22	4.54	5.71	6.70	5.35	3.99	2.51	0.52	0.00	1052
6	9290	0.00	0.53	1.38	2.91	4.21	5.23	5.95	4.90	3.65	2.37	0.58	0.00	969

APPENDIX E. Listing of VARIOWRT

Listing of the computer program VARIOWRT used to compute the experimental semivariograms for elevation.

```
'    ************************************************************
'    ***                                                      ***
'    ***                   Program VARIOWRT                   ***
'    ***                                                      ***
'    ***        Program to compute experimental direct        ***
'    ***       semivariograms for a single regionalized       ***
'    ***    variable with a maximum of 3240 sample values     ***
'    ***                                                      ***
'    ***    Author:  Antonio Martínez-Cob                     ***
'    ***             Water Resources Engineering Team         ***
'    ***             Department of Agricultural Engineering   ***
'    ***             Oregon State University                  ***
'    ***                                                      ***
'    ************************************************************

     REM $INCLUDE: 'c:\qb45\wret_lib\wret.icl'
     DIM PAIRLG(125), ADST(125), GAMMA(125)
     DIM EAST(3240), NORT(3240), ELEV(3240)
     CONST PI = 3.141592653#

40   CLS
     INPUT "Maximum distance?  ", MXDST
     NLGS = MXDST / 5
     INPUT "Direction?  ", DANG
     INPUT "Tolerance?  ", ANGTOL
     INPUT "Input file name?  ", INPF$
     INPUT "Output file name?  ", OUTF$

     IF DANG = 0 THEN ALP = 1
     IF DANG = 45 THEN ALP = 2
     IF DANG = 90 THEN ALP = 3
     IF DANG = 135 THEN ALP = 4
     TANTOL1 = TAN(ANGTOL * PI / 180)
     TANTOL2 = TAN((ANGTOL + 45) * PI / 180)
     TANTOL3 = TANTOL1 * (-1)
     TANTOL4 = TANTOL2 * (-1)

     J = 0
     FOR B = 1 TO NLGS
        PAIRLG(B) = 0
        ADST(B) = 0
        GAMMA(B) = 0
     NEXT B
```

```
    OPEN "I", #1, INPF$
    WHILE NOT EOF(1)
       J = J + 1
       INPUT #1, EAST(J), NORT(J), ELEV(J)
    WEND
    CLOSE #1

    FOR H = 1 TO J
       LEAT = 0
       LNORT = 0

    COLOR 31: LOCATE 12, 30: PRINT "Please, wait!"
    LOCATE 14, 30: PRINT "I am working very hard": COLOR 7
    LOCATE 17, 30: PRINT "Sample # "; H

       FOR S = 1 TO J
          IF H > S THEN 20
          IF LEAT = 0 AND LNORT = 0 THEN
             LEAT = EAST(S)
             LNORT = NORT(S)
             LELV = ELEV(S)
             GOTO 20
          ELSE
          END IF
          DIST = ((EAST(S) - LEAT) ^ 2 + (NORT(S) - LNORT) ^ 2) ^ .5
          IF ANGTOL = 180 THEN 50
          XDIV = EAST(S) - LEAT
          IF XDIV = 0 THEN XDIV = .00001
          ANGTAN = (NORT(S) - LNORT) / XDIV
          SELECT CASE ALP
             CASE 1: IF ABS(ANGTAN) > TANTOL1 THEN 20
             CASE 2: IF ANGTAN > TANTOL2 OR ANGTAN < TANTOL1 THEN 20
             CASE 3: IF ABS(ANGTAN) < TANTOL2 THEN 20
             CASE 4: IF ANGTAN < TANTOL4 OR ANGTAN > TANTOL3 THEN 20
          END SELECT
50        LG = INT(DIST / 5) + 1
          PAIRLG(LG) = PAIRLG(LG) + 1
          ADST(LG) = ADST(LG) + DIST
          GAMMA(LG) = GAMMA(LG) + (ELEV(S) - LELV) ^ 2
20     NEXT S

    NEXT H

    OPEN "O", #2, OUTF$
    PRINT #2, DANG; ANGTOL
    FOR A = 1 TO NLGS
      IF PAIRLG(A) = 0 THEN AVDST = 0: EXPGMA = 0: GOTO 30
      AVDST = ADST(A) / PAIRLG(A)
      EXPGMA = GAMMA(A) / (2 * PAIRLG(A))
30    PRINT #2, USING "###### ###.# #####.###"; PAIRLG(A); AVDST; EXPGMA
  NEXT A
```

```
CLOSE #2
BEEP: BEEP
INPUT "Other run?  ", RP$
IF UCASE$(RP$) = "Y" THEN 40
END
```

APPENDIX F. Experimental direct-semivariogram for ET_r

Experimental isotropic direct-semivariogram values for ET_r.

Region 2

Int	Avg. dist. *km*	# pair	Feb $mm^2 d^{-2}$	Mar $mm^2 d^{-2}$	Apr $mm^2 d^{-2}$	May $mm^2 d^{-2}$	Jun $mm^2 d^{-2}$	Jul $mm^2 d^{-2}$	Aug $mm^2 d^{-2}$	Sep $mm^2 d^{-2}$	Oct $mm^2 d^{-2}$	Nov $mm^2 d^{-2}$	Cum $mm^2 100^{-2}$
1	3.9	10	0.002	0.009	0.013	0.007	0.009	0.013	0.011	0.005	0.002	0.001	0.036
2	10.1	16	0.003	0.006	0.015	0.017	0.012	0.015	0.013	0.009	0.010	0.002	0.078
3	17.3	21	0.009	0.028	0.068	0.077	0.085	0.069	0.059	0.043	0.023	0.005	0.369
4	23.0	41	0.008	0.017	0.034	0.045	0.051	0.055	0.053	0.030	0.012	0.003	0.235
5	30.6	49	0.013	0.032	0.079	0.088	0.097	0.122	0.088	0.052	0.028	0.007	0.469
6	37.0	64	0.012	0.031	0.071	0.079	0.078	0.108	0.077	0.041	0.019	0.006	0.379
7	43.8	87	0.016	0.040	0.083	0.097	0.097	0.112	0.085	0.051	0.021	0.007	0.463
8	50.5	66	0.015	0.031	0.059	0.063	0.061	0.088	0.072	0.043	0.018	0.007	0.338
9	57.5	79	0.020	0.042	0.079	0.088	0.085	0.114	0.079	0.044	0.025	0.010	0.457
10	64.0	84	0.030	0.071	0.139	0.156	0.140	0.141	0.115	0.066	0.028	0.012	0.717
11	71.0	83	0.026	0.060	0.119	0.131	0.105	0.125	0.104	0.066	0.034	0.013	0.623
12	77.6	87	0.034	0.083	0.153	0.163	0.125	0.128	0.105	0.074	0.041	0.018	0.754
13	84.4	67	0.024	0.060	0.122	0.133	0.111	0.123	0.093	0.062	0.034	0.013	0.599
14	91.5	61	0.022	0.046	0.105	0.109	0.097	0.169	0.126	0.073	0.031	0.013	0.601
15	97.9	109	0.030	0.076	0.147	0.165	0.112	0.166	0.130	0.084	0.034	0.015	0.733
16	104.4	82	0.033	0.094	0.183	0.201	0.167	0.188	0.138	0.103	0.052	0.017	0.943
17	111.5	55	0.040	0.108	0.219	0.232	0.208	0.217	0.161	0.130	0.058	0.023	1.156
18	117.9	66	0.043	0.107	0.200	0.210	0.133	0.126	0.104	0.101	0.057	0.023	0.912
19	124.9	63	0.036	0.082	0.151	0.170	0.116	0.120	0.091	0.079	0.049	0.020	0.735
20	131.9	49	0.045	0.111	0.239	0.270	0.197	0.198	0.165	0.135	0.067	0.026	1.213

Region 4

Int	Avg. dist. *km*	# pair	Feb mm^2 d^{-2}	Mar mm^2 d^{-2}	Apr mm^2 d^{-2}	May mm^2 d^{-2}	Jun mm^2 d^{-2}	Jul mm^2 d^{-2}	Aug mm^2 d^{-2}	Sep mm^2 d^{-2}	Oct mm^2 d^{-2}	Nov mm^2 d^{-2}	Cum mm^2 100^{-2}
1	5.6	6	0.007	0.012	0.033	0.038	0.064	0.076	0.062	0.029	0.009	0.004	0.261
2	15.5	16	0.014	0.041	0.101	0.141	0.197	0.146	0.098	0.058	0.030	0.006	0.628
3	26.0	26	0.018	0.046	0.135	0.183	0.230	0.194	0.177	0.090	0.041	0.008	0.826
4	34.6	30	0.032	0.102	0.296	0.375	0.447	0.366	0.266	0.166	0.091	0.017	1.643
5	44.2	33	0.023	0.069	0.187	0.263	0.326	0.240	0.199	0.102	0.047	0.010	1.078
6	55.2	34	0.017	0.050	0.184	0.307	0.358	0.351	0.327	0.126	0.048	0.011	1.177
7	65.2	46	0.013	0.036	0.118	0.202	0.232	0.286	0.280	0.085	0.028	0.008	0.793
8	76.4	41	0.030	0.103	0.340	0.510	0.535	0.489	0.504	0.203	0.076	0.015	1.966
9	85.9	32	0.041	0.095	0.251	0.345	0.376	0.374	0.358	0.139	0.060	0.025	1.331
10	96.6	52	0.031	0.068	0.184	0.295	0.316	0.307	0.319	0.117	0.055	0.017	1.032
11	105.8	53	0.028	0.071	0.213	0.408	0.464	0.424	0.431	0.155	0.058	0.014	1.440
12	115.9	50	0.019	0.044	0.169	0.350	0.363	0.394	0.374	0.169	0.045	0.012	1.179
13	125.4	46	0.019	0.050	0.185	0.344	0.362	0.405	0.428	0.181	0.045	0.010	1.290
14	135.5	33	0.025	0.069	0.225	0.415	0.505	0.469	0.489	0.204	0.088	0.012	1.694
15	146.6	39	0.020	0.071	0.238	0.407	0.436	0.400	0.428	0.164	0.047	0.012	1.435

Region 5

Int	Avg. dist. *km*	# pair	Feb mm^2 d^{-2}	Mar mm^2 d^{-2}	Apr mm^2 d^{-2}	May mm^2 d^{-2}	Jun mm^2 d^{-2}	Jul mm^2 d^{-2}	Aug mm^2 d^{-2}	Sep mm^2 d^{-2}	Oct mm^2 d^{-2}	Nov mm^2 d^{-2}	Cum mm^2 100^{-2}
1	5.6	6	0.007	0.004	0.021	0.012	0.017	0.023	0.033	0.023	0.006	0.002	0.065
2	18.0	11	0.003	0.014	0.046	0.052	0.048	0.069	0.067	0.024	0.010	0.001	0.180
3	28.8	31	0.009	0.013	0.046	0.046	0.047	0.085	0.077	0.044	0.012	0.004	0.237
4	39.0	33	0.012	0.016	0.038	0.059	0.057	0.059	0.047	0.035	0.020	0.005	0.245
5	50.3	41	0.018	0.033	0.069	0.084	0.099	0.113	0.092	0.055	0.030	0.007	0.435
6	61.4	41	0.024	0.040	0.116	0.105	0.097	0.119	0.110	0.059	0.028	0.011	0.537
7	73.4	41	0.024	0.042	0.093	0.112	0.131	0.178	0.139	0.097	0.041	0.010	0.647
8	83.4	57	0.032	0.058	0.142	0.162	0.173	0.191	0.147	0.096	0.058	0.015	0.831
9	94.6	53	0.031	0.053	0.109	0.123	0.143	0.146	0.131	0.074	0.046	0.013	0.638
10	105.5	85	0.024	0.034	0.087	0.093	0.114	0.171	0.133	0.092	0.042	0.011	0.594
11	117.6	79	0.028	0.042	0.098	0.121	0.138	0.181	0.143	0.105	0.050	0.012	0.673
12	128.7	80	0.022	0.032	0.085	0.088	0.101	0.162	0.128	0.094	0.047	0.011	0.560
13	139.0	62	0.027	0.042	0.108	0.124	0.130	0.157	0.130	0.088	0.049	0.011	0.610
14	150.7	72	0.020	0.041	0.112	0.130	0.132	0.207	0.162	0.130	0.061	0.011	0.715
15	162.1	84	0.042	0.058	0.125	0.141	0.146	0.184	0.142	0.111	0.061	0.018	0.777

Region 6

Int	Avg. dist. *km*	# pair	Feb mm^2 d^{-2}	Mar mm^2 d^{-2}	Apr mm^2 d^{-2}	May mm^2 d^{-2}	Jun mm^2 d^{-2}	Jul mm^2 d^{-2}	Aug mm^2 d^{-2}	Sep mm^2 d^{-2}	Oct mm^2 d^{-2}	Nov mm^2 d^{-2}	Cum mm^2 100^{-2}
1	6.2	5	0.002	0.001	0.022	0.012	0.007	0.031	0.026	0.031	0.012	0.002	0.084
2	16.4	14	0.010	0.012	0.037	0.039	0.046	0.074	0.048	0.046	0.019	0.006	0.231
3	26.0	24	0.022	0.052	0.128	0.119	0.125	0.170	0.141	0.098	0.061	0.020	0.716
4	35.4	41	0.022	0.052	0.121	0.132	0.169	0.171	0.123	0.094	0.068	0.018	0.720
5	46.0	38	0.028	0.057	0.122	0.140	0.181	0.216	0.148	0.096	0.058	0.021	0.772
6	56.0	56	0.036	0.081	0.195	0.205	0.258	0.243	0.167	0.121	0.079	0.029	1.069
7	66.5	51	0.040	0.108	0.268	0.298	0.380	0.374	0.242	0.157	0.091	0.026	1.474
8	77.1	58	0.040	0.084	0.223	0.275	0.397	0.326	0.200	0.136	0.088	0.027	1.312
9	86.9	60	0.031	0.079	0.211	0.265	0.356	0.316	0.191	0.141	0.088	0.022	1.210
10	96.8	73	0.036	0.105	0.300	0.376	0.532	0.413	0.236	0.167	0.102	0.022	1.653
11	106.8	72	0.034	0.132	0.393	0.502	0.732	0.561	0.300	0.200	0.128	0.023	2.168
12	117.8	60	0.031	0.116	0.334	0.430	0.626	0.531	0.307	0.204	0.129	0.023	1.978
13	127.4	57	0.033	0.090	0.242	0.299	0.427	0.380	0.192	0.147	0.102	0.019	1.386
14	137.2	47	0.032	0.134	0.372	0.485	0.706	0.617	0.344	0.227	0.154	0.020	2.254
15	147.7	51	0.045	0.186	0.551	0.740	1.118	0.887	0.472	0.337	0.217	0.033	3.339
16	157.9	61	0.043	0.169	0.534	0.709	1.067	0.884	0.482	0.333	0.208	0.033	3.223
17	167.9	53	0.039	0.102	0.308	0.441	0.746	0.546	0.258	0.168	0.128	0.022	1.883
18	178.3	44	0.055	0.128	0.374	0.488	0.807	0.676	0.345	0.242	0.195	0.034	2.452
19	188.6	48	0.035	0.180	0.629	0.772	1.222	0.824	0.348	0.298	0.288	0.037	3.354
20	198.8	50	0.030	0.126	0.446	0.559	0.866	0.610	0.266	0.223	0.194	0.025	2.389

APPENDIX G. Experimental direct-semivariogram for elevation

Experimental isotropic direct-semivariogram values for elevation.

	Region 2			Region 4			Region 5			Region 6		
Int	Avg dist *km*	# pairs	Exp semvg dam^2	Avg dist *km*	# pairs	Exp semvg dam^2	Avg dist *km*	# pairs	Exp semvg dam^2	Avg dist *km*	# pairs	Exp semvg dam^2
1	4.8	2420	230.8	4.8	3015	158.5	4.8	3435	93.4	4.8	3954	280.9
2	8.0	5635	322.0	8.3	5960	250.6	7.3	12786	159.7	7.8	10035	348.7
3	12.4	10617	417.8	12.6	11792	346.3	12.2	25149	249.9	12.5	20048	459.3
4	17.5	15356	488.4	17.6	16327	446.0	17.2	32681	314.0	17.5	26532	578.9
5	22.8	19718	586.0	22.7	19976	543.7	22.4	45148	355.7	22.4	31395	636.3
6	27.7	19134	688.4	27.8	22846	629.3	27.5	50411	381.5	27.5	42172	727.9
7	32.5	23114	772.2	32.7	25208	711.0	32.4	56336	387.8	32.7	45215	790.2
8	37.6	28979	874.2	37.7	29491	809.1	37.4	67832	408.1	37.7	47205	890.2
9	42.8	26246	1020.9	42.8	30316	861.4	42.5	72058	401.8	42.6	56534	923.9
10	47.6	30539	1154.9	47.8	32413	926.0	47.5	79057	412.7	47.6	55152	984.3
11	52.5	30049	1294.8	52.7	33384	994.5	52.5	86076	412.7	52.6	64861	1004.9
12	57.6	36337	1444.5	57.7	37565	1019.8	57.6	91073	419.0	57.7	62180	1030.1
13	62.6	32061	1642.7	62.7	35165	1115.5	62.5	95058	424.9	62.6	68474	1047.3
14	67.6	36251	1776.7	67.6	38631	1158.6	67.5	99810	425.1	67.6	69153	1065.7
15	72.5	34452	1974.0	72.6	37824	1234.7	72.5	106867	428.5	72.6	70231	1074.5
16	77.5	36631	2089.3	77.7	39851	1300.7	77.5	107262	432.3	77.6	74021	1094.6
17	82.6	36539	2251.4	82.7	38823	1354.1	82.5	114659	435.8	82.6	73192	1100.2
18	87.5	34311	2402.0	87.6	39019	1418.7	87.5	115421	439.9	87.6	73990	1118.0
19	92.4	35906	2565.9	92.6	38831	1441.0	92.5	118396	443.2	92.5	74826	1136.3
20	97.5	34263	2588.5	97.6	38798	1482.8	97.5	122148	447.4	97.5	71936	1128.6
21	102.5	35087	2818.7	102.6	38182	1535.4	102.5	122636	453.1	102.4	73834	1155.3
22	107.4	31015	2859.6	107.5	37074	1600.2	107.5	127840	449.2	107.5	74652	1138.0
23	112.3	32136	2938.9	112.5	37276	1646.7	112.4	123154	452.8	112.5	70089	1162.8
24	117.3	30816	2935.9	117.5	35766	1761.6	117.4	130455	464.9	117.4	70126	1187.2
25	122.4	28199	3029.2	122.5	34783	1802.5	122.4	127971	468.6	122.3	68367	1196.1
26	127.2	25903	3030.9	127.5	33129	1906.1	127.4	128774	483.1	127.3	68645	1229.2
27	132.2	25883	2889.6	132.5	32958	2012.1	132.4	129550	489.1	132.3	69107	1247.5
28	137.2	24066	2975.1	137.5	30532	2089.0	137.4	130791	509.7	137.4	66392	1271.9
29	142.2	21485	2757.3	142.5	28807	2078.3	142.5	130397	506.1	142.4	66008	1306.0
30	147.3	21374	2774.4	147.5	27892	2121.1	147.5	127211	520.4	147.5	64702	1300.9
31	152.5	20167	2636.4	152.5	25238	2046.2	152.5	128487	527.1	152.5	63164	1293.0

	Region 2			Region 4			Region 5			Region 6		
Int	Avg dist *km*	# pairs	Exp semvg dam^2	Avg dist *km*	# pairs	Exp semvg dam^2	Avg dist *km*	# pairs	Exp semvg dam^2	Avg dist *km*	# pairs	Exp semvg dam^2
32	157.6	17830	2721.3	157.5	24188	2050.8	157.6	127037	528.9	157.6	62271	1277.6
33	162.6	16731	2640.0	162.4	22384	2032.3	162.5	123169	534.7	162.6	58685	1283.2
34	167.5	15553	2718.9	167.4	20919	2016.6	167.5	120976	537.3	167.6	59047	1256.1
35				172.4	19203	1943.1	172.5	119963	552.4	172.6	55627	1234.5
36				177.4	17911	1946.2	177.6	118852	559.5	177.6	55539	1215.4
37				182.4	16286	1876.9	182.5	112634	572.2	182.7	54568	1201.2
38				187.4	15087	1900.3	187.5	111543	586.5	187.7	51024	1184.8
39				192.4	13712	1871.2	192.5	108272	604.2	192.6	50956	1164.7
40				197.4	12480	1865.6	197.5	104829	607.1	197.6	48625	1120.3
41							202.5	100335	610.3			

APPENDIX H. Experimental cross-semivariogram

Experimental isotropic cross-semivariogram values.

Region 2

Int	Avg dist *km*	# pair	Feb *dam mm d^{-1}*	Mar *dam mm d^{-1}*	Apr *dam mm d^{-1}*	May *dam mm d^{-1}*	Jun *dam mm d^{-1}*	Jul *dam mm d^{-1}*	Aug *dam mm d^{-1}*	Sep *dam mm d^{-1}*	Oct *dam mm d^{-1}*	Nov *dam mm d^{-1}*	Cum *dam mm 100^{-1}*
1	3.9	10	-0.2	-0.3	0.0	-0.1	-0.2	0.1	-0.1	0.1	0.0	-0.1	-0.2
2	10.1	16	-0.2	-0.3	-0.5	-0.5	-0.5	-0.5	-0.4	-0.3	-0.3	-0.1	-1.2
3	17.3	21	-1.9	-3.4	-5.2	-5.6	-6.0	-4.9	-4.3	-3.8	-2.9	-1.3	-12.3
4	23.0	41	-1.1	-1.6	-2.4	-2.7	-2.9	-2.4	-2.4	-1.8	-1.1	-0.6	-6.0
5	30.6	49	-1.7	-2.8	-4.3	-4.5	-4.7	-4.4	-3.9	-3.3	-2.4	-1.2	-10.5
6	37.0	64	-1.7	-3.0	-4.6	-4.9	-4.7	-4.2	-3.7	-2.9	-1.8	-1.2	-10.4
7	43.8	87	-2.3	-3.8	-5.4	-5.8	-5.6	-4.8	-4.4	-3.6	-2.2	-1.4	-12.5
8	50.5	66	-1.7	-2.5	-3.5	-3.4	-3.2	-3.0	-2.9	-2.5	-1.7	-1.2	-8.2
9	57.5	79	-2.3	-3.6	-5.0	-5.1	-5.0	-4.9	-4.2	-3.4	-2.3	-1.6	-12.0
10	64.0	84	-4.5	-7.0	-10.0	-10.5	-9.8	-8.5	-8.0	-6.5	-4.1	-2.6	-22.9
11	71.0	83	-3.8	-5.9	-8.4	-8.6	-7.6	-6.4	-6.3	-5.7	-4.0	-2.7	-19.0
12	77.6	87	-5.2	-8.3	-11.4	-11.6	-9.9	-7.1	-7.3	-7.2	-5.6	-3.7	-25.0
13	84.4	67	-3.8	-6.0	-8.6	-8.7	-8.0	-6.7	-6.3	-5.9	-4.5	-2.8	-19.6
14	91.6	61	-3.5	-4.9	-7.4	-7.3	-6.8	-7.1	-7.1	-6.1	-3.9	-2.6	-18.3
15	97.9	109	-4.4	-6.8	-9.7	-10.0	-8.1	-6.6	-7.1	-6.7	-4.5	-3.1	-21.7
16	104.4	82	-5.3	-8.8	-12.6	-12.9	-11.9	-10.4	-10.1	-9.2	-6.3	-3.8	-29.3
17	111.5	55	-7.3	-11.7	-17.2	-17.4	-16.6	-15.0	-13.9	-13.2	-8.6	-5.2	-40.3
18	117.9	66	-7.2	-11.2	-15.6	-15.6	-12.7	-9.0	-9.9	-10.6	-7.8	-5.2	-33.6
19	124.9	63	-5.6	-8.2	-11.3	-11.2	-9.3	-7.0	-7.2	-7.8	-6.4	-4.2	-25.4
20	131.9	49	-8.6	-13.3	-19.4	-20.0	-16.8	-13.7	-14.3	-13.9	-9.7	-6.5	-43.4

Region 4

Int	Avg dist *km*	# pair	Feb *dam mm d^{-1}*	Mar *dam mm d^{-1}*	Apr *dam mm d^{-1}*	May *dam mm d^{-1}*	Jun *dam mm d^{-1}*	Jul *dam mm d^{-1}*	Aug *dam mm d^{-1}*	Sep *dam mm d^{-1}*	Oct *dam mm d^{-1}*	Nov *dam mm d^{-1}*	Cum *dam mm 100^{-1}*
1	5.6	6	-0.6	-1.0	-1.8	-1.9	-2.1	-2.2	-1.6	-1.4	-0.9	-0.6	-4.5
2	15.5	16	-3.0	-5.2	-8.1	-9.8	-11.6	-8.8	-6.6	-5.1	-4.3	-1.8	-19.8
3	26.0	26	-2.9	-5.2	-9.2	-10.4	-10.7	-8.7	-7.2	-6.3	-4.5	-2.0	-20.7
4	34.6	30	-7.2	-13.3	-22.4	-24.8	-26.9	-21.4	-16.7	-14.2	-11.8	-5.0	-50.3
5	44.2	33	-4.5	-8.4	-14.3	-16.7	-18.0	-14.1	-11.4	-9.3	-6.5	-2.7	-32.6
6	55.2	34	-3.3	-6.7	-13.5	-16.8	-17.5	-15.5	-14.2	-10.2	-6.0	-2.2	-32.6
7	65.2	46	-1.7	-3.4	-7.2	-9.6	-9.9	-9.0	-8.9	-5.5	-2.2	-0.7	-17.9
8	76.4	41	-4.9	-11.2	-21.2	-25.6	-25.7	-23.6	-22.3	-15.3	-8.9	-2.8	-49.7
9	85.9	32	-4.5	-9.6	-17.1	-19.4	-19.6	-17.5	-14.2	-11.0	-6.8	-3.0	-37.9
10	96.6	52	-2.9	-6.8	-13.0	-16.2	-16.5	-13.5	-11.9	-8.6	-4.4	-1.4	-29.2
11	105.8	53	-2.8	-8.1	-15.9	-21.9	-22.9	-20.3	-19.3	-12.7	-6.4	-1.0	-40.1
12	115.9	50	-1.1	-5.9	-13.2	-18.6	-18.7	-17.8	-16.5	-11.8	-4.7	-0.2	-33.1
13	125.4	46	-2.0	-6.9	-14.8	-19.5	-18.8	-19.0	-18.0	-13.2	-4.8	-1.0	-36.4
14	135.5	33	-3.5	-8.5	-16.3	-22.1	-23.5	-21.9	-21.1	-14.2	-7.0	-1.4	-42.7
15	146.6	39	-2.6	-9.0	-17.5	-22.2	-21.5	-20.5	-18.6	-13.5	-5.5	-1.2	-40.5

Region 5

Int	Avg dist *km*	# pair	Feb *dam mm d^{-1}*	Mar *dam mm d^{-1}*	Apr *dam mm d^{-1}*	May *dam mm d^{-1}*	Jun *dam mm d^{-1}*	Jul *dam mm d^{-1}*	Aug *dam mm d^{-1}*	Sep *dam mm d^{-1}*	Oct *dam mm d^{-1}*	Nov *dam mm d^{-1}*	Cum *dam mm 100^{-1}*
1	5.6	6	0.3	-0.2	-0.5	-0.2	0.3	0.4	0.8	0.6	0.2	0.1	0.5
2	18.0	11	-0.1	-1.3	-2.2	-2.3	-1.6	-1.0	-0.0	-0.2	-0.4	-0.1	-2.8
3	28.8	31	-0.8	-1.2	-2.2	-2.1	-2.0	-1.7	-1.1	-1.1	-0.9	-0.5	-4.1
4	39.0	33	-0.6	-1.1	-1.7	-1.8	-1.6	-1.4	-0.9	-0.9	-0.7	-0.4	-3.4
5	50.3	41	-1.4	-2.3	-3.3	-3.5	-3.4	-2.9	-2.2	-1.7	-1.6	-0.9	-7.1
6	61.4	41	-3.0	-4.4	-7.8	-7.1	-6.4	-6.1	-5.5	-3.8	-2.7	-2.0	-15.1
7	73.4	41	-2.3	-3.6	-5.3	-5.7	-6.0	-5.9	-4.9	-3.7	-2.4	-1.5	-12.7
8	83.4	57	-2.8	-4.6	-7.5	-7.7	-8.0	-8.1	-6.9	-5.3	-3.9	-1.8	-17.4
9	94.6	53	-2.0	-3.2	-4.5	-4.8	-4.7	-3.9	-3.1	-2.2	-2.1	-1.3	-9.8
10	105.5	85	-1.7	-2.6	-4.5	-4.6	-4.9	-5.2	-4.5	-3.6	-2.4	-1.2	-10.9
11	117.6	79	-1.7	-2.7	-4.1	-4.4	-4.7	-4.8	-3.8	-3.0	-2.2	-1.0	-10.0
12	128.7	80	-1.0	-1.6	-2.8	-2.6	-3.0	-3.9	-3.2	-2.7	-1.6	-0.7	-7.2
13	139.0	62	-1.4	-2.6	-4.6	-4.4	-4.2	-4.0	-3.1	-2.3	-1.8	-0.9	-9.0
14	150.7	72	-0.8	-1.8	-3.3	-3.2	-3.2	-3.5	-2.8	-2.2	-1.5	-0.6	-7.1
15	162.2	84	-2.4	-3.9	-6.1	-5.9	-5.9	-5.6	-4.5	-3.5	-3.0	-1.5	-13.0

Region 6

Int	Avg dist *km*	# pair	Feb *dam mm d^{-1}*	Mar *dam mm d^{-1}*	Apr *dam mm d^{-1}*	May *dam mm d^{-1}*	Jun *dam mm d^{-1}*	Jul *dam mm d^{-1}*	Aug *dam mm d^{-1}*	Sep *dam mm d^{-1}*	Oct *dam mm d^{-1}*	Nov *dam mm d^{-1}*	Cum *dam mm 100^{-1}*
1	6.2	5	-0.1	-0.1	0.2	0.1	-0.2	0.2	0.2	0.4	0.3	0.1	0.4
2	16.4	14	-0.6	-0.5	-0.8	-1.0	-0.9	-1.2	-0.9	-0.9	-0.4	-0.4	-2.3
3	26.0	24	-1.8	-3.1	-4.7	-4.7	-4.7	-5.0	-4.3	-3.6	-2.7	-1.6	-11.0
4	35.4	41	-1.7	-2.9	-4.2	-4.5	-5.0	-4.4	-3.7	-3.1	-2.7	-1.3	-10.2
5	46.0	38	-1.8	-3.2	-4.3	-4.4	-4.9	-5.1	-4.3	-2.9	-2.4	-1.5	-10.6
6	56.0	56	-3.5	-5.5	-8.2	-8.5	-9.3	-8.3	-6.8	-5.5	-4.6	-2.9	-19.2
7	66.5	51	-4.4	-8.0	-12.3	-12.6	-13.8	-12.9	-10.5	-8.2	-6.6	-3.4	-28.3
8	77.1	58	-3.4	-5.6	-8.5	-9.4	-10.9	-10.2	-8.3	-6.5	-4.9	-2.5	-21.4
9	86.9	60	-2.9	-5.3	-8.1	-9.0	-10.0	-9.4	-7.4	-6.0	-4.6	-2.3	-19.8
10	96.8	73	-3.6	-6.8	-11.3	-12.3	-14.0	-12.1	-9.4	-7.4	-5.6	-2.6	-26.0
11	106.8	72	-4.1	-8.8	-15.2	-16.7	-19.3	-17.0	-12.8	-10.0	-7.7	-3.2	-35.0
12	117.8	60	-3.3	-7.3	-12.2	-13.9	-16.2	-15.0	-11.6	-8.8	-6.3	-2.6	-29.7
13	127.4	57	-2.6	-5.5	-9.1	-10.1	-11.5	-10.8	-8.0	-6.2	-4.6	-2.0	-21.5
14	137.2	47	-3.0	-8.1	-13.6	-15.7	-18.0	-16.9	-13.0	-9.6	-6.6	-2.3	-32.5
15	147.7	51	-5.0	-11.8	-20.0	-22.8	-27.0	-24.8	-18.6	-15.0	-11.1	-4.1	-48.8
16	157.9	61	-3.8	-10.0	-17.9	-20.7	-24.4	-23.4	-17.6	-13.9	-9.6	-3.2	-44.1
17	168.0	53	-2.2	-5.4	-9.4	-11.0	-13.5	-12.5	-9.1	-6.9	-4.8	-1.7	-23.3
18	178.3	44	-3.5	-6.7	-11.1	-12.8	-16.3	-16.0	-12.0	-8.9	-6.4	-2.5	-29.3
19	188.6	48	-2.7	-7.8	-14.6	-16.3	-19.6	-16.3	-10.6	-9.5	-8.0	-2.6	-32.9
20	198.8	50	-1.7	-5.4	-11.0	-12.0	-13.6	-13.0	-9.0	-7.9	-5.5	-1.9	-24.7